Synthesis, Characterization and Stability Test of Silver Nanoparticles in Ecotoxicology Media

By

Mila Tejamaya

A thesis submitted to

The University of Birmingham

for the degree of

Doctor of Philosophy

Division of Environmental Health and Risk Management

School of Geography, Earth and Environmental Sciences

The University of Birmingham, UK

September 2013

Abstract

Currently silver nanoparticle (AgNP) is the most widely used NP due to its broad antimicrobial activity. Not less than 383 out of 1628 nanotechnology products contains AgNPs. Due to the substantial increase of AgNP commercialization, AgNP exposure to the environment become apparent. Potential hazard of AgNP to the environment, however, is largely unknown. Lack of NP characterization data in most of (eco)toxicology study, transformation of NPs in the test media and environment, etc. have challenged the attempt of presenting NP dose and toxic outcome. Therefore more control over NP ecotoxicology study need to be done to be able to draw a conclusion of NP dose-response relationship.

This study was aimed to synthesis a stable, fully characterized and tightly constrained PVP-capped AgNPs via bottom-up method. Modification of Mulfinger et al. (2007) synthesis protocol have been successful in generating spherical and monodisperse PVP-capped AgNPs. The average core size was 10-12 nm, hydrodynamic size = 27-29 nm, ζ= 12-15 mVA, and excellent stability in OECD *Daphnia* media and its variant (IS= 8.88 mM – 10.84 mM), and also in Algae media (IS= 8.02 mM).

Another straightforward and promising synthesis method of PVP-capped AgNPs was developed via ligand-exchanged (indirect method) from a monodisperse citrate-capped AgNPs. 2 mL of 30 g/L PVP_{10} $suspension_{(aq)}$ was adequate for recap 50 mL 11 ppm citrate-capped AgNPs without any effect into core AgNPs properties and improved AgNPs stability over OECD *Daphnia Magna sp.* media. Other polymers such as PEG-SH, Fulvic acid and Tween-80 polymers was also tried to recap citrate-coated AgNPs. There were no size and shape alterations as fuvic acid

replaced citrate coating, while PEG-SH and Tween-80 polymer did. All polymers, nevertheless improved the AgNPs stability in ecotoxicology media.

The stability of citrate; PEG-SH; and PVP-capped AgNPs due to incubation in several ecotoxicology media with variation in media ionic strength/concentration and composition was examined. The stability was evaluated in terms of SPR (λ_{max} and peak width), size, and shape stability. It was seen that PVP polymer showed a better stabilization effect than citrate and PEG-SH. In most of media, SPR extinction and size enlargement were found at greater extent for electrostatically capped AgNPs, citrate-capped AgNPs than sterically capped AgNPs. In algae media, nonetheless the SPR extinction of PEG-SH capped AgNPs was higher than citrate-capped AgNPs, potentially because of lower divalent cation content in algae media that caused lesser effect to citrate-capped AgNPs. Shape transformation was seen for AgNPs after incubated in media without chloride (nitrate and sulphate media), especiallay in concentrated media. Thus type of capping agent; media ionic strength and chemical composition determined the behavior and stability of AgNPs in ecotoxicology media.

Acknowledgements

I would like to express my deepest gratitude to my supervisor, Prof. Jamie R Lead, for giving me the opportunity to be one of his students in University of Birmingham. Because of his expertise, brilliant ideas and full support have made this thesis possible. I also would like to thank Prof. Kevin Chipman and Prof. Mark Viant for the encouraging discussion and introducing me to the Bioscience and daphnia world.

I would never have been doing this program without the financial support from the Directorate of Higher Education of Republic of Indonesia (DIKTI). Thank you for letting my dream come true. Thank you very much to my colleague in University of Indonesia, Ibu Daly, Mas Derriansyah and Mbak Galuh Puri for supporting me for the last 4 years. To Dean of School of Public Health, Pak Bambang Wispriyono PhD and his staffs, thank you very much for all the support and advices. To my colleague at Department of Occupational Health and Safety, all the support, advices and motivation are highly appreciated, especially Bu Fatma Lestari for her full and continuous support, Pak Doni Hikmat for backing me up for all the works in Dept.K3 , and Baiduri for sharing tears and laugh, Terimakasih banyaak…

My GEES Nanogroup, who always there to help me out with any lab and data problems, thank you so much. Especially to Yusuf Nur for sharing the skills, knowledge, faith, and coffee. All the moment we share together in the lab, office, masjid and Costa are unforgettable. Christine, my bestest advisor, for listening to my laments about work and family and checking my grammatical errors, thanks Mum. Special thanks also to Marie, Isabella and Laura for sharing the synthesis protocols and particles. Indrani, my thoughtful friend, many thanks for your advices. Willam Ho, thanks for taking me around the beautiful places in Birmingham. Paula Cole, Ruth Merrifield, Sue Cumberland, and Mohammed Baalousha for helping me out with instrumentation. Bjorn, my bestes mentor, thank you very

much for all effort that you have been given to me, with the AFM in particular. Thanks to other member of GEES Nanogroup for discussion and support.
Thanks to the people that teach me with the outstanding and complicated instrumentations, Theresa Morris for the TEM, and Steve Baker for the ICP-MS.

To 325 night-clubbers: Awwal, Issac, Soph Ia, Indrani and Marie (again), thanks for accompanying me to stay up late in the office and work even harder during weekend. Thank you so much, I'm gonna miss you all…

My family in UK, especially the member of Pengajian Asy-syifa and Forum Jumat, you help me to be istiqamah and remember Allah, Alhamdulillah… Special thanks to the lovely family of Bu Lina dan Uwa Undang, Mbak Lia and Pak Amet, Uni Mila and Brother Richard, Mbak Tini and Pak Riza, Mbak Tutik and Mas Pras, Mbak Laksmi and Mas Yulian, Teh Yossi and Brother Alex, Kak Rin and Brother Mohammad, Mbak Tyas, Mbak Een, Mas Hijrah and Mbak Lia Imran, I love you all… Thanks for all of support, dhua and advices.

To my dearest family, for the unconditional love and support, Mama, Papa, Ibu, Keluarga Uwa Mela, Uwa Nia, Mang Asep, adikku Bibi Hani and Om Teguh, without your support all this things are impossible. I love you all and may Allah rewards you for all the things you have given to me, your support, love, especially your dhua for me…

Last but not least, to my beautiful and bestest family, ayah Erik Ridwan, aa Fauzan Ridwan, Kaka Nadya Ridwan, your endless and infinite love and support , also our togetherness in Birmingham and Indonesia, have made this achievement never been easier. With all of my heart, I love you all unconditionally…forever and ever

Finally, I hope this thesis is useful for anyone who read this and especially for my students.

Table of content

List of Figures

CHAPTER I

CHAPTER II

CHAPTER III

CHAPTER IV

CHAPTER V

CHAPTER VI

List of Tables

CHAPTER I

CHAPTER II

CHAPTER III

CHAPTER IV

CHAPTER V

CHAPTER VI

CHAPTER VII

List of Abbreviation

AAS	Atomic Absorption Spectroscopy
AFM	Atomic Force Microscopy
Ag	Argentum (Latin), for Silver
$AgNO_3$	Silver Nitrate
AgNP/s	Silver nanoparticle/s
AM	Algae media
ASTM	American Standard Testing and Material
Au	Aurum (Latin), for Gold
BET	Brunauer-Emmet-Teller
BSI	British Standard Institution
^0C	Degree Celcius, unit of Temperature
CM	Chloride Media, refer to OECD *Daphnia sp*. media
CNT/s	Carbon Nanotube/s
CO_2	Carbon dioxide
d_H	Hydrodynamic diameter
DLS	Dynamic Light Scattering
DLVO	Derjaguin-Landau-Verwey-Overbeek
DNA	Deoxyribonucleic acid
EDL	Electric Double Layer
EDX	Energy Dispersive Spectoscopy
ENPs	Engineered Nanoparticles
EPA	Environment Protection Agency (US)
EPS	Exo-polysaccharides
FBS	Fetal Bouvine Serum
Fl-FFF	Flow-Field Flow Fractionation
FTIR	Fourier Transform Infra Red
FWHM	Full width half maximum
GA	Gum Arrabic
GaAs	Gallium Arsenide
HRP	Horseradish peroxidase
ICP-MS	Inductively coupled plasma mass spectrometry
IS	Ionic Strength
ISO	International standard organization

KDa	Kilo Dalton, is unit of mass. However Dalton is sometimes used to represent pore size, where 1KDa~ ±1 nm
kV	Kilo Volt
LC_{50}	Lethal concentration-50, is the concentration where 50% of population was killed
λ	Lamda (Latin) for wavelength
mM	Milli Molar
MWCO	Molecular Weight cut-off, where 90% of molecules larger than the pore size retained by the membrane
NaCl	Sodium Chloride
NM/s	Nanomaterial/s or Nitrate media (depends on context)
NOM	Natural organic material
nm	nanometer
NP/s	Nanoparticle/s
NTA	Nanoparticle Tracking Analysis
OECD	Organization for Economic Cooperation and Development
PAH	Polyaromatic hydrocarbon
PAS	Publicly Available Specification
PdI	Polydispersity Index
PEC	Predicted environmental concentration
PEG-SH	Thiolated-polyethylene glycol
pH	Potential of hydrogen, a measure for acidity
PNEC	Predicted no effect concentration
PVP	Polyvynilpyrrolidone
rpm	Rotation per minute
RQ	Risk quotient
S/SA	Specific/Surface area
SiO_2	Silicon dioxide
SM	Sulfate media
SPR	Surface Plasmon resonance
TEM	Transmission Electron Microscopy
THF	Tetrahydrofuran
TiO_2	Titanium dioxide
UFPs	Ultrafine Particles
UV-Vis	Ultraviolet-vissible
WWTP	Waste water treatment plant

CHAPTER I

INTRODUCTION

1.1. Overview

Nanoscience and nanotechnology have been successful in creating different types of nanomaterials (NMs), material with at least one dimension of the order of 100 nm or less (BSI, 2005). The novel mechanical, optical, electronic and magnetic properties exhibited by NMs over their corresponding bulk materials stimulates the interest in NMs. Inert substances such as gold for instance, will exhibit reactive properties when it is downsized to the nanoscale (Daniel and Astruc, 2004). Carbon nanotubes (CNTs), having the same chemical composition with brittle carbon compounds, show unique mechanical properties including a high tensile elastic modulus, flexibility and low density(Coleman et al., 2006). These distinctive properties may arise in part from the significant increase in the high surface-to-volume ratio as the particle size falls to the nanoscale and the domination of quantum effects on the properties of NMs (Owens and Poole Jr, 2008).

A number of methods of synthesizing NMs has been developed and can be grouped into top-down (physical methods), bottom-up (chemical methods) and biological methods (Wang and Xia, 2004; Ju-Nam and Lead, 2008; Christian, 2009; Tolaymat et al., 2010). The top-down method synthesizes NMs from the bulk material via inert-gas evaporation, laser ablation, sputtering, mechanical grinding and milling, etc. In contrast, the bottom-up method produces NMs from very small building blocks of materials such as atoms and molecules by the implementation of a wet chemical method. Through nucleation and growth processes, the small particles can be built-up into a more complex cluster (Ju-Nam and Lead, 2008; Lee, 2008).

Recently, exploration of the biological method has commenced for bio-synthesis of NMs, but the poorer control over NMs size by bio-methods mean that there are fewer application where this method is adopted.

The promising novel properties and well-developed synthesis technology of NMs have accelerated the production and utilization of NMs in many consumer products. Silver nanoparticles (AgNPs) are particularly widely used as AgNPs exhibit wide-range antimicrobial properties. According to Woodrow Wilson Centre study, 313 out of 1317 nano-products contain AgNPs, and this figure has increased by more than ten times within five years (PEN, 2013). This rapid increase of AgNP commercialization raises concern over its potential release to the environment and the consequent adverse effects (Nowack and Bucheli, 2007; Ju-Nam and Lead, 2008). Therefore the risk from NMs, as a function of exposure and the hazards, needs to be assessed either by an exposure-driven or a hazard-driven approach to prevent deleterious effect both on human and environmental health (Baalousha and Lead, 2007; Pettitt and Lead, 2013).

The release of AgNPs to the environment from washing machines, textiles, and paint containing AgNPs has been demonstrated (Benn and Westerhoff, 2008; Geranio et al., 2009; Kaegi et al., 2010; Farkas et al., 2011) with significant speciation alteration due to chemical reactions with the detergent and bleaching agent, and also effect of mechanical stresses from the washing machine (Impellitteri et al., 2009). Number of (eco)toxicology findings has also been reported (Fabrega et al., 2011; Batley et al., 2012), however, establishing an association between NP characteristics and the observed toxic effect was unsuccessful due to the lack of characterization data of most of the NPs used (Foss Hansen et al., 2007). Better

characterization of NPs in (eco)toxicology studies is very important as there may or may not be a relationship between NPs characteristics and toxic outcome.

NPs are also very reactive and dynamically transformed due to their interaction with biotic and abiotic components of the media. Thus undefined NP behavior during exposure in most (eco)toxicology studies complicates the dose-response relationship (Fabrega, Luoma et al., 2011). These complication is caused by concentration changes during incubation due to aggregation, dissolution, phase transformation, etc that lead to material losses (Figure 1.1) (Franklin et al., 2007; Navarro et al., 2008; Batley, Kirby et al., 2012; Levard et al., 2012; Lorenz et al., 2012; Lowry et al., 2012). Variation in characteristics of NMs between syntheses batches have to be controlled to obtain a consistent hazard identification result. Therefore a number of attempts has to be made to improve the course of NM hazard investigation: controlling synthesis processes to obtain consistent NM properties, fully characterizing the NMs, and examining the behavior of NPs in the media that the NMs are exposed to, especially within eco-toxicology studies in which oral dosing of NPs occurs (Crane et al., 2008).

Various lists of physico-chemical characteristics of NPs relevant to ecotoxicology studies have been proposed (Crane, Handy et al., 2008; Warheit, 2008; Scown et al., 2010) and the priorities according to Pettitt and Lead (2013) are presented in Table 1.1. The incubation conditions such as the media chemical composition, pH, total ion and divalent ion content, organic matter and ionic strength also needs to be reported (Handy et al., 2008).

This study, as part of larger eco-toxicology study that investigates the toxic effect of silver nanoparticle (AgNPs) with different capping agents on *Daphnia magna sp.*, examines the physico-chemical characteristics of AgNPs in pristine

suspensions and in eco-toxicology media, to be able to understand the behavior of AgNPs during the exposure studies. The AgNPs were synthesized during the course of this work, to ensure that NPs with well-controlled properties were used.

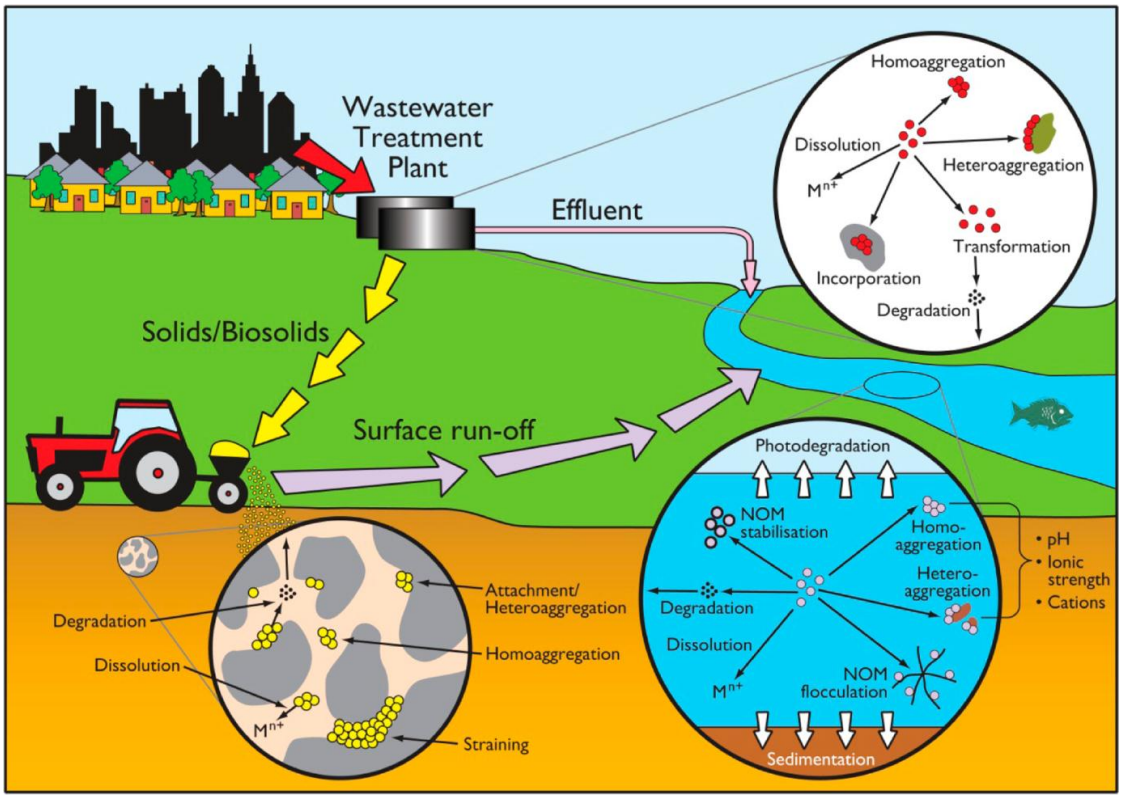

Figure 1. 1 The illustration of NMs behavior, fate and transformation in the aquatic and terrestrial environment (Batley, Kirby et al., 2012)

Table 1. 1 The priority list of NPs characterization in any eco-toxicology study(Handy, von der Kammer et al., 2008)

	Characterization	
	Pre-exposure	**Post-exposure**
Dose/concentration	Mass	Mass
	Particle number	Particle number
	Surface area	Surface area
Physical form	Particle size (mean)	Particle size (mean)
	Particle size (distribution)	Particle size (distribution)
	Agglomerate (morphology)	Agglomerate (morphology)
		Dissolution
Surface properties	Shell chemistry/coating	Shell chemistry/coating
	Surface charge/zeta potential	Surface charge/zeta potential

1.2. The aim, objectives and hypothesis of this study

The overall aim of this study is to investigate the behavior and stability of tightly controlled and well-constraint self-synthesized AgNPs in ecotoxicology media. The AgNPs is prepared with non-toxic chemicals to ascertain that the toxic outcome is attributed to NPs. In order to achieve this aim, the objectives of this study are described as:

- to tightly constrain the synthesis of PVP capped AgNPs to achieve intended core size ± 10nm with high stability in ecotoxicology media and well-controlled characteristics
- to develop an indirect synthesis method of polymer-capped AgNPs from electrostatically capped AgNPs via ligand-exchange method
- to examine the behavior and stability of citrate-, PEG- and PVP- coated AgNPs during 21 days incubation in Daphnia media and 3 days (72 hours) incubation in algae media

Hypothesis:

The works in this study is not fully hypothesis-driven, but some part is technology driven (synthesis and characterization). Thus the hypotheses are:

- spherical, PVP capped AgNPs can be synthesis via direct and indirect (ligand exchange) methods
- Behavior and stability of AgNPs in eco-toxicology media are influenced by the type of capping agent coating the AgNPs
- Behavior and stability of AgNPs in eco-toxicology media are influenced by the ionic strength and chemical composition of the ecotoxicology media

1.3. Structure of the thesis

This thesis is comprised of eight chapters covering the issues described below:

Chapter 1 is an introduction chapter which describes the general overview of NMs synthesis, production, exposure, hazards, and the corresponding risk assessments. The uncertainty of eco(toxicology) studies is reviewed in term of hazard identification and some suggestions to overcome the uncertainties are discussed. The aim, objectives and hypotheses of this study are presented.

Chapter 2 is the background chapter which explains about the NPs definition, classification, properties, transformation, synthesis, chracaterization and the reasons of choosing silver nNPs in this study.

Chapter 3 describes the practical methods implemented in this study, including descriptions of material and equipment used, the AgNPs synthesis methods, instrumentations and sample preparation for characterization purposes, and the methods adopted for the stability studies.

Chapter 4 presents and discusses the characteristics of AgNPs generated from the hot and the cold processes. The results from initial dissolution studies of PVP-capped AgNPs in different media performed by different techniques will also be presented.

Chapter 5 presents and discusses the synthesis of polymer-capped AgNPs from electrostatically-stabilised NPs via a ligand-exchange method. Characteristics of AgNPs before and after ligand-exchange will be presented and compared.

Chapter 6 presents and discusses the behavior of AgNPs in different eco-toxicology media. Three different types of NPs were prepared with different capping agents.The OECD *Daphnia magna* immobilization media and variants, and algae media were used for stability test of the AgNPs.

Chapter 7 is the summary and conclusions of this study. Some recommendations for future work are also presented.

Appendix A presents the ionic strength calculation of the media used in this study

Appendix B shows some TEM images of AgNPs after incubated in ecotoxicology media

CHAPTER II

BACKGROUND

2.1. History of nanotechnology

Although the term “nanotechnology” was coined later by the Japanese scientist Norio Taniguchi (1974)(RS, 2004), the concept of nanotechnology was originally introduced by the physicist Richard P. Feynman in his lecture “There’s plenty of room at the bottom”, given at the American Physical Society meeting in 1959 (Wang et al., 1999). Feynman set out the idea of manipulating and controlling materials by exploiting the laws of physics to produce materials at a very small scale. Feynman also described the potential of his application to the sciences (biology and chemistry) and predicted a range of application for example printing a book on the head of a pin, miniaturising the computers and machinery, and emphasized the importance of improving the electron microscopy for analysing very tiny materials(Wang, Xu et al., 1999).

Since 2001 nanotechnology has moved toward commercialization from research and development in the laboratory, and the value of nanotechnology products globally is forecast to grow from € 200 billion in 2009 into € 2 trillion in 2015 (EU, 2013). This emphasises that nanotechnology is expected to have a substantial impact into world economics.

Due to the range of applications of nanomaterials in different products, the potential for exposure and consequent risk to humans and the environment raises concerns. Since NMs show unique properties, their fate and behaviour in the environment and also the toxic effect following NPs exposure might be different from conventional chemical equivalent (Luoma, 2008). Therefore the growth of

nanotechnology has also stimulated the development of sciences exploiting the benefits and assessing the risk of nanoproducts such as nanoscience, nanomedicine, nano(eco)toxicology, etc (Curtis et al., 2006).

2.2. Definition of Nanomaterials

More than a 1,600 of nano-containing consumer products have been commersialised and are available in the market (PEN, 2013) and many more are waiting in the pipeline. A practicable and unambiguous definition of nanomaterials, however has not been agreed upon (Kreyling 2010) as different stakeholders have different points of view, for example, nanoengineers and nanotoxicologists focus the definition on the effect of NMs, and legislators need a reasonably simple definition with a clear-cut limit (Lidén, 2011). A consistent definition is also required for providing sufficient information to consumers, to promote consistency in the interpretation by producers, users and regulators, and for notification purposes if materials need closer inspection (Bleeker et al., 2013).

Even though the definition of NPs as material with size range 1-100nm has been widely used (BSI, 2005), other definitions have also been suggested. Figure 2.1 shows the length of the nanometer compared to other objects. In pharmaceutics, based on their biogenic properties the NP was defined as polymeric NPs in size range 10-1000nm, designed for carrying drugs (Oberdörster et al., 1994; Shi et al., 2013). The evidence of novel properties is also suggested as the criterion in defining metal and metal oxide NPs rather than the size alone, and 30nm has been proposed as the threshold size of NPs due to the appearance of novel properties at this size and smaller (Auffan et al., 2009). Some flexibility of the size threshold is also needed

in (eco)toxicology studies because the interest is in the evidence of novel toxic effect rather than size threshold only (Handy et al., 2008).

Recently, the Joint Research Centre (JRC) of the European Commission has published a recommendation for nanomaterial as (Rauscher et al., 2014):

"natural, incidental or manufactured material containing particles, in an unbound state or as an aggregate or as agglomerate and where, for 50% or more of the particles in the number size distribution, one or more external dimensions is in the size range 1nm-100 nm.

In specific cases where warranted by concerns for the environment, health, safety or competitiveness the number size distribution threshold of 50% may be replaced by a threshold between 1% and 50%"

Another issue arise. For practical application of the definition stated above, guidance on the size measurement method for a number-based size distribution is required as different methods give different dimensions (hydrodynamic, aerodynamic, core diameter, etc) (Bleeker, de Jong et al., 2013). Following the publication of the NMs definition, European Food Safety Authority (EFSA) recommends to use of at least two different techniques for NMs characterization and states that one of them should be an electron microscopy method (EFSA, 2011). For scientific purposes, especially for (eco)toxicology studies in which the knowledge about which characteristics of NMs can be attributed to toxic response is still largely unknown, multi-method characterization is recommended (Domingos et al., 2009).

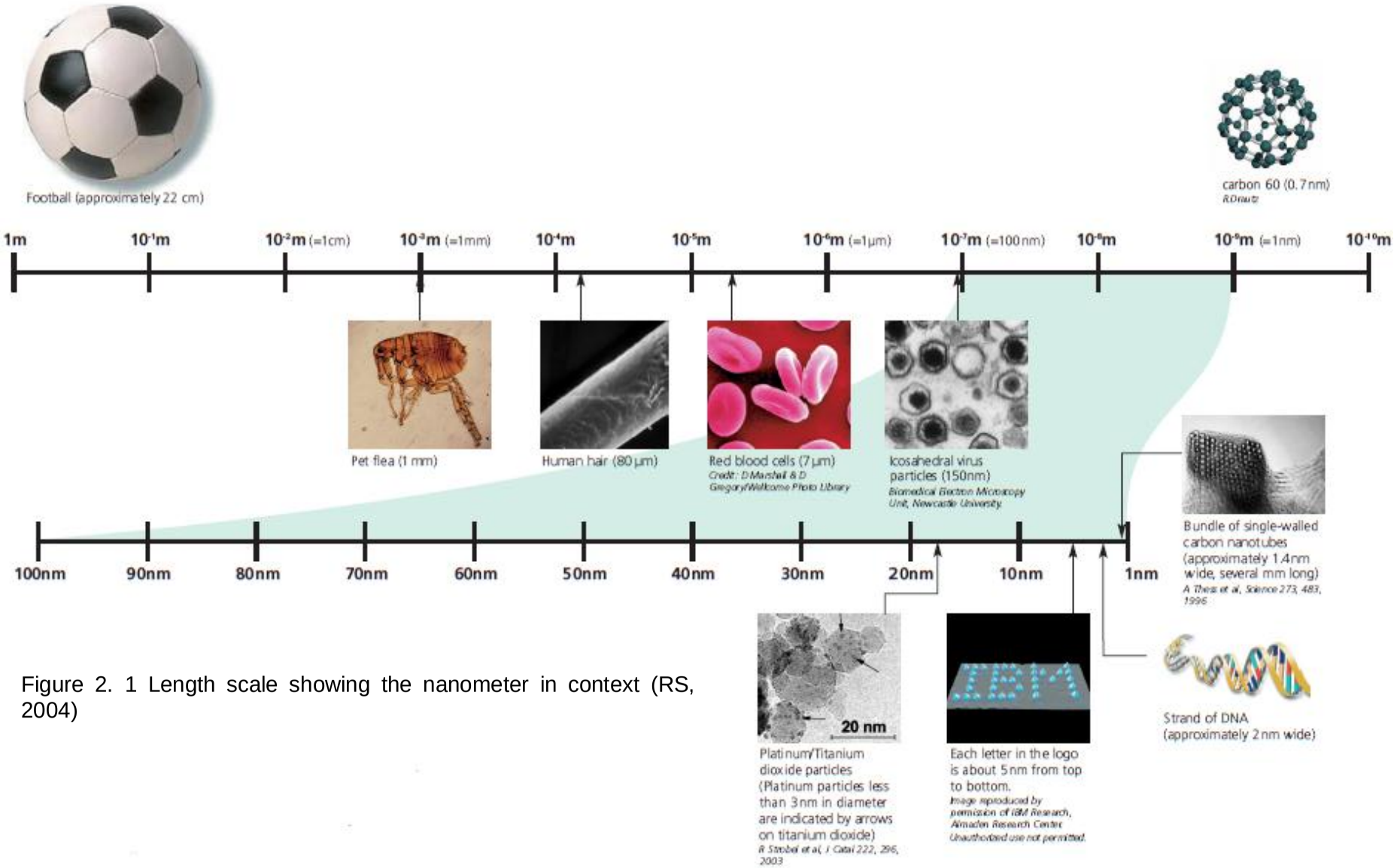

Figure 2. 1 Length scale showing the nanometer in context (RS, 2004)

2.3. Classification of nanoparticles

NPs can be grouped according to their origin and chemical composition as presented in Table 2. 1. In relation to their origin, NPs are classified as (1) natural, (2) incidental or unintentional, and (3) manufactured or engineered NPs (Nowack and Bucheli, 2007; Baalousha and Lead, 2009; Kendall and Holgate, 2012). According to their composition, NPs are categorized as organic (Carbon-containing) and inorganic NPs. Traditionally, NPs exist in the water and soil are referred to as colloids, and in the atmosphere are termed ultrafine particles (UFPs) with a minor difference in size ranges than the BSI definition (1nm - 1μm) (Krüger et al., 2001; Klaine et al., 2008).

Table 2. 1 Classification and some examples of nanoparticle according to their origin (Nowack and Bucheli, 2007; Lead and Smith, 2009)

Origin	Chemistry	Formation	Examples	
Natural	C-containing	Biogenic	Organic colloids	Humic acid
			Organism	Viruses
		Geogenic	Soot	Fullerenes, cristobalite, bismuth oxide
		Atmospheric	Aerosols	Organic acids
		Pyrogenic	Soot	CNT, Fullerenes, Nanoglobules, onion-shape nanosphere
	Inorganic	Biogenic	Oxides	Magnetite
			Metal	Ag, Au
		Geogenic	Oxides	Fe-oxides
			Clays	Allophane
		Atmospheric	Aerosol	Sea salt
Incidental	C-containing	Combustion by-products		CNT, nanoglobules, diesel soot, Ultrafine particulates
		Solvent spray		Solvent mist
	Inorganic			Platinum group metals, Other metals (oxides)
Manufactured	C-containing		Soot	Carbon black, Fullerenes
	Inorganics		Oxides	TiO_2, SiO_2, CeO_2
			Metals	Ag, Au, Fe
			Salts	Metal-phosphates
			Aluminosilicates	Zeolites, clays, ceramics

2.3.1. Natural nanoparticles

Natural NPs have existed as long as the earth's history and are generated by natural processes such as geogenic, biogenic, atmospheric, and pyrogenic origins without any human involvement (Klaine, Alvarez et al., 2008). Some examples of

natural occurring NMs are listed by Handy et al. (2008) and are presented in Table 2. 2. In some cases, the presence of natural NPs in the environment has supported the earth's life such as the iron oxide NPs generated from wind-blow mineral dust, which serves as a micronutrient for phytoplankton in controlling the CO_2 level in the environment (Keller et al., 2010; Prathna et al., 2011). Hygroscopic halide (NaCl) and hydrous sulfate produced from evaporated sea spray act as centres for cloud formation and control the global temperature (Parr et al., 1999). The action of a nanocrystalline vernadite-like mineral (a manganese oxyhydroxide), generated from catalytic oxidation of aqueous manganese on ferrihydrite surfaces, facilitates the mobilisation of heavy metal over hundreds of kilometres in rivers (Cumberland and Lead, 2009). Those findings highlight the occurrence and benefit of naturally occurring NPs.

Table 2. 2 Some examples of natural NPs (Handy et al., 2008)

Location of NPs	Particle types	Authors
Volcanic dust	Bismuth oxide nanoparticles released from volcanic eruptions	(Allen et al., 2008)
	Cristobalite (crystalline silica), extracted from volcanic ash Montserrat eruption causes lung inflammation and lymph node granuloma	(Allen et al., 2009)
Soil	A complex matrix containing mineral particles, colloids in pore water, and concerns about adsorption and binding of pollutants within the matrix	(Klein, 2007)
Ice cores	Carbon nanotubes, carbon fullerenes, and silicon dioxide nanocrystals were found in 10,000 year old ice cores, derived from natural combustion processes	(Cedervall et al., 2007)

2.3.2. Incidental or unintentional NPs

NPs can also be generated unintentionally, mostly as by product of combustion processes (generating carbon particles, diesel soot, etc), solvent spray (generating solvent mist), and foundry works (releasing metal fumes). The

automotive catalytic converters were found to release platinum and rhodium NPs unintentionally with traffic density and driving speed as the factors controlling their concentration level (Levard, Hotze et al., 2012; Lowry et al., 2012).

2.3.3. Engineered or manufactured NPs

Unlike the incidental NPs, engineered NPs (ENPs) are intentionally produced by humans for specific purposes and with particular composition, design, and properties. There are several classes of ENPs and these can be grouped as illustrated in Klaine et al (2008) and presented in Figure 2.2. Even though the abundance of ENPs in the environment is lower than that of the natural occurring NPs, ENPs can be toxic to life forms, and may persist longer in the environment due to the action of capping or fixing agents. They are also produced with specific sizes, shapes and functionality in order to exploit their unique physico-chemical properties. The risk associated with exposure to ENPs in the environment might be more significant than natural NPs and thus become the main focus of current research (Nowack and Bucheli, 2007; Handy, Owen et al., 2008; Handy, Kammer et al., 2008).

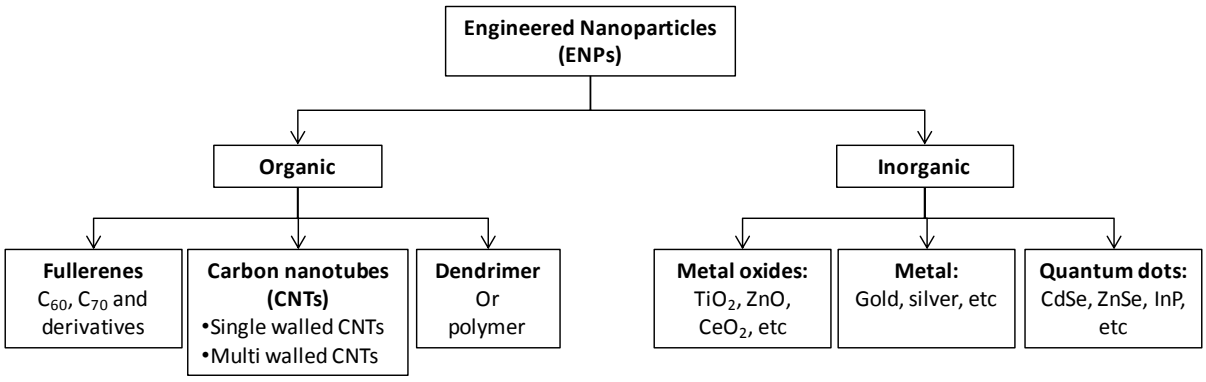

Figure 2. 2 Classification of Engineered Nanoparticles (ENPs)(Ju-Nam and Lead, 2008; Klaine, Alvarez et al., 2008)

2.4. Properties of nanoparticle

Scaling down material dimensions into the nanoscale may alter both physical and chemical properties of materials. The yellow colour of bulk gold material turns into deep-red colour when the gold size approach the nanoscale as has been recorded in the well-known work of Faraday in 1857 (Kelly et al., 2003; Daniel and Astruc, 2004). The absorbance of AuNPs at λ=520nm, generated by the interaction of the collective oscillation of free electrons on the NP surface and its interaction with incoming light termed as Surface Plasmon Resonance (SPR) can be used for AuNPs characterization (Kelly, Coronado et al., 2003; Lee, 2008; Vollath, 2008) and will be further discussed in section 2.7.2.1. Inert gold material turns chemically reactive when it is downsized according to the surprising discovery of Haruta et al. (1989). They observed catalytic reactivity of AuNPs supported on Co_3O_4.Fe_2O_3 for CO and H_2 oxidation, methanol combustion, NO reduction, etc (Haruta et al., 1989; Haruta, 1997; 2004) and the reaction rate depends on AuNPs size (Tsunoyama et al., 2005). Other novel optical, electronic, magnetic and biological properties of NPs have also been revealed (Daniel and Astruc, 2004; El-Sayed, 2004). Therefore size does matter in exploiting unique properties of materials.

There are at least two elementary consequences of reducing the size that drive the appearance of nanoparticles novel properties. They are the high ratio of surface area to volume and the domination of quantum effect (RS, 2004). The following paragraph will discuss the way that those two factors are driving the novel properties of NPs.

2.4.1. Specific surface area (SSA)

All NPs have a remarkably high surface area to volume ratios, for example, a spherical particle with diameter D or radius r will have:

surface area (a) $=\pi D^2$ Equation 2. 1

volume (v) = $\frac{\pi}{6} D^3$ Equation 2. 2

Ratio of surface area to volume Equation 2. 3

(R) = $\frac{\pi D^2}{\frac{\pi}{6} D^3} = \frac{6}{D} = \frac{3}{r}$

Thus the ratio is a function of particle diameter (Figure 2. 3).

(a)

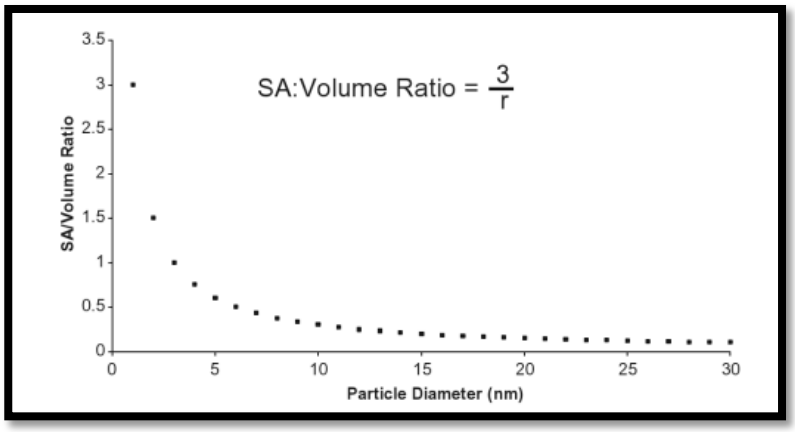

(b)

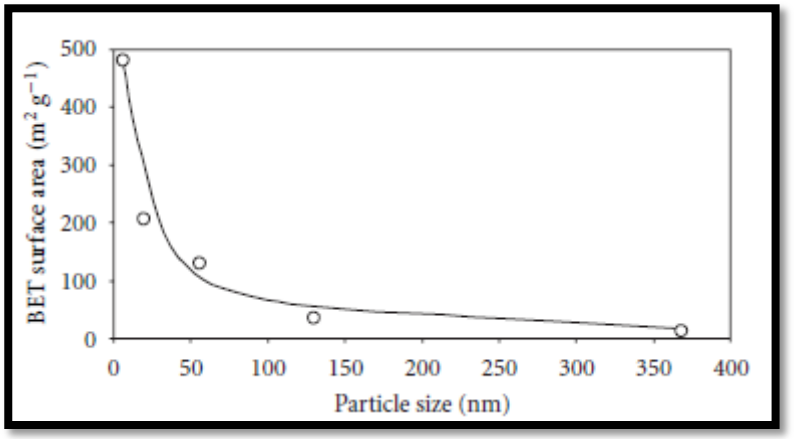

Figure 2. 3 (a) Surface area per volume of NPs as a function of NPs size (Shvedova et al., 2012); (b) Surface area of silica NPs according to particle sizes (Rahman and Padavettan, 2012)

Surface area per mol (A) is presented as:

$$A = Na = \frac{M}{\rho\frac{\pi D^3}{6}}\pi D^2 = \frac{6M}{\rho D}$$ Equation 2. 4

Where N is number of particle per mol, M the molecular weight, and ρ the density of the material (Vollath, 2008).

The greater specific surface area (SSA) of NPs results in the increase of the percentage of atoms available at the NPs surface. Gallium Arsenide (GaAs) NP for instance, has 2.9% of its atom on its surface when the size is 28.3nm and this increases to 51.1% when the size is decreased to 1.13nm (Table 2. 3) (Owens and Poole Jr, 2008). Another example is that 30nm and 3 nm Silica nanoparticles have 5% and 50% of their atoms on the surface respectively (Figure 2.3 (b))(Rahman and Padavettan, 2012).

Table 2. 3 Number of atoms available on the surface of GaAs NPs(Ju-Nam and Lead, 2008)

n	Size (nm)	Total number of atoms	Number of surface atoms	Percentages of atoms on the surface
2	1.13	94	48	51.1
3	1.70	279	108	38.7
4	2.26	620	192	31.0
5	2.83	1165	300	25.8
6	3.39	1962	432	22.0
10	5.65	8630	1200	13.9
15	8.48	2.84×10^4	2700	9.5
25	14.1	1.29×10^5	7500	5.8
50	28.3	1.02×10^6	3.0×10^4	2.9
100	56.5	8.06×10^6	1.2×10^5	1.5

n= unit cells (face centered cubic cell)

The increase of surface area will also increase the surface energy ($u_{surface}$) as presented in equation 2.5 and 2.6 (Vollath, 2008).

$u_{surface} = \gamma a$ Equation 2. 5

$U_{Surface}$ per mol of material = $N\gamma a = \gamma A = \frac{\gamma 6M}{\rho D}$ Equation 2. 6

Equation 2.6 states that the surface energy per mole increase as the particle size decrease, hence for NPs reducing the size of particle will have dramatic effect to the surface energy.

Since NP growth and catalytic reactions occur at the surface of material, the increase of surface energy due to scaling down the size of material will enhance those two processes. The aggregation or growth rate of smaller particles is higher than larger particles as shown by a syudy of hematite (He et al., 2008) where the decrease of surface energy was the driving force for aggregation. Further discussion of aggregation will be presented in section 2.5.2. Catalytic properties of AuNPs as discussed earlier, are imparted by size and surface energy effects (Lopez and Nørskov, 2002; Daniel and Astruc, 2004). Other nanoparticles such as Palladium, ceria and Pt_3Co also showed size-dependent catalytic properties (Zhang et al., 2003; Zhou et al., 2006; Wang et al., 2009).

The increase of surface area in crystalline solids will also enhance the mechanical properties of materials as the greater interface area within the materials is able to arrest the propagation of defects caused by stresses (RS, 2004; Meyers et al., 2006; Casals et al., 2011). For example, the hardness value (H) of nitride compounds such as TiN/NbN and TiN/ZrN film with ~180 layers (monolayer thickness ~ 10nm) is about 70-80 GPa, similar to that of diamond, due to the interface boundaries and lattice mismatch occurrence (Hu et al., 2011). The dependence of hardness to the particle size is found to follow Hall-Petch relationship (equation 2.7)(Meyers, Mishra et al., 2006).

$$H_{(L)} = H_0 + AL^{-0.5}$$ Equation 2. 7

Where $H_{(L)}$: is hardness of NPs size; H_0 is hardness friction stress in the absence of grain boundaries; A is a constant and L is grain size.

Biological activity of NPs was also enhanced by the increase of surface area as the degree of inflammation and generation of Reactive Oxygen Species (ROS) are shown to be surface-area dependence (Duffin et al., 2007; Monteiller et al., 2007; Hussain et al., 2009).

2.4.2. Quantum effect of NPs

The physical and chemical properties of materials are also influenced by the motion of electrons within the materials (El-Sayed, 2004). As the size of the material is reduced, the space for movement of the electrons is confined and the electronic energy levels are not continuous as in the bulk material, but discrete. The typical level spacing is in the order of 2-4 eV, corresponding to excitation by visible or ultraviolet light (Khanna and Castleman, 2003). The energy gap between the valence and conduction bands (Kubo gap, δ) in a small particle is increased by reducing the particle size as presented in Figure 2. 4. The evidence of δ alteration can be obtained by measuring the Fermi energy of the material and substituting this into the Equation 2. 8 (Hu, Peng et al., 2011).

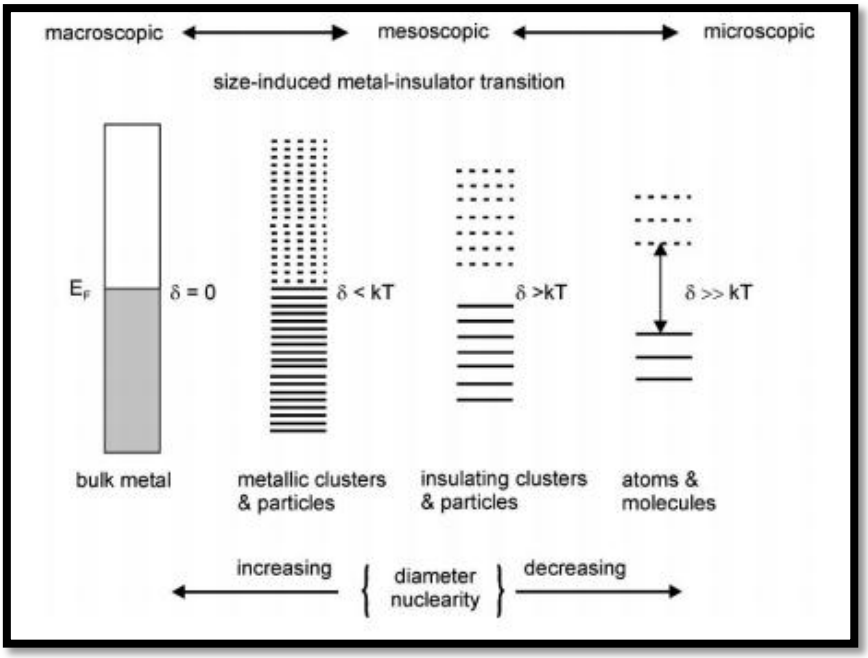

Figure 2. 4 Size dependence of band-gap energy(Taylor et al., 2002)

$$\delta = \frac{4\,E_f}{3n}$$ Equation 2. 8

Where E_f is Fermi energy of bulk material and n is total number of valence electrons.

The increase in band gap energy influences the optical, electrical and magnetic properties of NPs. The appearance of SPR in gold (520nm) and silver (400nm) nanoparticles is one of the optical consequences of the quantum confinement effect. The higher band-gap energy of NPs makes the free electrons in the incompletely filled conduction band attach more loosely to the nucleus and move collectively in discrete waves called 'plasmons' at particular a specific frequency, termed plasmon or resonance frequency (Lee, 2008; Vollath, 2008; Ledwith et al., 2009). When incoming light falls on metal NPs in suspension, the electric field of the light will induce the oscillation of the 'free electron cloud' (Figure 2. 5). The energy of the light at the same frequency as the NPs plasmon or resonance frequency will be absorbed to sustain the free electron oscillation (Novotny and Hecht, 2012). The absorbance at a distinct resonance frequency due to oscillation of the electron cloud, influenced by oscillation of electric field of the incoming light, is called surface plasmon resonance as has been briefly mentioned in early section (SPR)(Burda et al., 2000; Kelly et al., 2002; Wiley et al., 2006; Lee, 2008; Vollath, 2008; Ledwith, Aherne et al., 2009).

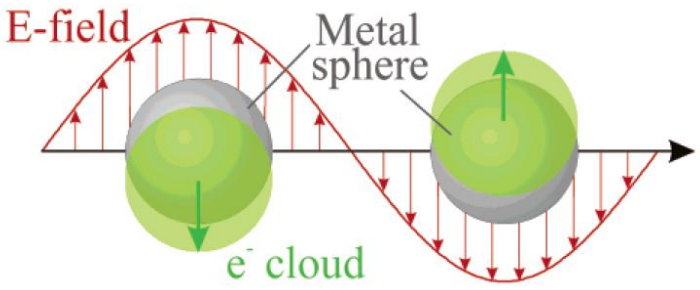

Figure 2. 5 The interaction between electric field oscillation of radiation and free electron oscillation (Kelly, Coronado et al., 2002)

Quantum confinement of nanoparticles also enhances the electrical conduction of NMs (Rao et al., 2002; Mak et al., 2009; Hu, Peng et al., 2011). The mechanism of conduction changes from diffusive to ballistics when the dimension of NPs reach the mean free path length of electrons and the conductance in NMs is no longer influenced the by type and geometry of the materials as in the case for the bulk material (Vollath, 2008).

Conductance of bulk wire $$G = \frac{\sigma L}{A}$$ Equation 2. 9

Conductance of nanowire $$G = \frac{2 m e^2}{h}$$ Equation 2. 10

Where δ is electrical conductivity (material-dependent property), L length of wire, A cross-section, e charge of electron, m active mode in wire and h plank constant.

Another important effect of down-sizing material is the enhancement of paramagnetic and ferromagnetic properties. Superparamagnetism and superferromagnetism of materials has been observed when the size of material is scalled down, such as shown by Ni-NPs embedded in SiO_2 (Fonseca et al., 2002). In fact, diamagnetic material such as gold shows size-dependent ferromagnetic properties (Hori et al., 2004). This enhancement of magnetic properties with decreasing size is due to the presence of single magnetic domains in a small size range of particles and can be exploited for developing highly sensitive sensor devices and high-density data-storage applications (Andrievski, 2009).

2.5. Transformation of NPs

Due to their high surface area, surface energy, and surface atom availability, NPs are very reactive to the immediate environment. Both biotic and abiotic components of the media, and also the ambient atmospheric environment have

shown to influence the stability and behavior of NPs (Elechiguerra et al., 2005; Bone et al., 2012; Unrine et al., 2012) . Stability of NPs in terms of size, shape, dispersion state, chemical composition and speciation stability, and the behavior of NPs such as aggregation and dissolution determine the NPs fate in the environment and the toxic effect following their exposure to organisms (Thomas et al., 1999; Crane, Handy et al., 2008; Handy, Kammer et al., 2008; Hassellov et al., 2008; EU, 2013). Thus understanding the types, rate and the magnitude of NPs transformation, which might be different from the reactivity of the corresponding bulk materials is very important in order to understand the NPs persistency, bioavailability/biouptake, reactivity and toxicity (Lowry, Gregory et al., 2012).

Lowry et al. (2012) categorized the nanomaterials transformation as chemical, physical and biological transformations in the environment. In the following section, those three processes will be discussed.

2.5.1. Chemical transformation

The chemical properties of NPs in the environment can be altered due to oxidation, reduction, dissolution, sulfidation, photo-reactivity, adsorption, etc. Even though the rate of reaction is largely unknown, but the occurrence of chemical transformation has been presented in number of studies. The release of ions such as Ag^{+} from Ag^{0} (Figure 2. 6 (a)) (Kittler et al., 2010; Liu and Hurt, 2010), Zn^{2+} from ZnO NPs and Cd^{2+} from TOPO-capped CdSe quantum dots (Figure 2. 6 (b)) due to oxidation was presented in various studies and rendered the material toxic to organisms (Franklin et al., 2007; Navarro et al., 2008; Kittler, Greulich et al., 2010; Yang et al., 2011). Oxidising environments such as natural water, atmospheric

conditions and aerated soil might induce the oxidation process, but carbon-rich sediments and stagnant water result in NPs reduction (Lowry, Gregory et al., 2012).

Photo-oxidation was also found to chemically transform the NPs. C_{60} for instance, in the form of a C_{60} monolayer on TiO_2 particles showed photo-oxidation (laser photolysis) and fullerene epoxides were generated (Kamat et al., 1997). Functionalized single-walled carbon nanotubes (SWCNs) in oxic conditions became chemically reactive to solar light and generated reactive-oxygen-species (ROS) such as singlet oxygen ($^1O_2$), superoxide anion ($O_2^{\cdot -}$) and hydroxyl radical ($^{\cdot}OH$) due to surface defects caused by functionalization (Chen and Jafvert, 2011) (Figure 2. 6 (c)).

The oxidation-reduction process was found to be very dynamic in NPs bound to surfaces. In the vicinity of humidity and light, the surface-bound 75 nm PVP-capped AgNPs were oxidized. Silver ions were released, confined by and reduced within the adsorbed water layer on the NPs surface under environmental conditions. Smaller particles were formed by the parent particles. The formation of incidental small particles were also found to form spontaneously from non-nanoscale silver and Cu surfaces such as utensils, jewelry, etc. due to chemical or photo-oxidation (Glover et al., 2011).

(a)	$4Ag^0 + O_2 \rightarrow 2Ag_2O$ $2Ag_2O + 4H+ \rightarrow 4Ag^+ + 2H_2O$
(b)	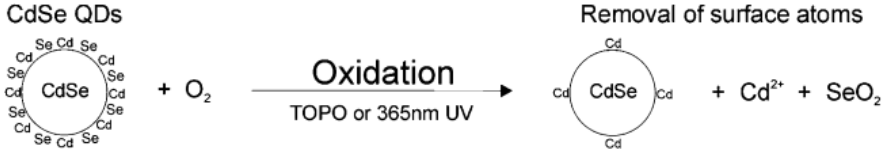 TOPO: tri-n-octylphosphine oxide

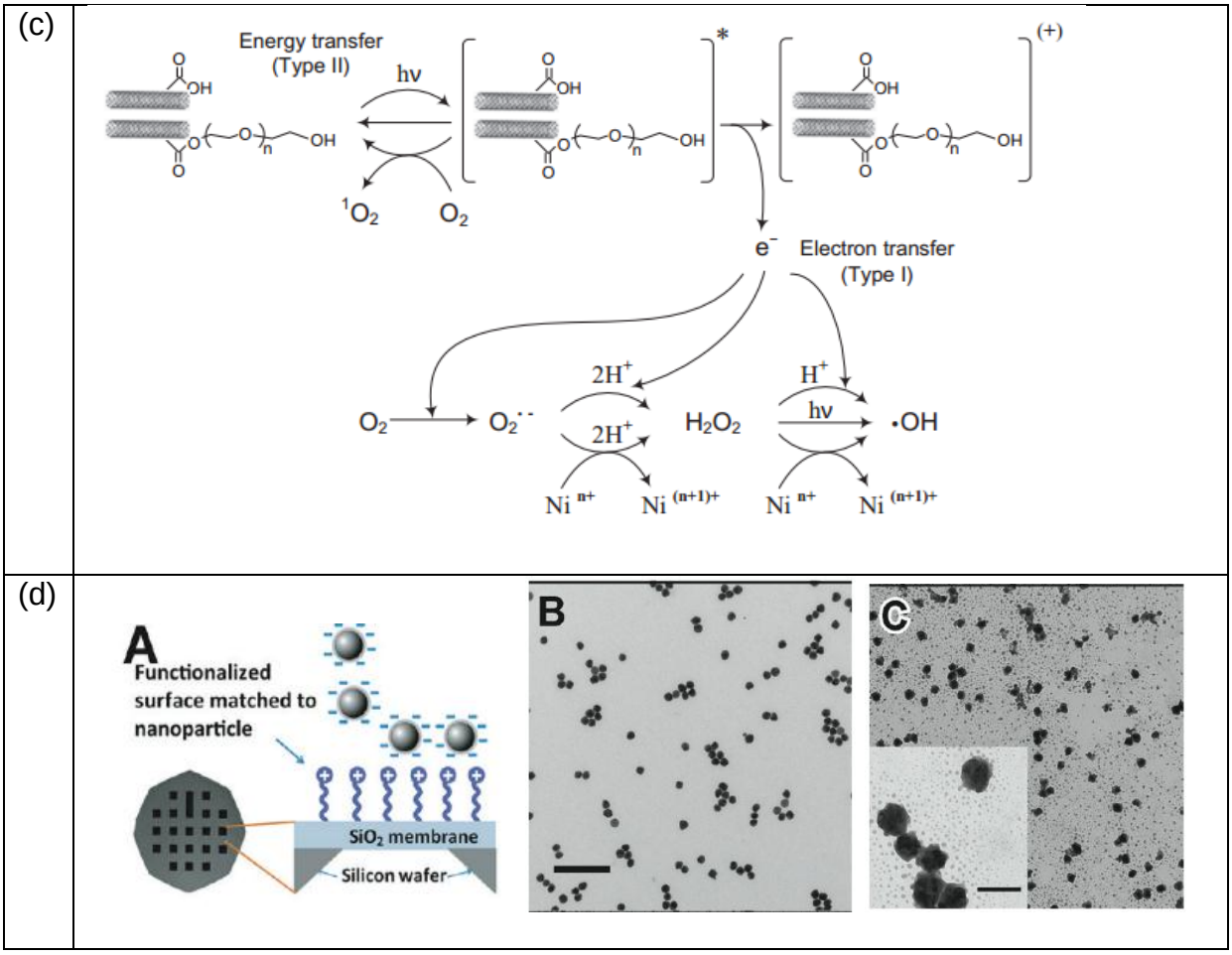

Figure 2. 6 Some examples of NPs chemical transformation: (a) AgNPs dissolution due to oxidation (Liu and Hurt, 2010); (b) Cd^{2+} dissolution from CdSe quantum dot (Derfus et al., 2003); (c) ROS production of SWCNTs photoreduction(Chen and Jafvert, 2011). (d) dynamic redox reaction of AgNPs.

Sulfidation is another reaction that chemically transforms the NPs. Ag_2S (acanthite) bridges were formed following Na_2S solution addition to PVP-capped AgNPs suspension. Chain-like structure appeared and limited the dissolution and reduced the toxicity of AgNPs (Levard et al., 2011). PVP-capped nanowaire was found to be corroded by H_2S and carbonyl sulfide (OCS), the principal corrodents of silver with the action of water. H_2S was generated from OCS when in contact with water according to Equation 2.11 and subsequently corroded the Ag-NPs and Ag-nanowire (Equation 2. 12) (Elechiguerra, Larios-Lopez et al., 2005). The O_2 and NO_2 content in the air enhanced the corrosion reaction; as presented in equation 2.13 and 2.14.

$OCS + H_2O \rightarrow H_2S + CO_2$ Equation 2. 11

$H_2S + 2Ag \rightarrow Ag_2S + H_2$ Equation 2. 12

$2Ag + H_2S + ½\ O_2 \rightarrow Ag_2S + H_2O$ Equation 2. 13

$2Ag + H_2S + NO_2 \rightarrow Ag_2S + 2HNO_2$ Equation 2. 14

Apparently, sulfidation was not only enhanced in aerobic condition. In anaerobic condition with high content of sulfide, sulfidation of AgNPs was discovered e.g. in final stage sewage sludge materials in one of metropolitan waste water treatment plant (Kim et al., 2010). Kaegi et al. (2013) also found that the spiked NPs into the trunk sewer turned into their sulphide compound irrespective of NPs type (Ag or Au), size (10 and 100nm) and coating agent (citrate and PVP). The biofilm within the sewer pipe controlled the extent of sulfidation (Kaegi et al., 2013) yet, in the incinerator, the Ag_2S was reconverted to Ag (Impellitteri et al., 2013).

Adsorption of organic and inorganic ligands on NPs surfaces is another reaction that can cause chemical transformation of NPs. Even though a variety of organic polymers can improve the stability of NP dispersions (e.g. Citrate, PVP, SDS, PEG, Fulvic and humic acid) the interaction of some polymers, such as thiolated PEG with NPs was also found to increase the dissolution of AgNPs (Li et al., 2010; Zook et al., 2011), and the surface charge alteration (El Badawy et al., 2010). Other polymers, such as PVP, yet preserved AgNPs from dissolving (Ho et al., 2010). It has also been reported that the polymer concentration could control the extent of transformation (Li, Lenhart et al., 2010; Miao et al., 2010). Anionic ligands, such as Cl^- together with SDS were found to control the dissolution of AgNPs and induce shape transformation in oxic-conditions (Yang et al., 2007).

It was also found that the dissolution was also exagerated by chloride content in a media. The influence of chloride content was even more significant than the effect

of media's ionic strength (Chambers et al., 2014). Chloride ions acted catalytically in the dissolution of AgNPs (Mulvaney et al., 1991; Kapoor, 1998) and subsequently chemically reacts with the generated silver ion to form silver chloride bridge between AgNPs, indicated by d_H size incease of AgNPs suspension (Chambers, Afrooz et al., 2014).

2.5.2. Physical transformation or aggregation

NPs in suspension are kinetically stable (i.e. over long time scales) but thermodynamically unstable as the NPs collide due to three fundamental processes (Handy, von der Kammer et al., 2008):

1. Brownian motions of particles, that can lead to perikinetic aggregation
2. Particles traveling at different velocities in a shear flow, that can lead to orthokinetic aggregation (shear aggregation)
3. Differential settling of particles with different sizes.

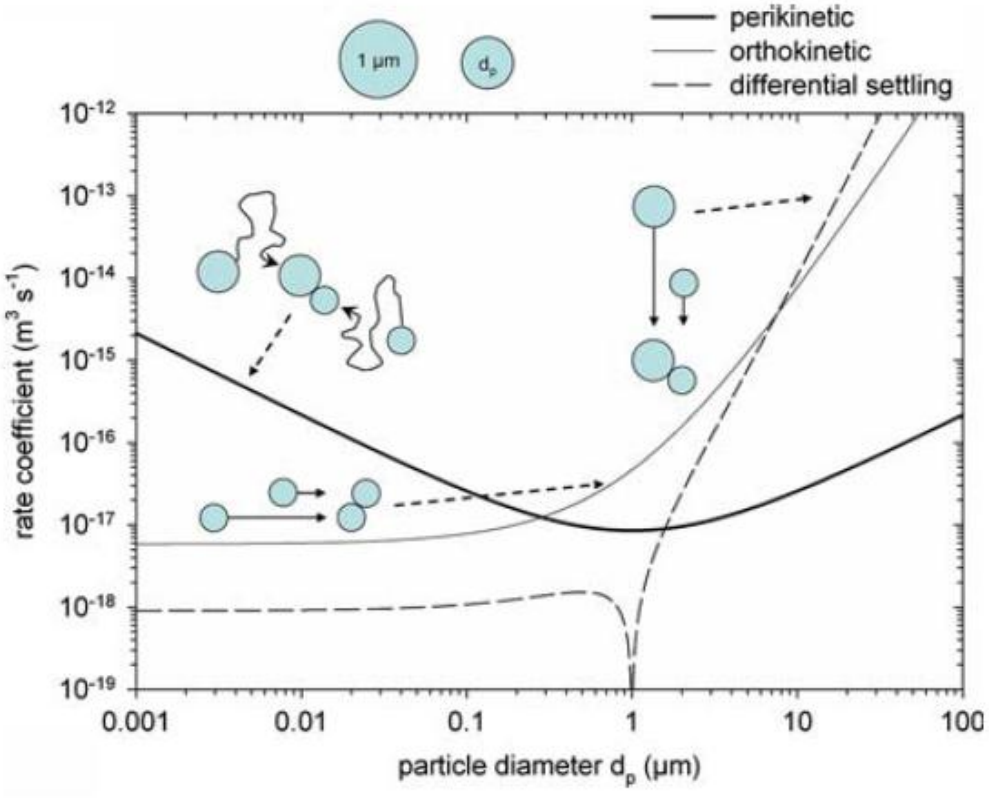

Figure 2. 7 Three collision mechanism and aggregation rate coefficient of 1 µm particles, with diameter d_p, temperature 12^0C, particle density 2.6 g mL^{-1} and share rate 35 s^{-1}. The figure represents domination of perikinetik aggregation in smaller particle sizes and ortokinetic aggregation for particle larger than 1 µm (Handy, von der Kammer et al., 2008)

Elimelech and O'melia (1990) have shown that collision efficiency (α) or sticking probability represents the fraction of collisions that are successful in making an attachment, and is presented as:

$$\alpha = \frac{\eta}{\eta_0} \qquad \text{Equation 2. 15}$$

Where η is the actual dimensionless deposition rate of particles and η_0 is the dimensionless deposition rate under barrier-less interaction(Elimelech and O'Melia, 1990).

In a stable dispersion, the collision efficiency is < 1 and the collisions do not stick the particles together. According to Derjaguin-Landau and Verwey-Overbeek (DLVO) theory of colloid stability, the stabilization originates from forces between

particles and they affect each other via attractive and repulsion forces acting on the particles on different length scale (equation 2.16).

$V_T = V_A + V_R + V_S$ Equation 2. 16

where V_T= total potential energy; V_A = attractive force between particles (Van der waals interaction); V_R= repulsive force between particles (due to the electric double layer or capping action) and V_S= interaction with solvent. As the V_S relatively small compared with V_S and V_R, the stability of the NP suspension is usually presented as $V_T = V_A+V_R$ where:

$$V_A = \frac{-A}{12\,\pi\,D^2}$$ Equation 2. 17

where A is Hamaker constant and D is particle separation

$$V_R = 2\,\pi\,\varepsilon\,a\,\xi^2\exp(-kD)$$ Equation 2. 18

where a is particle radius, π: solvent permeability, k: function of ionic composition

And ξ : zeta potential

Since zeta potential, a potential at the slipping plane or shear plane of the particles is a measurable parameter, it is commonly used as a measure of NP stability and the potential must be at least 30 mili-volt (mV) to ensure the NP suspension stability (Riddick, 1968). If the attraction force outweighs the repulsion force, according to DLVO, the particles will attach to each other and physical transformation occurs.

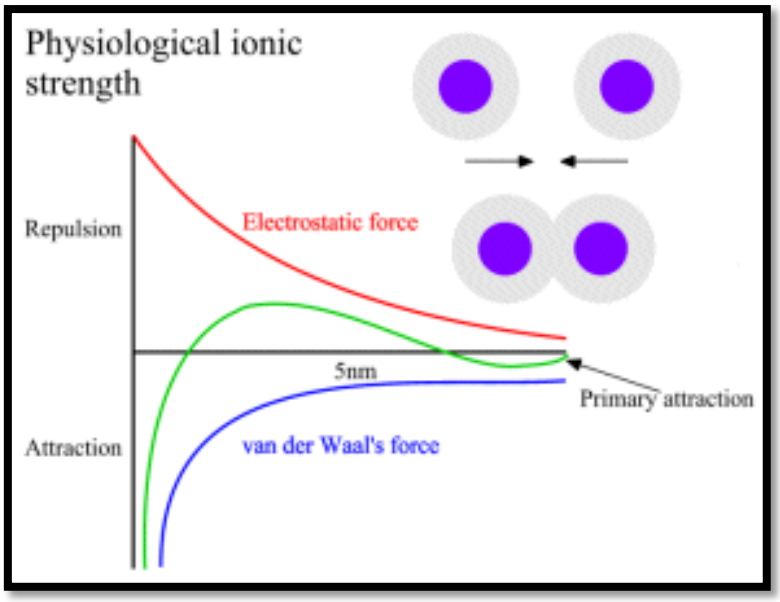

Figure 2. 8 Schematic diagram of the variation of free energy with particle separation according to DLVO theory. The net energy is given by the sum of the double layer repulsion and the van der Waals attractive forces that the particles experience as they approach one another (downloaded from http://www.ncl.ac.uk/dental/oralbiol/oralenv/tutorials/electrostatic.htm on 21st august 2014)

Formation of aggregates and agglomerates due to the imbalance of repulsion and attraction forces is one of the physical transformation of particles. ISO TS 27687:2008 differentiate between the definition of aggregates and agglomerates. An aggregate is defined as a particle comprising of strongly bound or fused particles where the resulting external surface area may be significantly smaller than the sum of calculated surface area of the individual components; while agglomerate refers to a collection of weakly bound particles or aggregates, or a mixture of the two in which the resulting external surface area is similar to the sum of the surface areas of individual components (Reidy et al., 2013). The difference between aggregates and agglomerates is presented in Figure 2. 9, however in some of the literature the aggregation and agglomeration are used interchangeably. Thus, the measurement of the change of the hydrodynamic size, zeta potential and surface area of particles can be used to evaluate the aggregation and stability properties of NPs.

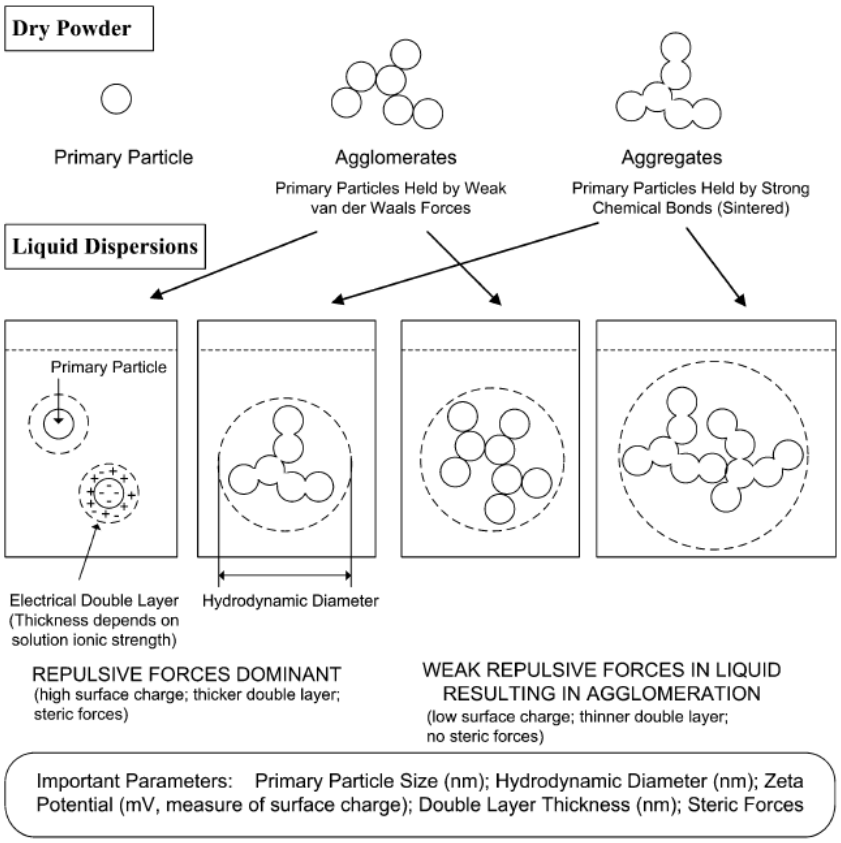

Figure 2. 9 Dispersion state of nanoparticles and the forces acting on each state(Baun et al., 2008)

There are two types of aggregation: heteroaggregation (particles attaching to other particle types) and homoaggregation (the same type of particles aggregating together). In the environment, attachment of particles to suspended solid (SS), organism and surfaces are examples of heteroaggregation, and the attachment of the same particles is homoaggregation (Handy, Kammer et al., 2008). In (eco)toxicology studies aggregation was found to reduce the toxic effect of NPs (Rehn et al., 2003; Panáček et al., 2006; Kvitek et al., 2008), although aggregation does not always reduce the bioavailability of NPs (Handy, Kammer et al., 2008; Tourinho et al., 2012). Although stabilizing NPs is commonly implemented to maintain the availability and dispersibility of NPs in (eco)toxicology studies, it has been suggested that aggregation need not be prevented in (eco)toxicology study

because it will occur during NPs exposure in the environment (Baun, Hartmann et al., 2008).

Providing a barrier to the close approach of two particles, either by addition of charged material (to generate an electrostatic double layer (EDL) surrounding the particles) or polymer and surfactants (tethering a relatively long molecules on the particle surface) have been widely implemented to improve the stability of NPs (Figure 2.10). While steric stabilization is relatively insensitive to the ionic content of the media, the thickness of the EDL layer of electrostatically-capped NPs will be influenced by the media ionic content (Debye- Hückel approximation).

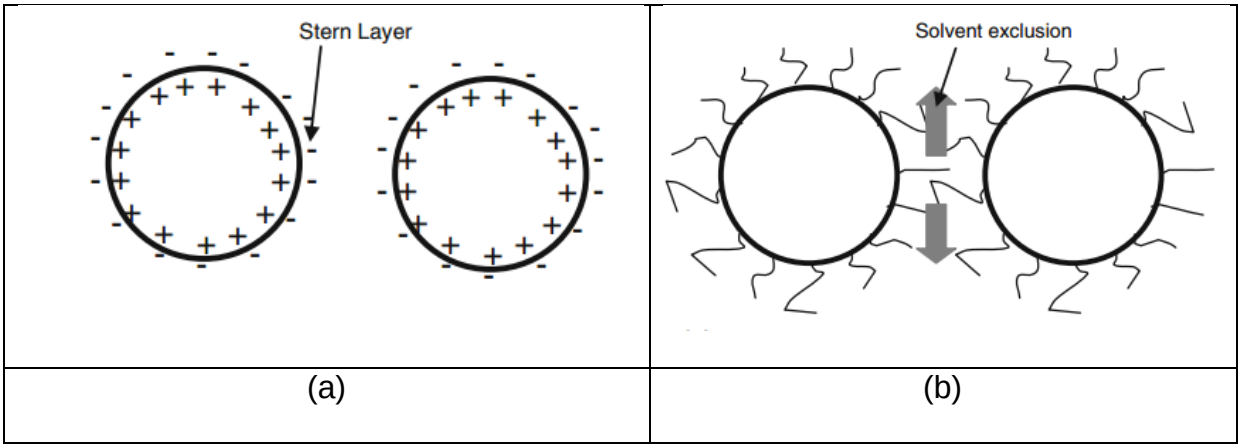

Figure 2. 10 Stabilization of NPs: (a) electrostatic, and (b) steric stabilization(Christian et al., 2008)

According to the Debye-Hückel approximation, the thickness of EDL (by the size of $1/\kappa$) depends on the temperature and the bulk electrolyte concentration as presented in (Equation 6. 2)(Hunter, 1986) :

$$K = \sqrt{\frac{2000\,F^2}{\varepsilon_0 \varepsilon_r RT}} \times \sqrt{I} \ \text{(meter)}^{-1} \qquad \text{Equation 2. 19}$$

where K is Debye-Hückel parameter, ***F*** is Faraday's constant (96,485 C.mol^{-1}), ***I*** is ionic strength, $\boldsymbol{\varepsilon_0}$ is permittivity of a vacuum (8.85 x 10^{-12} farad.m^{-1}), $\boldsymbol{\varepsilon_r}$ is dielectric constant of solution, ***R*** is gas constant (8.31 J.K^{-1}.mol^{-1}) and ***T*** is temperature (K). At

25^0C in water (ε_r at 25^0C = 78.57), than the $K = 3.288\sqrt{I}$ (nm^{-1}), shows that the EDL ($\sim 1/\kappa$) is only influenced by media's ionic strength where

$$\boldsymbol{I} = \frac{1}{2}\sum c_i z_i^2 \qquad \text{Equation 2. 20}$$

where c_i is ionic concentration and z_i is the ionic charge.

Therefore the stability of EDL-coated NPs is partly influenced by the ionic strength (Cumberland and Lead, 2009; French et al., 2009; Badawy et al., 2010).

Other factors both biotic (plant, animal, exudates, etc) and abiotic (pH, light) have also been shown to influence stability of NPs and cause aggregation/disaggregation. The release of dissolved organic material (DOM) from plants in a microcosm stabilized PVP-capped AgNPs while in a microcosm without plants the AgNPs aggregated. However DOM was found to oxidize and dissolve Gum arrabic (GA)-capped AgNPs (Unrine, Colman et al., 2012). Algal exopolymeric exudates (EPS=exo-polyssacharide) were found to bind the TiO_2 and reduce the particles bioavailability and toxicity (Hartmann et al., 2010; Dalai et al., 2013).

Irradiation of artificial light and sunlight induced fragmentation of NPs, which was subsequently followed by fusion of particles to form agglomerates as was presented by Cheng et al (2011). Both PVP- and gum Arabic-capped AgNPs have been physically transformed by formation of larger particles due to irradiation. Alteration of the available surface area and the morphology of AgNPs (as indicated by loss of SPR and larger particle size by TEM) after 4 days of sunlight exposure has been shown to reduce the toxicity of NPs (Cheng et al., 2011; Li et al., 2011).

Re-precipitation and shape transformation following NP dissolution has been observed as another type of physical transformation (Yang, Zhang et al., 2007; An et al., 2008). Yang et al. (2007) showed the formation of triangular plate AgNPs due to

the O_2/Cl^- corrosion effect to nano spherical SDS-capped AgNPs. An et al. (2008) found that Cl^- etched the triangular NPs and formed discal AgNPs. These shape transformations might alter the toxicity of AgNPs since shape has been found to influence the NPs toxicity (Handy, Kammer et al., 2008).

2.5.3. Biological transformation

Physical and chemical reactions between the NPs surface and biological components (protein, membrane, phospholipid, DNA, organelles, etc) have been presented in various studies of the bio-nano interface. This interaction will not only change the physico-chemical properties of NPs but also the properties of the biological materials. Novel cryptic peptide epitopes, for instance, were released from the protein in contact with NPs and this caused a change the protein function to some extent (Cedervall, Lynch et al., 2007; Klein, 2007). Formation of soft and hard coronas on NPs surfaces, resulted from competitive absorption of proteins onto the NPs surface, and was found to decrease the reactive oxygen production and lesser its toxic effect (Casals, Pfaller et al., 2011).

NPs degradation within the biological environment is another important transformation that needs to be considered. Graphene oxide and CNTs toxicity was found to be mitigated by fetal bouvine serum (FBS) and horseradish peroxidase (HRP) enzyme respectively showing the potential degradation of NPs in biological environments (Allen, Kichambare et al., 2008; Allen, Kotchey et al., 2009; Hu, Peng et al., 2011). However current knowledge of NPs biotransformation within biological system leaves many questions that need to be addressed (Treuel and Nienhaus, 2012).

Due to active transformation of NPs in the environment, full characterization of NPs in ecotoxicology studies needs to be performed for both the pristine NPs and after exposure to the media used in the studies.

2.6. Synthesis method of nanoparticles

Due to the observation of NPs's novel properties and their promising application in many sectors, numerous synthesis protocols have been examined extensively and can be grouped into top-down and bottom-up methods as illustrated in Figure 2. 11 (RS, 2004; Wang and Xia, 2004; Ju-Nam and Lead, 2008; Christian, 2009). The former method produces NPs from their bulk material. By implementing physical processes such as grinding and milling (Tsuzuki and McCormick, 2004), laser ablation (Mafune et al., 2000; Dolgaev et al., 2002), DC arc thermal (Shinde et al., 2009), etc, macro scale materials are mechanically broken-down into nanosize particles. Nanoscale patterned material can also be produced using some of these methods, and this type of material can be further used as a mold for NPs large scale production (Christian, 2009).

On the other hand, bottom-up methods produce NPs from very small building blocks of material such as ion, atoms and molecules by implementing wet chemical, self-assembly and positional assembly processes (RS, 2004). Through reduction, nucleation and growth process, the ions can be built-up into a more complex clusters of NPs, by wet chemical methods (Powers et al., 2006; Ju-Nam and Lead, 2008; Lee, 2008).

Top-down methods have been known as versatile strategies for producing NPs in industrial scale (Skandan and Singhal, 2006). Nonetheless, they are less favored by the scientific community. Physically breaking-up bulk materials into smaller nano-

size particles makes controlling the size, shape and purity of the NPs difficult (Skandan and Singhal, 2006; Klaine, Alvarez et al., 2008). Moreover, those processes require expensive and complex instrumentation.

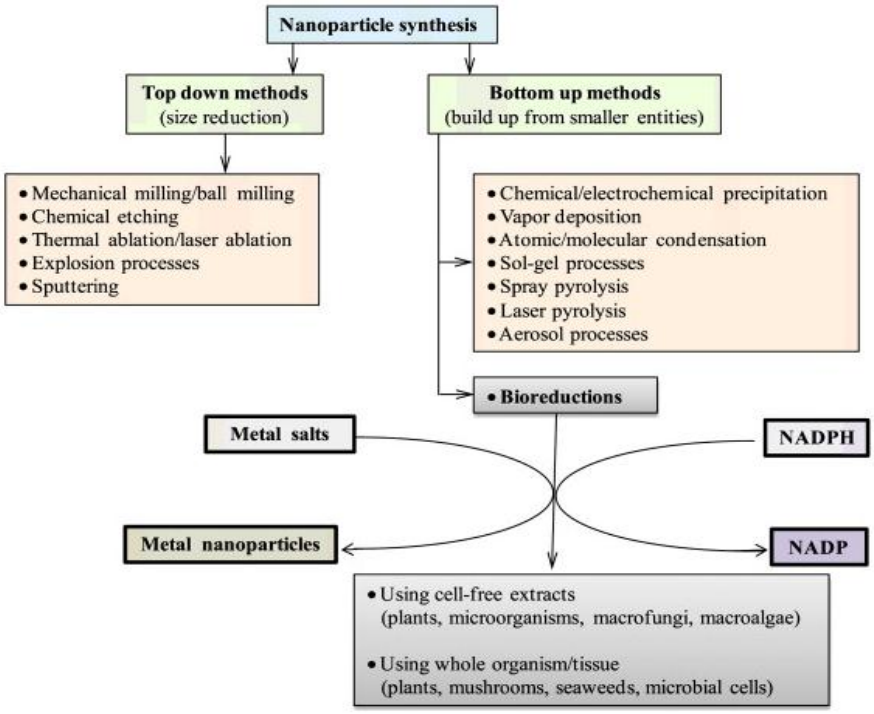

Figure 2. 11 Top-down and bottom-up methods (Powers, Brown et al., 2006).

Conversely, bottom-up methods offer some advantages. Mostly they can be adjusted relatively easily to generate monodisperse particles with controllable shape and size as well as creating functionality by encapsulating NPs (Lin and Samia, 2006; Ledwith et al., 2009). Moreover these methods can offer straightforward routes with lower production costs (Brust and Kiely, 2002). Thus, bottom-up or scale-up strategies have been preferred experimentally and have been developed intensively. Bottom-up method will be discussed in further detail in the following section.

2.7. Characterization of nanoparticles

Determination of the NP's physico-chemical properties is an important step in nanotechnology and nanoscience in order to elucidate the NP's homogeneity,

stability, reactivity, behavior and bioavailability (Lajunen and Perämäki, 2004; Ju-Nam and Lead, 2008). Characterization is also critical in understanding the dose in eco(toxicology) studies as the traditional definition of dose, the mass concentration, may not be the critical factor controlling the observed toxic outcome (Oberdörster, Ferin et al., 1994; Oberdörster et al., 2005). Number of studies suggested that number concentration (Barillet et al., 2010), size (Verwey et al., 1999; Baalousha and Lead, 2007; Baalousha et al., 2011), shape, surface area, surface functionality are the main determinants that control the toxic outcome (Barillet, Simon-Deckers et al., 2010). Incomplete presentation of characterisation data, thus makes the interpretation of dose-response association challenging (Hansen et al., 2007). As there is no single ideal characterization techniques (Domingos, Baalousha et al., 2009) and unconfirmed of which characteristics corresponds to their toxic outcome, multi technique analysis need to be performed (Hassellöv et al., 2008; Warheit, 2008; Silva and Unali, 2011).

Attempts have been made to prioritize the essential NP's characteristics that need to be performed in (eco)toxicology study (Handy, von der Kammer et al., 2008; Tantra et al., 2011; Pettitt and Lead, 2013). Following paragraphs will discuss some essential characteristics of NP and methods available for characterization purposes.

2.7.1. Size

Particle diameter is the most commonly used metric for presenting NP size. However, since NP shape is not always spherical, other size measures equivalent to spherical have been widely used (Hassellov et al., 2007). For example, hydrodynamic diameter, projected area, equivalent molar mass, etc have been commonly used for presenting NPs size. In the following section, number of method for size measurement will be discussed.

2.7.1.1 Dynamic Light Scattering

Dynamic light scattering (DLS) also known as photon correlation spectroscopy (PCS) has been widely used for nanoparticle characterization. The short duration of measurement, simple operation of the instrument and minimum perturbation of the sample are some benefits of DLS, although the presence of large aggregates might overestimate the result (Sartor; Thomas, 1987). DLS measure the diffusion coefficient (D) of the NPs suspension which then converted to obtain NPs hydrodynamic diameter ($\boldsymbol{d_H}$) size by implementing the Stokes-Einstein relationship (Equation 2. 21).

$$D = \frac{K_B T}{6\pi\eta d_H}$$ Equation 2. 21

where $\boldsymbol{k_B}$ is Boltzmann's constant (1.38 x 10^{-23} J.molecule^{-1}.K^{-1}); $\boldsymbol{T}$ is absolute temperature (K) and $\boldsymbol{\eta}$ is the viscosity of the solvent. d_H is a measure of particle size including the electric double layer or steric capping agent thickness surrounding the particles (Figure 2. 12).

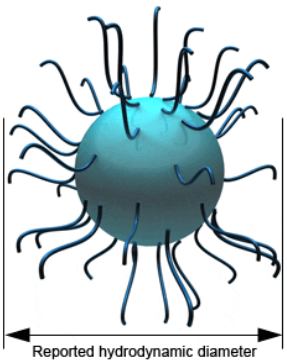

Figure 2. 12 Hydrodynamic size of a steric capped particle (downloaded from http://www.malverninstruments.fr/labfre/technology/dynamic_light_scattering/dynamic_light_scattering.htm)

2.7.1.2 Flow-Field Flow Fractionation

Field-flow fractionation (FFF) is an elution technique, developed for the first time in the 1960s by the work of J. Calvin Giddings and co-workers. Although FFF is a relatively new technique, it has been widely used for environmental studies (colloids and macromolecules) (Baalousha and Lead, 2007; Alasonati et al., 2010; Stolpe et al., 2010) as well as NP separation and characterization (Baalousha et al., 2011; Poda et al., 2011; Gigault et al., 2012). The FFF ability in separating species in greater size ranges (10^{-3} to 10^{2} μm); can be coupled with other instrumentations for physical and chemical characterization; fast separation; ready fraction collection for further analysis; and gentleness in separating delicate species (Giddings, 1993; Hassellov et al., 2007) are some benefits offered by Fl-FFF. NPs-membrane interaction, however makes the attempt of finding a perfect flow rate for the instrument is difficult.

FFF utilizes the nature of viscous flow in ribbon-like (narrow) channel for separation (Figure 2. 13) (Williams et al., 1996; Hassellov, von der Kammer et al., 2007). The laminar flow of the suspension in the channel retards the motion of particle close to the wall relative to the particle in the flow section further away from the wall. By employing an external field perpendicular to the channel flow, the particles are pushed down to the accumulation wall. Particles with higher diffusivity (smaller particle) will diffuse back to the channel due to concentration gradient, entering the least retarded area of the laminar flow, so the particles are selectively separated. The magnitude and type of the field, channel dimensions, interaction between particles and the field, particle-solvent diffusion coefficient, are factors governing the particle elution rate in the FFF (Williams, Moon et al., 1996).

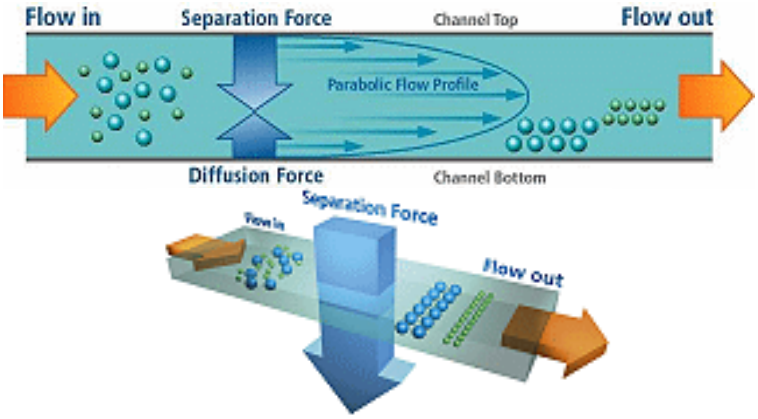

Figure 2. 13 Fractionation of NPs sample with two size distributions by as-Fl-FFF (downloaded from http://www.field-flow-fractionation.com/field-flow-fractionation.htm on the 7th August 2013)

2.7.1.3 Transmission Electron Microscopy

In NPs characterization, TEM has been widely used for imaging purposes (aimed for visualization of the synthesized NPs and NPs interaction with organism), size and shape characterization, etc (Hassellöv, Readman et al., 2008; Fabrega et al., 2009; Fabrega et al., 2011; MacCuspie et al., 2011; Silva et al., 2011). Another important application of TEM is single particle elemental analysis of an object whenever the TEM is complimented by spectroscopy detector/s (Kim, Park et al., 2010).

In general, the TEM consists of electron gun, series of focusing and magnifying lenses, sample stage and fluorescence screen or monitor for visualization (Figure 2. 14). A hot filament of Tungsten (T 2500-3000 K) and Lanthanum hexaborides (LaB_6, T 1400-2000 K) are some examples of electron gun, with accelerated voltage 30 kV-1,000kV or more. An ultra high vacuum needs to be applied to the interior of TEM to avoid the collision of electron with molecules within the air. The condensing coil(s) focus the electron beam on a small area of specimen (2-3 μm) placed in the specimen stage.

Sufficient contrast, a relative difference in intensity between an object and background is necessary to generate an image. Contrast of an image is determined by the nature of the samples and the interaction between the sample and the electron . The high density and thin sample (<100nm) will scatter the electron and creates low intensity, but the lesser density (i.e. background) area of the sample will creates a higher intensity so the contrast is produced. However, for thicker sample, contribution of electron absorption and multiple scattering will interfere the contrast generation Thus preparing a very thin sample is very important in EM.

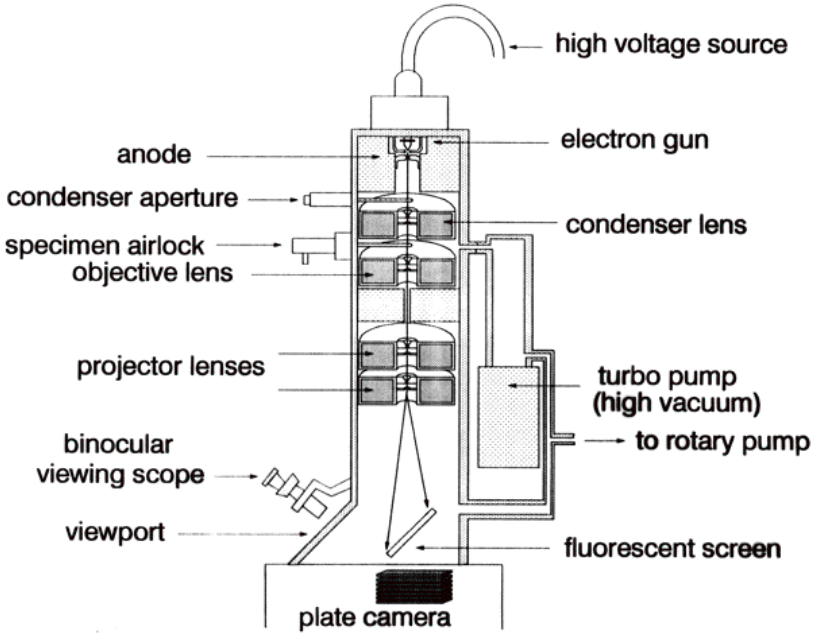

Figure 2. 14 The layout of TEM instrument (downloaded from http://www.udel.edu/biology/Wags/histopage/illuspage/lec1/mIcroscopyppt.htm)

The TEM images can be further analyzed for measuring the size, quantifying shape factor of NPs, etc by using a software (i.e Gatan Digital Micrograph and ImageJ). For shape analysis, equation 2.22 is applied (Wilkinson and Lead, 2007) and the SF value of different shapes of particles is presented in Figure 2.15.

$$SF = \frac{4\pi\ x\ area}{perimeter^2}$$ Equation 2. 22

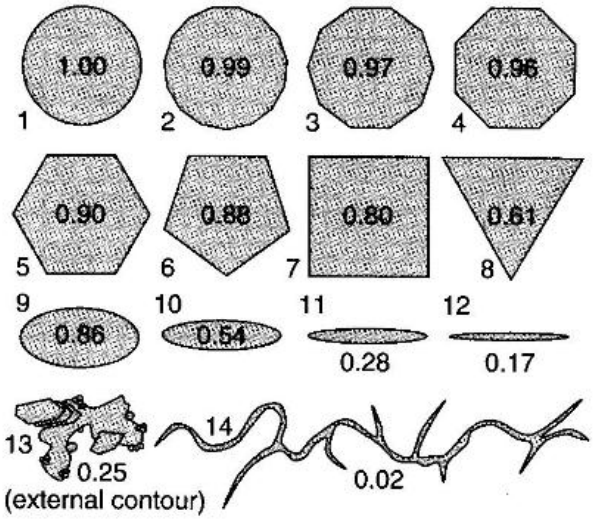

Figure 2. 15 Variation of shape factors value (Wilkinson and Lead, 2007)

2.7.1.4. Atomic Force Microscopy (AFM)

Atomic force microscopy (AFM) is one variety of scanning probe microscopy (SPM) technique widely used for surface analysis of material. The interaction forces between the atom at the end of a sharp tip attached to a cantilever-type spring, and the atom on the scanned surface is sensed by a cantilever spring, the most critical component of AFM (Binnig et al., 1986; Binnig et al., 1987; Balnois et al., 2007). According to Hooke's Law, interaction force is influenced by spring constant (c) and spring deflection (***Δz)*** (equation 3.30)

$$F = c.\Delta z$$ Equation 2. 23

where ***c*** is spring constant and ***Δz*** is the spring deflection. The spring has to be soft enough to maximize the deflection and stiff at the same time to minimize the influence from background vibration noises (Binnig, Quate et al., 1986).

According to the interaction force being measured, there are two types of interaction forces utilized in AFM: short range interaction (repulsive force) and long-range interaction forces (attractive force) (Rugar and Hansma, 1990). For short range forces measurement, the tip remains in contact with the sample surface during measurement and then known as Contact mode AFM (C-AFM) or repulsive mode AFM. However, long-range forces measurement is done by slightly moving the tip away from the sample at around 10-100nm and known as non-contact AFM or NC-AFM (Jalili and Laxminarayana, 2004; Eaton and West, 2010). Since the attractive force between the tip and the sample is weaker than repulsive force, a small oscillation or vibration is given to the cantilever (dynamic cantilever mode) in NC-AFM mode so the cantilever will be much more sensitive to the small forces(Jalili and Laxminarayana, 2004).

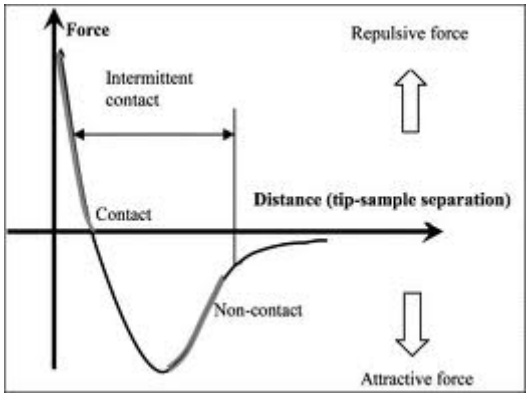

Figure 2. 16 Force- displacement curve (Jalili and Laxminarayana, 2004)

In nanoscience and nanotechnology, AFM has been mainly used for the surface characterization of materials, as well as size and shape characterization of nanoparticles deposited onto a flat surface (Schmitt et al., 1997; Chi and Rothig, 2000). It has also been used for material manipulation (Baur et al., 1998; Resch et al., 2000; Liu et al., 2006). Recently AFM has also been used for dissolution study of particles on the surface by monitoring the shape and size changes of particles

attached to a surface (Kent and Vikesland, 2011). Due to the ability of AFM to analyse many different materials, it has extremely rapidly been developed and commercialized. AFM provides topography image and height size of NPs adsorbed on a surface, and aggregation state of the samples, however it has poor lateral accuracy and need a high skill for operating the instrument.

2.7.2. Elemental analysis

There are two methods available for analyzing the elemental composition of NP sample, bulk sample analysis by UV-Vis spectrometry and single NP analysis by Energy Dispersive X-Ray Spectroscopy (EDX).

2.7.2.1. UV-Vis spectroscopy

Some metals show unique optical properties by absorbing a characteristics wavelength at visible region which is not exhibited by their corresponding bulk metal material. Noble metal such as silver and gold for example, absorb wavelength at 400nm and 520nm respectively, manifested as yellow and red color separately as has been recognized since 17^{th} century by working of Faraday(Faraday, 1857). The origin of the unique optical properties of metal NPs is due to surface plasmon resonance (SPR) of NPs as has been discussed in section 2.4.2.

Theoretical approaches and experimental results have shown that the SPR of NPs is influenced by many factors such as size, size distribution and shape of NPs, and the dielectric constant at the NP surface (Slistan-Grijalva et al., 2005; MacCuspie, 2011). If the size of NPs increase, the band-gap energy between conduction and valence band decrease and as consequence the SPR will be red shifted (Slistan-Grijalva, Herrera-Urbina et al., 2005; Smitha et al., 2008) (Equation

2. 24). The width of SPR peak, termed as full width half maximum (FWHM), broader in larger and more polydisperse NPs suspension (Slistan-Grijalva, Herrera-Urbina et al., 2005; MacCuspie, Rogers et al., 2011) (Equation 2. 25). Different shapes of the same NPs chemical composition will give different SPR spectrum (Figure 2. 17) (Mock et al., 2002). The presence of capping agent has been found to increase the maximum absorbance, red shift and broaden the SPR (Yan et al., 2006). Thus SPR spectrum provides a lot of information about NPs suspension characteristics.

$$\sigma\,(\lambda) = \left(\frac{18\pi VNl\varepsilon_m^{3/2}}{2.303\lambda}\right)\frac{\varepsilon_2}{(\varepsilon_1 + 2\varepsilon_m)^2 + \varepsilon_2^2}$$

Equation 2. 24

Where V is the volume of one particle, ε_m is dielectric constant of the medium, ε_1 and ε_2 are real and imaginary part of dielectric constant of the metal and λ is wavelength in vacuum.

$$\Gamma = \Gamma_0 + A\frac{v_f}{R}$$

Equation 2. 25

Where T (damping constant of NPs) ≈ FWHM of the SPR, A is the constant (depend on the nature of the scattering), v_f is velocity of the conduction band electron at Fermy energy, and R is the size of NPs.

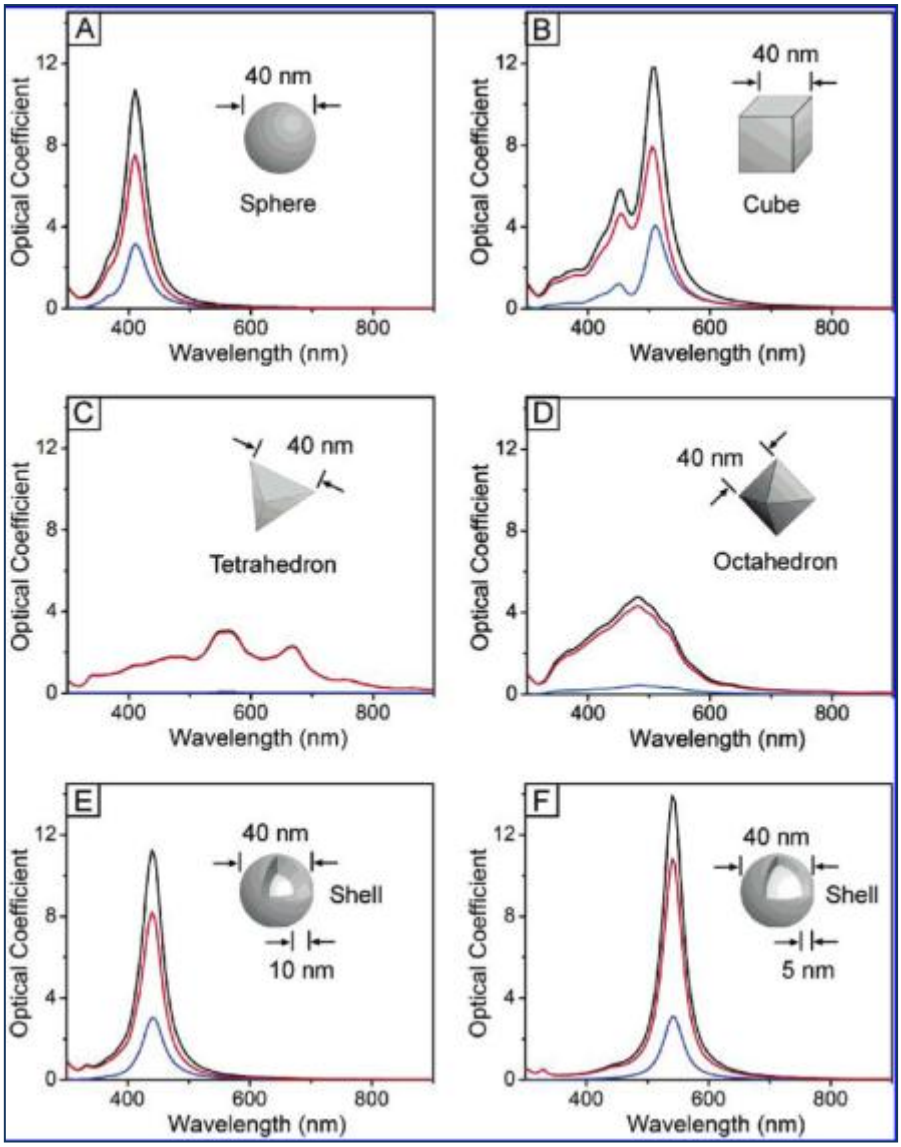

Figure 2. 17 Different SPR for different silver nanoparticle shape and size (Wiley, Im et al., 2006)

Even though this method is only applied for particular metal NP, the advantage of this method, non-destructive and fast analysis, makes this method is extensively used for NP characterization.

2.7.2.2. Energy dispersive X-Ray Spectroscopy

When the electron beam comes into contact with the specimen, the electrons can be: (1) elastically scattered due to the Coloumb potential of a nucleus with no

energy loss of the electron; (2) inelastically scattered when the electron excite or ionize inner-shell of the atom/s of the specimen (Figure 2. 18) (Reimer, 1997; Vollath, 2008).

The elastically scattered electron is more localized and contributes to the image contrast and thus is exploited for imaging purposes. On the other hand, the inelastically scattered electrons are less localized and do not contribute to the imaging process. These electrons, however, provide the information about chemical content of an object because the electron energy loss and emitted excitation energy of the object is fingerprint of the element of the object and can be used for qualitative chemical analysis. Energy dispersive X-ray spectroscopy (EDX) for example, analyze the X-ray emission from the specimen for single particle elemental analysis purposes. By combining an EDX detector into the TEM, more information can be derived from this technique and TEM becomes a more powerful for NPs characterization purposes (Reed, 1993; Reimer, 1997).

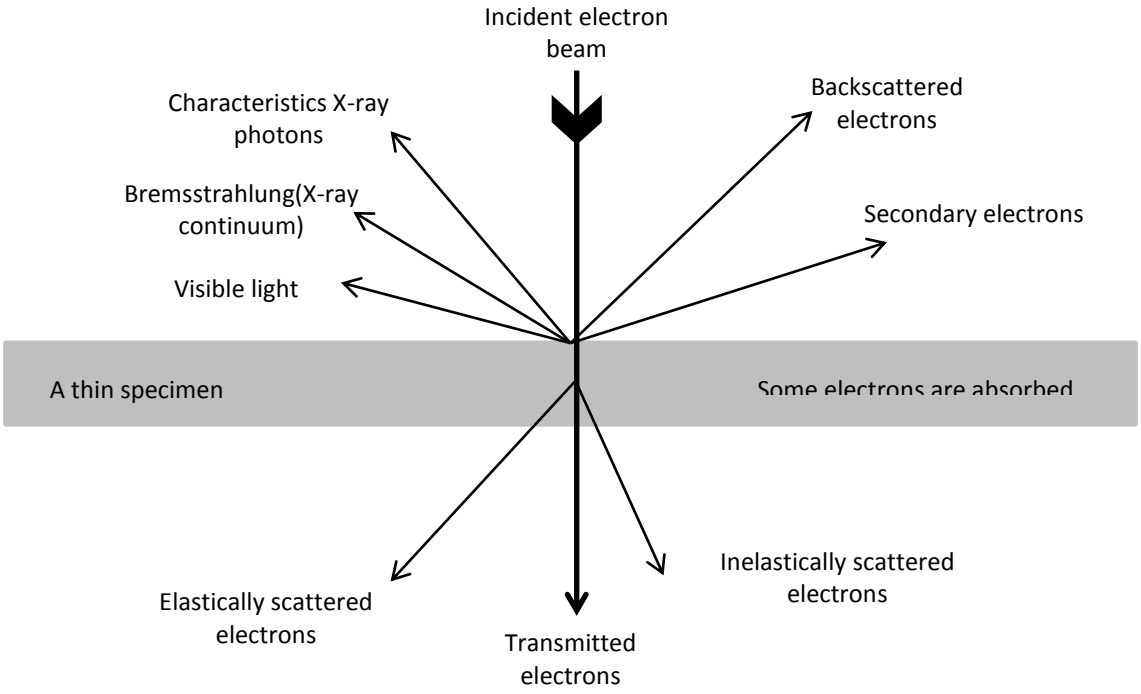

Figure 2. 18 Interaction between electrons and specimen in electron microscopy(Rochow and Tucker, 1994)

2.7.3. Surface Charge measurement

When NPs are suspended in a media, the NPs can acquire charge due to ionization of functional groups (protonation or de-protonation), adsorption of solvated ions to the charge-neutral NPs surfaces and ion exchange where higher valence ions replace lower-valence ions bound to the surface; lattice defect; and other reaction equilibria (Derjaguin, 1989; Kirby and Jr, 2004). Surface charge is an important characteristic of NPs and has a major influence into NPs fate and behavior. However measuring surface charge directly is difficult. Zeta potential, potential at slipping plane or surface of hydrodynamic shear or shear plane, in which the ions and particle inside the plane form a stable entity and move along together due to Brownian motion (Hunter, 1986) can be measured by electrophoresis and used for estimating the surface charge of NPs. The electrophoretic mobility (***U_E***- electric-field driven particle mobility) of NPs can be converted into zeta potential (ζ) by using Henry equation (Equation 2. 26).

$$U_E = \frac{2\,\varepsilon\,\zeta\,f(ka)}{3\eta} \qquad \text{Equation 2. 26}$$

where ε is dielectric constant; η is viscosity of the media; ζ is zeta potential and f(ka) is Henry's function. The value of henry's function refer is 1.5 (for particle larger than 0.2 microns dispersed in salt containing media with concentration more than 10^{-3} molar, according to Smoluchowski approximation) or 1.0 (for small particle in low dielectric constant media, according to Huckel approximation) (Malvern). If the ζ close to zero, the repulsive force between particles is reduced and the particles are allowed to come into contact and start to aggregated.

2.7.4. Surface area measurement

The Brunauer, Emmett, Teller (BET) method has been widely used for measuring specific surface area of solid material, and shown to be useful for measuring NPs surface area (Hassellov, von der Kammer et al., 2007). By letting the Nitrogen (N_2) gas to occupy the surface of NPs, the amount of adsorbed N_2 onto NP surface can be calculated to measure the area of NP. Since the N_2 are very small adsorbate molecules, degree of aggregation gives minor effect into measurement (Powers, Brown et al., 2006). This method shows high precision and direct measure the surface area, but artifacts and NPs morphology changes due to sample preparation would give a false result (Hassellöv, Readman et al., 2008).

2.7.5. Concentration measurement

Nanoparticle concentration in a suspension can be measured by using Atomic Absorption Spectroscopy (AAS) and Inductively coupled plasma-mass spectrometry (ICP-MS). Since ICP-MS has a lower detection limit (limit detection 1-10 $ng.L^{-1}$) than AAS, it has been widely used for NPs elemental characterization and quantification. ICP-MS also can analyze multi-element at the same time with a wide range of linearity. Another advantage of ICP-MS is its possibility to be coupled with other separation techniques such as chromatography (liquid chromatography and HPLC) and FFF (Taylor, Garbarino et al., 2002). One limitation of ICP-MS is this instrument can only measure metal.

2.8. Reasons for choosing silver nanoparticles

Silver (Ag) is a rare element (67^{th} in abundance among the elements) with atomic weight of 47. It has been known as an environmental hazard and has been

classified as one of the priority pollutants since 1977, even though the history of human life has been closely related to silver for about 7000 years. In the 18th century, for example, silver was used in medication (as eye drops, antibiotic, disinfectant, etc) due to its antibacterial properties. However, toxic, persistent and bioaccumulation properties of silver, especially in the environment, meant that it was necessary to control silver usage and exposure (Hwang et al., 2007; Luoma, 2008; EPA, 2013).

Recently, exploiting the novel properties of material nanoscience and nanotechnology, nanosilver (AgNPs) has been introduced to the market. Although nanosize silver shows unique optical, electrical, magnetic and theurapetic properties, most of AgNPs applications use silver's antimicrobial properties (Elechiguerra et al., 2005; Lu et al., 2008; Luoma, 2008; Jo et al., 2009; Panacek et al., 2009; Rejeski, 2009), as has been exploited in the conventional silver form.

Recently, more than three hundred consumer products containing AgNPs have been marketed and making nanosilver or silver nanoparticles (AgNPs) the most rapidly growing classes of nanoproducts (Figure 2. 19) (Fauss, 2008; Rejeski, 2009). Because AgNPs have been commercialised, the exposure of humans and the environment to these materials is bound to occur. Thus the hazard identification and exposure evaluation of AgNPs need to be performed immediately.

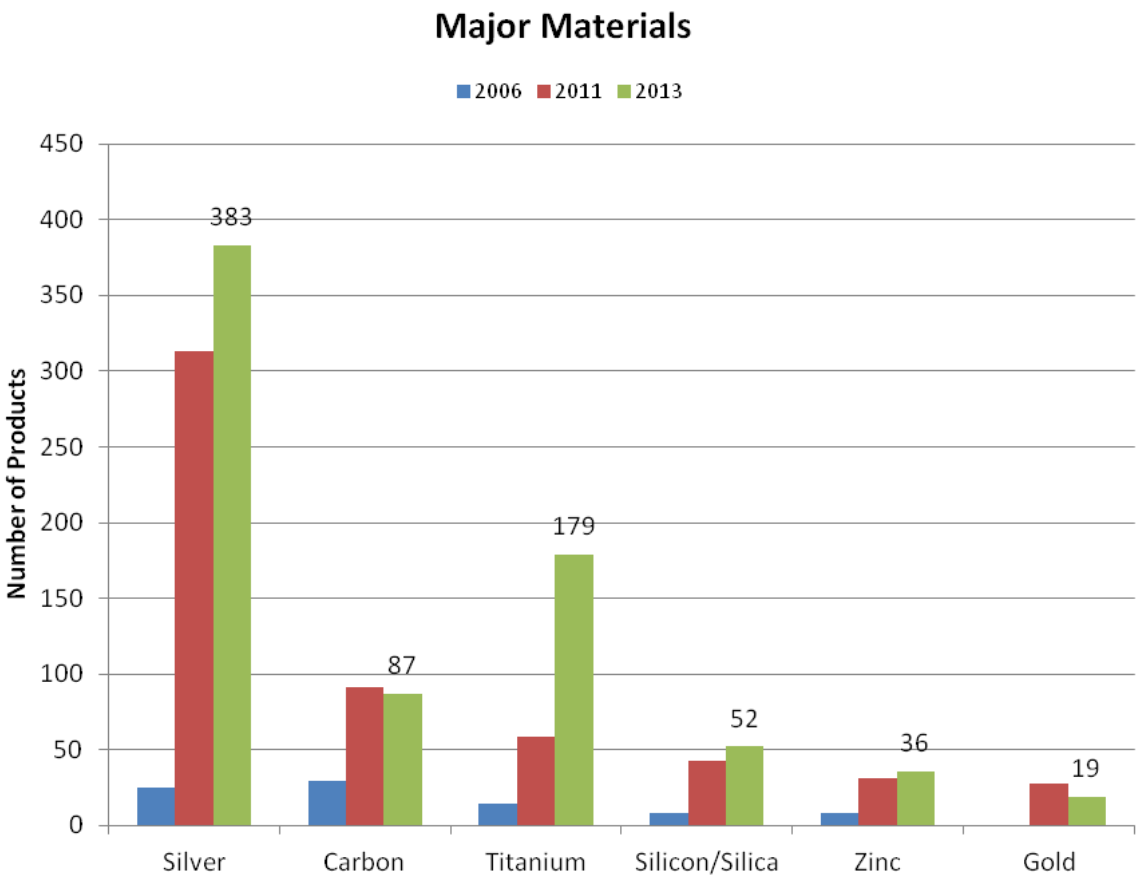

Figure 2. 19 The number of nanomaterial products categorized by its major component (http://www.nanotechproject.org/cpi/about/analysis/ ,downloaded 31st March 2014).

Different types of AgNPs has been synthesized with different shapes (sphere, rods, wire, triangle, etc), coatings (citrate, polymer, carbon, silica, sugar, peptide, ect), and different sizes, generated both by bottom-up and top-down methods (Reidy, Haase et al., 2013). This huge variety of AgNPs was synthesized in order to obtain novel and unique properties for ranges of applications.

A number of studies on the toxic effect of AgNPs is vast and the majority of studies found that the toxic response of AgNPs was associated with the release of silver ions, and the dissolution was revealed as the effect of oxidation (Liu and Hurt, 2010):

$$O_2 + H^+ \xrightarrow[\text{slow}]{Ag^0} Ag^+ + \text{peroxide intermediates} \xrightarrow[\text{fast}]{Ag^0} Ag^+ + H_2O$$ Equation 2. 27

The oxide form which can be further transformed into Ag-ligand complexes in media containing ions such as chloride, sulphate, carbonate, etc. These influence the silver bioavailability. The complex interaction between AgNPs occurring in the media is likely to complicate some of the (eco)toxicology findings (Thomas, Judd et al., 1999; Misra et al., 2012; EU, 2013; Reidy, Haase et al., 2013).

However determination of trends in AgNPs toxicity is complex owing to the various types of AgNPs, different sizes and shapes, presence or absence of capping agent, transformation of AgNPs and diverse types of evaluation test (Batley, Kirby et al., 2012). Chernosova argue that depot function for the silver ion is the only obvious findings, but beyond these features, a specific nano effect cannot be derived from present data (Ahamed et al., 2010; Chernousova and Epple, 2013). From the existing data, some highlights from eco-toxicology findings revealed that AgNPs show a lower toxicity than silver ions, and the capping agent, size and shape of AgNPs influence the biological response from organism, with human cells seen to be the most resistant culture to the toxicity of silver. Full characterization in any eco(toxicology) study is important and the possibility that biosynthesised AgNPs may be less toxic than the AgNPs generated by chemical process has been examined (Ahamed, AlSalhi et al., 2010; Marambio-Jones and Hoek, 2010; Fabrega, Luoma et al., 2011; Batley, Kirby et al., 2012; Chernousova and Epple, 2013).

2.9. Summary

Development of nanotechnology and nanoscience have increased the production of engineered nanoparticles significantly as well as the potential of their exposure to the environment. AgNPs has been reported as the most widely used NP in different types of product due to its wide microbial activity. Even though the concentration of engineered NPs in the environment is less than natural NP, their size, shape, composition and functionalization might be different with natural NPs in which the nature has not be adapt to and pose diverse risk to the environment.

Large specific surface area and unique properties due to quantum effect of NPs will influence NP fate and behavior in the environment. Chemical, physical and biological transformation of NP in various media and environment have been reported. Thus aggregation, dissolution, re-precipitation and other transformation of NPs need to be anticipated and evaluated in any (eco)toxicology study as they might influence the “real dose” exposing the organisms or cells. Therefore, more NP eco(toxicology) studies need to be performed with recommendations of fuller characterization of the NPs properties before, during and after exposure studies.

CHAPTER III

METHODOLOGY

3.1. Introduction

This chapter illustrates the practical methodology that was performed for this study. In general, three main activities covered by this study, which were: (1) synthesis and characterization of PVP-capped AgNPs, (2) ligand-exchange of citrate-capped AgNPs by different polymers, and (3) stability assessment of citrate-, PVP- and PEG-capped AgNPs in ecotoxicology media. This study was part of larger study that examines the ecotoxicity of AgNPs into *Daphnia magna sp*.

The PVP-capped AgNPs, in this study, were synthesized according to two protocols, termed the hot process and the cold process, modified from Hoppe and Mulfinger method (Hoppe et al., 2006; Mulfinger et al., 2007). Changes of precursor and PVP concentration ratio to the Hoppe method and PVP addition into Mulfinger method were applied in this study. The characteristics of the generated PVP-capped AgNPs by the two processes are presented in Chapter 4. PVP-capped AgNPs were also synthesised from citrate-capped AgNPs via ligand-exchange. Given the success of the PVP replacement of citrate, further investigation of the replacement of citrate with other capping agents (PEG-SH, fulvic acid and Tween-80) was investigated. The method of ligand-exchange is presented in this chapter and the characterization results of polymer-capped AgNPs compared to the original citrate-capped AgNPs are presented in Chapter 5.

The stability of citrate-, PVP-, and PEG-capped AgNPs toward aggregation in the OECD *Daphnia magna sp*. and Green Algae media (Bold Basal Medium) were

evaluated. The methodology of the stability test is presented in this chapter and the result of stability evaluation is presented in Chapter 6.

3.2. Materials and Equipments

Lists of chemicals, water, media and laboratory wares used for this study are presented in the following discussion.

3.2.1. **Materials**

Materials used for this study is presented in Table 3. 1. All the chemicals were used as received and without further purification. All chemical used are analytical grade (purity > 90%).

Table 3. 1 List of chemicals used in this study

No	Chemical name	Chemical structure	MW (gram.mol^{-1})	Supplier
1	Silver Nitrate	$AgNO_3$	169.87	Analab
2	Polyvinylpyrrolidone (PVP)	$(C_6H_9NO)_n$	10,000	Sigma-Aldrich
3	Sodium borohydride	$NaBH_4$	37,83	Sigma-Aldrich
4	Sodium citrate dihydrate	$C_6H_5O_7.2H_2O.3Na$	294,10	Sigma-Aldrich
5	Acetone	C_3H_6O	58.08	Fisher Scientific
6	Thiolated-metoxy polyethylene glycol	$CH_3O(CH_2CH_2O)_nCH_2CH_2SH$	5,000	Sigma-Aldrich
7	Suwanne River Fulvic acid	(in section 6.3.3)	750-860	IHSS, USA
8	Tween-80 (Polysorbate-80)	$C_{64}H_{124}O_{26}$	1,310 (density= 791.00 kg.m^{-3})	Sigma-Aldrich
9	Nitric acid	HNO_3	63.01	Fisher Scientific
10	Calcium nitrate	$Ca(NO_3)_2$	164.09	Sigma-Aldrich

3.2.2. **Ultrapure water**

The water used in this study, both for preparing the suspension of reagents and media, and for cleaning the equipments was ultrapure water (18.2 MΩ at 25^0C), dispensed from Barnstead and Purelab flex water system.

3.2.3. **Media**

The OECD *Daphia magna sp*. media immobilization test (OECD 202) and the Green Algae media (Bold Basal Medium) were used for testing the stability of AgNPs. Nitrate and sulphate media (NM and SM) which are the modification of OECD *Daphnia magna sp*. media, by replacing the chloride anion with an equivalent ionic strength of nitrate and sulphate, respectively, were also employed. So, for the purpose of this study, the OECD *Daphnia magna sp.* media was termed as citrate media (CM). The composition of CM; NM and SM are presented in Table 3. 2 and Algae media composition in Table 3. 3. The media were prepared by DR. Thomas White and DR. Nadine Taylor, School of Bioscience, University of Birmingham.

Table 3. 2 Chemical composition of *Daphnia magna sp.* immobilization test media (OECD No. 202) and its variants

Chloride media (CM-1)		**Nitrate media (NM-1)**		**Sulphate media (SM-1)**	
Composition	**concentration ($mg.L^{-1}$)**	**Composition**	**concentration ($mg.L^{-1}$)**	**Composition**	**concentration ($mg.L^{-1}$)**
$CaCl_2 . 2H_2O$	294	$Ca(NO_3)_2 . 4H_2O$	472.25	$CaSO_4$	271.75
$MgSO_4 . 7H_2O$	123.25	$MgSO_4 . 7H_2O$	123.25	$MgSO_4 . 7H_2O$	123.25
$NaHCO_3$	64.75	$NaHCO_3$	64.75	$NaHCO_3$	64.75
KCl	5.75	KNO_3	7.5	K_2SO_4	6.75
Na_2SeO_3	2	Na_2SeO_3	2	Na_2SeO_3	2

Note: CM-1, NM-1, and SM-1 are full strength media; and CM-10, NM-10, and SM-10 are ten-fold dilution of concentrated media.

Table 3. 3 Chemical composition of Green Algae media or known as Bold Basal Medium (OECD No. 201)

No	Name	Formula	g/L
1	di-potassium hydrogen orthophosphate	K_2HPO_4	0.075
2	Potassium di-hydrogen orthophosphate	KH_2PO_4	0.175
3	Magnesium sulphate	$MgSO_4.7H_2O$	0.075
4	Sodium Nitrate	$NaNO_3$	0.25
5	Calcium chloride	$CaCl_2.2H_2O$	0.025
6	Sodium Chloride	NaCl	0.025
7	Ferrous sulphate	$FeSO_4.7H_2O$	0.00498
8	Sulphuric acid conc. (wt per mL = 1.84g)	H_2SO_4	0.018
9	Boric acid	H_3BO_3	0.01142
10	Zinc sulphate	$ZnSO_4.7H_2O$	0.001412
11	Manganese chloride	$MnCl_2.4H_2O$	0.000232
12	Cupric sulphate	$CuSO_4.5H_2O$	0.000252
13	Cobaltous nitrate	$Co(NO_3)_2.6H_2O$	0.00008
14	Sodium molybdate	$Na_2MoO_4.2H_2O$	0.000192

(http://www.phycol.ca/system/files/BBM.pdf)

3.2.4. **Treatment to filter paper, glass ware and plastic ware**

The regenerated cellulose membrane with nominal pore size 1 KDa molecular weight cut-off (MWCO) from Millipore was used for ultrafiltration. Before used, the membrane was soaked in 0.1% $HNO_{3\ (aq)}$ to prevent contamination. All the glass- and plastic-ware used within this study were also acid washed by soaking them in 10% $^{v}/_{v}$ $HNO_{3(aq)}$ for at least one day and followed by washing with plenty of ultrapure water. After washed, the glass- and plastic-ware were dried at room temperature before used.

Further treatment for the plastic-wares, used for dissolution experiments were done by soaking them in 0.1 M $Ca(NO_3)_{2\ (aq)}$ for one night, re-washing with plenty of high purity water, and subsequently soaked in ultrapure water for at least another night. Those further treatment was done in order to prevent material (Ag^+) loss due

to adsorption onto container surfaces. All the plastic-ware used were made of high density polyethylene (HDPE).

3.3. Synthesis of PVP-capped AgNPs by the hot process

A method developed by Hoppe et al. (2006) was adopted for this study with reactans concentration modification. About 100mL of accurately measured 2.9 mM $AgNO_{3(aq)}$ and 100mL 20 mM $PVP_{10\ (aq)}$ (PVP with MW 10,000 $g.mol^{-1}$) were mixed in a round-bottomed flask and stirred for 5 minutes (Figure 3.1). Then the mixture was heated with vigorous stirring until the temperature reached 70^0C and kept on that temperature for 7 hours. After heating, the solution was removed from the heat and left overnight to cool down and for completion of the reaction. Subsequently, the particles were cleaned by series of centrifugation and re-dispersion procedures in acetone and ultrapure water to remove excess reactants. The clean up procedure will be discussed in section 3.6.

(a)

(b)

Figure 3. 1 PVP capped AgNPs was synthesised with hot process

3.4. Synthesis of PVP-capped AgNPs by the cold process

The cold process was an adjustment of synthesis method developed by Mulfinger et al. (2007) to obtain PVP-capped AgNPs. Five set of reaction conditions

were exercised to have a monodisperse PVP-capped AgNPs. A 240mL of 2 mM $NaBH_{4\ (aq)}$ was stirred and cooled in an ice bath for 20 minutes. A volume of 1 mM $AgNO_{3\ (aq)}$ was added drop-wise using a burette at about 1 drop per second with continuous stirring (Figure 3. 2). A 0.3% m/v $PVP_{10(aq)}$ was added either before or after addition of $AgNO_{3\ (aq)}$ at 5% v/v of total volume of $NaBH_{4\ (aq)}$ and $AgNO_{3\ (aq)}$. Variation of stirring duration was applied to find out its effect to AgNPs monodispersity. Then the solution was removed from the ice bath and left in the fridge overnight. The surface plasmon resonance (SPR) of as-synthesized AgNPs was monitored. Once the spectra was visualized and stable, the process was complete and the NPs were washed before characterised.

Table 3. 4 Volume of reactans added to the cold process reaction

Experiment	$AgNO_{3\ (aq)}$ (mL)	$NaBH_{4\ (aq)}$ (mL)	Stir (hour/s)[a]	PVP (aq) 0.3% V/V	
				Addition time[b]	volume
CP1	20	240	1	After	5%
CP2	20	240	3	After	5%
CP3	20	240	5	After	5%
CP4	40	240	1	After	5%
CP5	80	240	0	Before	5%

[a]: stirring time after addition of $AgNO_{3\ (aq)}$

[b]: before or after addition of $AgNO_{3\ (aq)}$

(a) **(b)**

Figure 3. 2 PVP capped AgNPs were synthesised with cold process

3.5. Replacing citrate with polymer

Citrate-capped AgNP were synthesized by reducing silver nitrate with sodium borohydride and sodium citrate. 10nm citrate capped AgNPs were generated by mixing 100 mL 0.25 mM $AgNO_3$ (aq), 100 mL 0.31 mM sodium citrate (aq) and 6 mL 0.25 mM $NaBH_4$ (aq) according to Römer et al (Römer et al., 2011). The mixture was brought into boil for 90 minutes while stirred vigorously and then left overnight to complete the reaction. The generated NPs suspension was then purified from excess reactants with diafiltration (1kDa cellulose membrane and Amicon stirred ultrafiltration cell).

Solutions of PEG-SH; PVP_{10}, fulvic acid, and Tween-80 were added separately into the washed citrate-capped AgNPs and stirred for at least an hour for capping agent substitution. Since citrate-capped AgNPs gave a red colour in Nitrate Media (NM), yellow colour preservation of AgNPs in NM after ligand-exchange suggesting steric stabilization of AgNPs and used as an indication of capping agent replacement. The polymer solution was continuously added into AgNPs until the sample of ligand-exchange product sustained its yellow colour in NM. The result will be discussed in Chapter 5.

3.6. Clean-up of polymer-capped AgNPs

It is very important to have clean and uncontaminated AgNPs suspensions in toxicology studies to be able to draw a dose-response relationship attributed to NPs exposure alone. There are three aims of the clean-up process: 1) to remove residual dissolved Ag (Ag^+) ; 2) to remove excess capping agents, and 3) to ensure the NPs are as monodisperse as possible.

Two different cleaning methods were adopted. For HP-AgNPs, i.e. AgNPs generated by the hot process, clean up the NPs consists of three steps: NPs separation; washing; and re-dispersion.

The AgNPs was separated by addition of acetone (five times in volume) and centrifugation at 4000 rpm for 15 minutes (Chou and Lai, 2004) by using an Eppendorf 5804R bench-top centrifuge. The supernatant was thrown away and the pellet AgNPs was collected. The separated particles was then washed up with water and acetone mixture (volume ratio 1:3); shaken by hand and followed by separation by acetone and centrifugation. The washing process and separation were repeated at least three times. Finally, the clean AgNPs was re-dispersed in high purity water and ultrasonicated for not more than 5 minutes with Branson ultrasonic bath.

Diafiltration/ultrafiltration (UF) was implemented for clean up CP-AgNPs, i.e. AgNPs synthesized by the cold process, citrate-capped AgNPs and citrate-replacement products. Pressurized nitrogen gas was used to provide force to push solvent through the membrane pores (nominal pore size 1 KDa, regenerated cellulose membrane). The membrane retained materials larger than 1KDa and allow the ions, water and other materials smaller than 1 KDa to be removed as the filtrate (Figure 3. 3). The volume of the NPs suspension was kept constant by adding high purity water for CP-AgNPs and 0.15mM Na-citrate for citrate-capped AgNPs.

The filtrate was collected and Ag^+ concentrations within the filtrate were analyzed by ICP-MS. The washing process was repeated several times until the Ag^+ concentration in the filtrate was leveled off.

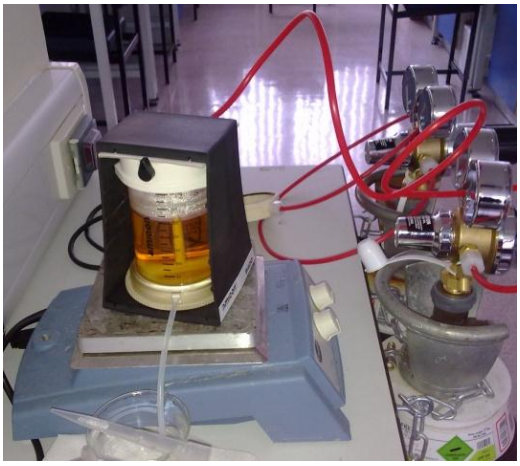

Figure 3. 3 The set-up of diafiltration cell

3.7. Characterization

A number of methodologies were employed for characterizing the size, shape, and chemical composition of AgNPs and will be discussed in the following section. The characterization however was done to single batch of AgNPs sample due to the technical complexity and equipment restriction.

3.7.1. **Surface Plasmon resonance with UV-Vis spectrometer**

Qualitative analysis of AgNPs SPR both in pristine suspension and in ecotoxicology media was analysed by Jenway 6800 UV-Vis spectrophotometer, with a tungsten halogen and deuterium lamps as the light source and scanning wavelength ranges from 190 - 1100nm. The absorbance was scanned between 200-800nm with a 1 cm disposable plastic cuvette. The qualitative characterization of AgNPs with UV-Vis spectrophotometer was used for:

(1) Chemical identification of as-synthesized AgNPs as AgNPs absorbs the UV-Vis wavelength at around 400nm.

(2) SPR comparison between citrate-capped AgNPs and its ligand-exchange products (PEG-, PVP-, fulvic acid and Tween-80 capped AgNPs).

(3) Analysing the AgNPs stability in eco-toxicology media

3.7.2. **Size distribution by dynamic light scattering**

The DLS Zetasizer nanoseries nano-ZS from Malvern Instrument UK was used for hydrodynamic diameter and PdI characterization of AgNPs both in pristine suspension and in ecotoxicology media. Size and polydispersity index (PdI) stability of AgNPs during incubation in ecotoxicology media was monitored over 21 days (in CM, NM and SM, both concentrate and dilution media) and 3 days (in algae media). With a 4mV He-Ne laser source, wavelength 633nm and avalanche photodiode as the detector, the instrument can measure the particle at size range 1-1,000 nm. The measurement was done at temperature 20^0C. By using a disposable plastic cuvette, a 1mL sample was loaded and measured for ten times and ten runs for each measurement. There was no sample preparation before the measurement.

3.7.3. **pH measurement**

The pH of the suspension was measured by Orion 3 star pH meter which was calibrated with standard pH 4; 7 and 10 each time before measurement.

3.7.4. **Zeta potential**

In this study, zeta potential of AgNPs both in pristine suspension and in ecotoxicology media were measured by Laser Doppler Velocimetry in zetasiers nano-ZS from Malvern Instrument UK at temperature 25^0C. A laser was used as the source of light and was split into incident and reference beam. The incident beam passes through the sample cell and the attenuated scattered light at angle 17^0 was detected by a detector. When an electric field is applied, the particles will be moving toward the electrodes and creates a fluctuation of the scattered light. The intensity of

fluctuating scattered light will be converted to particle speed and then further computed into zeta potential.

3.7.5. **Flow field flow fractionation**

In this study, an Assymetric-FlFFF Postnova Analytics AF2000 MT coupled by UV-Vis and multi angle light scattering (MALS) detector were used for size (d_H) characterization of NPs suspended as pristine suspension and in ecotoxicology media. Dilute salt solution (10mM $NaNO_3$) was used as the carrier liquid with a 1kD molecular weight cut-off regenerated cellulose membrane was used for filtering the cross-flow out. The channel-flow rate was set constantly at 1mL/min, and the cross-flow rate was adjusted manually to have the best resolution between void peak and sample's peak (ranges from 0.3 to 1.5 mL/min). 10 minutes focusing time was set for all the experiment. The volume of sample injected into the instrument was between 0.5 – 1.5mL, depend on the concentration of the sample.

For size quantification, polystyrene NPs standard from Duke scientific with known size (20±2; 40±2 and 60±2nm) were used as the standard. The retention time of the sample was compared with the standard to obtain the size of the NPs.

3.7.6. TEM and AFM sample preparation

In this study, TEM samples were prepared by a drop deposition technique. A drop of suspension was placed onto a 300 mesh copper grid, fully covered with carbon film (Agar scientific). After 2 hours (nearly dry), the grid was then washed with drops of ultrapure water and let the grid to dry for another hour. Within the same day the prepared specimens were analyzed by TEM to avoid the risk of physical and chemical changes of the sample.

On the other hand, the AFM samples were prepared by ultracentrifugation deposition method using Beckman counter type SW40 with average rotation axis (r_{max})= 112.7 and K factor = 137. By using a 30,000 rpm rotation speed for one hour at temperature 10^0C, particles were brought down to be deposited onto the mica surface. Then the mica was rinsed with ultrapure water and dried in a room temperature prior to the analysis.

3.7.7. AgNPs core size and shape characterization by Transmission Electron Microscopy (TEM) and single particle elemental analysis by Energy Dispersive X-Ray (EDX) Spectroscopy

In this study, two different TEM instruments, Jeol 1200EX and TecnaiF20 were used for size, shape and elemental characterization both for pristine suspension and AgNPs in media. Most of the imaging taken for size and shape characterization was done by Jeol 1200EX, but the Tecnai F20 was primarily used for EDX chemical analysis because the Tecnai F20 is complemented with Oxford ISIS EDX. The condition of those two instruments is presented below:

Jeol 1200EX	LaB_6 electron gun
	Resolution: 0.34 nm
	Accelerating voltage: 40-120 kV (80kV was used for this study)
	Magnification up to 500kx
FEI Philips Tecnai F20	Schottky field emitter as the electron gun
	Point resolution: 0.24nm
	Line resolution: 0.12nm

Accelerating voltage: 200kV

Equipped with Oxford ISIS EDX and Gatan digiPEELS detectors

Magnification: 30x -1280 kx

The images were taken and analyzed with Gatan DigitalMicrograph and ImageJ software. The size of NPs were averaged from at least 100 NPs from each grid, but the shape factor were calculated from about 50 Nps.

3.7.8. Size and shape characterization by Atomic Force Microscopy (AFM)

In this study, AFM was used for core size analysis of AgNPs in pristine suspension. The XE-100 PSIA from Park system was used and operated by non contact mode by using a silicon cantilever (PPP-NCHR, tip radius < 10nm). Decoupled and motorized XY scanner moves the sample and the Z scanner drives the probe for sample imaging and measurement. Super luminescent diode (830 nm) with low coherency was used for cantilever deflection detection. Maximum sample size of 100 mm x 100 mm, 20 mm thick, up to 500 g, 780x magnification and 1 µm optical resolution are offered by this instrument. The microscope was kept in an acoustic foam box to reduce the background effect of noise and vibration on the imaging acquisition process.

Several softwares were employed. XEC and XEP were used for data acquisition and data visualization of the sample, and XEI software was used for image processing and analysis. The size of NPs was averaged from at least 100 NPs by implementing the XEI system.

3.8. Stability study of AgNPs in eco-toxicology media

The stability of citrate-, PVP- and PEG-capped AgNPs in full strength and ten-fold dilution of CM; NM, and SM, and in full strength of algae media (AM) was assessed because this study is part of ecotoxicology study of AgNPs into Daphnia magna. The use of ten-fold dilution media was suggested for ecotoxicology study as NPs, especially electrostatic-capped NPs was unstable in high ionic strength media and apparently no significant negative effect induced by diluting media by 10% to organisms (Gubbins et al., 2011; Römer, White et al., 2011; Park et al., 2013). Thus both concentrated and 10-fold dilution media was used in this stability test.

For incubation purposes, a clean AgNPs were mixed with the media at volume ratio 1:4 to have AgNPs concentration at ± 4 ppm. This concentration was chosen because it lies within range of LC_{50} of AgNPs ecotoxicity findings (<7 ppm) (de Lima et al., 2012) and can be clearly detected by instrumentation, especially UV-Vis spectrometry.

Four replicates of each suspension were prepared and stored in acid washed HDPE plastic vials. The incubation time of AgNPs in *daphnia sp.* media and its variants (NM and SM) was 21 days, and 3 days in algae media according to OECD standard ecotoxicology test (OECD, 2002; 2004). Since the aim of this study was to examine the capping-agent and media effect into the AgNPs stability, the confounding factor such as light and organism (Freitas and Müller, 1998; Cheng et al., 2011) were controlled by performing the experiment in the absence of light and organism. Characteristics of AgNPs during and after incubation media were assessed by multi-method characterization techniques as presented earlier.

Dissolution of AgNPs in full strength and diluted OECD daphnia media (CM-1 and CM-10 respectively), and full strength and diluted nitrate media (NM-1 and NM-10) were assessed and will be described further in following paragraph.

3.9. Preliminary dissolution study of PVP capped AgNPs

The release of silver ion from pristine AgNPs suspension during storage (at 7 and 10 days storage) and during incubation in ecotoxicology media was quantified. The experiments were done in HDPE plastic containers as silver ion adsorptivity into borosilica glass was found to be high (West et al., 1966; Struempler, 1973). A 1 to 4 volume ratio of AgNPs suspension to the media were prepared and stored in an acid washed HDPE plastic bottle. The AgNPs-media mixture was kept for 21 days in temperature and light controlled room, having the same condition with *Daphnia sp.* exposure condition set-up with temperature 18-19^{0}C and 18 hours light and 6 hours dark (OECD, 2004).

The concentration of released silver ion were measured by performing two steps of work: ion species separation and concentration measurement. Two methods of ion separation used in this study were ultrafiltration and dialysis, and concentration measurement by Inductively Coupled Plasma-Mass Spectrometry (ICP-MS).

3.9.1. Silver ion separation by ultrafiltration

Silver ion released from PVP-capped AgNPs, both during storage and after 21 days incubation in ecotoxicology media was quantified. The set-up of ultrafiltration instrumentation was presented in section 3.6. and Figure 3. 3. A 10 mL of AgNPs sample, both pristine and incubation AgNPs was ultra-filtered with 1KDa (MWCO) regenerated cellulose membrane under N_2 pressurised gas to have a 5mL filtrate

and a 5mL retentate. The collected filtrate and the retentate were then acidified before analysis by ICP-MS (will be further described in section 3.9.3). The increase of Ag^+ concentration in the filtrate was calculated as an indication of dissolving behavior of AgNPs.

3.9.2. **Dissolution study with dialysis**

The instrument set up of dissolution study by dialysis technique is presented in Figure 3. 4, adopted from previous study (Franklin, Rogers et al., 2007; Rogers et al., 2010). The external suspension was prepared by mixing 20 mL clean PVP-capped AgNPs and 800 mL media to have about 0.5 ppm AgNPs suspension. Dialysis bags were made of about 5 cm long of Cole Parmer Spectra/Por 7 dialysis membranes with nominal pore size 1KDa MWCO and 45 mm diameter, filled with the same media as external suspension and clipped with universal plastic dialysis clip (from Cole Parmer) at both ends. Prior to use, dialysis membrane was washed with ultra pure water and the clips were soaked in 1% v/v HNO_3 and 0.1 M $Ca(NO_3)_2$ as described in section 3.2.4. Ten bags were immersed into an external suspension and then left mildly stirred. Each bag was sampled at particular time and the solution from the dialysis bags were acidified for ICP-MS analysis.

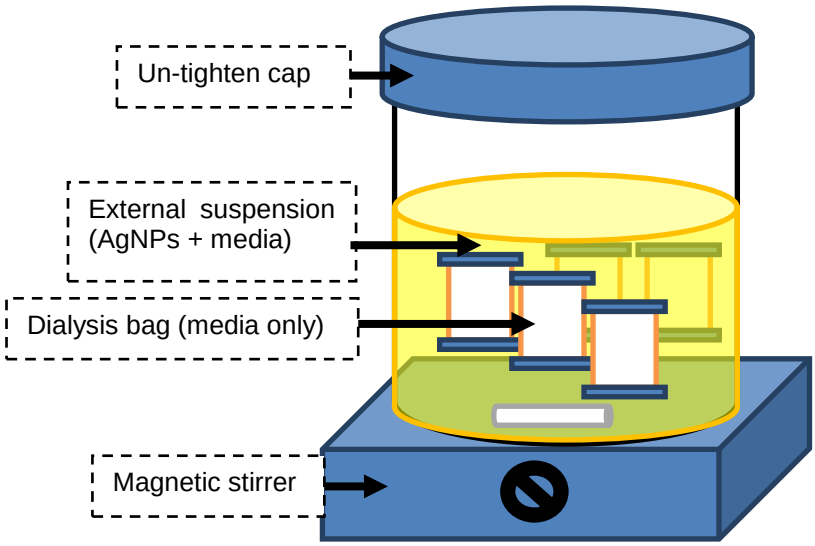

Figure 3. 4 Dissolution study by using dialysis method

3.9.3. **Inductively coupled plasma-mass spectrometry**

In this study, the Agilent 7500 ICP-MS instrument were employed for AgNPs and silver ion (Ag^{+}) concentration measurement. High frequency quadrupole (3MHz) was used for ion separation after the beam passed through an octopole collision or reaction cell where the helium gas removed the polyatomic ion interferences.

All the samples were acidified prior to ICP-MS analysis. The AgNPs samples were acid digested by adding concentrate HNO_3 to have 20% $^{v}/_{v}$ acid concentration within the sample and then shaken it for at least 2 hours until the yellow colour of AgNPs disappeared. Then the suspensions were ten-fold diluted with ultrapure water to have 2% $^{v}/_{v}$ acid concentration in the sample before ICP-MS analysis. For ion samples, however, the samples were acidified by HNO_3 to have 2%$^{v}/_{v}$ acid in the sample. All of the ICP-MS samples were kept in the acid washed and $Ca(NO_3)_2$ treated HDPE plastic bottles prior to the analysis. All the measurement and data analysis were done by Dr. Stephen Baker, University of Birmingham UK.

CHAPTER IV

SYNTHESIS AND CHARACTERIZATION OF PVP-CAPPED SILVER NANOPARTICLES

Summary

This study examined two existing protocols for the synthesis of PVP-capped AgNPs, termed hot process and cold process. In the hot process, the PVP polymer was used to reduce the silver ion and to cap the generated AgNPs. In the cold process, $NaBH_4$ was used as the reducing agent, and the PVP polymer was added to replace the electrostatic layer of BH_4^- ion surrounding the AgNPs, providing stability to the AgNPs. One set of reaction conditions was used for the hot process, and five conditions for cold process. The characteristics of the synthesized AgNPs, such as UV-Vis absorbance, $d_{H,}$ core size, zeta potential, and shape factor were evaluated. It was shown that the cold process generated more monodisperse NPs than the hot process, and addition of PVP polymer prior to the nucleation process gave a better PdI value of NP generated by cold process. Preliminary solubility measurements showed that the amount of released 'dissolved' Ag from AgNPs incubated in chloride containing media was lower than in nitrate containing media, possibly due to formation of Ag-Cl complexation and subsequent precipitation.

4.1. Introduction

A number of methods have been developed for AgNPs synthesis, classified as top-down or bottom-up methods. Other biological methods have also been used and all methods can utilize 'green synthesis' principles. The bottom-up synthesis approach is the most widely implemented method according to 200 reviewed publications (Tolaymat, El Badawy et al., 2010). It was revealed that most of the AgNPs were synthesized from $AgNO_3$ as the main precursor (83%), using $NaBH_4$ as reducing agent (≈23%), citrate (27%) and PVP (18%) as the main capping agents, and water as the solvent (80%). Generally, the synthesized AgNPs were spherical and less than 20nm in diameter (Tolaymat, El Badawy et al., 2010).

Other reducing agents which have been used to synthesize AgNPs including hydroquinone (Patakfalvi et al., 2007), hydrazine hydrate (Zhang et al., 1996), and ethylene glycol (Ducamp-Sanguesa et al., 1992; Silvert et al., 1997). Some polymers such as Polyvinylpirrolydone (PVP), polyethylene glycol (PEG) and polyvinyl alcohol (PVA) have also been used both as the reducing agent and the stabilizer concurrently (Porel et al., 2004; Hoppe, Lazzari et al., 2006; Popa et al., 2007). A strong reducing agent such as $NaBH_4$ may lead to a fast reduction and nucleation process, which then produces small monodispersed AgNPs (Patakfalvi, Papp et al., 2007). With a weaker reducing agent, such as a polymer however, a slower reaction occurs, so the NPs growth can be controlled for generating particular shapes and sizes (Washio et al., 2006; Patakfalvi, Papp et al., 2007).

PVP-capped AgNPs in particular has been synthesized by number of method, such as electrochemical (Yin et al., 2003), ɣ-irradiation (Huang et al., 1996; Shin et al., 2004), with and without heating (Mulfinger, Solomon et al., 2007) and generated different shapes of AgNPs such as triangular(Washio, Xiong et al., 2006), nano-wire,

nanoplate(Xiong et al., 2006) and spherical (Mulfinger, Solomon et al., 2007; Patakfalvi, Papp et al., 2007). Since slow reduction reaction of Ag^+ by hydroxyl end of PVP, the reduction rate can be promoted by adding alkaline or heating (Chou and Lai, 2004; Hoppe, Lazzari et al., 2006; Xiong, Washio et al., 2006).

Characterization of as-synthesized NPs is another important attempt. Since the behavior in the environment and effect following exposure of NPs are governed by its intrinsic properties, proper characterization is very important. Hansen et al. (2007) reviewed 428 toxicology and ecotoxicology studies and was not able to draw a correlation between NPs specific properties with the observed outcome due to incomplete characterization data (Foss Hansen, Larsen et al., 2007). Moreover, the transformations of NPs due to its interaction with ecotoxicology media, such as aggregation and dissolution, need to be characterized (Levard, Hotze et al., 2012; Shvedova, Pietroiusti et al., 2012). For that reason, establishing the characteristics of the as-synthesized NPs is imperative. Multi-method characterizations need to be performed as there is no single best method of NPs characterization (Domingos, Baalousha et al., 2009).

This study is intended to synthesize and fully characterize PVP-capped AgNPs with core size ± 10nm. Since there were no “off the shelf” method available to meet the aim of this study, the existing methods were modified. Two methods were chosen according to their practicality, which were method developed by Hoppe et al. (2006) and Mulfinger et al. (2007). Changing the chemical concentration ratio between $AgNO_3$ precursor and PVP polymer to the synthesis protocols developed by Hoppe et al (2006) and adding PVP capping agent to the Mulfinger et al (2007) procedure were applied in order to obtain a monodisperse AgNPs, defined by low polydispersity indices (PdI).

4.2. Aims and objectives

The aim of this study was to tightly constrain the synthesis of PVP-capped AgNPs to achieve intended core size ± 10nm with high stability in ecotoxicology media.

The objectives were:

1. To synthesis PVP-capped AgNPs with core size ±10 nm by modifying available synthesis protocols
2. To fully characterize the as-synthesised PVP-capped AgNPs by multi-method techniques to check the SPR, core and hydrodynamic size and zeta-potential
3. To assess the dissolution of PVP-capped AgNPs in pristine suspension and in ecotoxicology media.

4.3. Methodology

Details of synthesis and characterization method of PVP capped AgNPs have been presented in Chapter 3, section 3.3 – 3.7.

4.4. Results and discussion

4.4.1. Operationalizing the synthesis

Silver NPs were successfully synthesized in this study via bottom up methods. Heating and cooling processes were exercised in order to get a monodispherse PVP-capped AgNPs. At first glance, the colour change of the colourless silver nitrate solution to yellow was a preliminary indication that AgNPs were formed (Figure 4. 1). To verify this, the UV-Vis spectra were taken. An intense UV-Vis absorption peak around 400nm observed for all the samples and attributed to the AgNPs Surface Plasmon Resonance (SPR), confirmed the formation of AgNPs in the suspension

(Jana et al., 2001; Hoppe, Lazzari et al., 2006). The SPR was further analysed after the NPs were cleaned (section 4.4.3.1).

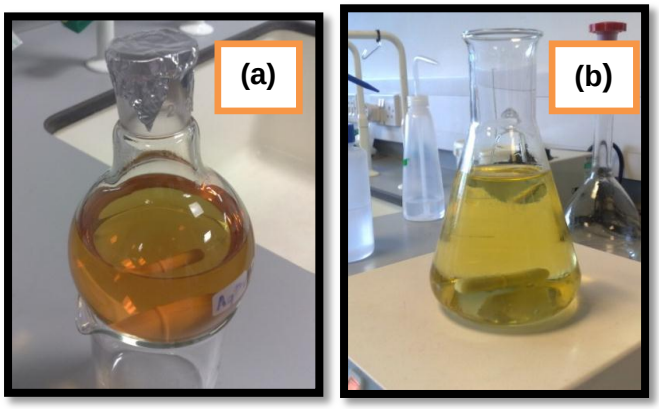

Figure 4. 1 PVP capped AgNPs generated from: (a) Hot process; and (b) Cold Process

In hot process, PVP were used as a steric stabilizer or capping agent as well as reducing agent. Dual function of PVP has been studied previously (Hoppe, Lazzari et al., 2006; Xiong, Washio et al., 2006). The reaction mechanism of AgNPs formation by the hot process has been proposed by Hoppe, et al. (2006). First, the metal ion promotes degradation of the PVP polymer by abstracting the hydrogen atom from the PVP molecule as presented in Figure 4. 2. Then the generated radical polymers responsible for silver ion reduction into metal silver (Hoppe, Lazzari et al., 2006).

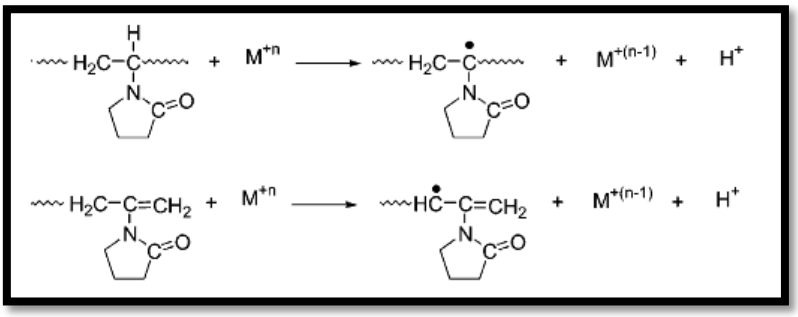

Figure 4. 2 Illustration of PVP molecule – metal ion interaction in metal NPs synthesis (Hoppe, Lazzari et al., 2006)

Zhang and colleagues proposed a different mechanism. Instead of forming the polymer radical, the metal ions form a coordination complex with the PVP polymer due to loan pair electrons donated from the oxygen and nitrogen atoms from

the pyrine ring of the PVP polymer to the *sp* orbital of silver ions as illustrated in Figure 4. 3 (Zhang, Zhao et al., 1996; Pattanaik and Bhaumik, 2000). The complexed Ag^+ ion is more easily reduced than the hydrated Ag^+ ion. By the action of the reducing agent, such as hydrazine or the hydroxyl end of the PVP molecule (Zhang, Zhao et al., 1996; Washio, Xiong et al., 2006), the nucleation occurs and silver ions turn into silver metal (Figure 4. 4).

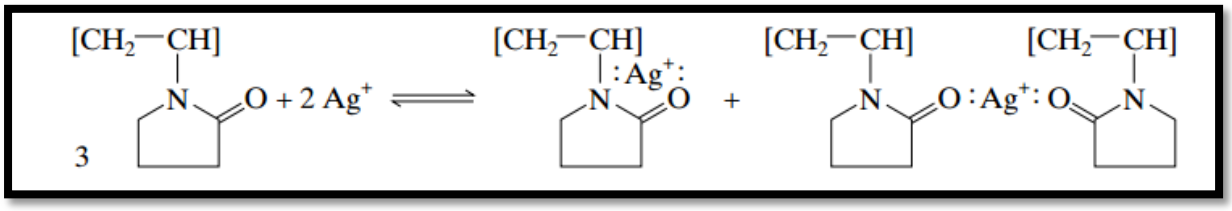

Figure 4. 3 Formation of silver ion-PVP complex (Zhang, Zhao et al., 1996)

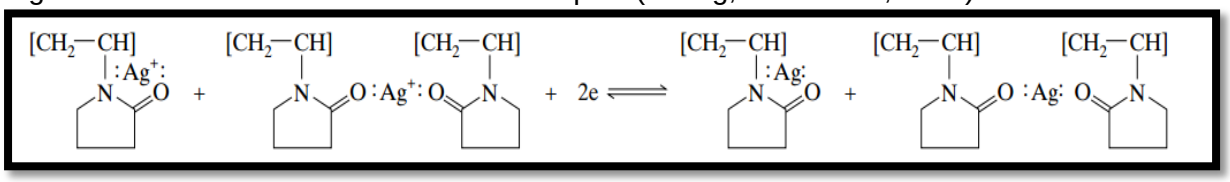

Figure 4. 4 Formation of PVP capped AgNPs (Zhang, Zhao et al., 1996)

In the hot process of this study, no additional reducing agent was added. Either formation of organic radicals (Hoppe, Lazzari et al., 2006) or weakly reducing hydroxyl-end of the PVP (Washio, Xiong et al., 2006) was exploited for reduction of Ag^+ into Ag^0. To improve the reaction rate, heat was employed (70^0C for 7 hours). The generated AgNPs from hot process (HP-AgNPs) was then capped by the PVP and protected from further growth and aggregation (Hoppe, Lazzari et al., 2006). The excess PVP from the AgNPs suspension is subsequently removed by a method of washing presented in section 3.6.

PVP-capped AgNPs were also generated by the cold process (CP-AgNPs). Since the $NaBH_4$ is a strong reducing agent, in this study the reaction speed was decelerated by cooling the temperature of the $NaBH_4$ solution and performing the

reaction in an ice bath as about 10nm particle diameter was the target size of this study. The mechanism of AgNPs formation by the cold process has also been proposed (Mulfinger, Solomon et al., 2007) and is presented in Equation 4. 1.

$$AgNO_3 + NaBH_4 \rightarrow Ag + \tfrac{1}{2} H_2 + \tfrac{1}{2} B_2H_6 + NaNO_3 \qquad \text{Equation 4. 1}$$

In case of no other capping molecule present in the suspension, the BH_4^- ion acts as an electrostatic capping agent and protect the NPs from aggregation as illustrated in Figure 4. 5.

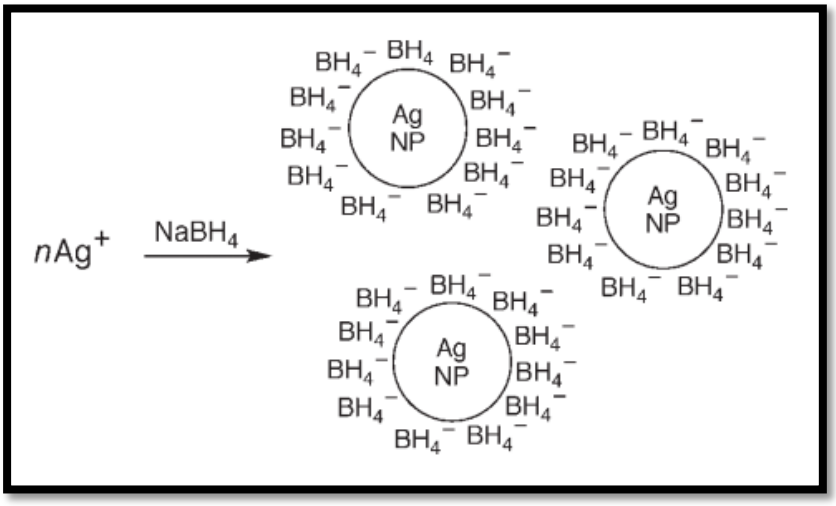

Figure 4. 5 Action of borohydride ion as the electrostatic capping agent of synthesized AgNPs generated by cold process (Mulfinger, Solomon et al., 2007)

In this study, the CP-AgNPs were further re-capped by PVP molecules. The occurrence of ligand-substitution (BH_4^- replacement by PVP polymer) was evaluated by analyzing the SPR alteration. Since the SPR is generated due to oscillation of the electron cloud on the NPs surface (Kelly, Coronado et al., 2003), the interruption of the NPs surface electron will be manifested as the alteration of the SPR (λ_{max}, FWHM, and or the A_{max}) (Malinsky et al., 2001; Haes and Van Duyne, 2002; El-Sayed, 2004; Endo et al., 2005). In this study, the addition of two different volumes of 0.3% $^m/_v$ $PVP_{(aq)}$ (5% and 15% of NPs suspension volume) into as-synthesized CP-AgNPs red-shifted the plasmon peak (about 25-30nm), and the SPR was further

shifted when more volume of PVP (aq) was added. PVP addition also increased the FWHM (38% and 48%, by 5% and 15% PVP, respectively) and maximum absorption (A_{max}) at about 70% for both PVP volume (Figure 4. 6), indicating the formation of PVP steric layer on the NPs surface.

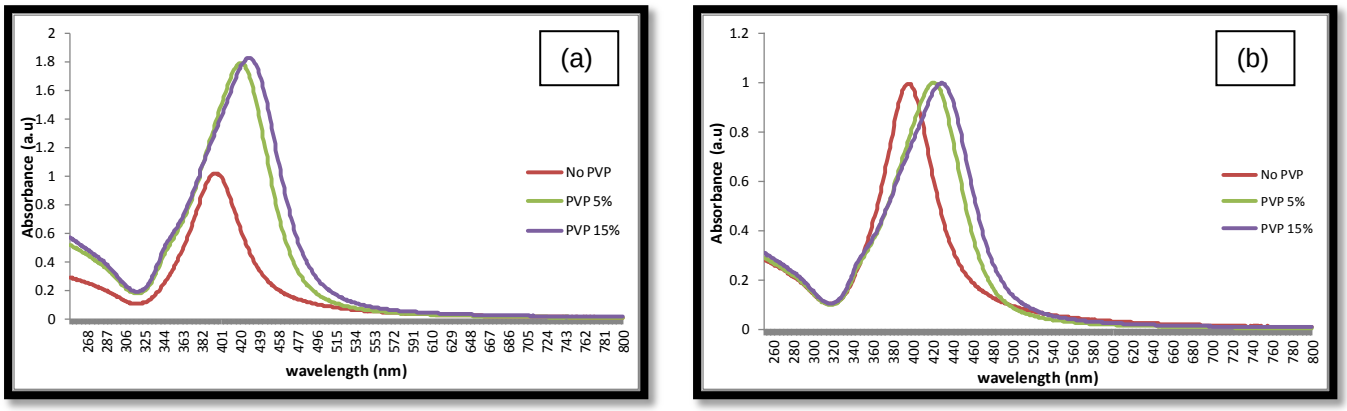

Figure 4. 6 (a) SPR comparison of AgNPs without and with two different volume of 0.3% m/v (5% and 15% v/v), (b) normalized of SPR peak at (a)

The un-reacted silver ions and other reactants were removed from the CP-AgNPs suspension to prevent further growth of AgNPs, using an ultrafiltration cell and 1 KDa regenerated cellulose membrane as presented in section 3.6.

4.4.2. Sample washing

The PVP-capped AgNPs synthesized by both processes were washed to remove excess reactants and reduce polydispersity. The washing methods were discussed in earlier section (3.6). No further analysis was performed on the removed PVP from HP-AgNPs but removed silver ion from CP-AgNPs was analysed by ICP-MS. At least six washes were needed to properly clean the CP-AgNPs suspension, indicated by constant silver ion concentration within the ultrafiltrate (Figure 4. 7). The convenience of using ultrafiltration for washing the nanoparticle suspensions has also been shown in other studies (Aymonier et al., 2002; El Badawy, Silva et al.,

2010). The relative concentration of the removed silver ions from each filtration step during the CP-AgNPs washing process was calculated using Equation 4. 2 and is shown in Table 4. 1.

$$\text{Relative silver ion concentration} = \frac{[Ag^+]_n}{[Ag^+]_{n=1}} \times 100\% \qquad \text{Equation 4. 2}$$

$[Ag^+]_n$: concentration of silver ion in the filtrate from each filtration step (n= 1 to 6)

$[Ag^+]_{n=1}$: concentration of silver ion in the 1st filtrate

Table 4. 1 Relative concentration of silver ion removed from CP-AgNPs washing process

Washing step	Normalised Ag^+ concentration
1st	100
2nd	44.39 ± 5.75
3rd	25.93 ± 5.52
4th	12.66 ± 3.42
5th	8.62 ± 3.48
6th	8.62 ± 1.69

± is a standard deviation of measurement, not a true replicate

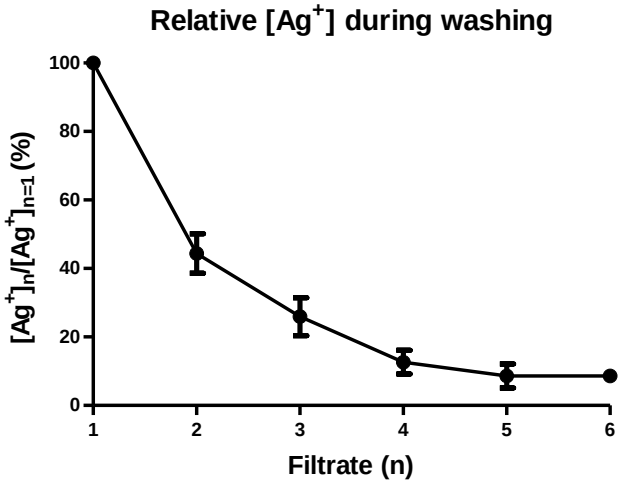

Figure 4. 7 The relative concentration of silver ion in the ultra-filtrate removed from the CP-AgNPs during NPs washing by ultrafiltration tabulate relative to total concentration.

After washing, the HP-AgNPs and CP-AgNPs were characterized to analyze their optical properties (SPR), hydrodynamic size, core size, shape factor and zeta potential. The characterization results are presented in the following section.

4.4.3. Characterization

The properties of HP-AgNPs and CP-AgNPs were characterized by multi method approach, using UV-Vis spectrometry to quantify SPR, DLS and Fl-FFF for measuring the AgNPs hydrodynamic diameter (d_H), TEM and AFM for NPs core size and shape factor analysis, and laser doppler velocimetry for NPs zeta potential measurement.

4.4.3.1. SPR characteristics

The SPR of HP-AgNPs and CP-AgNPs was compared. Figure 4. 8 and Figure 4. 9 show the SPR of HP-AgNPs and CP-AgNPs (CP1-CP5). The peak position (λ_{max}) and full width of half maximum (FWHM) of AgNPs plasmon peak are presented inTable 4. 2.

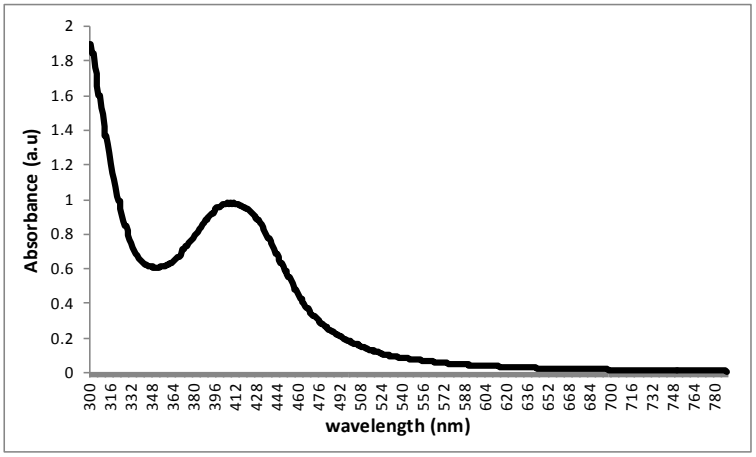

Figure 4. 8 The SPR of PVP capped AgNPs generated from hot process (HP-AgNPs)

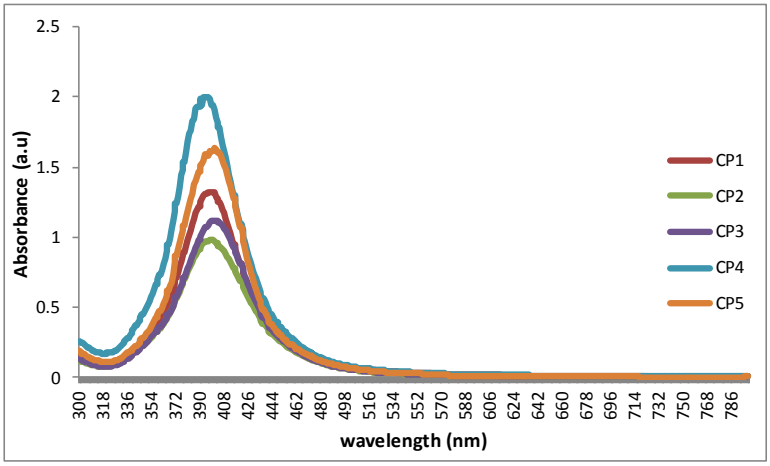

Figure 4. 9 SPR of PVP capped AgNPs generated by cold process with various reactant ratio and reaction condition

Table 4. 2 The peak position and width of HP- and CP-AgNPs plasmon

AgNPs	λ_{max} (nm)	FWHM (nm)
Hot Process	406 - 408	73
CP1	397	54
CP2	397	62
CP3	399	54
CP4	393-396	55
CP5	401	55

As presented inTable 4. 2, the SPR characteristics, both the λ_{max} and FWHM of HP- and CP-AgNPs were different. HP-AgNPs showed a longer λ_{max} and broader FWHM than CP-AgNPs. Since the optical properties of NPs depends on size, shape, polydispersity, refractive index, strength of the ligand-NPs interaction, etc, there were possible differences of those characteristics between HP- and CP-AgNPs. However, longer wavelength of λ_{max} and wider FWHM is usually attributed to larger and more polydisperse NPs sample (Heard et al., 1983; Schenk et al., 2012). Stronger interaction between capping-agent and NPs has also been reported to shift the Plasmon peak into longer wavelength (Ghosh et al., 2004). These qualitative

estimations were then further corroborated by other analysis techniques as will be discussed in the following section.

4.4.3.2. Hydrodynamic diameter (d_H) and size distribution by DLS and Fl-FFF

The d_H measurement result by DLS is presented as size distribution by intensity (), and as the zeta-average, peak 1 size by intensity and PdI of HP- and CP-AgNPs (Table 4. 3).

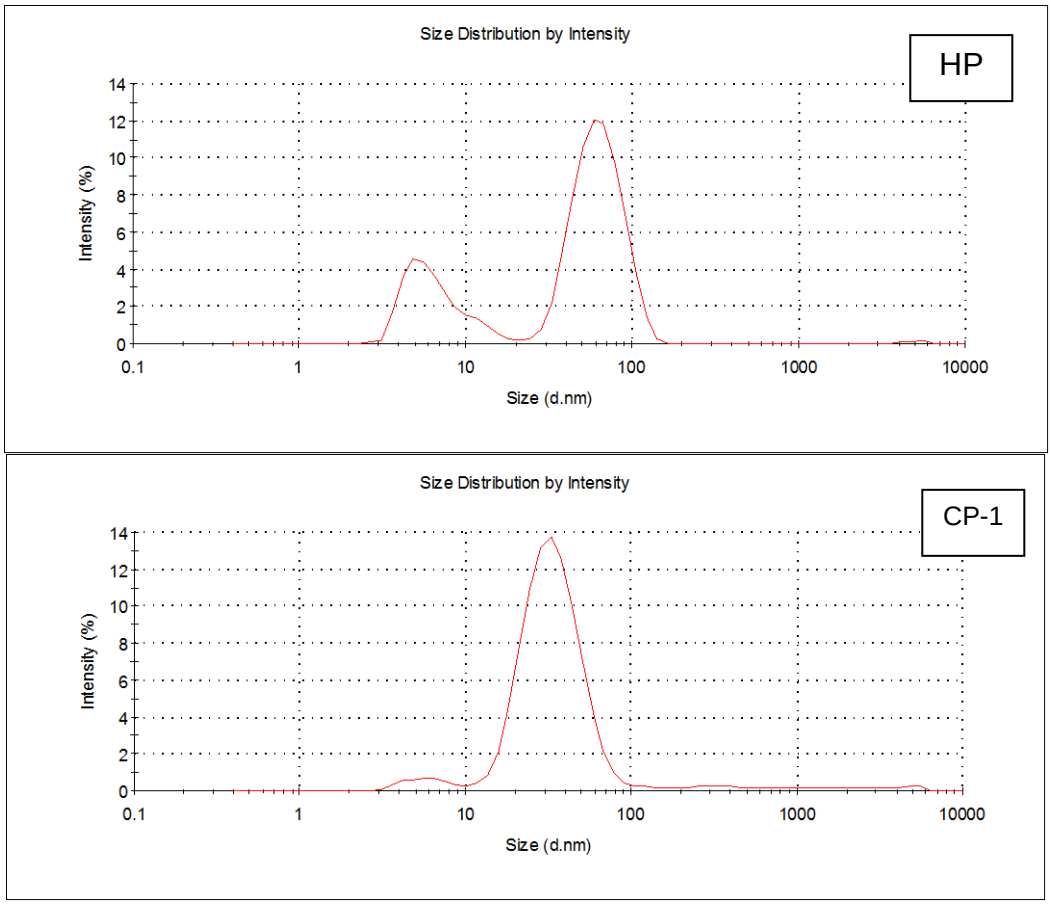

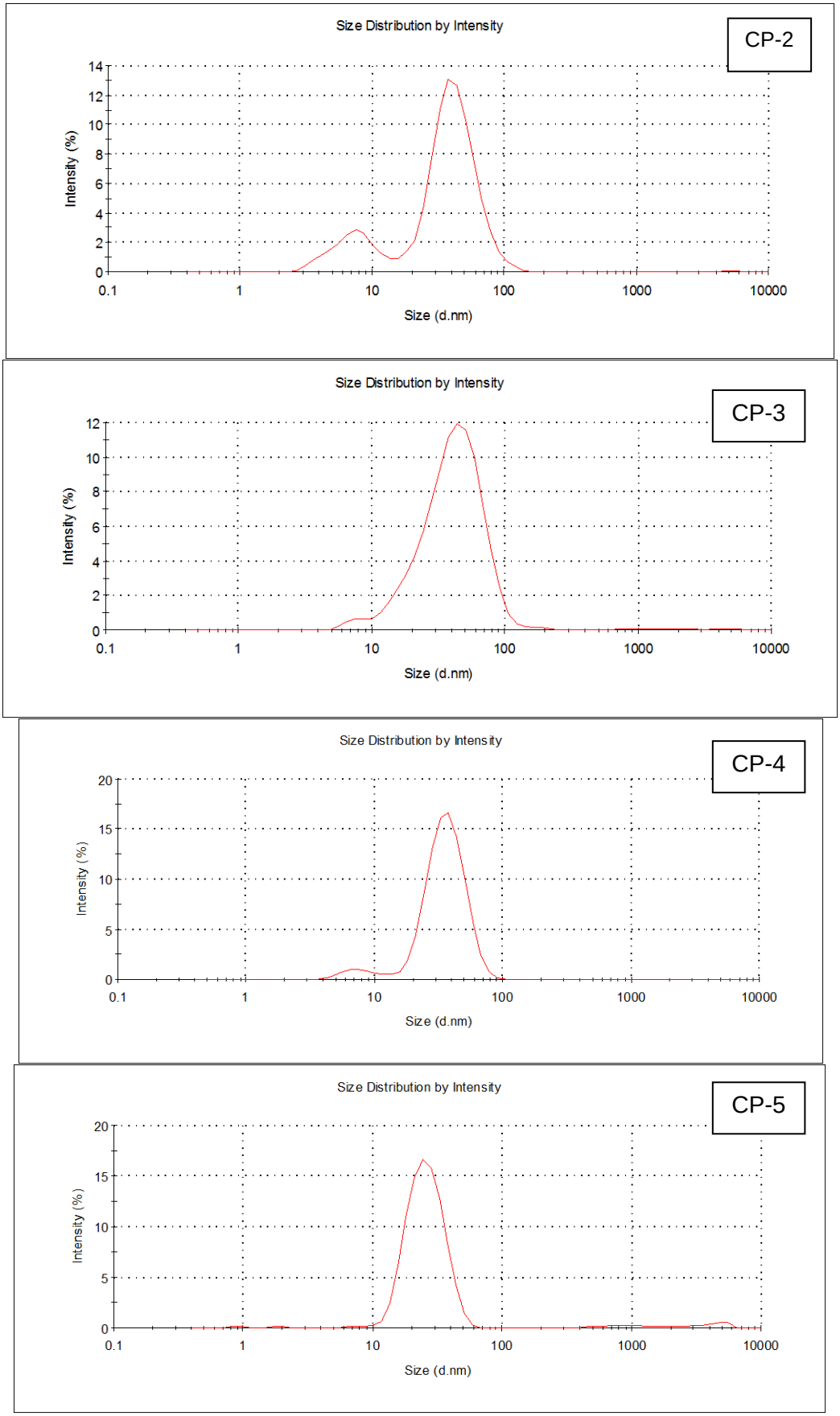

Figure 4. 10 Size distribution by Intensity of AgNPs from hot process and cold process measured by DLS

Table 4. 3 The d_H and PdI of HP-AgNPs and CP-AgNPs measured by DLS

AgNPs	z-average (nm)	PdI	Peak 1 size by intensity
Hot process	22.23 ± 0.69	0.66 ± 0.03	64.62 ± 4.38 (72.2%)
CP1	25.90 ± 0.13	0.48 ± 0.00	51.18 ± 6.91 (80.4%)
CP2	22.79 ± 0.45	0.42 ± 0.03	34.6 ± 3.99 (90.5%)
CP3	28.99 ± 0.56	0.39 ± 0.03	42.23 ± 4.91 (85%)
CP4	26.48 ± 0.83	0.28 ± 0.01	34.42 ± 2.19 (94%)
CP5	21.62 ± 0.26	0.27 ± 0.02	25.55 ± 0.41 (96%)

± represent standard deviation of the measurement, not standard deviation of true replicates.

As can be seen from the DLS results (Figure 4.10), most of the NPs samples gave a bimodal size distribution. Only CP-5 showed a monodisperse size distribution (96% by intensity) as confirmed by the lowest PdI value (0.27). As has been mentioned earlier that SPR width indicates the polydispersity of particle suspension, the correlation was seen in this study where HP-AgNPs with its wider plasmon peak showed highest PdI value Table 4. 4. However no statistical analysis can be presented due to limited number of data.

Table 4. 4 FWHM and PdI of as-synthesised AgNPs

AgNPs	FWHM (nm)	PdI
Hot process	73	0.66 ± 0.03
CP1	54	0.48 ± 0.00
CP2	62	0.42 ± 0.03
CP3	54	0.39 ± 0.03
CP4	55	0.28 ± 0.01

The d_H of synthesized AgNPs was further measured by Fl-FFF. Figure 4. 11 and Figure 4. 12 illustrate the d_H distribution of HP-AgNPs and CP-AgNPs respectively. The fractogram of HP-AgNPs and CP-1 were positively skewed, confirmed the presence of larger particles that make higher polydispersity of the

samples as shown by higher PdI value from DLS. Table 4. 5 presents the calculated weight average (d_w) of AgNPs after compared with standard polystyrene 20nm and 30nm.

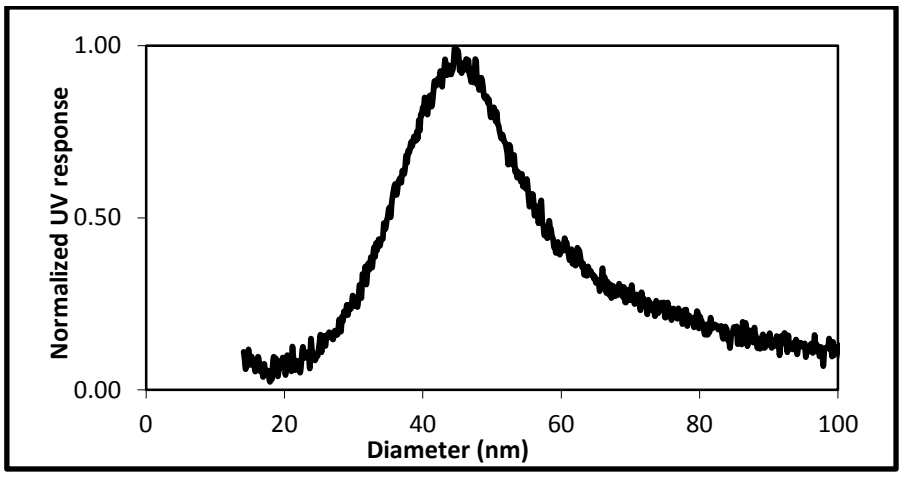

Figure 4. 11 d_H size of HP-AgNPs analysed by Fl-FFF

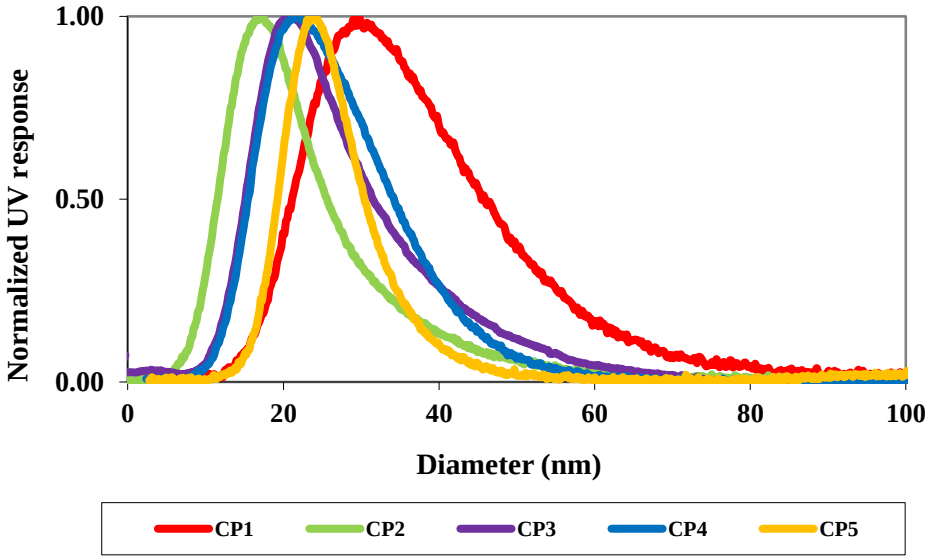

Figure 4. 12 d_H size of CP-AgNPs analysed by Fl-FFF

Table 4. 5 Calculated d_H of AgNPs analysed by Fl-FFF and standardize by 20nm and 30nm polystyrene NPs

AgNPs	d_H size by Fl-FFF
Hot Process	34.93 ± 2.24
CP1	41.90 ± 0.38
CP2	27.88 ± 0.47
CP3	27.22 ± 2.20
CP4	29.23 ± 0.95
CP5	28.14 ± 1.75

± represent standard deviation of the measurement, not standard deviation of true replicates.

From the d_H measurement results, it was corroborated that the HP-AgNPs was the most polydisperse synthesized AgNPs (PdI= 0.66). Gradual increase of the temperature and also mild strength of reducing agent lead to relatively slow reduction and nucleation rate (Kim et al., 2006; Patakfalvi, Papp et al., 2007) which allow the NP nucleation and growth process to occur at the same time. If the nucleation and growth process could not be separated temporally it would potentially lead to the generation of polydisperse particles (Sugimoto, 1987; Patakfalvi, Papp et al., 2007) as was found with HP sample.

The cold process, on the other hand, allowed faster reduction of Ag^+ into Ag^0 as it used $NaBH_4$, a strong reducing agent. Varying the stir duration as well as the mass ratio of reactant, however, could not control the generated particle size as the reducing action of $NaBH_4$ was extremely strong. Fast reduction endorsed fast nucleation step and then the PVP polymer arrested the growth of particles. Thus, in general, CP-AgNPs were more monodisperse than HP-AgNPs, and the lowest PdI (0.27) was achieved by adding the capping $PVP_{(aq)}$ in advance, before the reduction and nucleation took place (reaction condition 5). Since the intended particles has been generated by experiment condition 5, no further experiment conditions were examined.

4.4.3.3. Core size by TEM and AFM

The core sizes of HP- and CP-AgNPs were analysed by TEM and AFM. The TEM micrographs of HP- and CP-AgNPs were taken and the size and shape factor were analysed by using Gatan Digital Micrograph and ImageJ software. The core size was then averaged from > 100 particles and the shape factor from > 50 NPs, and the results are presented in Table 4. 6.

The topographic images of AgNPs adsorbed onto a mica surface were taken using AFM. The core size (height) of AgNPs was measured using XEI software from at least 100 particles, apart from CP2 (only 53 particles) and the result is presented in Table 4. 7.

Table 4. 6 TEM images and core size analysis of PVP-capped AgNPs

AgNPs and average size	TEM Images	Size distribution
HP-AgNPs Size = 25.81 ± 9.44 nm (n=117) Shape factor = 0.93 ± 0.04	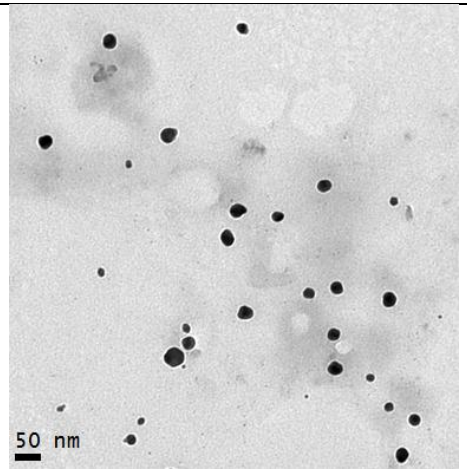	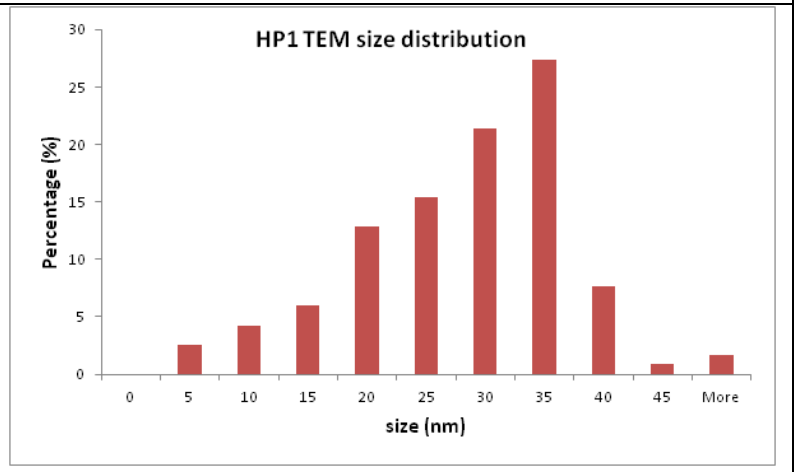
CP1 Size = 16.02 ± 8.42 (n=118) Shape factor = 0.94 ± 0.03	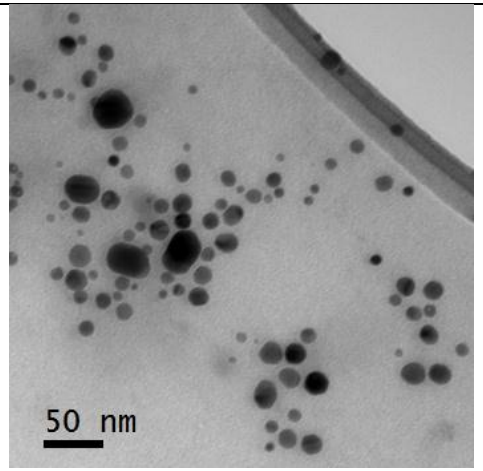	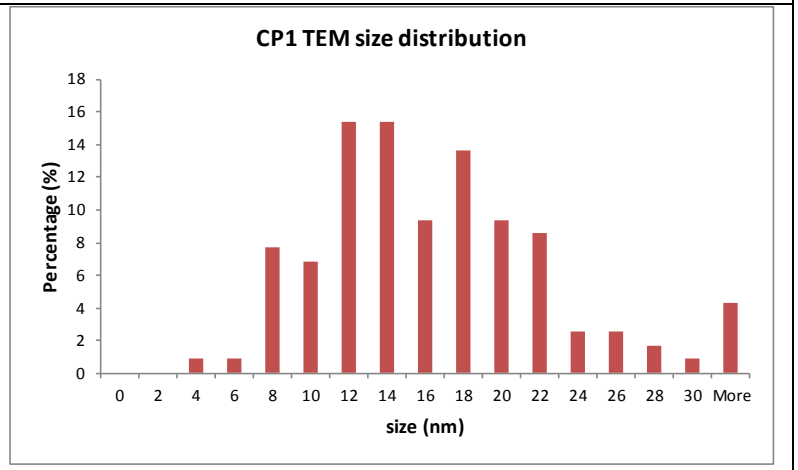

CP2 Size = 11.1 ± 2.9 (n=116) Shape factor = 0.92 ± 0.05	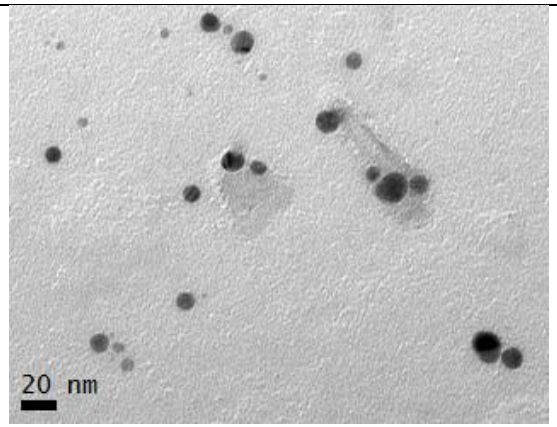	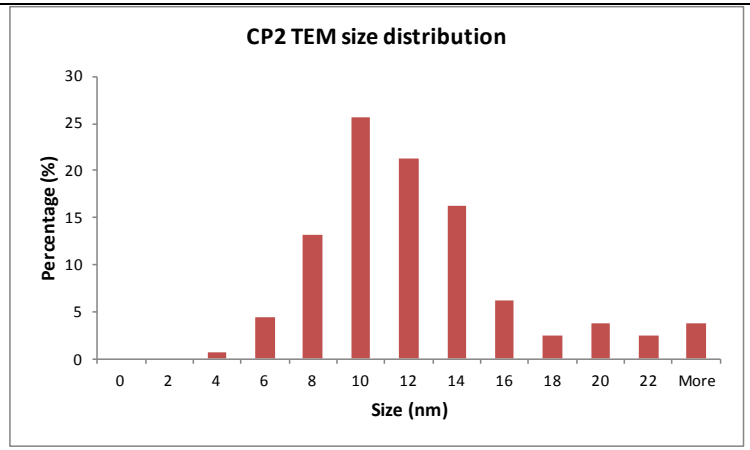
CP3 Size = 12.04 ± 4.52 (n=143) Shape factor = 0.87 ± 0.06	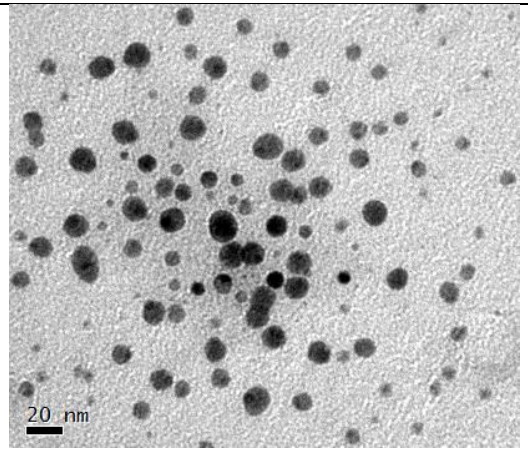	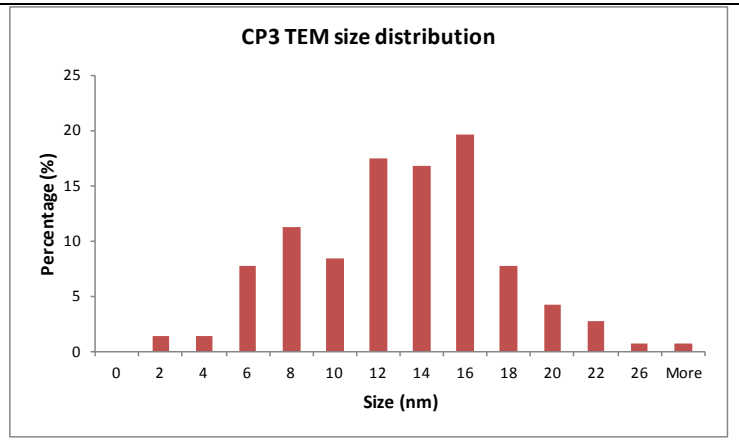

CP4 Size = 10.56 ± 3.16 (n=113) Shape factor = 0.89 ± 0.07	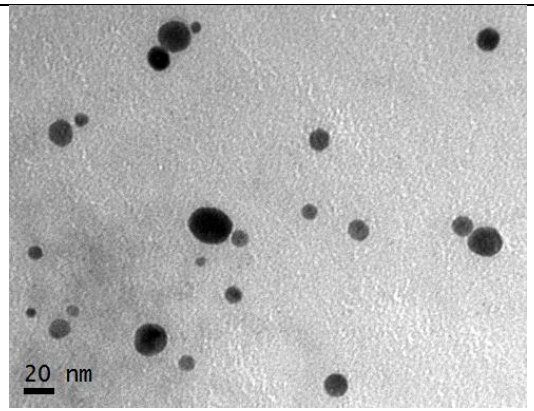	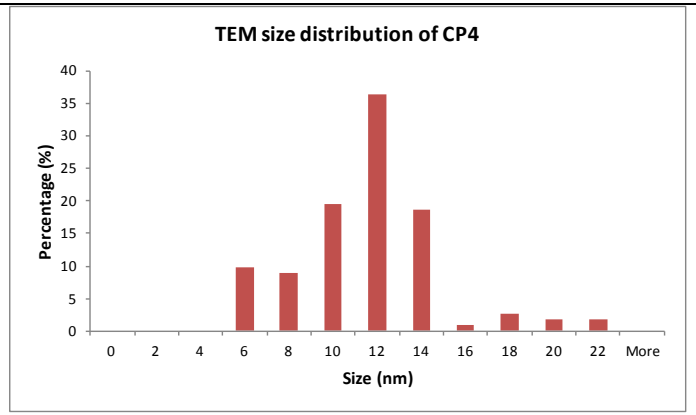
CP5 Size = 10.83 ± 3.30 (n=158) Shape factor = 0.88 ± 0.05	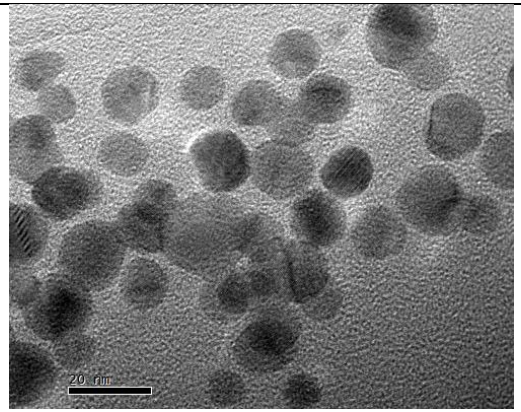	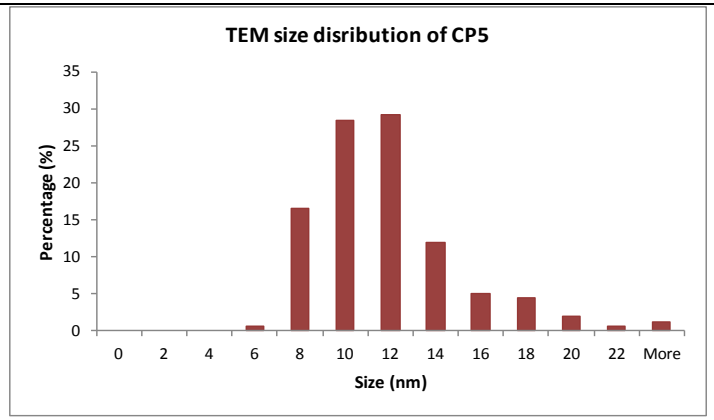

± represent standard deviation of the measurement, not standard deviation of true replicates

Table 4. 7 AFM topographic image and core size analysis of PVP-capped AgNPs

HP 11.68 ± 5.86 nm (n= 100)	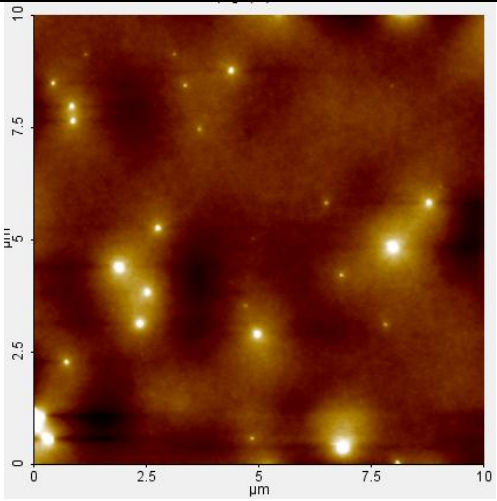	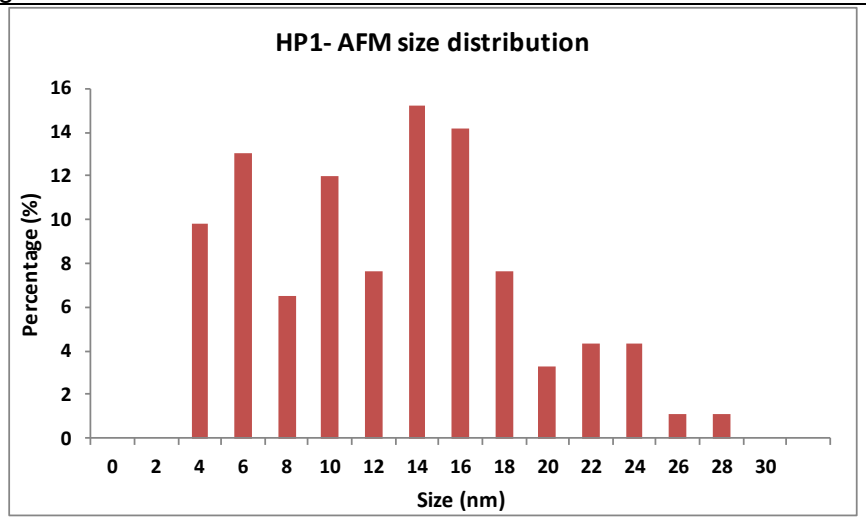
CP 1 8.79 ± 4.06 nm (n=136)	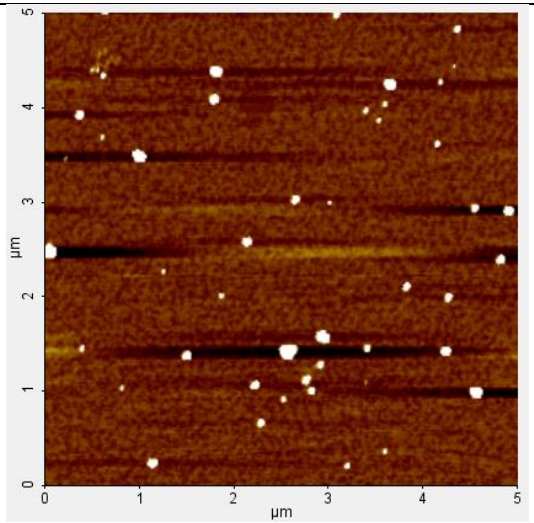	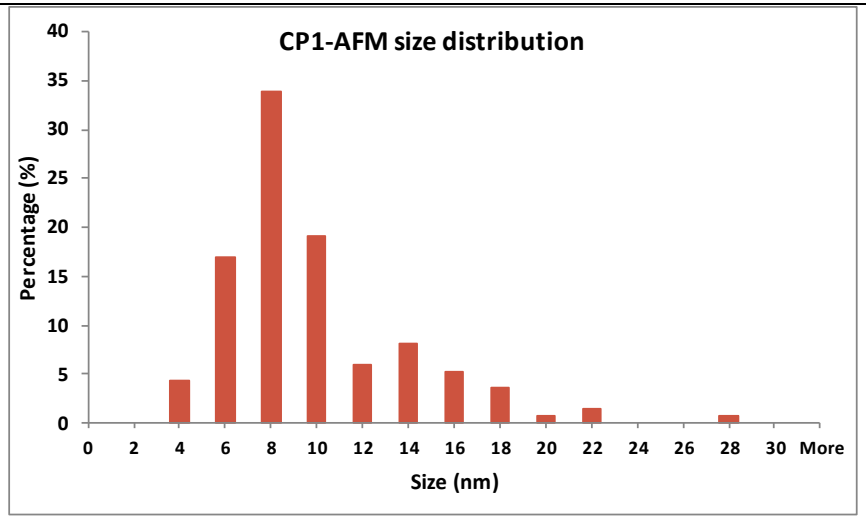

CP2 15.22 ± 9.04 (n=53)	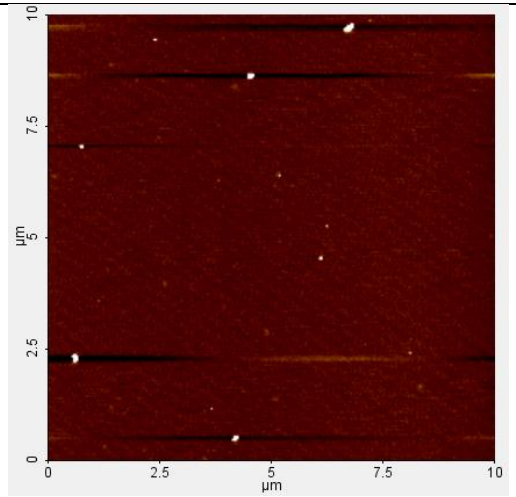	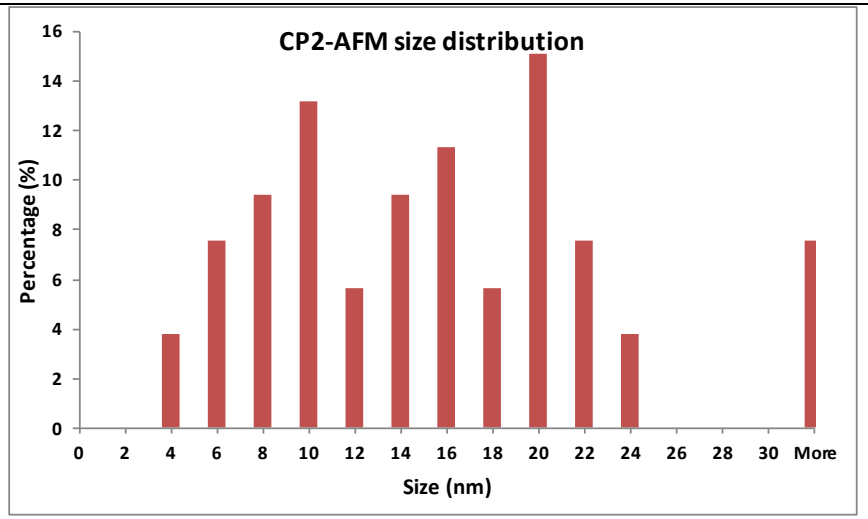
CP3 18.00 ± 11.27 (n=104)	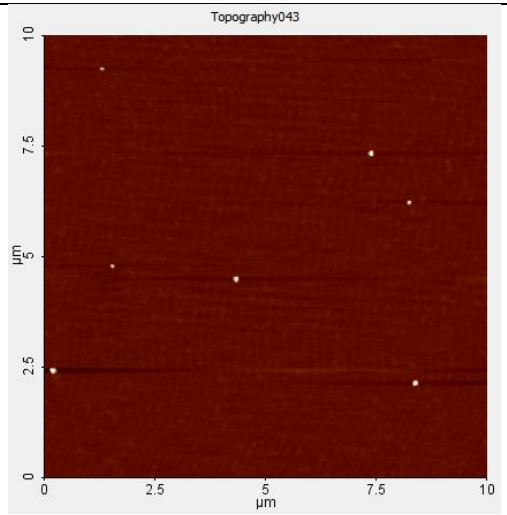	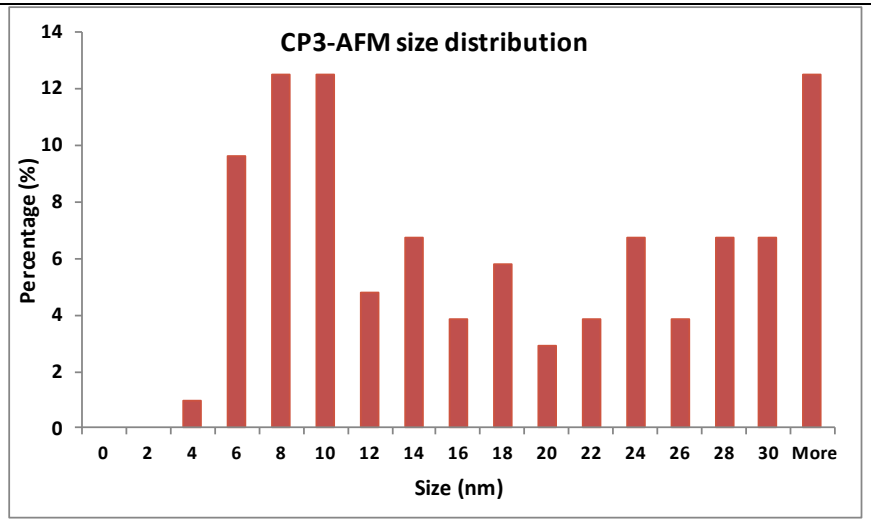

CP4 10.17 ± 8.44 (n=100)	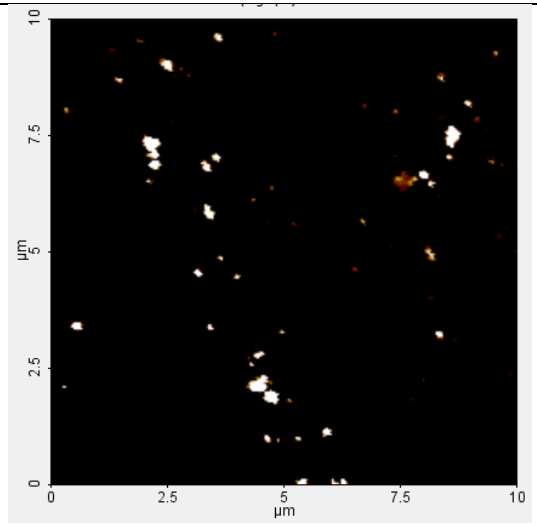	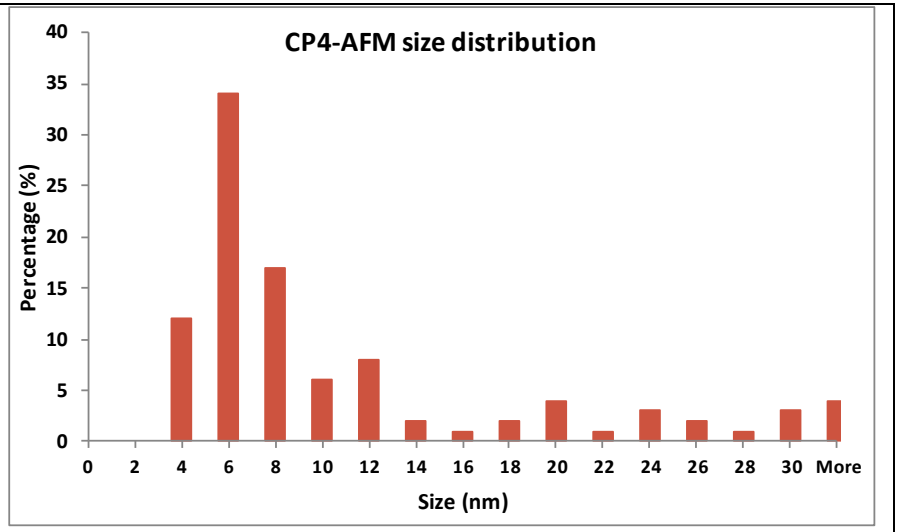
CP5 11.93 ± 5.13 (n=110)	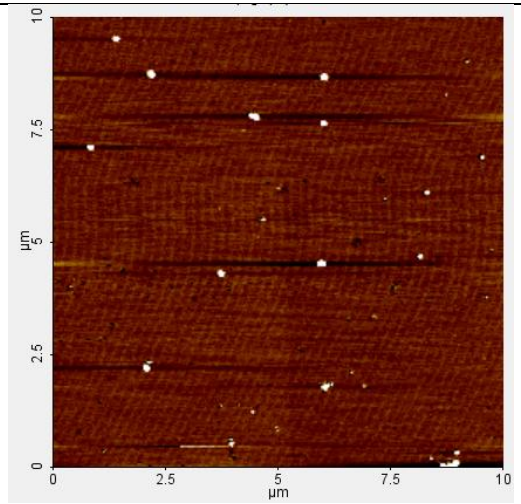	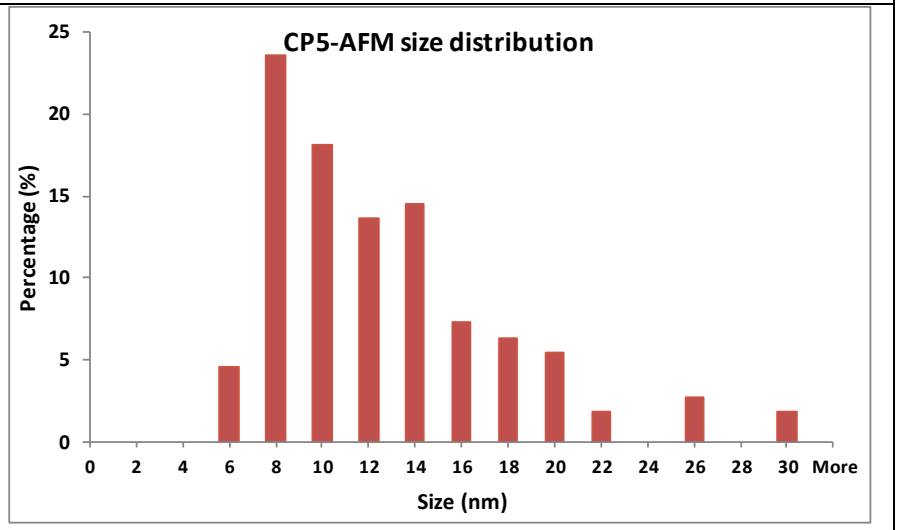

± represent standard deviation of the measurement, not standard deviation of true replicates

Table 4. 8 Comparison of core size measured by TEM and AFM

AgNPs	d_{TEM} (nm)	d_{AFM} (nm)	d_{TEM}/d_{AFM}
HP	Size = 25.81 ± 9.44 nm	11.68 ± 5.86 nm	2.21
CP1	Size = 16.02 ± 8.42	8.79 ± 4.06 nm	1.82
CP2	Size = 11.1 ± 2.9	15.22 ± 9.04	0.73
CP3	Size = 12.04 ± 4.52	18.00 ± 11.27	0.67
CP4	Size = 10.56 ± 3.16	10.17 ± 8.44	1.04
CP5	Size = 10.83 ± 3.30	11.93 ± 5.13	0.91

The shape factor of the NPs was analysed by ImageJ and are presented in Table 4. 6. The shape factor of all the NPs was close to 1 (0.88 – 0.94), a value for a spherical shape (Wilkinson and Lead, 2007), as also seen from the TEM micrograph. Since the TEM and AFM measure the lateral diameter and topographic height of the particle respectively, the shape factor can also be inferred from the ratio of TEM and AFM size (d_{TEM}/d_{AFM}) (Domingos, Baalousha et al., 2009) and the ratio of d_{TEM}/d_{AFM} from particles generated in this study ranged from 0.67 – 2.21 (Table 4. 8). The $d_{TEM}/d_{AFM} \approx 1$, however, was only obtained from CP4 and CP5, the particles which have the lowest PdI in this study. The highest ratio of d_{TEM}/d_{AFM} was found from HP-AgNPs (2.21), and the lowest from CP3 (0.67). The discrepancy between the shape factor analysis result from TEM and the ratio of d_{TEM}/d_{AFM} was due to the broadness of the TEM and the AFM size distributions. Thus, shape factor determination by ImageJ software might be more accurate than comparing the d_{TEM}/d_{AFM} for polydisperse NPs suspensions.

4.4.3.4. Elemental analysis by EDX

The EDX spectrums of single particle and clumps of AgNPs from CP5 sample were also taken and are compared with the EDX spectrum of the background (grid only) (Figure 4. 13).

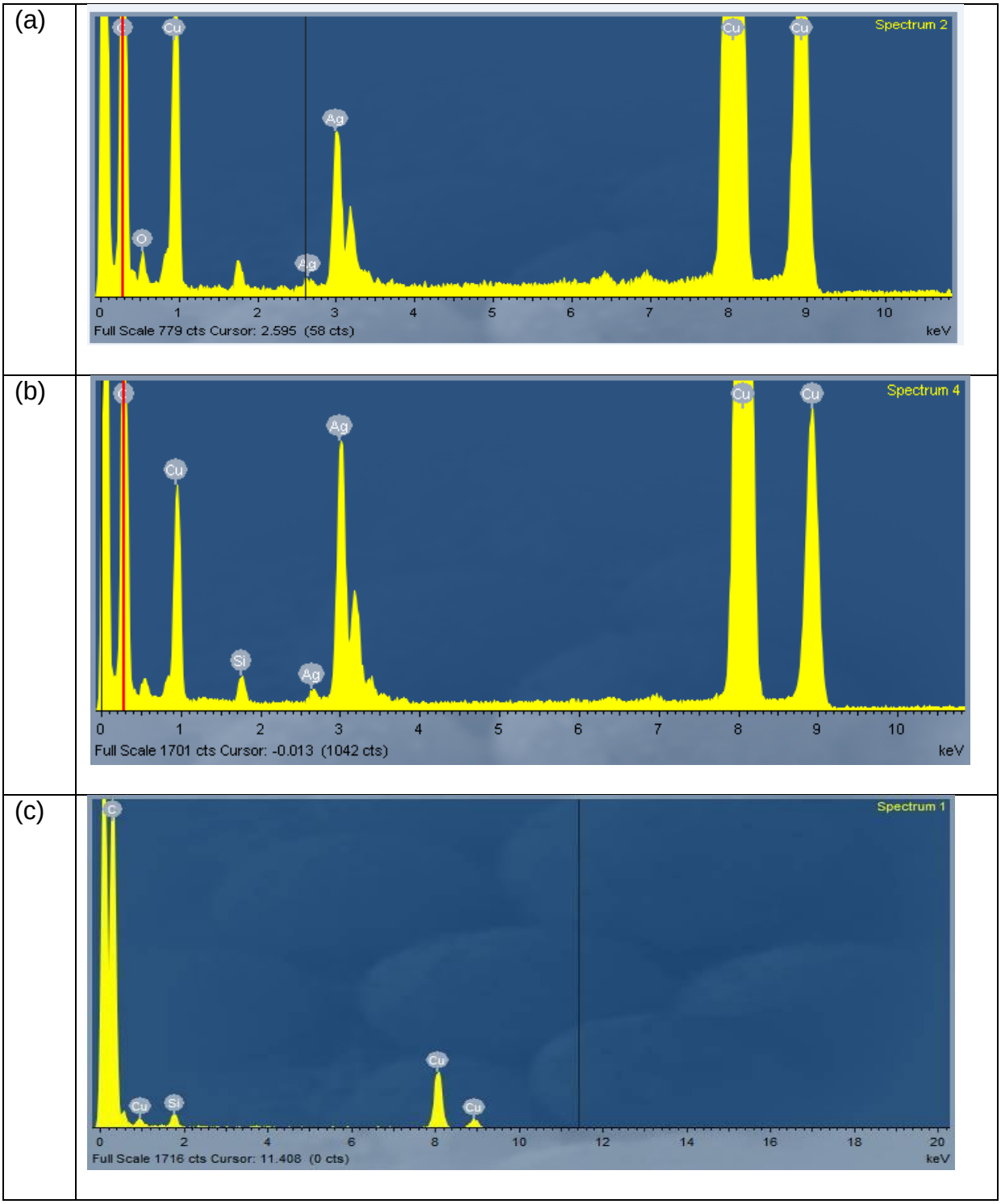

Figure 4. 13 EDX spectrum of (a) single particles, and (b) clumps of particles from CP5 sample, and (c) background (EDX spectrum of Cu drid only)

In Figure 4. 13.(a), and (b) Ag peaks are clearly seen, verify the formation of AgNPs. The Cu and Si peak were also found from the sample spectrum, as well as from the background (Figure 4. 13.(c)), which correspond to the Cu grid that was used for preparing the TEM sample. The oxygen peak is also seen (at 0.5 keV), which might be attributed to the presence of either oxygen-containing polymer coating the AgNP, surface silver oxide, or other source of oxygen contamination. Nonetheless, clearly, the formed NPs were AgNPs.

4.4.3.5. Zeta potential

The zeta potential of HP- and CP-capped AgNPs are presented in Table 4. 9. It is seen that the HP-AgNPs has less negative zeta potential and closer to zero value than the zeta potential of CP-AgNPs, suggesting a thicker layer of PVP polymer coated the HP-AgNPs as was seen by AFM.

Zeta potential was correlated with NPs stability as lower than -30mV of larger than +30mV has been used as cut-off for NPs stability. Those correlation, however was only for electrostatically capped particles(Torrey et al., 2006). In this case, the particles were capped sterically by PVP polymer and the stability could not accurately represented by their zeta potential value.

Table 4. 9 Zeta potential of PVP capped AgNPs

AgNPs	Zeta potential (mV)
Hot process	-01.03 ± 0.32
CP1	-15.6 ± 0.63
CP2	-10.0 ± 2.61
CP3	-20.7 ± 3.86
CP4	-10.2 ± 0.31
CP5	-12.4 ± 2.39

4.4.4. Summary of characterization result

The summary of characterization result is presented in Table 4. 10.

Table 4. 10 Summary of PVP capped AgNPs characteristics, analysed by different instruments

Characteristics		HP	CP1	CP2	CP3	CP4	CP5
SPR	**λ_{max}**	401-404	397	397	399	393-396	401
	FWHM	73	54	62	54	55	55
DLS	**d_H size**	22.23 ± 0.69	25.90 ± 0.13	22.79 ± 0.45	28.99 ± 0.56	26.48 ± 0.83	22.55 ± 0.41
	PdI*	0.66 ± 0.03	0.48 ± 0.00	0.42 ± 0.03	0.39 ± 0.03	0.28 ± 0.01	0.27 ± 0.02
FFF	**d_H size**	34.93 ± 2.24	41.90 ± 0.38	27.88 ± 0.47	27.22 ± 2.20	29.23 ± 0.95	28.14 ± 1.75
TEM	**Core size**	25.81 ± 9.44	16.02 ± 8.42	11.1 ± 2.9	12.04 ± 4.52	10.56 ± 3.16	10.83 ± 3.30
	Shape factor	0.93 ± 0.04	0.94 ± 0.03	0.92 ± 0.05	0.87 ± 0.06	0.89 ± 0.07	0.88 ± 0.05
AFM	**Core size**	11.68 ± 5.86	8.79 ± 4.06	15.22 ± 9.04	18.00 ± 11.27	10.17 ± 8.44	11.93 ± 5.13
Zeta potential (mV)		-01.03 ± 0.32	-15.6 ± 0.63	-10.0 ± 2.61	-20.7 ± 3.86	-10.2 ± 0.31	-12.4 ± 2.39

*PdI < 0.1 : monodisperse
0.1 < PdI < 0.2 : narrow size distribution
0.2 < PdI < 0.5 : broad size distribution
(Lohrke et al., 2008)

4.4.5. Sizes ratio and polydispersity indices

The correlation between the ratio of sizes (Table 4. 11) and polydispersity indices (Table 4. 12) was evaluated (Table 4. 13). Very strong correlation was shown between the PdI and the ratio of d_H -DLS/d_{TEM} (r= -0.9) and d_{TEM}/d_{AFM} (r= 0.79) (Figure 4. 14) but only moderate correlation with d_H-DLS/ d_H-Fl-FFF (d=0.68). Lesser correlation was also found between RSD-Fl-FFF and the ratio of d_H Fl-FFF/d_{TEM} (r= -0.5) and d_H Fl-FFF/$d_{AFM,}$ (r= -0.57). Stronger correlation was shown between RSD-TEM and d_{TEM}/d_{AFM} (r= 0.58) than RSD-AFM with d_{TEM}/d_{AFM} (r= -0.39). From the result above, it was found that PdI from DLS showed a better measure of polydispersity of the samples than relative standard deviation (RSD) from other techniques for these samples due to relatively broad size distribution (DLS PdI > 0.27) (Lohrke, Briel et al., 2008; Baalousha and Lead, 2012).

Table 4. 11 The ratios of AgNPs sizes measured by different technique

	d_H-FlFFF/d_H-DLS	d_H-DLS /d_{TEM}	d_H-DLS /d_{AFM}	d_H-FlFFF /d_{TEM}	d_H-FlFFF /d_{AFM}	d_{TEM}/d_{AFM}
HP	1.57	0.86	1.90	1.35	2.99	2.21
CP1	1.62	1.62	2.95	2.62	4.77	1.82
CP2	1.22	2.05	1.50	2.51	1.83	0.73
CP3	0.94	2.41	1.61	2.26	1.51	0.67
CP4	1.10	2.51	2.60	2.77	2.87	1.04
CP5	1.25	2.08	1.89	2.60	2.36	0.91

Table 4. 12 Polydispersity indices of AgNPs from different size measurement technique

	PdI	**RSD-Fl-FFF**	**RSD-TEM**	**RSD-AFM**
HP	0.66	0.06	0.37	0.50
CP1	0.48	0.01	0.53	0.46
CP2	0.42	0.02	0.26	0.59
CP3	0.39	0.08	0.38	0.63
CP4	0.28	0.03	0.30	0.83
CP5	0.27	0.06	0.30	0.43

Table 4. 13 Pearson's correlation between the size ratio and polydipersity indices

Pearson Correlation (r)	Size ratio					
	d_H-DLS/d_H-Fl-FFF	d_H-DLS /d_{TEM}	d_H-DLS /d_{AFM}	d_H-Fl-FFF /d_{TEM}	d_H-Fl-FFF /d_{AFM}	d_{TEM}/d_{AFM}
PdI	**0.68**	**-0.9**	-0.05			**0.79**
RSD-Fl-FFF	-0.41			-0.5	-0.57	
RSD-TEM		-0.37		-0.08		0.58
RSD-AFM			0.1		-0.28	-0.39

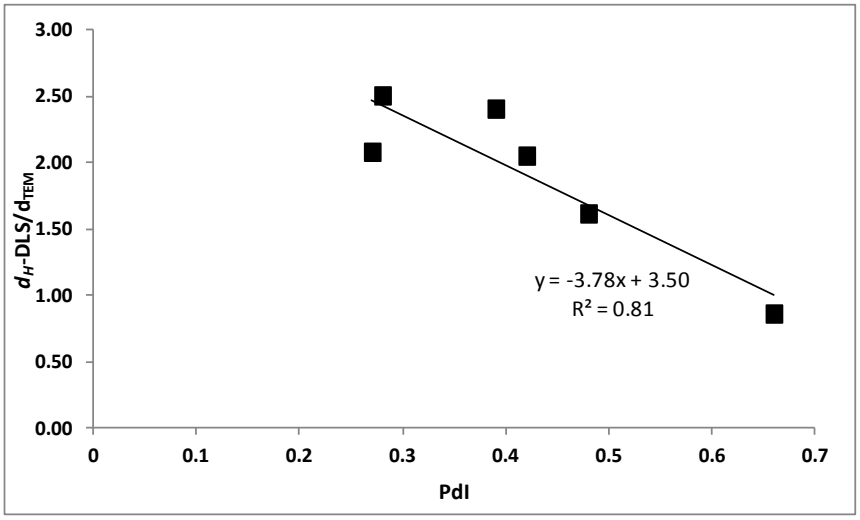

Figure 4. 14 Linear correlation between the ratio of dH-DLS/dTEM and PdI value

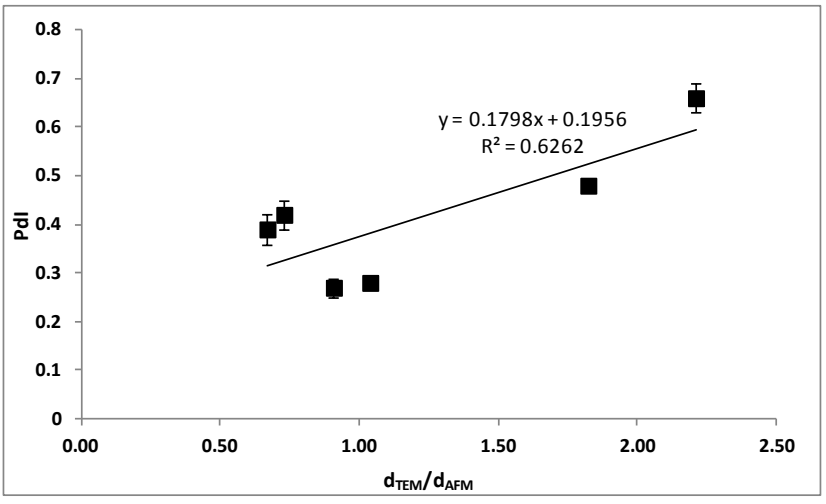

Figure 4. 15 Linear correlation between the ratio of d_{TEM}/d_{AFM} with PdI value

4.4.6. Preliminary solubility study of AgNPs in pristine suspension and ecotoxicology media

AgNPs has been revealed to be dissolving during storage (Templeton et al., 2006) as well as during incubation in an electrolyte media (Liu and Hurt, 2010; Liu et al., 2010; Li and Lenhart, 2012). It was agreed that the dissolution of AgNPs was preceded by an oxidation process as presented in following chemical reaction (Liu and Hurt, 2010):

$$4Ag^0 + O_2 \rightarrow 2Ag_2O \qquad \text{Equation 4. 3}$$

$$2Ag_2O + 4H^+ \rightarrow 4Ag^+ + 2H_2O \qquad \text{Equation 4. 4}$$

Presenting solubility and dissolution of NPs as part of the characterization in eco(toxicology) study is very recommended (Thomas, Judd et al., 1999; Lin et al., 2006; Foss Hansen, Larsen et al., 2007; Stone et al., 2010) as the toxicity of AgNPs might be associated with the released ion. Thus, in this study, the preliminary solubility of CP5, was characterized. The challenge was to avoid material Ag^+ loss due to adsorption as it is known that Ag^+ adsorptivity to surfaces is high, especially to borosilica glass (West, West et al., 1966; Struempler, 1973). All the experiments, thus were performed using acid and $Ca(NO_3)_{(aq)}$ treated HDPE plastic container to minimize Ag^+ loss due to adsorption to the container walls as has been mentioned earlier in section 3.9.

Ecotoxicology media used for dissolution study were full strength (CM-1) and ten-fold dillution (CM-10) *Daphnia sp.* media (CM-1) and modification of CM-1 (Nitrate media or NM), both full strength (NM-1) and ten-fold dilution (NM-10). The media composition are illustrated in section 3.2.3, page 56.

4.4.6.1. Dissolution in pristine suspension, a preliminary study

In this study, the amount of silver ion released from CP5-AgNPs in pristine suspension and after 21 days incubation in OECD *Daphnia magna sp*. media (CM-1) and its modification (NM-1), both the concentrate and dilution media (section 3.2.3) were analyzed. Ultrafiltration technique was used for ion separation. There was a 39% increase of Ag^+ concentration in the stock suspension within 7 days storage time, and continue to increase up to 58% at day 10 (Table 4. 14). Since the NPs were not stored in an anaerobic condition, the oxidation process might cause the AgNPs to dissolve.

Table 4. 14 Amount of dissolved silver ion (ppb) in pristine suspension over time

Time (day)	Stock 1 (n=1)	Stock 2 (n=1)
0	78.72	218.27
7	109.18	
10		345.82
% increase of Ag^+	38.69	58.44

In a full strength OECD media (CM-1) and its dilution (CM-10), surprisingly, the Ag^+ concentration decreased significantly at the end of 21 days of incubation, by 68.6% and 32.3% respectively (Table 4. 15). Apparently, the presence of soft bases in the media, especially chloride, controlled the amount of Ag^+ concentration in the suspension by forming silver-base complexes. These phenomena has also been reported in many other studies (Mehra and Gubeli, 1971; Ratte, 1999; Choi et al., 2009; Park et al., 2009; Liu and Hurt, 2010; Xiu et al., 2011; Levard, Hotze et al., 2012).There is also possibility of Ag^+ attachment to the filter and plastic ware but was not evaluated in this study.

Table 4. 15 Amount of dissolved silver ion (ppb) in test media after 21 days incubation

Time (day)	Media (n=1)			
	CM-1	CM-10	NM-1	NM-10
0	38.38	38.38	38.38	38.38
21	12.06	25.98	163.1	614.9
% increase of Ag^+	-68.6	-32.3	325.0	1502.1

Different species of silver-base complexes and the corresponding solubility equilibrium constant (K_{sp}) are presented in Table 4. 16. Minimal amount of Ag^+ required for formation of silver-base complexes was calculated according to the Ksp data (Table 4. 16) and are presented in Table 4. 18. It is seen that the lowest Ag^+ concentration required for Ag-complex formation was for the AgCl formation in CM-1 (4.4×10^{-8} M), followed by AgCl formation in CM-10 (4.4×10^{-7} M). Then Ag^+ was also required at relatively higher concentration (1.1×10^{-4}M) for Ag_2CO_3 formation both in CM-1 and NM-1. For that reason, potentially, the released Ag^+ from the suspension of AgNPs CP5 in CM-1 and CM-10 was consumed for, likely AgCl complex formation.

Table 4. 16 Silver-anion complexes and the Ksp (Jonte and Martin Jr, 1952; Shakhashiri et al., 1980)

Silver compound	Ksp
Silver sulfide, AgS	8×10^{-51}
Silver phosphate, Ag_3PO_4	8.89×10^{-17}
Silver carbonate, Ag_2CO_3	8.46×10^{-12}
Silver Chloride, AgCl	1.77×10^{-10}
Silver sulfate, Ag_2SO_4	1.20×10^{-5}
Silver nitrate, $AgNO_3$	6.0×10^{-4}

Taken from: www.ktf-split.hr/periodni/en/abc/kpt.html and

Table 4. 17 The minimal Ag^+ concentration required for silver-complex formation in CM and NM media are illustrated in, calculated from the K_{sp} equations below:

K_{sp} AgCl	$[Ag^+] \times [Cl^-]$
K_{sp} Ag_2CO_3	$[Ag^+]^2 \times [CO_3^{2-}]$
K_{sp} Ag_2SO_4	$[Ag^+]^2 \times [SO_4^{2-}]$
K_{sp} $AgNO_3$	$[Ag^+] \times [NO_3^-]$

Table 4. 18 The Ag^+ concentration (Molar) required for Ag-complexes formation (in grey shading)

Ag-complex (Ksp)	CM-10 (M)			CM-1 (M)			NM-10 (M)			NM-1 (M)		
	Cl^-	**CO_3^{2-}**	**SO_4^{2-}**	**Cl^-**	**CO_3^{2-}**	**SO_4^{2-}**	**NO_3^-**	**CO_3^{2-}**	**SO_4^{2-}**	**NO_3^-**	**CO_3^{2-}**	**SO_4^{2-}**
	4×10^{-4}	7.7×10^{-5}	5×10^{-5}	4×10^{-3}	7.7×10^{-4}	5×10^{-4}	4.1×10^{-4}	7.7×10^{-5}	5×10^{-5}	4×10^{-3}	7.7×10^{-4}	5×10^{-4}
AgCl (1.77×10^{-10})	**4.4×10^{-7}**			**4.4×10^{-8}**								
Ag_2CO_3 (8.46×10^{-12})		**3.3×10^{-4}**			**1.1×10^{-4}**			**3.3×10^{-4}**			**1.1×10^{-4}**	
Ag_2SO_4 (1.20×10^{-5})			**0.45**			**0.15**			**0.45**			**0.15**
$AgNO_3$ (6.0×10^{-4})							**1.47**			**0.15**		
Ag_2SeO_3 (unknown)												

Note: Example of calculation of concentration Ag+ required for formation Ag-Cl complexes in CM-10:

Ksp AgCl= 1.77×10^{-10}

Concentration of Cl- in CM-10 = 4×10^{-4}

Minimal concentration of Ag+ to have AgCl formed = $\frac{Ksp\ AgCl}{[Cl^-]} = \frac{1.77 \times 10^{-10}}{4 \times 10^{-4}}$ = 4.4 x 10-7

There are different species of Ag-Cl complexes can be formed ($AgCl_x^{(x-1)-}$). According to Levard et al. study (2013), the concentration ratio of Cl/Ag determines the species of Ag-Cl complexes formed in a media, and solid AgCl is expected to be the dominant species if the ratio of Cl/Ag < 2675 (Levard et al., 2013). In this study, the concentration ratio of Cl/Ag was about 1124 (CM-1) and 112,4 (CM-10), thus the main form of Ag-Cl complexes was likely to be the solid AgCl.

Not only in the bulk media, the AgCl complex has been shown to be formed on the AgNPs surface due to Cl^- adsorption and the formed Ag-Cl complex inhibited AgNPs from oxidation and dissolution (Choi, Clevenger et al., 2009). Since the concentration of Cl^- in CM-1 was 10 fold higher than in CM-10, the extent of Ag-Cl complex formation both in the media and on the AgNPs surface was possibly more obvious than in CM-10 and led to higher decrease of Ag^+ concentration in CM-1 as also shown by this study.

In contrast, the concentration of Ag^+ released from CP5 after 21 days incubation in the media where the chloride anion was replaced by nitrate, increased significantly. The increase of Ag^+ concentration in NM-10 (1,502.1%) was much higher than in concentrated NM-1 (325%), showing that even in the absence of chloride ion, other anions (such as carbonate and sulfate) significantly influence the Ag^+ concentration. In NM-1, the level of Ag^+ released from CP5 was potentially controlled by formation of Ag_2CO_3 and minimal Ag^+ concentration required for Ag_2CO_3 formation is 1.1×10^{-4} M (≈ 11,858 ppb,Table 4. 17). In this study, since the Ag^+ concentration in NM-1 was lower than NM-10 after 21 days incubation, the formation and sedimentation of Ag_2CO_3 was likely to occur.

4.4.6.2. Dissolution of AgNPs in CM-1 and NM-1

Concentrations of Ag^+ released over 504 hours time (21 days) from CP5-AgNPs incubated in full strength of OECD Daphnia media (CM-1) and modification of CM-1, NM-1 where the chloride content was replaced by nitrate ion, were also examined (Figure 4.16). Dialysis method were employed for separation the Ag^+ ion. All the experiment mentioned above was single experiment only.

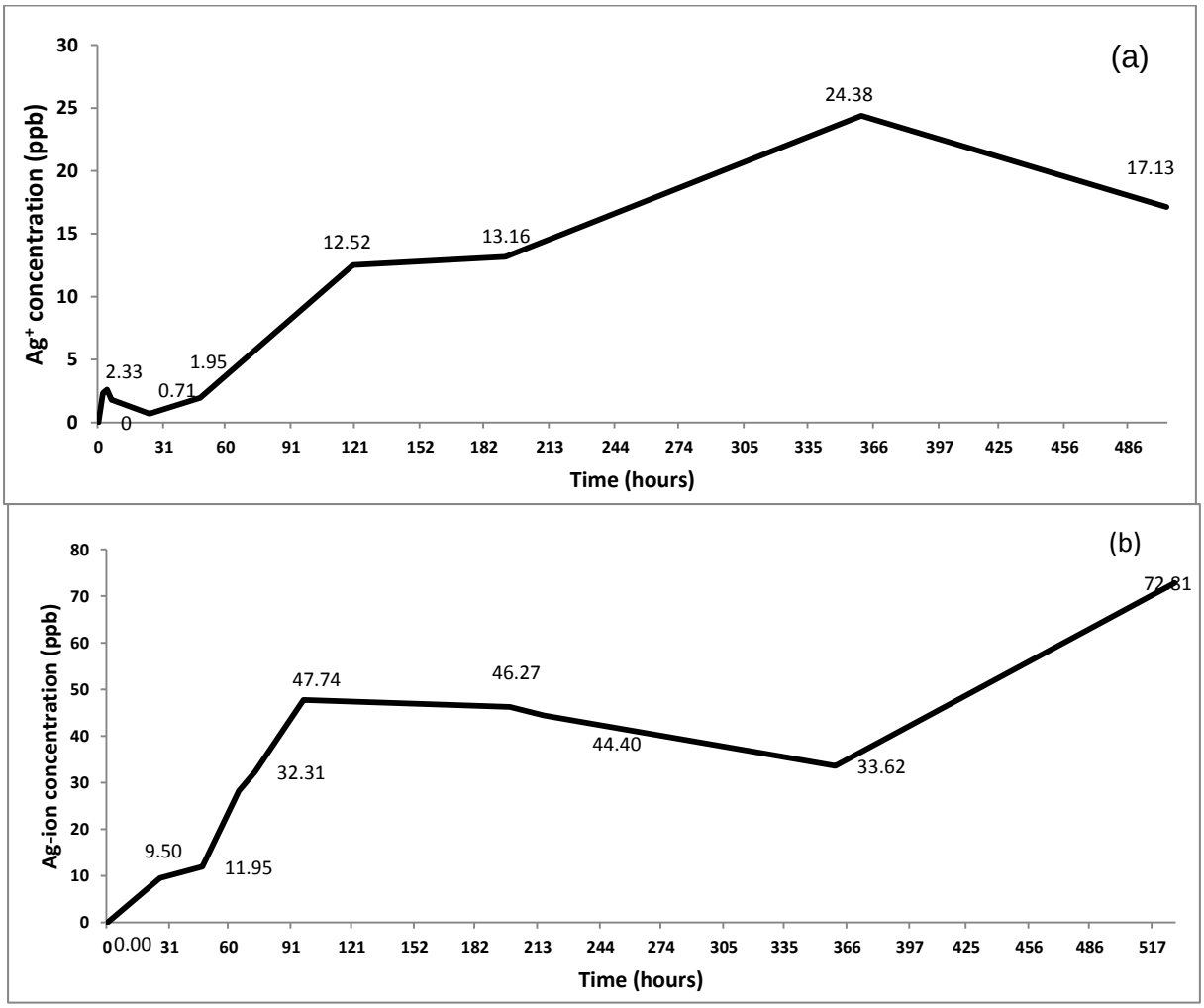

Figure 4. 16 The amount of Ag^+ inside the dialysis bag over time. The dialysis bags were immersed into (a) AgNPs-CM1 suspension, (b) AgNPs-NM1 suspension and the sample was removed at particular sampling time. The initial and final $[Ag]_{total}$ concentration in the external suspension of (a) was 420.24 ppb; and 169.70 ppb, respectively; and (b) was 586.10 ppb; 124.4 ppb, respectively

In order to mimic the exposure study, the NPs was mixed with the media used as the external suspension and the amount of ion passed through the dialysis bag immersed into the external suspension was measured. It was found that the Ag^+ concentration increased significantly after 48 hours incubation in both CM-1 and NM-1 (Figure 4. 16 (a) and (b)). Consistent with previous findings, higher concentration of Ag^+ was found in NM-1 media than in CM-1 at all sampling time, suggesting that the AgNPs was more dissolving in NM-1.

Interestingly, after t=360 hours, the Ag^+ concentration in CM-1 dropped for about 30% but continuously increased in NM-1 although slight Ag^+ concentration decreased was seen between t= 97 to t=360 hours. At t=360 hours, the Ag^+ concentration in CM-1 reached 24.38 ppb (≈ 2.3×10^{-7} M), just above the minimal concentration of Ag^+ required for AgCl formation (4.4×10^{-8} M). As the Ag^+ concentration dropped afterwards, it was suggested that the Ag^+ was consumed for AgCl formation.

The remaining AgNPs from the external suspension after the solubility study was analysed by TEM and EDX (Figure 4. 17 and Figure 4. 18). The size and shape factor of remaining AgNPs were re-measured and compared with the size and shape factor distribution of AgNPs in pristine suspension (Figure 4. 19 and Figure 4. 20).

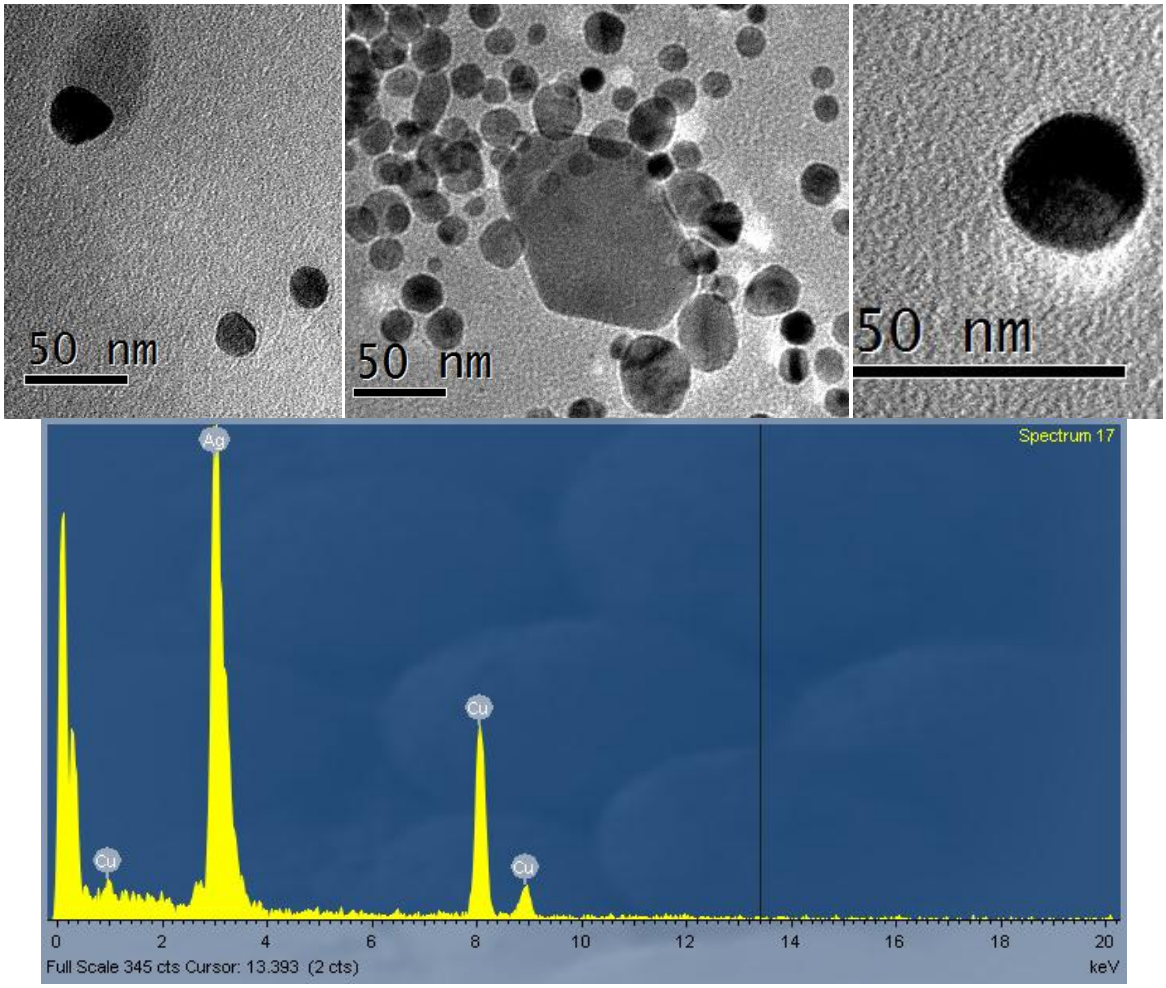

Figure 4. 17 TEM image and EDX spectrum of CP5-AgNPs after incubated in CM-1 for 21 days

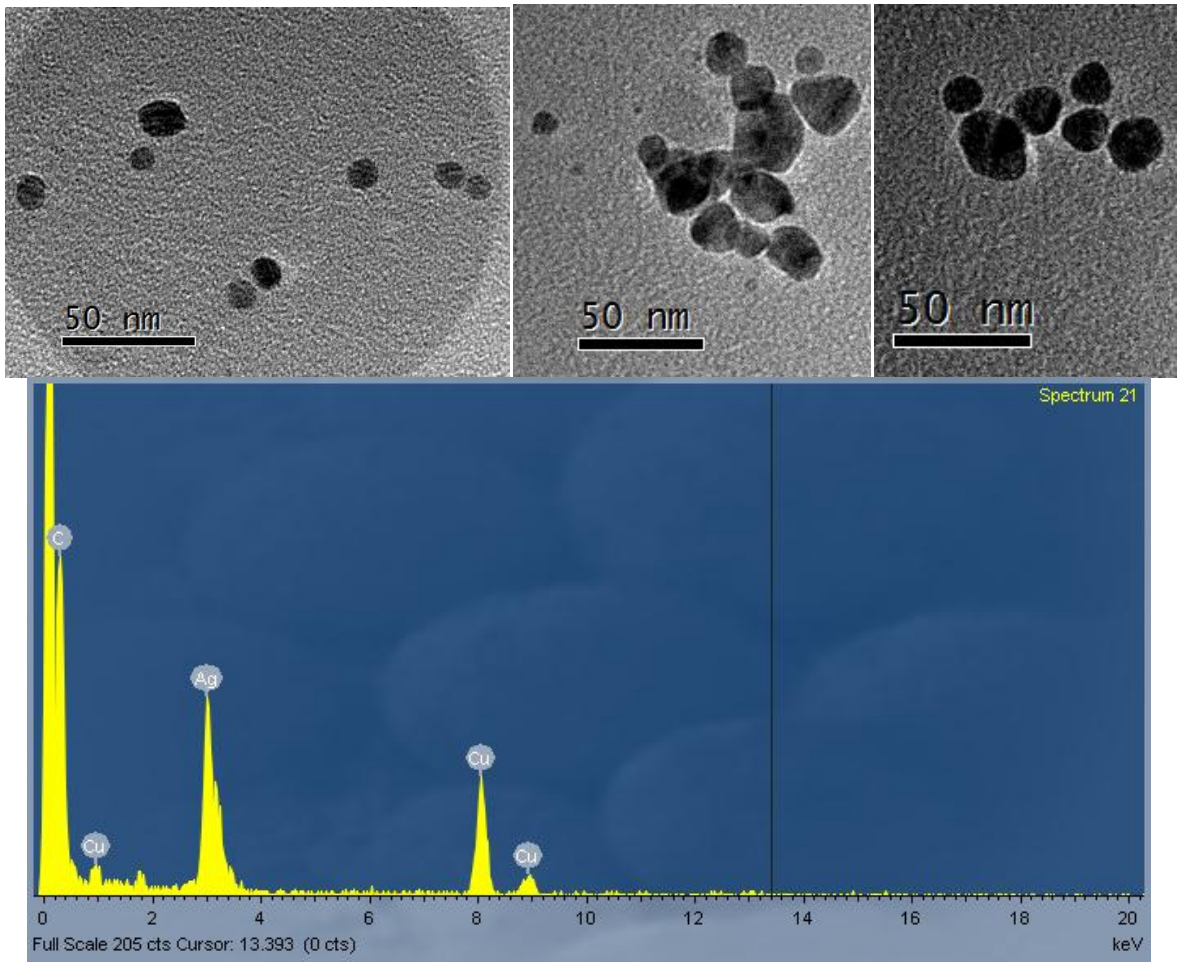

Figure 4. 18 TEM images and EDX spectrum of CP5-AgNPs after incubated in NM-1 for 21 days

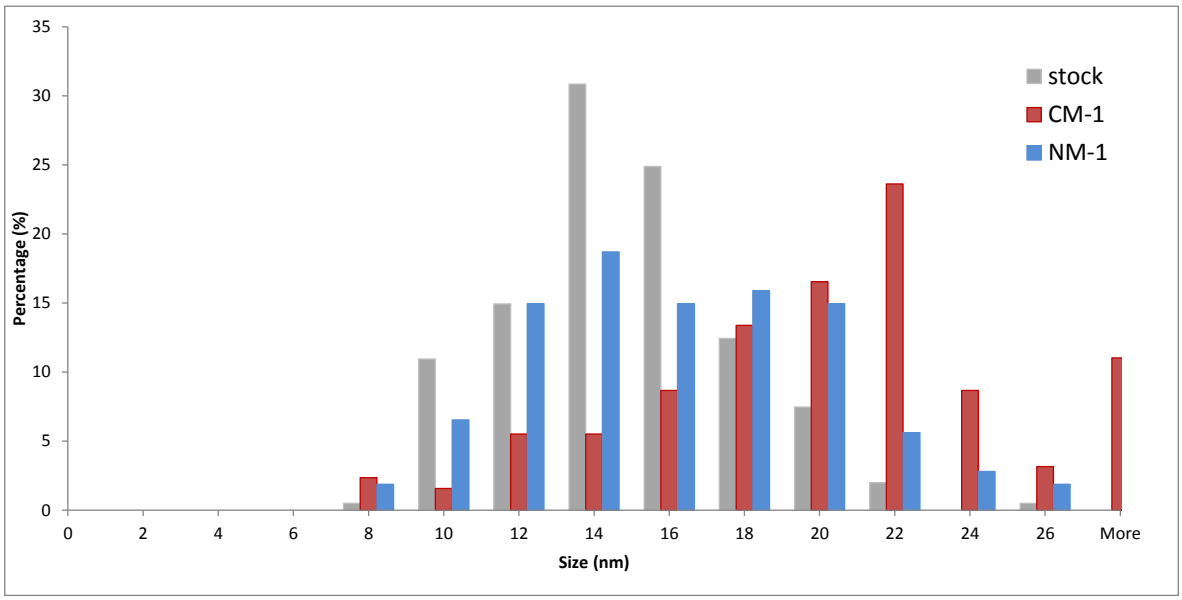

Figure 4. 19 Size distribution of CP5 in stock suspension (grey) and after 21 days incubation in CM-1 (red) and NM-1(blue)

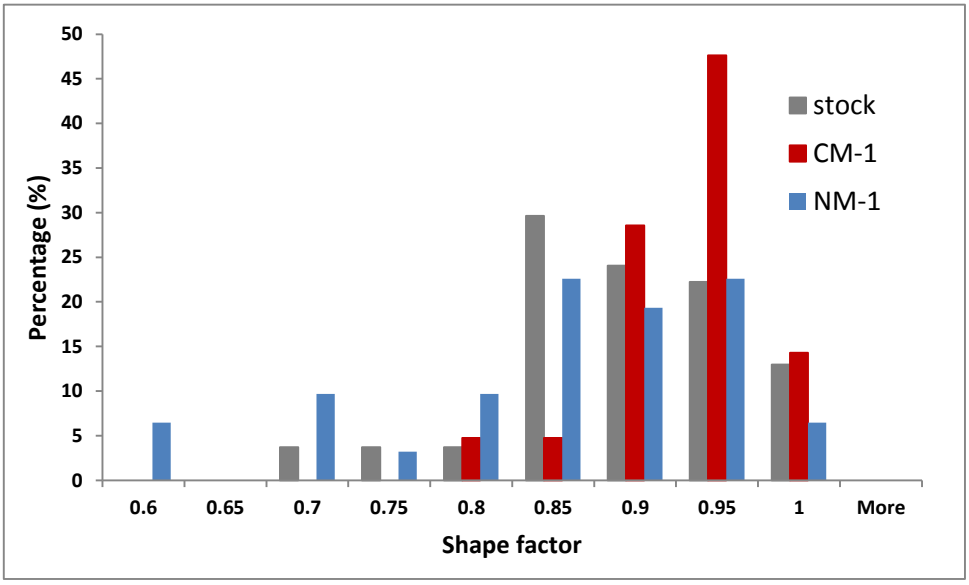

Figure 4. 20 Shape factor of CP5 in stock suspension (grey) and after 21 days incubation in CM-1 (red) and NM-1(blue)

As has been shown by other study that there was significant correlation between dissolution and TEM size reduction of NPs (Borm et al., 2006; 2011), the size of remaining AgNPs were measured. Surprisingly, instead of decreasing due to dissolution, the size of AgNPs after 21 days incubation in CM-1 was skewed into larger size and the averages size was significantly larger than pristine AgNPs size (19.47 ± 6.17nm with t-exp (336) = 9.63; 95% CI). On the other hand, the size distribution of AgNPs after 21 days incubation in NM-1 became broader, with average size significantly larger than the pristine suspension (15.41 ± 4.55nm with t-exp (233)= 3.21, 95% CI), but significantly smaller than remaining AgNPs in CM-1 (t-exp (316)= 6.64, 95% CI). By EDX, there was no chloride element was detected from the remaining AgNPs surface after incubation in CM-1, possibly because of the relatively thin layer of AgCl or even no formation of AgCl layer on the AgNPs surface.

The shape factors of remaining AgNPs in external suspension of CM-1 and NM-1 were also evaluated and compared with the shape factor of AgNPs pristine suspension (Figure 4. 20). It was found that the shape factor of AgNPs after incubation in CM-1 significantly shifted into larger value (0.91 with t-exp (76)= 3.14), became much closer to one, or in another word, became more spherical. In NM-1, even though the shape alteration is visually seen from the TEM images, there was no significant alteration of the NPs shape (0.83 with t-exp (87)= 1.75, 95% CI) compare to pristine NPs.

The increase of AgNPs core size and more spherical AgNPs in CM-1 indicated the growth of AgNPs. Since no chloride peak was detected by EDX from the surface of AgNPs after 21 days incubated in CM-1, re-deposition of the Ag^{+} onto AgNPs surface might be another mechanism of reduction of Ag^{+} ion in the bulk suspension.

Loss of total Ag in external suspension was also determined after 21 days incubation. It was found that lower Ag concentration remained in NM-1 than in CM-1, at about 11.23% and 40.3% respectively. Thus a better recovery was found in CM-1. Floating and sedimenting aggregates, however, were also found in both CM-1 and NM-1 suspension and contributing to the lost of total Ag content in the suspension suggesting that complex behavior of AgNPs such as dissolution, aggregation and re-precipitation took place in both media.Again,there is possibility of material loss due to adsorption into container wall and other surfaces (magnetic stirrer, dialysis clip, etc) but was not quantified in this study.

4.4.6.3. Dissolution of AgNPs in CM-10

Three replicates of solubility experiment of CP5-AgNPs in CM-10 were performed. Dialysis was used for separation the Ag^+ ion. The normalized [Ag^+] concentrations from those experiments are presented inTable 4. 19. The concentration of total Ag in the external suspension at time =0 hour and at the end of the study (t= 625 hours or 26 days) were measured and compared for recovery analysis.

Table 4. 19 Normalised [Ag^+] released form incubated AgNPs in CM-10 within 26 days

Time (hours)	Normalised [Ag^+] (n=3)	Time (hours)	Normalised [Ag^+] (n=3)
3	0.14 ± 0.04	123	0.45 ± 0.37
6.5	0.11± 0.03	192	0.33 ± 0.03
24	0.32 ± 0.13	360	0.23 ± 0.04
30	0.21 ± 0.05	480	0.36 ± 0.16
48.5	0.76 ± 0.24	624	0.30 ± 0.01
93	0.85 ± 0.26	Initial concentration	591.54 ppb
		Final concentration	115.33 ± 10.33 ppb

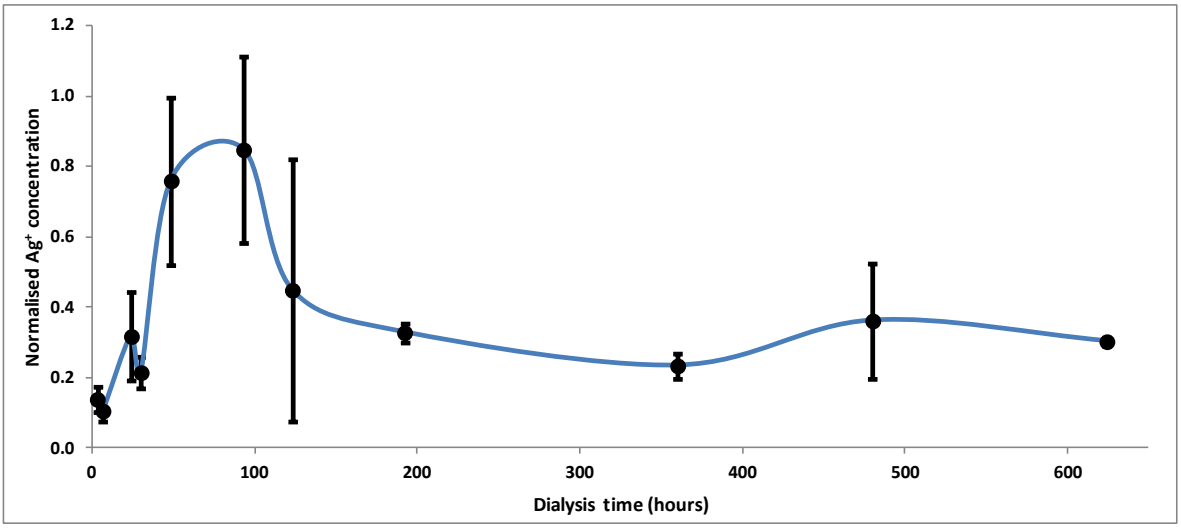

Figure 4. 21 The solubility of CP5-AgNPs in CM-10 within 625 hours

It was shown that the Ag^+ concentration from t=0 hours increased up to its maximum concentration (approximately by 1450%) at t= ± 80 hours. Then the

concentration decreased by approximately 80% at t= 192 hours and remained stable up to t=624 hours (26 days). Maximum concentration of Ag^+ pass through the dialysis membrane from the experiment above was approximately 2.0 x 10^{-6} M, and then dropped into approximately 0.4 x 10^{-6} M (the lowest ion concentration). According to the calculation, about 4 x 10^{-6} M is needed for the formation of Ag-Cl complexes in CM-10, thus the decrease of silver ion concentration in phase 2 was possibly because of solid AgCl formation and its separation from the bulk media due to sedimentation. Then the stabil Ag^+ concentration after t=120 hours indicate the equilibrium state, where the formation of Ag^+ ion and Ag-complex formation were finished. Thus three phases of AgCl dissolution in CM-10 is suggested (Figure 4. 22).

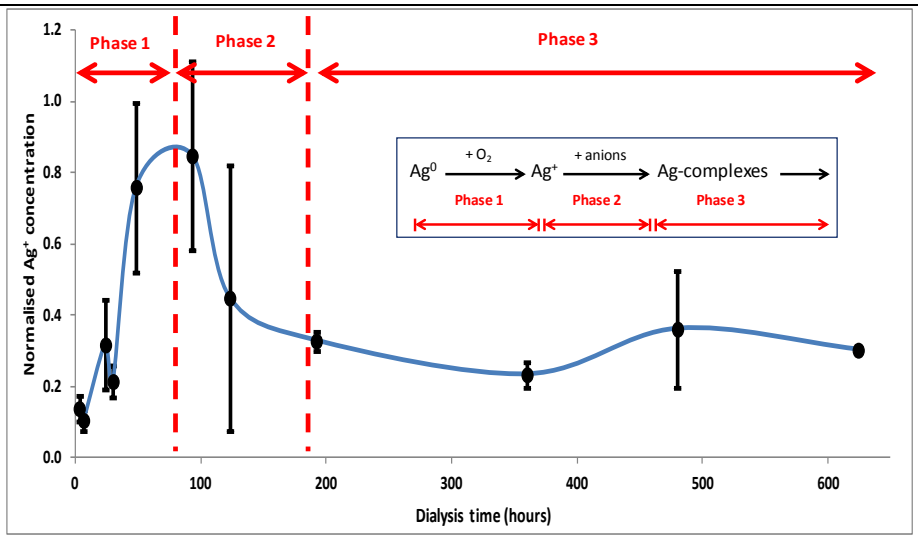

Phase-1: Dissolution of Ag^0 into Ag^+

Phase-2: Formation and sedimentation of solid AgCl, suggested by the decrease of Ag+ concentration in the suspension

Phase-3: equilibrium state, where the concentration of remaining ion or soluble Ag-complexes in the suspension leveled off

Figure 4. 22 Suggested three dissolution phases of AgNPs and media-Ag^+ interaction during incubation in CM-10

4.5. Conclusion

This study compared two protocols of PVP-capped AgNPs synthesis. First protocol exploits the PVP polymer in reducing the Ag^{+} from the salt precursor and capping the generated AgNPs. Since the PVP is a weak reducing agent, the reaction was accelerated by heating the reaction at 70^{0}C for 7 hours. The second method was using cold $NaBH_4$ as reducing agent and the reaction was performed in an ice bath to decelerate the strong reducing action of $NaBH_4$. It was found that the hot process generated more polydisperse PVP-capped AgNPs. The lowest PdI value was shown by one of the cold process reaction where the PVP polymer was added in advance, before the reduction and nucleation took place. The characteristics are presented in Table 4. 20. The summary of CP-PVP-capped AgNPs synthesis method is illustrated in **Error! Reference source not found.**.

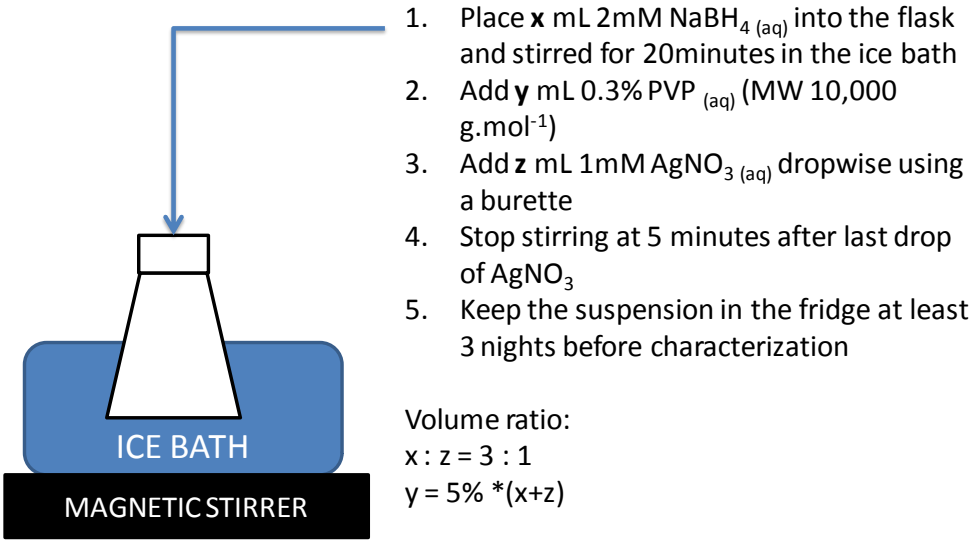

Figure 4. 23 The PVP-capped AgNPs methods via cold process

Table 4. 20 Characteristics of CP5 PVP-capped AgNPs generated by the protocol presented in Figure 4. 23

SPR (λmax)	401 nm
dH size by DLS (z-average)	21.78 ± 0.82
dH size by Fl-FFF	28.14 ± 1.75
PdI	0.27 ± 0.02
Core size by TEM	10.83 ± 3.30
Core size by AFM	11.93 ± 5.13
Shape factor	0.88 ± 0.05
Zeta potential	-12.4 ± 2.39
7 days solubility in pristine suspension	0.12- 0.15%
10 days solubility in pristine suspension	0.19%

The concentration of released Ag^+ in dissolution study of PVP-capped AgNPs was shown to be influenced by chemicals content of the media, especially the Cl^-. Unlike in NM, both in CM-1 and CM-10, the concentration of Ag^+ in the ultra-filtrate decreased after 21 days incubation. By dialysis, the Ag^+ concentration in CM-1 was lower than in NM-1, and dropped significantly as the Ag^+ concentration close to $4.4x10^{-7}$ M, the minimal Ag concentration for AgCl formation in CM-1. Interestingly, the size of remaining AgNPs in CM-1 after 21 days incubation shifted significantly into larger size, and the shape factor became closer to 1, suggesting re-deposition of Ag^+ ion onto AgNPs surface. Findings of floating aggregates and sedimenting material after study suggested that complex behaviour of dissolution, aggregation and sedimentation took place simultaneously in media. In CM-10, the dissolution of AgNPs showed a three phase process: (1) dissolving of Ag^0 into Ag^+, (2) reduction of Ag^+ concentration due to AgCl formation, and (3) equilibrium state.

CHAPTER V

THE EFFECT OF LIGAND-EXCHANGE ON NANOPARTICLE CHARACTERISTICS AND STABILITY

Chapter summary

The purpose of this study was to evaluate the ligand-exchange synthesis protocols from electrostatically-stabilised AgNPs to generate sterically-capped AgNPs. Different polymers suspensions were added into citrate-capped AgNPs, and the occurrence of ligand-exchange was analysed. The practicability of indirect recapping method (ligand-exchange) compared to direct synthesis (chapter IV), alteration of physico-chemicals properties of core AgNPs because of ligand-exchange, and AgNPs stability in ecotoxicology media before and after ligand-exchange in ecotoxicology media were evaluated.

It was found that PVP polymer and Fulvic acid preserved the NPs core size and increased the stability of AgNPs in a full strength OECD *Daphnia sp.* media for up to 21 days incubation. PEG-SH and Tween-80 polymers, however, significantly changed the core size of NPs although increased the stability of AgNPs in the media. The polymer structure, number and position of functional head group in the ligand molecules and the interaction strength between ligand and NPs, influence the SPR, d_H and core size, zeta potential, and stability of AgNPs in full strength OECD *Daphnia sp.* media. Finding concentration ratio of NP suspension and polymer solution to form a stable steric-capped AgNPs, and effect of polymers into NPs core characteristics are novelty of this study.

5.1. Introduction

It has been shown that ligand-exchange of electrostatically-capped nanoparticles with a polymer significantly increases the stability of the NP in high ionic strength media (Rao, Kulkarni et al., 2002; Kvitek, Panaček et al., 2008; Kvitek et al., 2009). Ligand-exchange by polymer also allows further manipulation of NP properties as the adsorbed ligand polymer shell is associated with the increase of NPs chemical reactivity (Stobiecka et al., 2010; Park and Advincula, 2011), electrical and thermal conductivity (Brown and Hutchison, 2001; Seo et al., 2009), and other properties (Balazs et al., 2006). Recently, it was found that the transport of NPs in porous media was also influenced by capping-ligand (El Badawy et al., 2013)

Additionally, polymer-capped NPs have a potential for application in a broad range of areas such as in material, chemical and biological sciences as discussed in Templeton (1999) and presented in Figure 5. 1. An example of this is the prospective application of polymer-capped AgNPs as a sensor in detection of amine and thiol vapour (Marques-Hueso et al., 2012), streptavidin (Haes and Van Duyne, 2002), chiral molecules (Zhang and Ye, 2011), etc. Moreover, ligand-exchange can also be adopted to build up a diverse library of steric-capped AgNPs generated from a single source of uncapped NPs for research purposes (Woehrle et al., 2005), which is the main focus of this study. Due to diverse advantages of polymer-capped NPs, the understanding of the ligand-capped NPs synthesis, characterization and stability study need to be further explored.

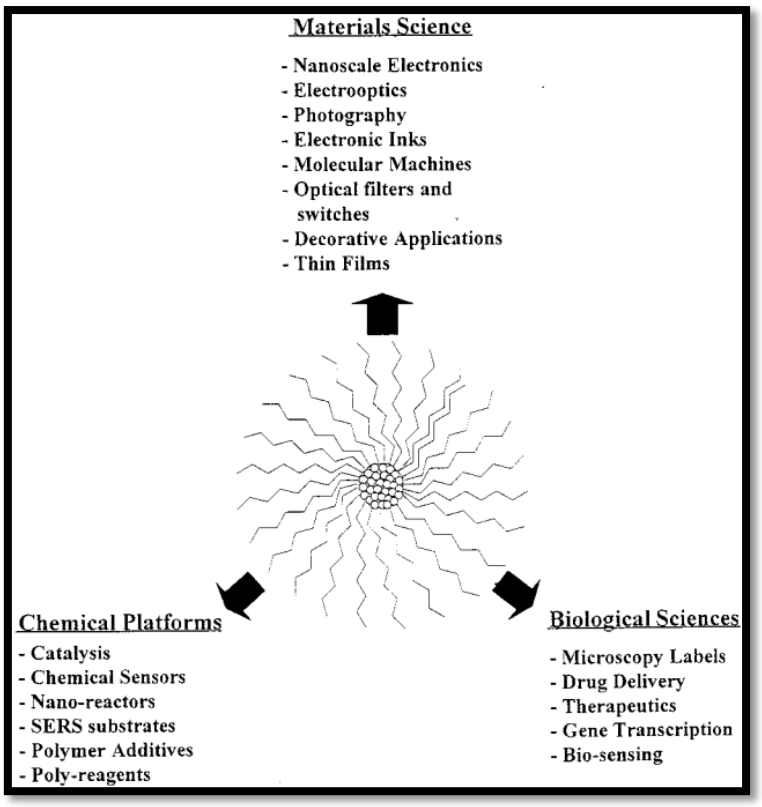

Figure 5. 1 Outline of some possible application of ligand protected NPs (Templeton et al., 1999)

Polymer-capping can be generated via various methods such as: (1) by following a nucleation-growth-passivation process (direct method) where the polymer is added during the primary synthesis of the NPs (Templeton, Wuelfing et al., 1999; Hoppe, Lazzari et al., 2006); (2) by re-capping existing electrostatically-capped NPs with a polymer (Mulfinger, Solomon et al., 2007; Kvitek, Panaček et al., 2008; Li and Lenhart, 2012) or (3) by recapping weakly-bound ligand-stabilised NPs with a stronger ligand (Napper, 1977; Rao, Kulkarni et al., 2002). Method number (1) has been widely implemented, but a number of challenges limit the adoption of the ligand-exchange or indirect methods (methods (2) and (3)) because of the difficulties of controlling the core size uninfluenced by the replacing ligand (Sau et al., 2001), and achieving the complete removal of the original capping agent (Woehrle, Brown

et al., 2005). Furthermore the reaction conditions such as concentration, solvent, temperature, etc, (Hostetler et al., 1998) and ligand structure such as chain length, bulkiness of terminal functional head group, charge, etc, determine the characteristics of re-capped NPs (Hostetler, Wingate et al., 1998). For these reasons, there are only a limited number of publications showing recapping of electrostatic or weakly-bonded ligand NPs.

In this study, the electrostatically citrate-stabilised AgNPs were recapped with different polymers. Four polymers with different functional group were employed for recapping the citrate-capped AgNPs. The re-capped AgNPs were re-characterised by number of methods and the characteristics of AgNPs before and after ligand-exchange were compared. Then the stability towards aggregation of all particles in OECD *Daphnia magna sp.* media was assessed over 21 days. The methodology adopted for ligand-exchange, characterization and stability study is presented in section 3.5 – 3.7.

5.2. Aim and objectives

The aim of this study was to develop an indirect synthesis method of polymer-capped AgNPs from electrostatically capped AgNPs via ligand-exchange method. The effect of ligand replacement into NP (core) characteristicssubsequently was assessed.

The objectives of this study were:

1. To find a concentration ratio of citrate-capped AgNPs and polymer suspension (PVP, thiolated PEG, Suwanne River Fulvic acid and Tween-80 polymers) to make polymer-capped AgNPs via ligand-exchange method

2. To characterize the as synthesized polymer-capped AgNPs by multi method characterization techniques
3. To compare the characteristics of AgNPs before and after ligand exchange
4. To examine the effect of ligand-exchange into AgNP's SPR stability in Daphnia media

5.3. Results and discussion

Nitrate media (NM) was used as an indicator for the occurrence of AgNPs ligand exchange. Since yellow citrate-capped AgNP turned into red if mixed with NM while yellow polymer-capped AgNPs stayed stable, the occurrence of ligand-exchange was seen as yellow colour preservation of AgNPs in NM. Figure 5.2 show colour changes of AgNPs, capped by different concentration of polymer, in NM. Complete citrate-ligand replacement by polymer was corroborated by total colour conservation in NM. Polymer concentration and volume for complete citrate-ligand replacement found in this study is presented in Table 5.1.

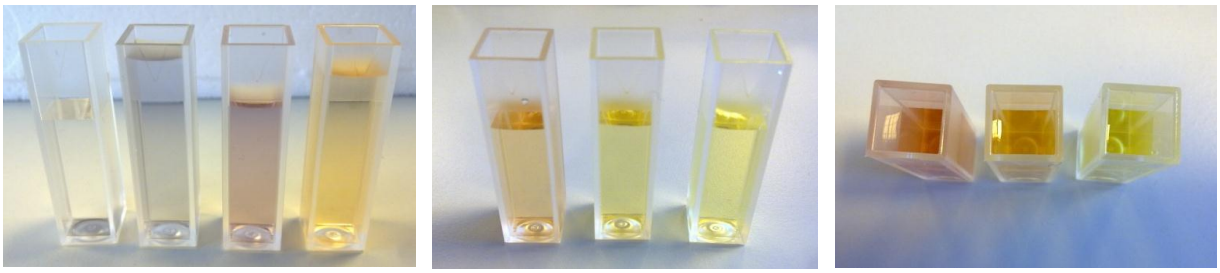

(a) (b) (c)

Figure 5. 2 The colour changes of recapped citrate AgNPs with different volume of (a) PVP solution (1-4% v/v); and (b) and (c) Tween-80 solution (1%; 2% and 4% v/v) when mixed with NM.

Table 5. 1 Concentration and volume of polymer added into 50 mL citrate capped AgNPs

Polymer	Concentration	Volume of polymer (mL)
PEG-SH	500 mg/L	2.1
PVP	30,000 mg/L	2
Fulvic acid	500 mg/L	20
Tween-80	10% $^{v}/_{v}$	2

The characteristics of the original and recapped AgNPs were analysed by multi-method characterization using the UV-Vis spectrometer, transmission electron microscopy (TEM), dynamic light scattering (DLS), and asymmetric flow field flow fractionation (Fl-FFF) to characterize the SPR (both the plasmon position (λ_{max}) and the FWHM), hydrodynamic diameter (d_H), core size, shape factor, and zeta potential of NPs. The nature of AgNPs properties after ligand-exchange was compared with the original citrate-capped AgNPs. The stability of citrate- and polymer-capped AgNPs in full strength OECD *Daphnia* media over an incubation time of 21 days was monitored with UV-Vis spectrometer only.

5.3.1. SPR Characteristics

Uv Vis as a tool to provide data on the SPR of NPs has been employed as a simple and inexpensive tool for characterizing NPs-polymer interactions, because the replacement of citrate with other ligands can be manifested as the alteration in the NPs plasmon peak, either shifting the peak position (λ_{max}) or broadening the FWHM, or both (Malinsky, Kelly et al., 2001; McFarland and Van Duyne, 2003). Thus the occurrence of polymer attachment onto the NP surface can be corroborated by analysing the changes in the SPR.

In this study the slight changes of AgNPs's SPR was observed, indicating the occurence of ligand-exchange. The position of λ_{max} red-shifted and the FWHM

broadened after NPs were sterically capped (Figure 5. 3 and Table 5. 2). There was no observed colour change due to polymer addition.

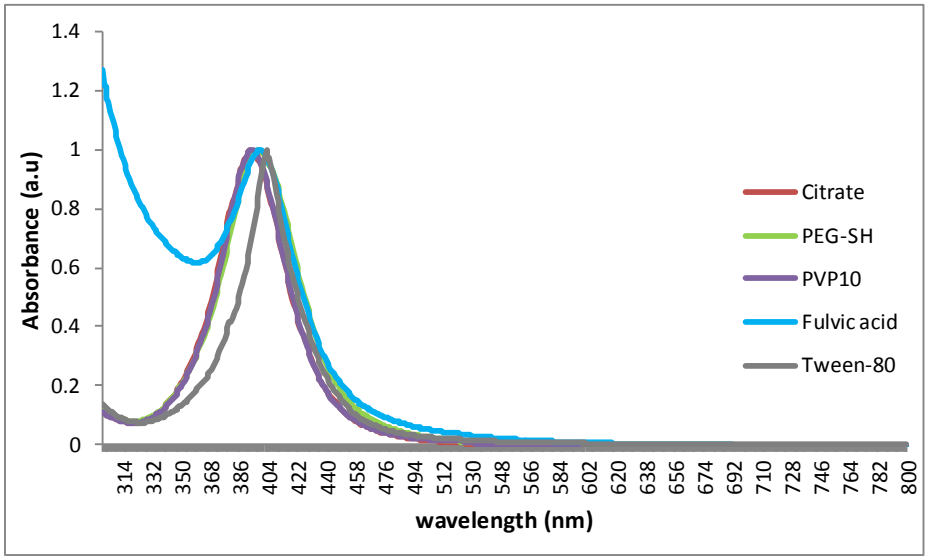

Figure 5. 3 The normalised SPR of citrate-capped AgNPs and polymer-capped AgNPs generated by re-capping the citrate-capped AgNPs

Table 5. 2 The plasmon peak position and width of AgNPs capped with different capping agent (citrate; PEG-SH; PVP10; Fulvic acid and Tween-80)

	Citrate	PEG-SH	PVP10	Fulvic acid	Tween-80
λmax	392	397	397	399	404
FWHM	57	66	64	74	73

Henglein (1993) proposed two mechanisms for the SPR alteration: (1) due to changes of refractive index of the medium surrounding the NPs; or (2) changes of NPs dielectric properties (Linnert et al., 1993; Liz-Marzán et al., 1996). Gray et al highlighted that chemisorptions of the polymer reduces the density of electrons in the conduction band as illustrated as “t” in Figure 5. 4; and this affects the dielectric constant of the NPs (Sun et al., 2011). As a consequence, plasmon damping and peak shift are induced (Sun, Gray et al., 2011). Charge localization due to covalent

bond formation was also another possible mechanism of chemical interface damping because the electrostatic charge damps the oscillation of remaining free electrons (Marques-Hueso, Abargues et al., 2012). Based on this, the shifting of λ_{max} in this study suggested the chemisorption of the polymer onto the surface of NPs and replacement of citrate.

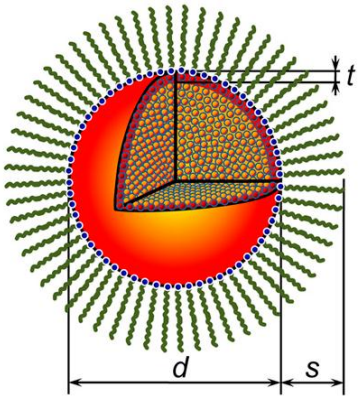

Description:

1. NPs core radius = r – t
2. Surrounding metal shell (electron damping) = t
3. Capping thickness = s

Figure 5. 4 Illustration of schematic model of steric capped NP(Sun, Gray et al., 2011)

In regards to the changes of Plasmon width, it was proposed that the width of SPR offers an alternative or complimentary method for predicting the core size of a NP. Although this idea is still under discussion, Shinca (2008) found that FWHM have a strong dependence with the core size of AgNPs (Schinca and Scaffardi, 2008). Kreibig and Persson also emphasize the particle size effect of plasmon width as shown in Equation 5. 1 (Sau, Pal et al., 2001; El-Sayed, 2004).

$$\Gamma = \Gamma_0 + A\frac{v_f}{R} \qquad \text{Equation 5. 1}$$

Where Γ= bandwidth of the SPR spectrum; Γ_0= SPR bandwidth of bare AgNPs, A= phenomenological parameter (electron damping constant); v_f= Fermi velocity; R= core diameter of the particles.

In the case of chemisorb polymer-NPs interaction, as it has been discussed earlier that the bond decreases the electron density of the NPs, Garcia and

Hernando proposed another model of the SPR width-core size dependence (Park et al., 2007). They argued that the R in Equation 5. 1 should be corrected by surrounding metal shell (t) (Figure 5. 4) and represented the as:

$$\Gamma = \Gamma_0 + A\frac{v_f}{(R-t)} \qquad \text{Equation 5. 2}$$

where the thickness of t depends on the strength of interaction between capping molecule and NPs (El-Sayed, 2004). Following from this, Garcia et al. explained why 1.5 nm thiol capped-AgNPs do not demonstrate a plasmon peak (Zhang and Sham, 2003; Crespo et al., 2004) as the strong interaction between thiol functional group and NPs lead to an infinite damping (R = t). However, in linking the FWHM with the core size of NPs it is necessary to consider the effect of aggregation, as it is well known that aggregation make the plasmon peak wider (Haes and Van Duyne, 2002; Park, Papaefthymiou et al., 2007).

In this study, different extent of the FWHM changes was shown by each polymer. Fulvic acid and Tween-80 polymer broadened the plasmon peak more notably than PEG-SH and PVP, suggesting greater core size changes according to Equation 5. 2 and or aggregation. The fact that the thiolated polymer modifies the size of NPs has been corroborated by some studies especially for gold NPs (Rao, Kulkarni et al., 2002; Park, Papaefthymiou et al., 2007; Huang et al., 2011). Although some studies refuted that ligand-exchange alters the core size of NPs (Seo et al., 2004; Woehrle, Brown et al., 2005; Caragheorgheopol and Chechik, 2008), it is an interesting question whether the adsoption of polymer in this study could modify the core size of the NPs or the observed alteration is only due to aggregation. To answer this question, TEM was employed for further analysis.

5.3.2. TEM core size and measurement and shape factor analysis

Figure 5. 5 shows the TEM images, core size and shape factor of AgNPs. Since the TEM used could not capture a clear image of Tween-80 capped AgNPs, an estimate of the size was made.

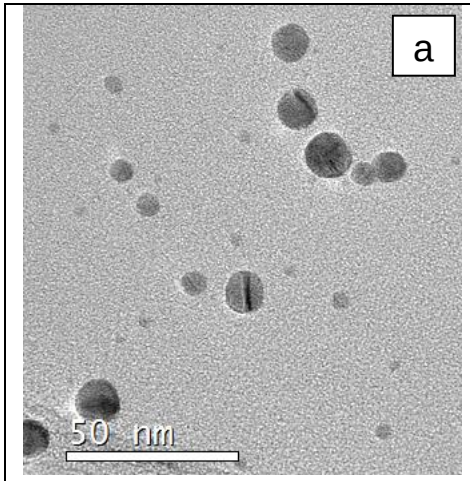

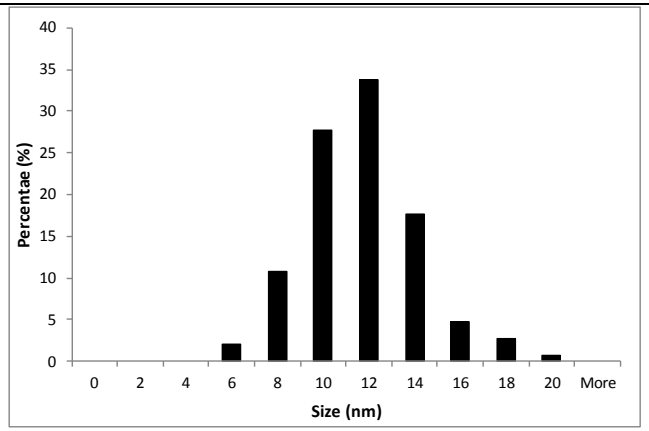

Average size = 10.65 ± 2.52 (n=148)

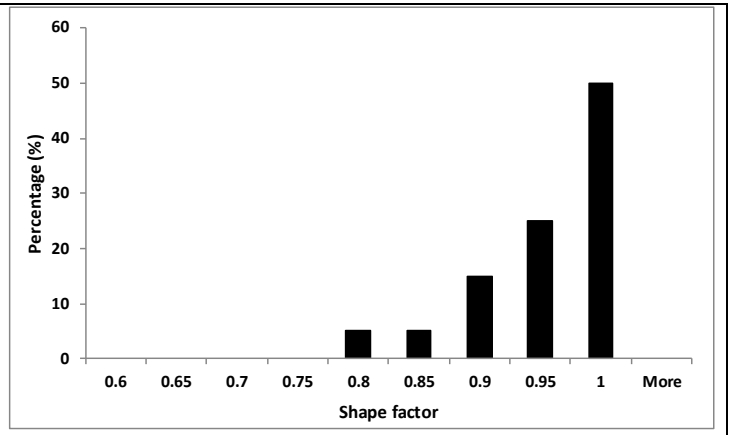

Shape factor = 0.93 ± 0.06 (n > 50)

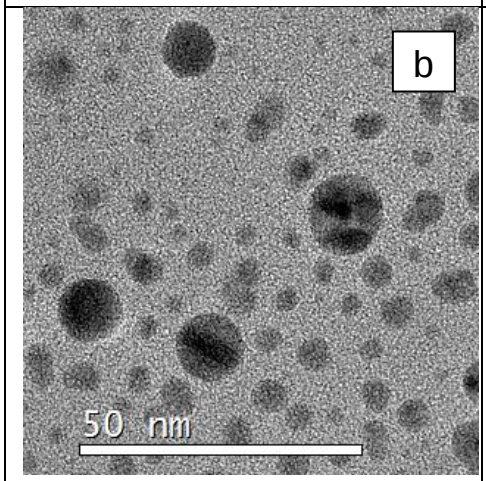

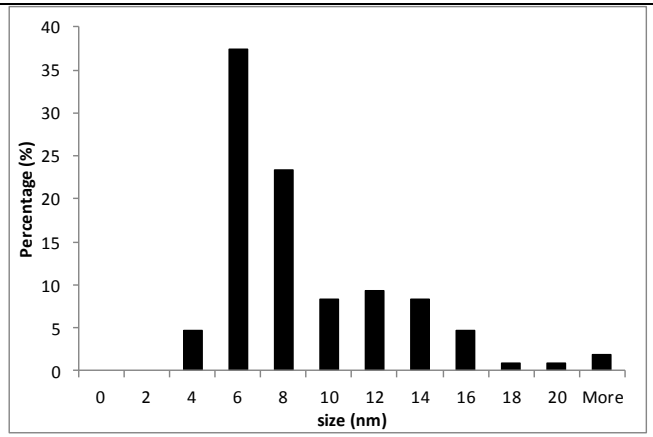

Average size = 7.81 ± 3.85 (n= 141)

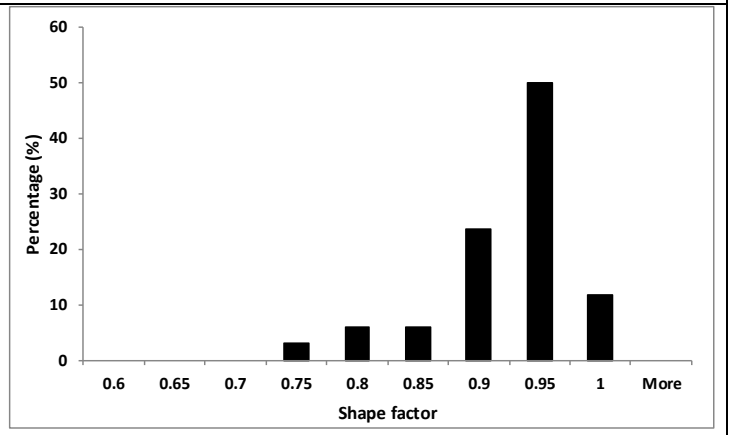

Shape factor = 0.90 ± 0.06 (n > 50)

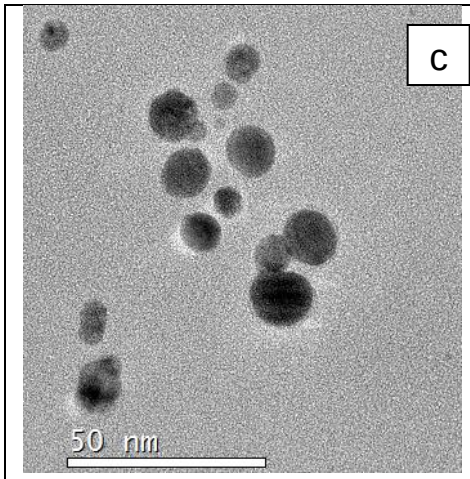

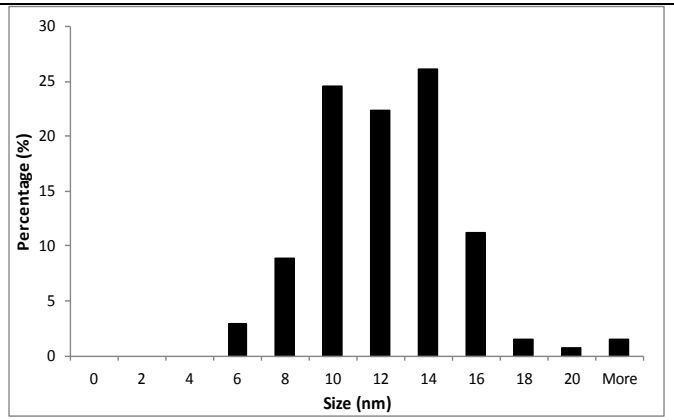

Average size = 11.31 ± 3.05 (n= 134)

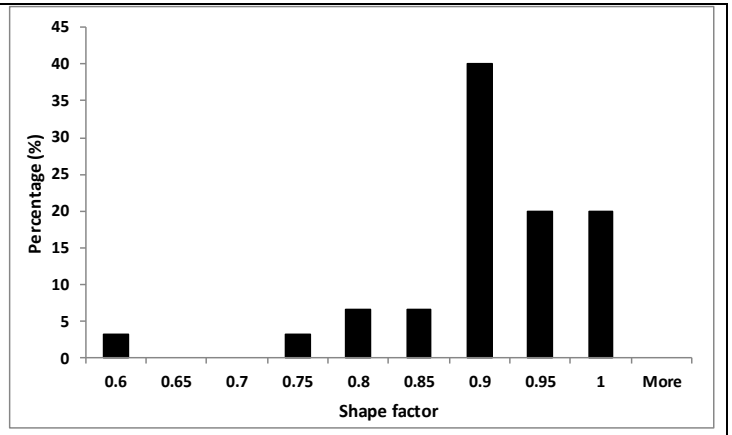

Shape factor = 0.90 ± 0.06 (n > 50)

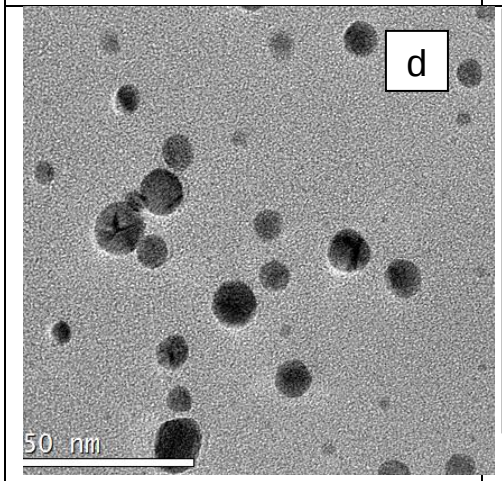

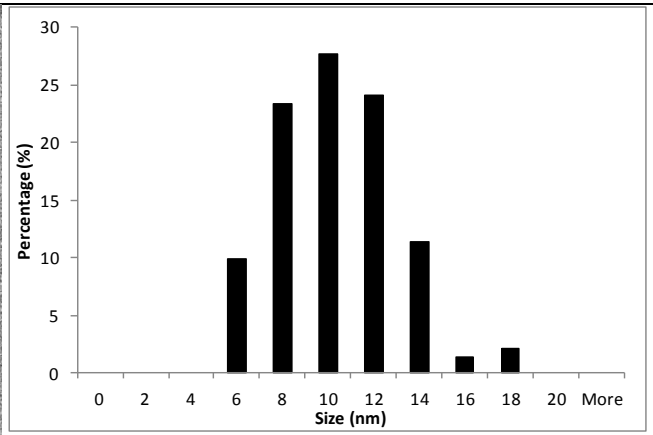

Average size = 9.37 ± 2.66 (n= 141)

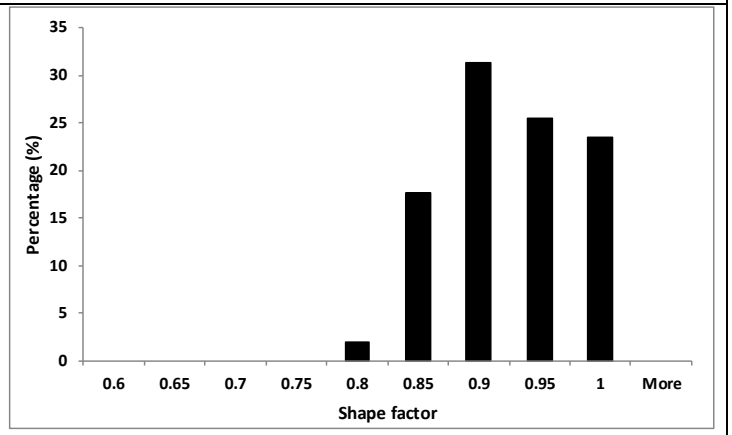

Shape factor = 0.90 ± 0.05 (n > 50)

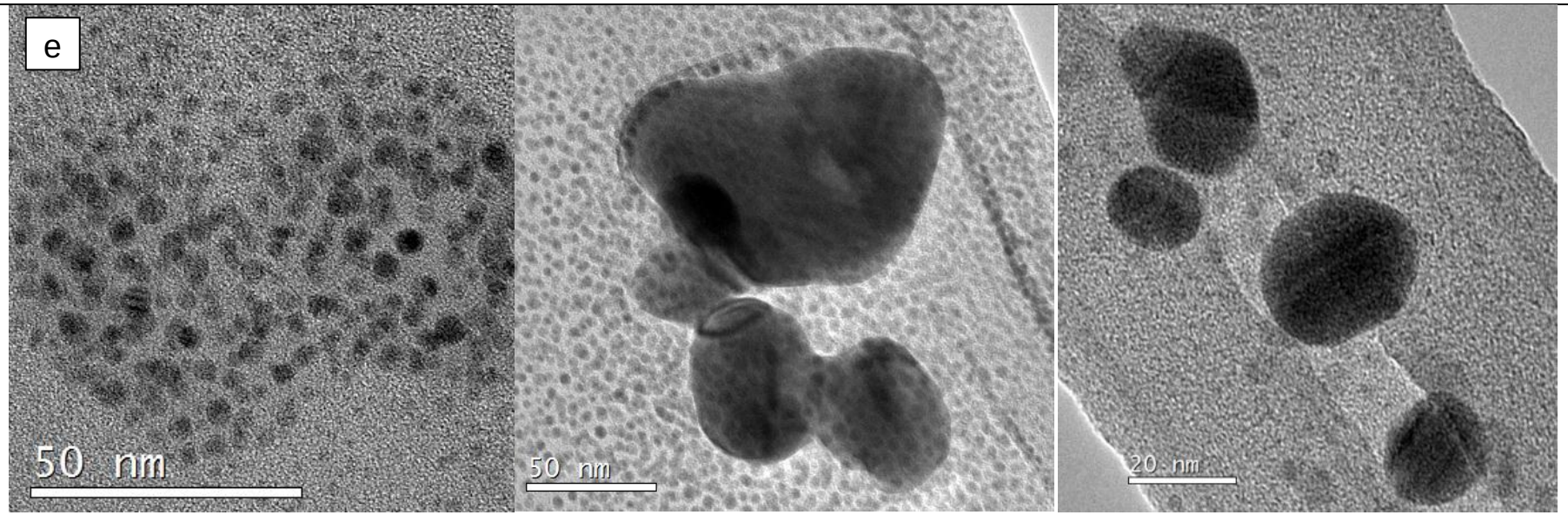

Figure 5. 5 TEM images and size distribution of (a) citrate; (b) PEG-SH; (c) PVP; (d) Fulvic acid; and (e) Tween-80 capped AgNPs

The TEM micrographs show that the ligand-exchange with Tween-80 polymer gave rise in a significant change of the core size of AgNPs, and that is resulted in generation of very small particles (approximately < 5 nm) and some large clumps (approximately > 50 nm). As has been discussed in an earlier section, that the changes of SPR width could be linked with NPs size or aggregation, in case of Tween-80-capped AgNPs, both processes were observed.

Core size reductions were also induced by PEG-SH polymer, at around 3 nm as indicated earlier by the alteration of its plasmon width. The most likely mechanism responsible for the observed NPs core-size reduction in PEG-SH and Tween-capped AgNPs was dissolution. As has been reported by other studies, thiol-functional group has the ability to etch or corrode the surface of copper and gold NPs which then reconstructs the NP's surface and make the NPs vulnerable to oxidation (Sondag-Huethorst et al., 1994; Driver and Woodruff, 2000; Wilcoxon and Provencio, 2003; Kanninen, Johans et al., 2008). The increase of AgNPs dissolution due to thiolated-PEG polymer capping action has also been revealed (Zook, Long et al., 2011).

Henglein proposed the mechanism of nucleophile-NPs interaction that cause oxidative-dissolution of NPs. Electron donation from the charged functional head group of polymer changes the electron density on the NPs surface and creates preoxidation or precomplexation state as presented in Figure 5. 6 (Henglein, 1993). The presence of oxygen in the system could oxidize the δ^- surface and dissolve the NPs.

A study from Ho (2010) found that size, capping agent, pH, presence of halide ion influence the dissolution rate (Ho, Yau et al., 2010). Measuring the extinction of SPR spectra using UV-Vis, spectrophotometric titration with oxidator, and ion separation using ultrafiltration, centrifugation, dialysis, etc are widely used for

oxidation rate determination (Ho, Yau et al., 2010; Liu and Hurt, 2010; Li and Lenhart, 2012; Misra, Dybowska et al., 2012).

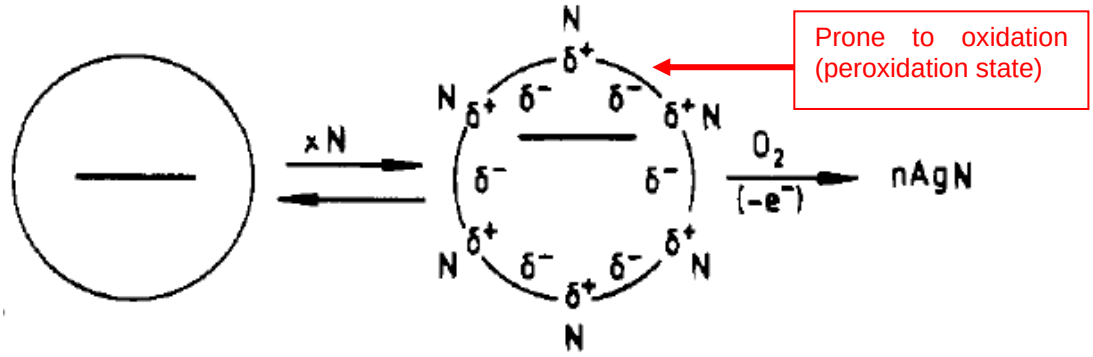

Figure 5. 6 Illustration of nuchleophiles and AgNPs interaction which lead to dissolution of AgNPs.

In this study, the concentration of silver ion released from thiolated-PEG-capped AgNPs after one week storage was found to be higher than ions released from citrate-capped AgNPs (Table 5. 3). For that reason, the decrease of core size of AgNPs after ligand-exchange by PEG-SH might be due to increase of dissolution.

Table 5. 3 Silver ion concentration (Ag^+) in ppb released from the pristine suspension of citrate- and PEG-SH-capped AgNPs, separated by ultrafiltration

UF	Citrate-capped AgNPs	PEG-SH-capped AgNPs
1	104.4	243.5
2	22.34	198.4
3	15.59	168.7

In case of Tween-capped AgNPs, formation of small particles and large aggregates might be due to dissolution and re-deposition of Ag species. Li and Lenhart (2012) reported that the Tween-capped AgNPs dissolved more than citrate-capped AgNPs in the first 6 hours of incubation in natural water. 3 days later, however, the Ag^+ concentration in the suspension started to decrease and subsequent size increased possibly due to re-adsorption of the ion into the NPs surface (Li and Lenhart, 2012). Moreover the tween-80 polymer has shown its ability

as a reducing agent (Premkumar et al., 2007; Lee et al., 2009), thus re-conversion of Ag^{+} into Ag^{0} is another possibility. In this study, no dissolution study was performed for tween-capped AgNPs but dissolution and re-deposition might be the case.

On the other hand, slight core size changes were shown by PVP and fulvic acid polymers. Since the PVP is a reducing agent (Bonet et al., 1999; Hoppe, Lazzari et al., 2006; Tolaymat, El Badawy et al., 2010) the equilibrium state between Ag^{0} and Ag^{+} on the NPs surface will be suppressed, maintaining the Ag^{0} state and retarding dissolution. Reversible dissolution and formation of AgNPs has also been presented in other studies (Pal et al., 1997) due to O_2 purging in the vicinity of reducing agent.

Fulvic acid, interestingly, was found previously to stabilise NPs and retard NP dissolution at lower concentrations, but liberated ions at higher Fulvic acid concentration (Li, Lenhart et al., 2010; Miao, Zhang et al., 2010). Therefore concentration of FA is an important parameter of FA stabilization effect and for aggregation. In this study, the concentration of FA could maintain the core size of AgNPs.

The shape factor of AgNPs before and after ligand-exchange was analysed from the TEM micrograph. The shape factor was reduced by 0.03 after the AgNPs was re-capped by polymers. However, the shape factor of Tween-capped AgNPs could not be analysed as the TEM image of this particle was not sharp enough for analysis.

5.3.3. DLS size measurement

The hydrodynamic diameter (d_H) of the AgNPs, attributed to both the core diameter and thickness of capping-layer of the AgNPs, was measured with DLS

(Table 5. 4). The results are presented as 'Peak 1 size by intensity' (the d_H size of the particle fraction that scattered the light with higher intensity) and z-average (cumulant mean d_H of the NPs). The size distributions by intensity of AgNPs with different capping agents are illustrated in Figure 5. 7. DLS also gave the value of polydispersity index (PdI) of the NPs which referred to the homogeneity of the size of the NPs. It was found that the addition of the polymer capping agent altered both the d_H and PdI values of the AgNPs.

Table 5. 4 d_H average and polydispersity index of AgNPs with different capping agent, analysed by DLS

Capping agent	Peak 1	z-average	PdI
Citrate	23.01 ± 0.47	20.13 ± 0.17	0.17 ± 0.01
PEG-SH	42.54 ± 0.58	35.78 ± 0.26	0.23 ± 0.01
PVP	31.69 ± 1.02	26.34 ± 0.44	0.25 ± 0.01
Fulvic acid	24.79 ± 0.27	21.52 ± 0.19	0.18 ± 0.00
Tween-80	30.80 ± 2.55	19.58 ± 0.23	0.31 ± 0.00

z-average dz = $\frac{\Sigma n_i d_1^6}{\Sigma n_i d_1^5}$ and Peak 1 dn = $\frac{\Sigma n d_i}{\Sigma n}$ (Balnois, Papastavrou et al., 2007)

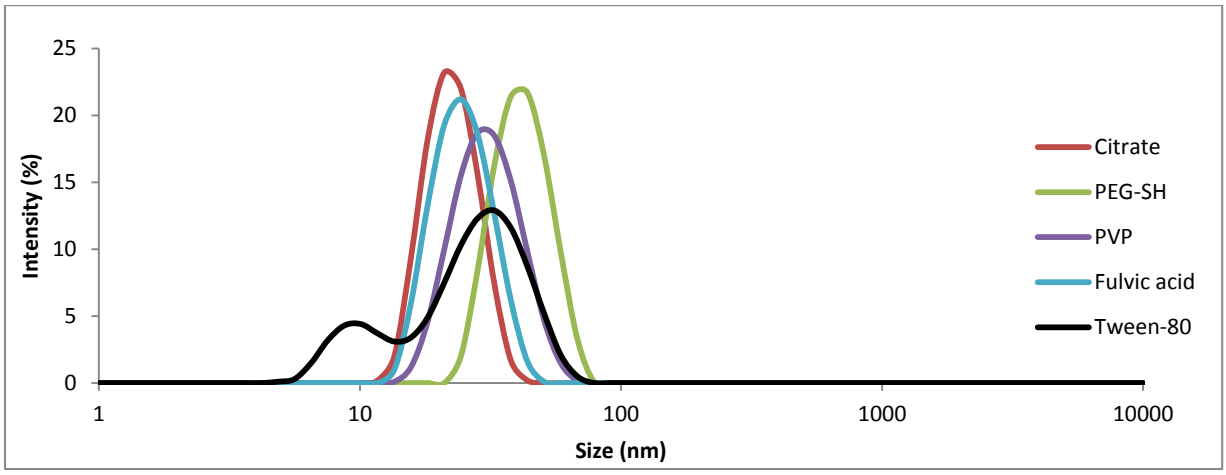

Figure 5. 7 Size distribution (by intensity) of AgNPs with different capping agent, analysed by DLS

Since the DLS measures the size of AgNPs and take the adsorbed outer layer into account, it was expected that ligand-exchange by polymer would increase the d_H size of AgNPs as the size of polymers in this study are larger than citrate. In general,

this study showed that addition of polymer increased the d_H size (Peak 1 size) and PdI value of AgNPs. This finding can be explained by looking at the polymer structure, such as molecular weight (molar mass) and both position and number of functional head group in a polymer (Table 5. 5) and the likelihood of its interaction with NPs (Hostetler, Wingate et al., 1998).

Table 5. 5 Chemical structure of PEG-SH, PVP, Fulvic acid and Tween-80 polymer

Polymer	Chemical structure
Citrate MW=189 g.mol^{-1}	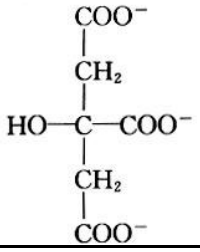
PEG-SH MW=5,000 g.mol^{-1}	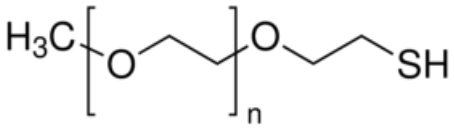
PVP MW=10,000 g.mol^{-1}	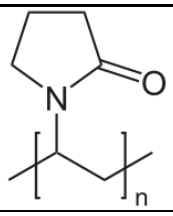
Fulvic acid** MW= ca 1000 g.mol^{-1}	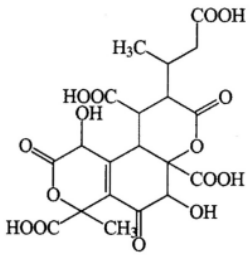 Subfraction 2/1, MW = 500 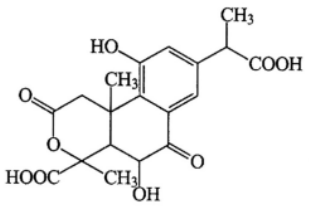 Subfraction 2/4, MW = 392 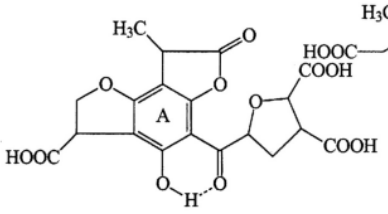 Subfraction 3/2, MW = 436 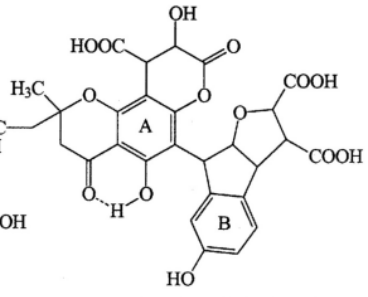 Subfraction 4/6, MW = 628

Tween-80

MW=1,310 g.mol^{-1}

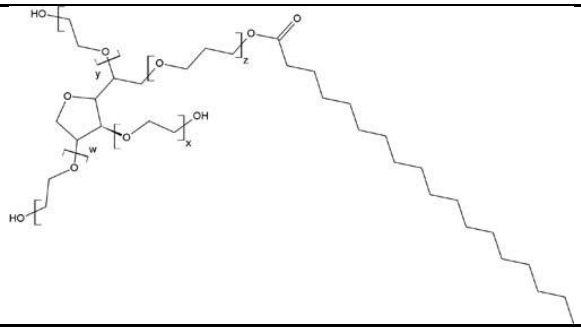

**(Beckett et al., 1987)

Theoretically, there are different functional head groups that have been shown to attach sterically to the NPs surface as a result of covalent and non covalent (adsorption) interaction (Nobs et al., 2004). Thiol, carboxyl, amine and phosphine groups are some examples of functional head group that have been widely used for colloid and NPs stabilization purposes (Hunter, 1986). In this study, the functional groups employed were thiol (of PEG-SH); amine (of PVP); and carboxyl (of Fulvic acid and Tween-80) (Table 5. 5). Unlike the PEG-SH and PVP which only contain one functional group per molecule (monodentate ligand), fulvic acid has a number of functional groups per molecule (polydentate ligand) and allow the fulvic acid to adsorb onto the NPs surface in a train or loop form (Figure 5. 8).

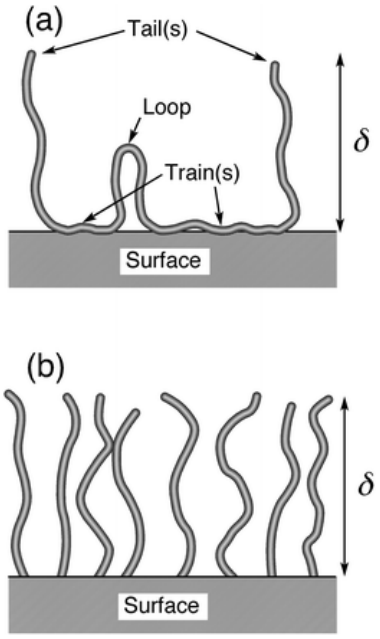

Figure 5. 8 Possible attachment mode of polymer onto the NPs surface (a) trail, loop and train, (b) surface-anchored polymer brushes (Araki, 2013)

In contrast, since the thiol functional head group of PEG-SH molecule is located at the end of the molecular structure, the polymer will likely to attach in a tail form. The thiol head group anchored to the NPs surface and the long carbon tail of the PEG-SH molecule exposed to the bulk medium as has been shown in thiolated-capped gold NPs (Figure 5. 9). Thus it was expected that the PEG-SH polymer to give the thickest coat. This was found to be the case as the d_H size of PEG-capped AgNPs was the most increased both by DLS (Table 5. 4) and Fl-FFF (Figure 5. 10), will be discussed in section 5.3.4) even though the core size decreased according to the TEM result.

Figure 5. 9 Thiolated-polymer capped Gold NPs(Daniel and Astruc, 2004)

In the case of Tween-80 capped AgNPs, consistent with the TEM finding, the z-average size was smaller than citrate capped AgNPs at approximately 1 nm with formation of large clumps simultaneously. This is shown as two populations of the NPs size (Figure 5. 7) and the increase of PdI value into 0.31. As has been discussed in earlier section, the formation of two size populations of tween-capped AgNPs might be due to dissolution and recrystalization or re-deposition of silver.

On the other hand, only one peak was shown by PEG; PVP and Fulvic acid and lower PdI value, indicated better NP's size homogeneity than Tween-80 coated NPs. However, ligand-exchange by any polymer in this study increased the PdI value of AgNPs significantly.

5.3.4. Fl-FFF Size measurement

The Fl-FFF was also employed for d_H measurement of the NPs, both before and after ligand-exchange. The weight (*dw*), number (*dn*), and peak (*dp*) average of d_H distributions calculated from Fl-FFF fractograms (Figure 5. 10) are presented inTable 5. 6. The calculation of those average sizes can be found in Romer et al. (2011).

Table 5. 6 The weight, number and peak d_H average of the AgNPs, measured by Fl-FFF

Capping agent	*dH* by Fl-FFF		
	dw	*dn*	*dp*
citrate	13.12 ± 0.63	10.5 ± 0.10	11.28 ± 1.00
PEG-SH	36.06 ± 0.27	31.54 ± 0.20	32.29 ± 0.01
PVP	22.92 ± 1.12	18.11 ± 0.70	20.64 ± 0.88
Fulvic acid	23.36 ± 0.65	15.17 ± 1.37	13.68 ± 0.22
Tween	18.35 ± 4.06	13.25 ± 2.76	7.50 ± 0.67

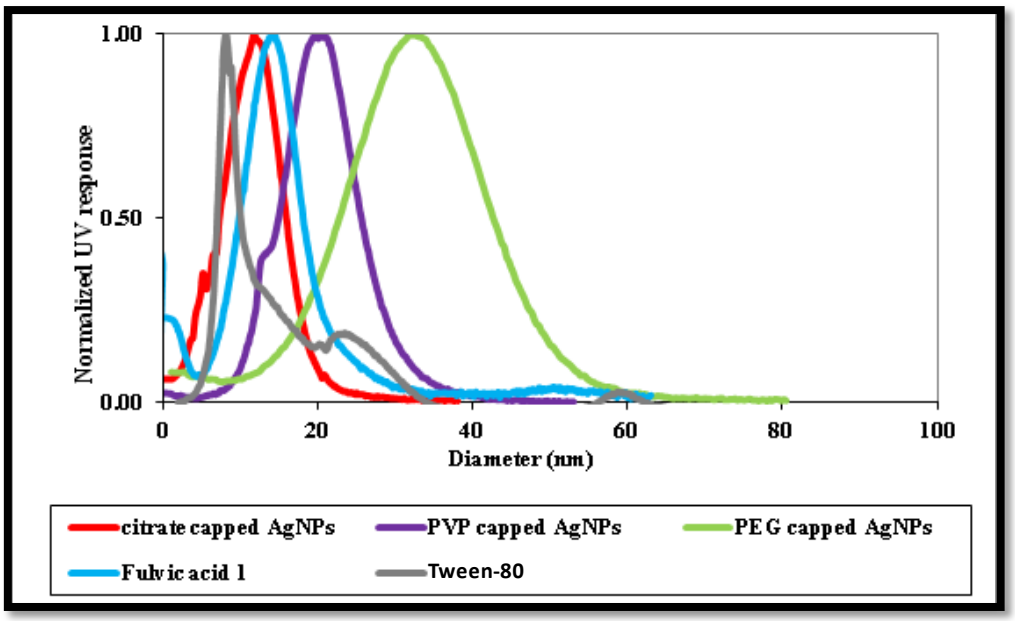

Figure 5. 10 The d_H distributions fractogram by Fl-FFF of AgNPs with different capping agents

Significant alteration of size averages (*dw*, *dn* and *dp*) was shown by most of the polymer. Only tween-capped AgNPs showed minor size alteration (dp, *dw* and *dn*) even though more than one peak of Tween-capped AgNPs fractogram appeared (Figure 5. 10) as indicated earlier by higher PdI value of tween-capped AgNPs than other polymer-capped AgNPs. Consistent with d_H-DLS, d_H by Fl-FFF of PEG-capped AgNPs was the largest.

Interestingly, comparing DLS (Figure 5. 7) and Fl-FFF (Figure 5. 10) d_H size distribution qualitatively, it is seen that there are discrepancies of the areas under peak 1 and 2 of Tween-capped AgNPs. By DLS, Peak 2 area is larger than peak 1 but it is the other way around for Fl-FFF. This is understandable as the DLS signal correlates with the intensity of scattered light to the six power ($\approx I^6$), so higher intensity arising from small numbers of large particles masked the intensity from higher number of smaller particles. In contrast, the diffusion coefficient of Fl-FFF depends on concentration of NPs, so response from the more concentrated fraction

(in this case smaller NP fraction) will be presented as larger peak area by Fl-FFF. Thus, for tween-capped AgNPs by Fl-FFF, the area of peak 1 is larger than peak 2.

5.3.5. Zeta potential result

The attachment of polymer onto the surface of AgNPs brought the zeta potential of the AgNPs closer to zero as presented in Table 5. 7. Recapping the AgNPs with all polymers resulted in a reduction of the zeta potential relatively to the original citrate-capped AgNPs. The largest change was shown by Tween-80, followed by PEG-SH; PVP and fulvic acid.

Table 5. 7 The zeta potential and electrophoretic mobility of AgNPs with different capping agent

Capping agent	Zeta potential (mV)	Electrophoretic mobility (μmcm/Vm)
Citrate	-35.4 ± 2.51	-2.77 ± 0.20
PEG-SH	-19.5 ± 2.28	-1.53 ± 0.18
PVP	-24.6 ± 1.65	-1.93 ± 0.13
Fulvic acid	-26.1 ± 1.23	-2.04 ± 0.10
Tween-80	-10.6 ± 2.32	-0.83 ± 0.18

It was shown that the adsorption of the non-ionic polymer (Tween-80) altered the zeta potential the most significantly compared to the anionic (PEG-SH and Fulvic acid) and cationic polymer (PVP). The alteration of zeta potential due to ligand-exchange has also been observed in other studies (Laaksonen et al., 2006; Park and Hamad-Schifferli, 2008; Gangula et al., 2012).

5.3.6. Comparison between size measurement result

The size measurement results of the different AgNPs are summarized up in Table 5. 8. Clearly, there is size variability as a result of different measurement techniques used.

Table 5. 8 Summary of AgNPs size measurement result, by DLS, Fl-FFF and TEM

Capping agent	DLS	Fl-FFF			TEM
	z-average ± σ_r	d_w-Fl-FFF + σ_r	dn-Fl-FFF + σ_r	dp-Fl-FFF + σ_r	$d_{DLS}/d_{Fl\text{-}FFF}$
Citrate	20.13 ± 0.17	13.12 ± 0.63	10.5 ± 0.10	11.28 ± 1.00	10.65 ± 2.52
PEG-SH	35.78 ± 0.26	36.06 ± 0.27	31.54 ± 0.20	32.29 ± 0.01	7.81 ± 3.85
PVP	26.34 ± 0.44	22.92 ± 1.12	18.11 ± 0.70	20.64 ± 0.88	11.74 ± 3.63
Fulvic acid	21.52 ± 0.19	23.36 ± 0.65	15.17 ± 1.37	13.68 ± 0.22	9.37 ± 2.66
Tween-80	19.58 ± 0.23	18.35 ± 4.06	13.25 ± 2.76	7.50 ± 0.67	Approx.5 nm

σ_r = repeatability of the measurement
RSD (relative standard deviation)= (σ_r/d)

5.3.7. SPR Stability of AgNPs in electrolyte media

The stability of AgNPs in full strength OECD *daphnia sp.* media was examined by monitoring the SPR of AgNPs in the media during 21 days incubation. The results are illustrated in Figure 5. 11. The SPR of citrate-capped AgNPs extinct rapidly and totally disappeared within 3 days of incubation. However, after ligand-exchange by polymer, the stability of AgNPs increased significantly as shown by the preservation of the SPR within 21 days incubation. The alteration of maximum absorbance of citrate- and polymer capped AgNPs in the media are also illustrated in Figure 5. 12 and Figure 5. 13.

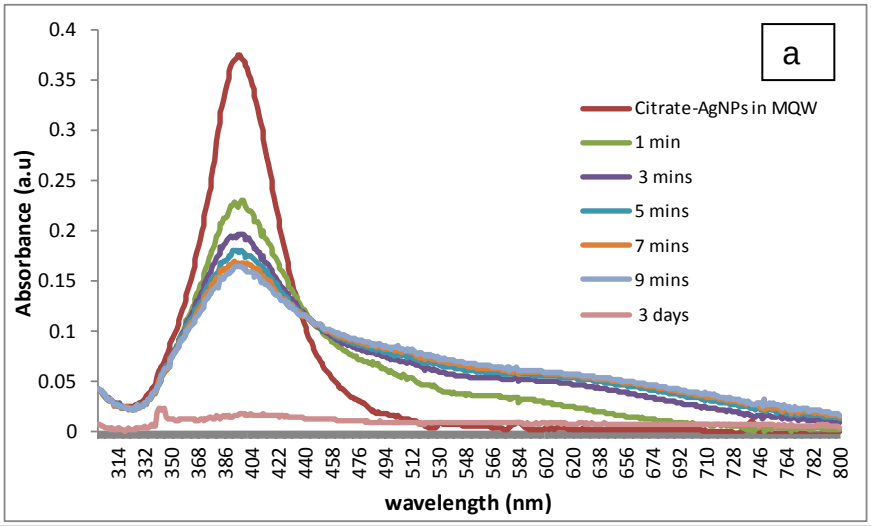
a
Absorbance (a.u)
wavelength (nm)
Citrate-AgNPs in MQW
1 min
3 mins
5 mins
7 mins
9 mins
3 days

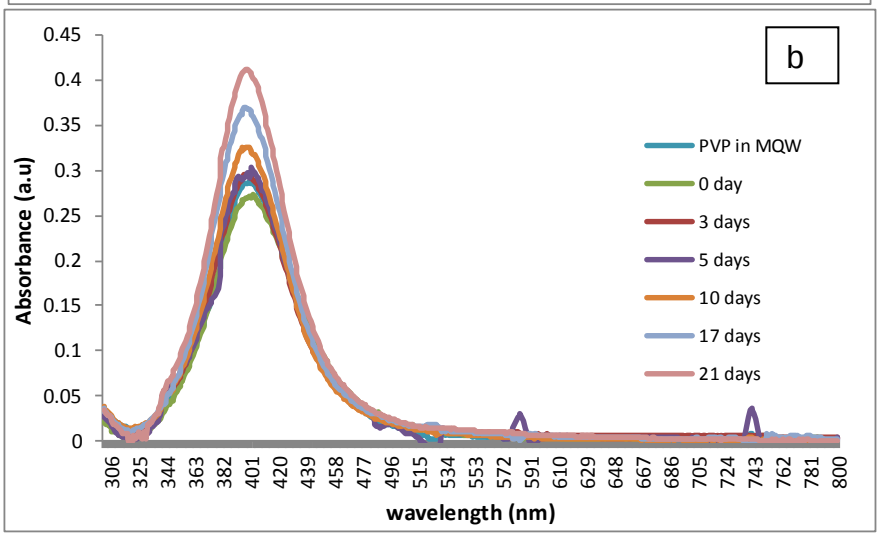
b
Absorbance (a.u)
wavelength (nm)
PVP in MQW
0 day
3 days
5 days
10 days
17 days
21 days

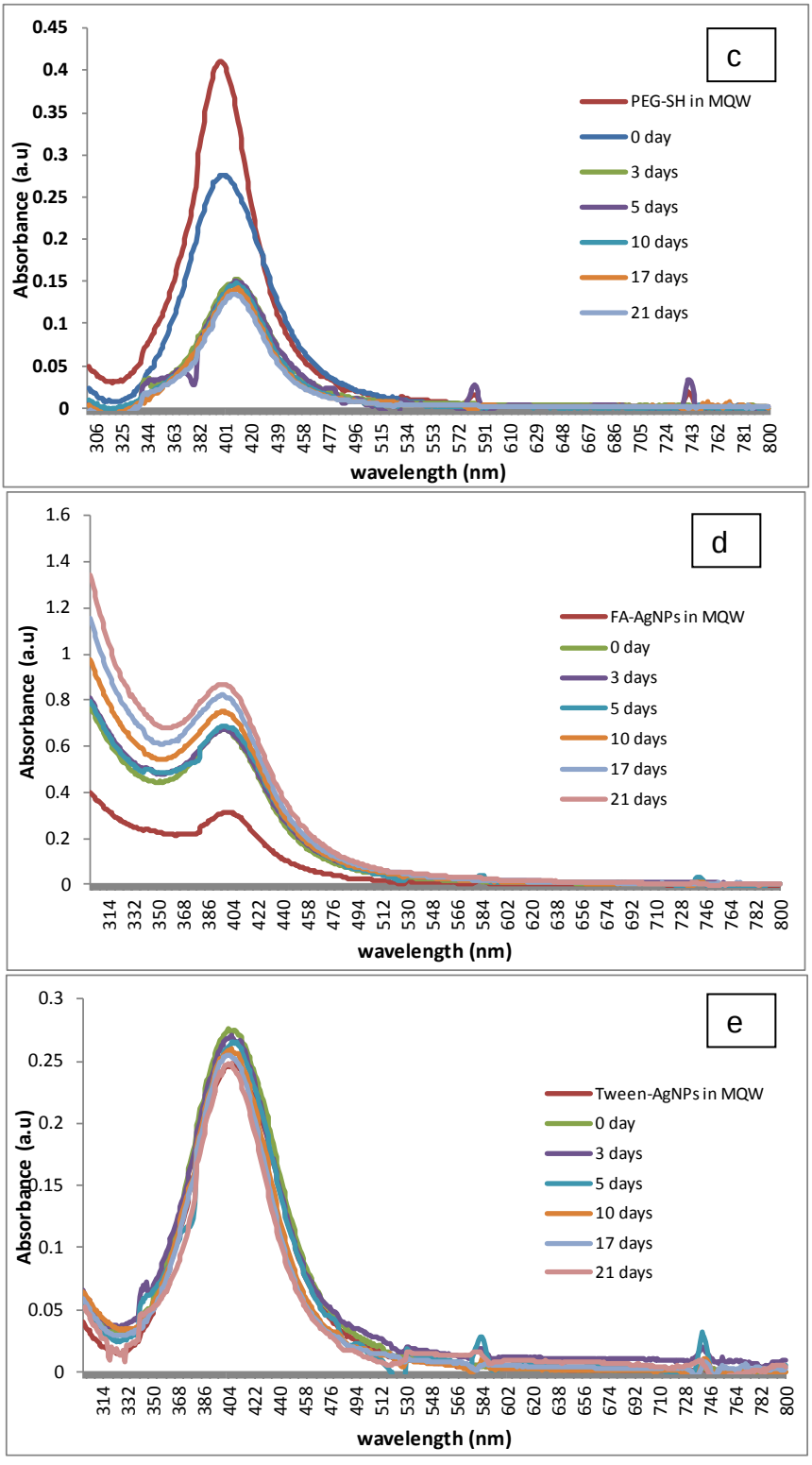

Figure 5. 11 The SPR of AgNPs with different capping agent in CM-1 within (a) 3 days incubation for citrate-capped AgNPs, and 21 days of incubation for (b) PEG-SH capped AgNPs; (c) PVP-capped AgNPs; (d) FA-capped AgNPs; (e) Tween-capped AgNPs

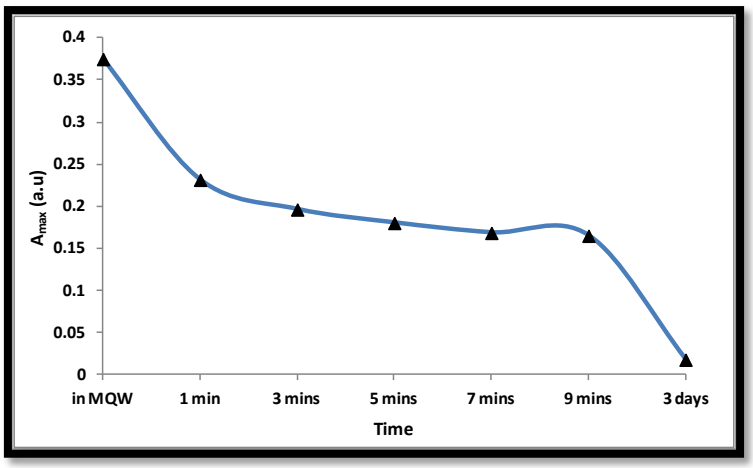

Figure 5. 12 The SPR extinction of citrate capped AgNPs in CM-1

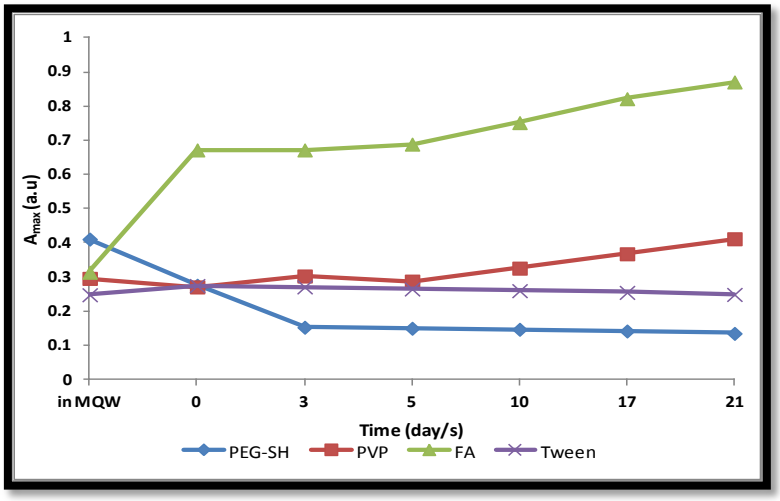

Figure 5. 13 Comparison of A_{max} changes of steric-capped AgNPs in full strength OECD media within 21 days (error bar was less than 0.01)

It was expected that the occurrence of ligand-exchange by polymer into citrate-capped AgNPs would be observed as the increase of the NPs stability in a high ionic strength media. It was seen that ligand-exchange by polymer enhanced the stability of AgNPs in CM-1 while the SPR of citrate-capped AgNPs extinct very rapidly. This stability enhancement of polymer-capped AgNPs was due to the increase of repulsive forces between the NPs as the ligand sterically cap the NPs (Hunter, 1986).

Figure 5. 12 and Figure 5. 13 illustrate the A_{max} of citrate-capped AgNPs and polymer-capped AgNPs in CM-1, respectively. Within minutes, the A_{max} of citrate-capped AgNPs in CM-1 vanished but recapping the NPs with polymers improved the AgNPs stability. The SPR of polymer-capped AgNPs was remained detected until end of 21 days of incubation.

A more significant increase of A_{max} was shown by fulvic-acid capped AgNPs. The A_{max} continuously increased until the end of 21 days study. This phenomenon could be explained by the fact that less aggregation will be seen as A_{max} intensification (Baalousha et al., 2013). By using TEM analysis, it was seen that well dispersed fulvic-acid capped AgNPs was still found after 21 days incubation in CM-1 (Figure 5. 14).

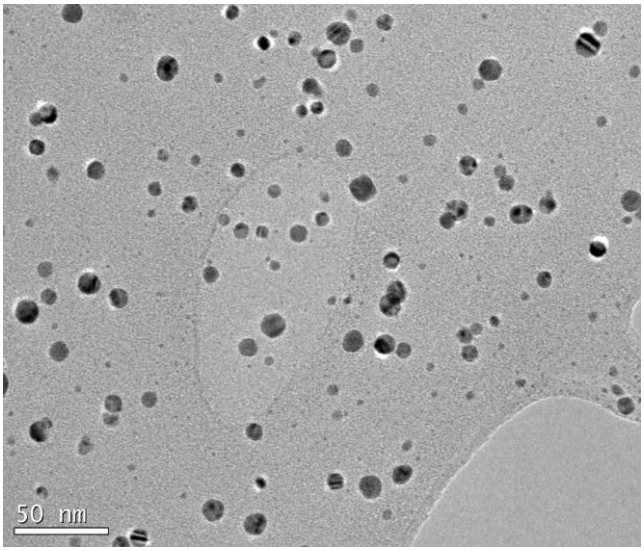

Figure 5. 14 Dispersion of fulvic-acid capped AgNPs after 21 days incubated in CM-1

Unexpectedly, the A_{max} of PEG-SH capped NPs decreased in the beginning of the study and then levelled off after 3 days incubation. This observation might be due to rapid dissolution of AgNPs as has been discussed in section 5.2.2. The A_{max} of Tween-80-capped AgNPs was also relatively stable during 10 days

incubation in CM-1, with minor decrease within the first 5 days, and remain unchanged over the rest of the trial.

5.4. Conclusion

This study demonstrated convincingly that the synthesis of polymer-capped AgNPs was more simple and practical than direct synthesis method. Substitution of electrostatic- with steric- capping agent increased the stability of AgNPs in a full strength ecotoxicology media. Ligand-exchange by PEG-SH and Tween-80 polymers, however, altered the original NPs characteristics. On the other hand, PVP and fulvic acid polymer preserve the core size of AgNPs. Therefore re-characterization of AgNPs generated by ligand-exchange is very important.

The chemisorptions of thiol-functional group of the PEG-SH polymer onto the AgNPs surface caused significant SPR and size changes. The λ_{max} was red-shifted and the FWHM broadened. The core size of AgNPs became smaller and the shape factor became less spherical (SF<1) possibly due to NP dissolution. On the other hand, the d_H size of AgNPs after recapped by PEG-SH, both measured by DLS and Fl-FFF, increased significantly as a thick ligand-shell surrounding the NPs was created. High ratio of d_H/d_{TEM} of PEG-capped AgNPs indicated softness or permeability of the capping layer compare to other ligands in this study, and lead to more dissolution of PEG- than citrate-capped AgNPs. The dissolution was manifested as the decrease of AgNPs core size in pristine suspension and A_{max} of AgNPs SPR in CM-1.

The PVP and fulvic acid polymer, on the other hand, did not affect the NPs core size. Incubated in CM-1 for 21 days showed the enhancement of A_{max}, suggesting grow of NPs and or because of less aggregation.

Formation of very small particles and large aggregates at the same time, due to tween-80 polymers capping action was another interesting finding in this study. Dissolution and re-deposition of Ag species might responsible for the size alteration. Multi peaks were shown by DLS and Fl-FFF size distribution corroborated the polydispersity of tween-capped AgNPs as also shown by the highest PdI value amongst other ligand-capped AgNPs. However, the tween polymer retained the AgNPs stable in the CM-1.

This study also verifies that full strength nitrate media is a good indicator for rapid examining of ligand-exchange occurence. Since the incomplete ligand-exchange was indicated by the appearance of red colour after mixed with NM-1, there is potential for the use of NM-1 as an indicator. Moreover it was demonstrated that UV-Vis, TEM, DLS, Fl-FFF and zeta potential were powerful tools for ligand-exchange analysis.

CHAPTER VI

STABILITY OF SILVER NANOPARTICLES IN ECOTOXICOLOGY MEDIA

Some part of this study has been published in Tejamaya, M. (2012) Environmental Science and Technology (ES&T) Journal, 46 (13), pp. 7011-7017 (the paper is attached)

Chapter Summary

Establishing the dose-response relationship of NPs in any (eco)toxicology studies is challenged by understanding of which characteristics of NPs can be referred as the dose. Providing full characteristics of NPs in any eco(toxicology) study thus become very important to be able to draw an association (Handy, Owen et al., 2008; Fabrega, Luoma et al., 2011).

In this study, the behaviour of well-characterized and tightly constrained AgNPs separately capped with one of three coatings (citrate, thiolated PEG and PVP) in selected ecotoxicology media was examined. As has been predicted, the characteristics of electrostatically, citrate-stabilised AgNPs was the most altered in all of tested media due to the dependence of electrostatic double layer (EDL) thickness into the ionic strength and media composition of the media. However citrate-capped AgNPs showed a better stability in algae media than in Daphnia media due to lower content of bivalent cation and Ca^{2+}, as well as lower ionic strength.

PEG- and PVP-capped AgNPs were more stable in all media as corroborated by color and SPR preservation, even though the d_H and PdI increased to some

extent. Yet, the decrease of SPR area of PEG-capped AgNPs was greater than citrate-capped AgNPs in Algae media, potentially due to dissolution-redeposition of NPs.

Shape transformation of citrate-capped AgNPs was found in dilution media without chloride. PEG- and PVP-capped AgNPs also generated non-spherical shape after incubated in concentrated media without chloride. Chloride content of the media, therefore imparted better stability of AgNPs, potentially due to formation Ag-Cl complex on the NPs surface. Thus, factors affecting behaviour and stability of AgNPs in ecotoxicology media were the type of capping agent, ionic strength and chemical composition of media.

6.1. Introduction

AgNPs are potentially toxic both to humans and the environment as has been presented in number of review papers (Handy, Kammer et al., 2008; Klaine, Alvarez et al., 2008; Fabrega, Luoma et al., 2011; Batley, Kirby et al., 2012; Reidy, Haase et al., 2013). As with exposure, there are many uncertainties about mechanisms of action, dose measurement, dose-response relationships and the physico-chemical form of the AgNPs during and after exposure in a complex media. In particular, the change in exposure dose and the nature of the toxicant in ecotoxicological media, due to aggregation, dissolution, shape and surface chemistry changes, is poorly quantified (Thomas, Judd et al., 1999; Alvarez et al., 2009; Handy et al., 2012). For AgNPs, there is little information about changes such as aggregation, dissolution and shape at high ionic strength and chloride concentrations relevant to such media.

Understanding both the dynamics of exposure concentration changes and the alteration in physico-chemical properties of NPs during ecotoxicology exposure is

essential in the interpretation of dose-response relationships. Those changes are likely to occur over relevant exposure periods which are poorly accounted for in the literature to date (Auffan et al., 2009; Stone, Nowack et al., 2010). A few studies have shown that aggregation (Shrivastava et al., 2007; Kvitek, Panaček et al., 2008) and dissolution(Brunner et al., 2006; Franklin, Rogers et al., 2007) of AgNPs have occurred in toxicology media with consequent changes in bioavailability and toxicity(Chen et al., 2010; Fabrega, Luoma et al., 2011). Systematic investigations of temporal changes over exposure are required and changes may be influenced by factors such as solution chemistry (Gao et al., 2009; Jin et al., 2010) and sunlight (Cheng, Yin et al., 2011).

This study examined the influence of capping agent, ionic strength and media composition to the AgNPs stability, in the absence of light. Three different capping agents which are representative and have been frequently used in other studies (Tolaymat, El Badawy et al., 2010) were utilised. They are citrate, which stabilizes NPs by charge repulsion (Henglein and Giersig, 1999) and is weakly bound to the core Ag; and thiolated-polyethylene glycol (PEG-SH) and polyvinyl pyrrolidone (PVP), which sterically-stabilize nanoparticles (Huang, Ni et al., 1996; Zhang, Zhao et al., 1996; Yoo, 1998), strongly bound to the core and potentially permeable to solutes and solvents. Standard OECD (Organisation for Economic Co-operation and Development) media for *Daphnia. Sp* (OECD/OCDE, 2004) for acute and chronic studies, its dilution and variants by replacement of specific ions, were employed to examine NP changes over both acute and chronic exposure timescales and under different media chemistry. The ISO algae media or also known as Bold Basal medium as one of media commonly used for eco(toxicology) study was also used to examine the stability of AgNPs coated with three different capping agents.

6.2. Aims and Objectives

The aim of this study was to examine the behavior and stability of citrate-, PEG- and PVP- coated AgNPs during incubation in Daphnia media for 21 days and in algae media during 3 days (72 hours).

The objectives were:

1. To analyse behavior and stability of citrate-, PEG-, and PVP-capped AgNPs in ecotoxicology media by evaluating the visual color preservation, size, zeta potential and shape alteration of AgNPs during and at the end of incubation period.
2. To evaluate the effect of capping agent to the stability of AgNPs
3. To evaluate the effect of media ionic strength to the stability of AgNPs
4. To evaluate the effect of media ionic composition to the stability of AgNPs

6.3. Methodology

The methods of NPs-media suspension preparation and characterization have been presented in section 3.8 and 3.7, respectively. The media composition used for this study has been presented in section 3.2.3. Briefly, OECD Daphnia media (CM) and Algae media (AM) were used for incubation. Two OECD Daphnia modifications, nitrate and sulphate media (NM and SM) were also used to examine the specific ion effect into AgNPs behavior during incubation. NM and SM were prepared by replacing the chloride content from CM media with nitrate and sulphate ion respectively. Both full strength and ten-fold dilution media concentration were used for testing the stability of AgNPs in CM, NM and SM, however single full concentration of Algae media (AM) was used.

6.4. Result

This section shows the behaviour of citrate-, PEG- and PVP-capped Ag NPs, incubated in OECD Daphnia media and variants (CM, NM, SM, section 6.4.1) and in algae media (section 6.4.2). The behaviour of AgNPs in eco-toxicology media was evaluated in the state of SPR, size and shape stability, analysed by UV-Vis instrument, DLS, and TEM and the results are presented in the following paragraph. Fl-FFF was also used for characterization of AgNPs in algae media only.

6.4.1. Behaviour of citrate-capped AgNPs in CM, NM and SM

It was observed that the characteristic yellow colour of the citrate-capped AgNPs turned into grey, red and purple within seconds in full strength of CM, NM and SM respectively (Figure 6.1.a) and totally disappeared after 24hrs (Figure 6.1.b) with the appearance of metal precipitate apart from CM-1 (Figure 6. 2). These changes were then confirmed with SPR analysis after 2 hours of incubation in the media (Figure 6. 3) and compared with the control.

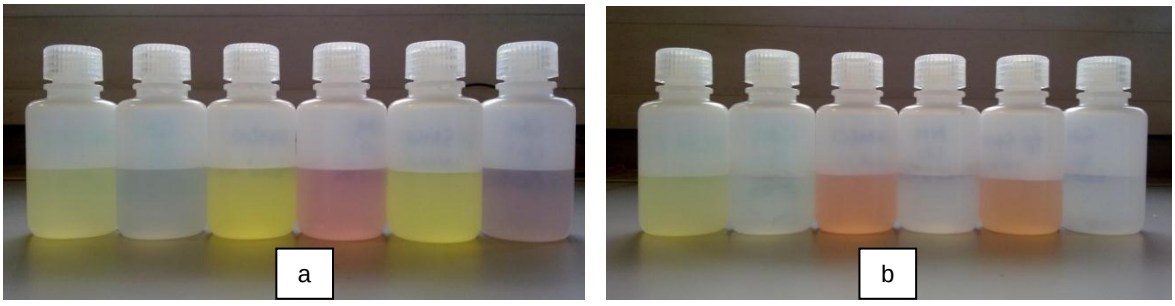

Figure 6. 1 Colour changes of citrate-coated AgNPs in different media (from left to right: CM-10; CM-1; NM-10; NM-1; SM-10 and SM-1). [a] immediately after media addition; [b] after 24 hours.

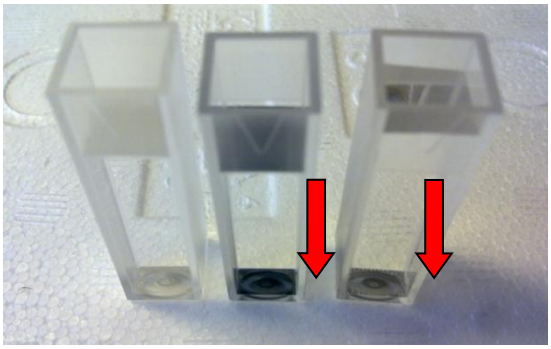

Figure 6. 2 The colour loss and appearance of sediment after citrate-capped AgNPs incubated in concentrated media for 24 hrs (from left to right: CM-1; NM-1 and SM-1)

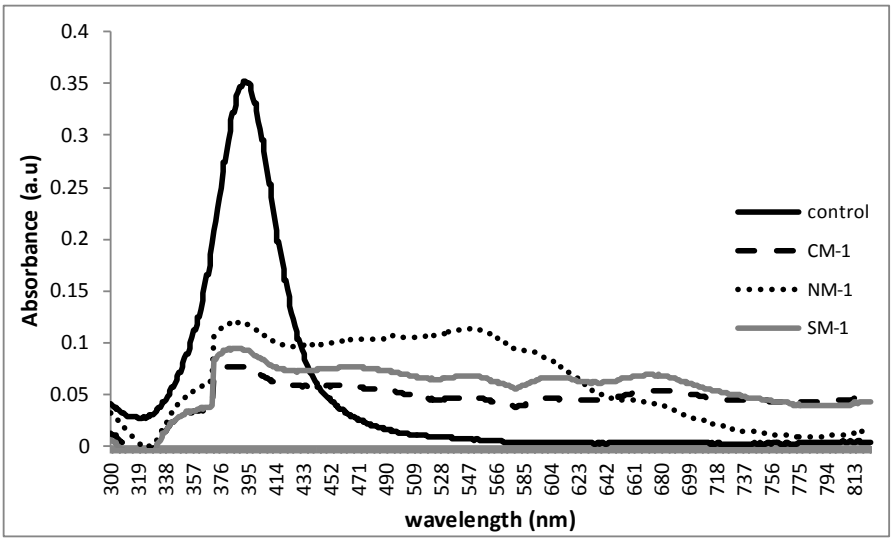

Figure 6. 3 The SPR of citrate-capped AgNPs after 2 hours of incubation in concentrated media, compared to the SPR of control

The absorbance kinetics (A_t/A_0) of citrate-capped AgNPs within first hour of incubation in concentrated media were measured at λ=392nm, the λ_{max} of citrate-capped AgNPs in pristine suspension (Figure 6. 4).

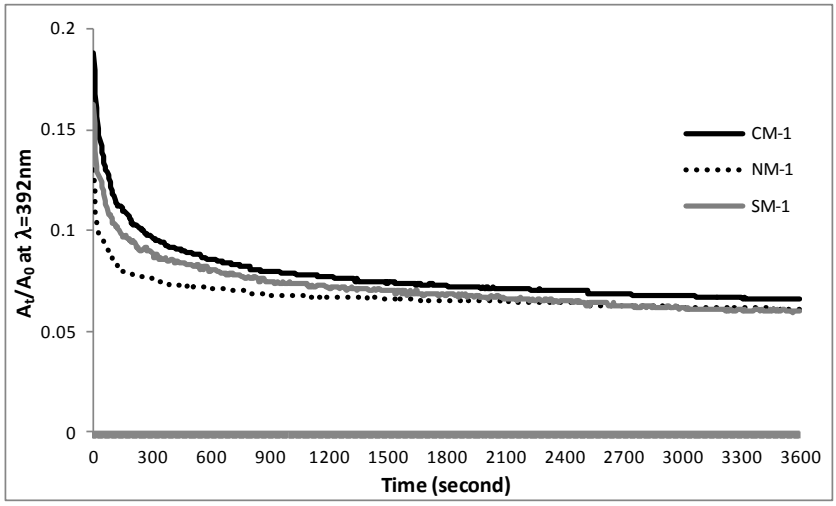

Figure 6. 4 The kinetics of absorbance decrease of citrate-capped AgNPs at λ_{max}=392nm during the first hour in concentrated media

A large absorbance decrease of citrate capped AgNPs at a λ_{max} 392 nm was observed in all concentrated media, corresponding to the loss of AgNPs yellow colour. Interestingly, a new (broader) absorbance peak appeared at longer wavelength which indicates the appearance of large aggregates (Liu et al., 2011; MacCuspie, Rogers et al., 2011; Tantra et al., 2011). Aggregation was followed by significant loss of signal interpreted as sedimentation and the appearance of sediment was primarily found in NM-1 (Figure 6. 2).

SPR behaviour of citrate-capped AgNPs was also evaluated in ten-fold dilution media (CM-10; NM-10 and SM-10), measured after 2 hours of incubation. In dilution media, different SPR changes were observed after 2 hours of incubation (Figure 6. 5). There was a slight absorbance decrease at λ_{max} of citrate-coated AgNPs in CM-10 for about 5% (Figure 6. 6 and Table 6. 1), but both NM-10 and SM-10 showed a more significant absorbance reduction at λ_{max} and appearance of a shoulder at around 470nm as indicated by the colour changes of AgNPs in NM-10 and SM-10.

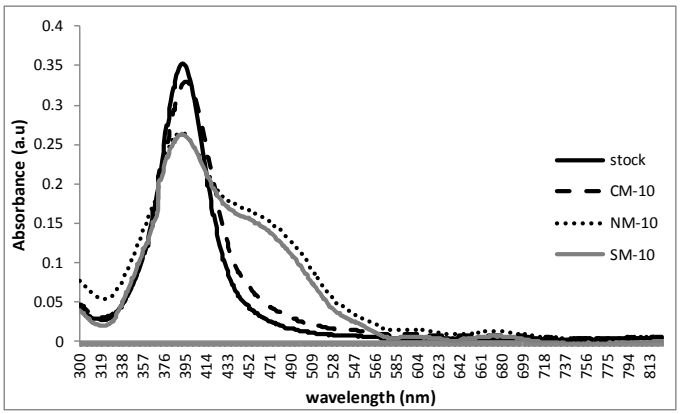

Figure 6. 5 The SPR of citrate-capped AgNPs in dilute media after 2 hours of incubation compare with the SPR of the control

Then the SPR characteristics of citrate-capped AgNPs, both in full strength and diluted media were continuously monitored within 21 days of incubation and the results are presented in Figure 6. 6. The total area under the SPR peak was measured and the decrease of SPR area compared to the control (%) was calculated according to Equation 6. 1.

$$Area\ decrease\ (\%) = \frac{Area_{(control)} - Area_{(t)}}{Area_{(control)}}\ x\ 100\% \qquad \text{Equation 6. 1}$$

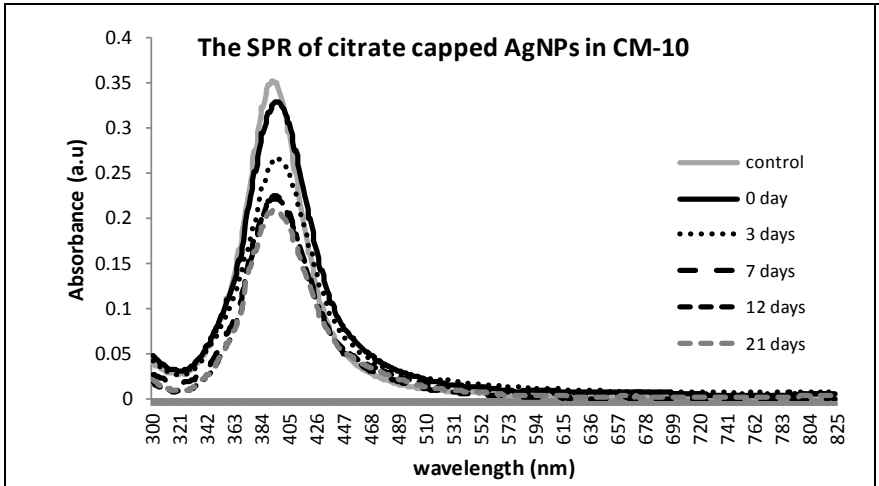
The SPR of citrate capped AgNPs in CM-10
Absorbance (a.u)
wavelength (nm)
control
0 day
3 days
7 days
12 days
21 days

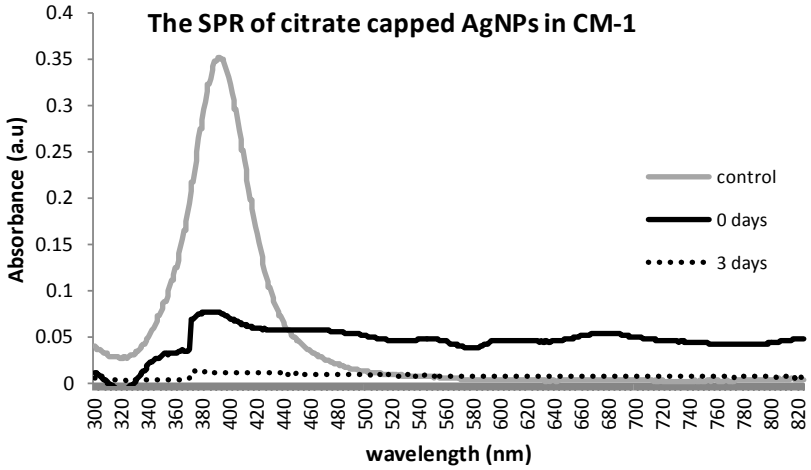
The SPR of citrate capped AgNPs in CM-1
Absorbance (a.u)
wavelength (nm)
control
0 days
3 days

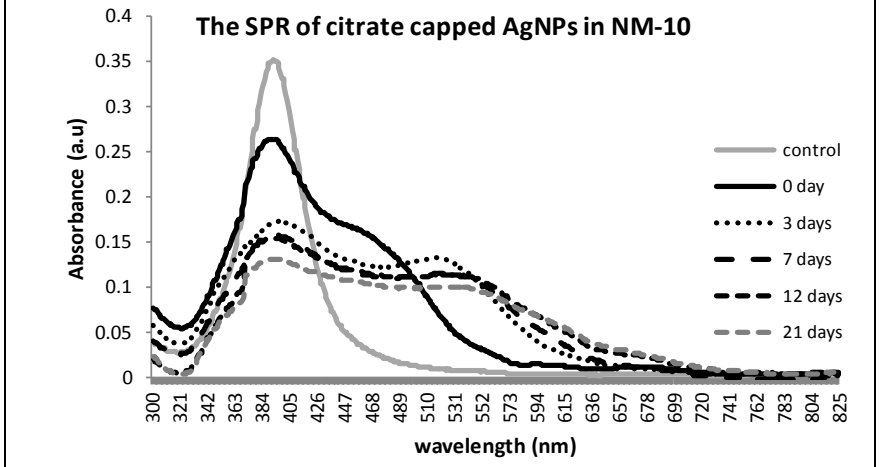
The SPR of citrate capped AgNPs in NM-10
Absorbance (a.u)
wavelength (nm)
control
0 day
3 days
7 days
12 days
21 days

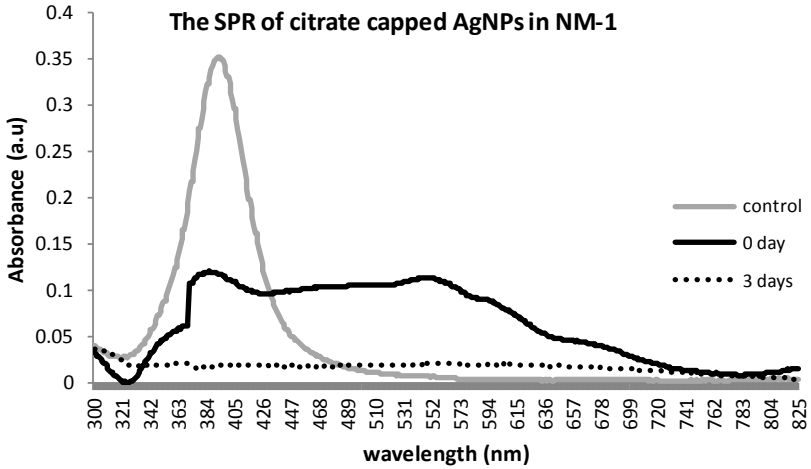
The SPR of citrate capped AgNPs in NM-1
Absorbance (a.u)
wavelength (nm)
control
0 day
3 days

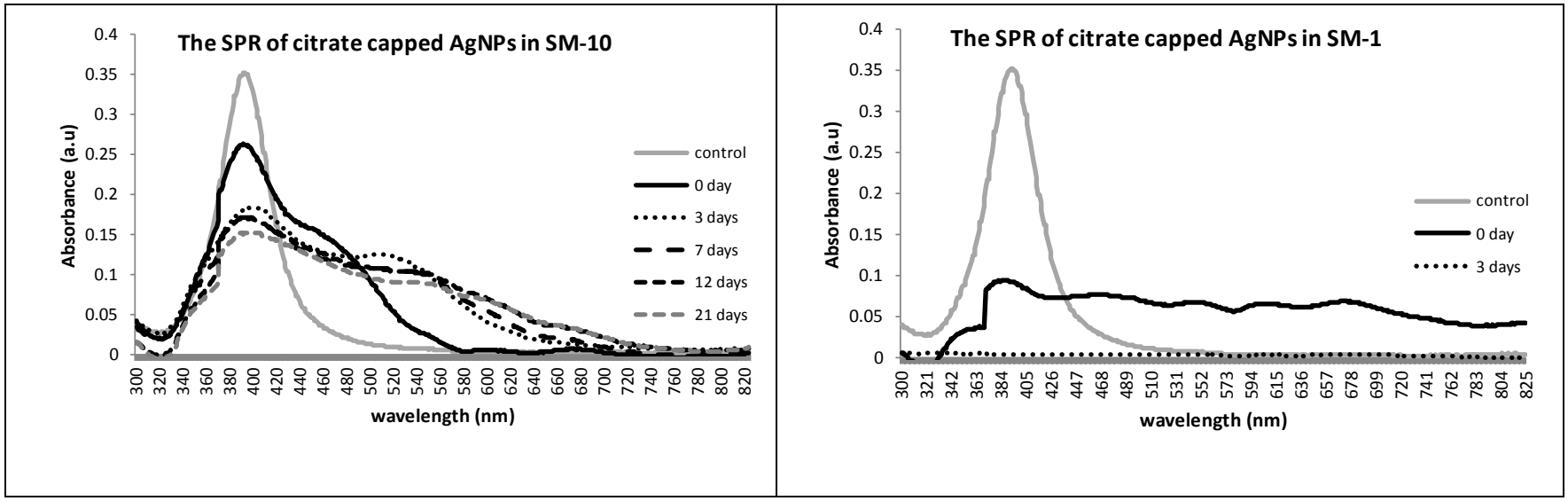

Figure 6. 6 The SPR stability of citrate capped AgNPs in various media within 21 days

Table 6. 1 The SPR area changes (%) of the citrate-capped AgNPs's in different media after 21 days incubation

SPR Area alteration (%)	**CM-10**	**NM-10**	**SM-10**
t= 2hrs	+5.01 ± 2.50	-9.21 ± 7.48	-14.34 ± 2.89
t= 3days	-9.66 ± 1.72	-14.75 ± 2.12	-13.87 ± 5.45
t= 7 days	-31.14 ± 2.80	-31.80 ± 3.18	-31.50 ± 1.2
t= 12 days	-34.30 ± 8.19	-46.00 ± 1.73	-44.57 ± 4.97
t= 21 days	-42.88 ± 8.21	-58.31 ± 1.31	-46.65 ± 2.71

(+) when the SPR area increased; and (-) when the area decreased compare to the control.

During 21 days of incubation, in all media, the SPR of citrate capped AgNPs changed over this time period. CM-10 was the only media where a minor qualitative change of the AgNP's SPR occurred, but the absorbance (peak area) decreased by approximately 43% over 21 days. Both in NM-10 and SM-10 the absorbance at λ_{max} continuously decreased and broadened with a shoulder shift to longer wavelengths (from 470 to 550nm). In all concentrated media, there was a total loss of this peak between 0-3 days, indicating losses through aggregation or other changes. These data indicate such changes are likely to be very rapid, in agreement with previous studies.

The d_H size average and size distribution of citrate-capped AgNPs after incubation in different media were measured by DLS and compared with the size of the control suspension (citrate-capped AgNPs in ultrapure water). Table 6. 2 presents the average size (z-average and Peak 1 size by intensity) and polydispersity index (PdI) of citrate-capped AgNPs after 24 hours incubation in different media. Figure 6. 7 illustrates the size distribution changes due to 24 hrs incubation in different media.

Table 6. 2 The dH size average and PdI of citrate-capped AgNPs after 24hrs incubated in variety of media,n measured with DLS

Property / Media	Z average	PdI	Peak 1 by intensity
High purity water	24.9 ± 1.5	0.2 ± 0.1	26.8 ± 1.4
CM-1	189.1 ± 7.6	0.4 ± 0.0	230.1 ± 28.6
NM-1	790.0 ± 166.0	0.7 ± 0.1	607.1 ± 75.3
SM-1	1104.5 ± 409.1	0.7 ± 0.4	601.8 ± 108.2
CM-10	76.0 ± 2.2	0.4 ± 0.0	116.9 ± 8.6
NM-10	42.9 ± 0.5	0.3 ± 0.0	57.1 ± 2.8
SM-10	42.4 ± 0.3	0.3 ± 0.0	59.7 ± 1.8

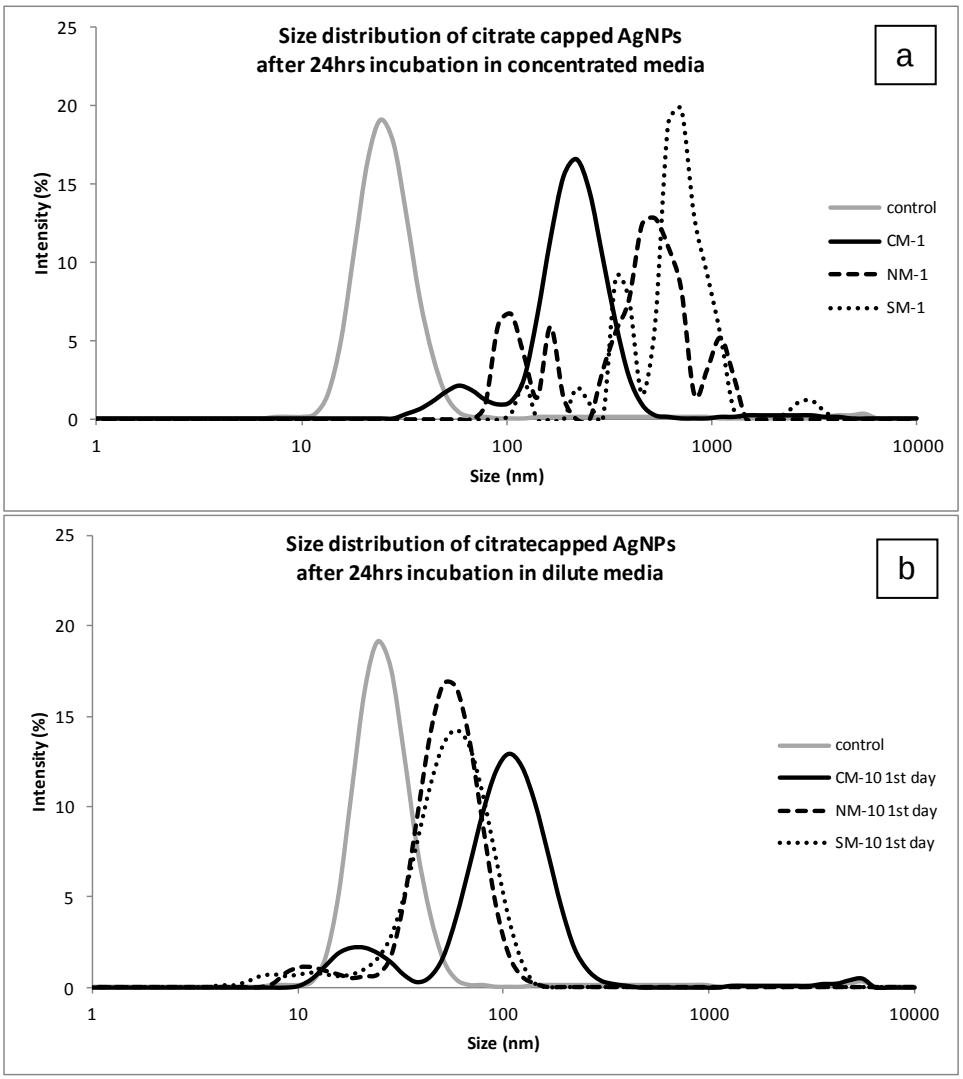

Figure 6. 7 Size distribution of citrate-capped AgNPs in (a) concentrated media; and (b) dilute media; after 24hrs incubation, compared to the control; and measured by DLS.

The DLS corroborated the size enlargement of the NPs after 24 hrs incubation in all media (Table 6. 2) and concentrated media caused extensive size changes of NPs. The z-average of AgNPs in SM-1 for example, grew enormously from about 25nm (d_H) into up to 1.1 micrometer and the 'Peak 1 size by intensity' changed from approx. 27nm size into around 600nm, corroborates the occurrence of aggregation.

The size distribution of citrate-capped AgNPs in diluted media was continuously measured within 21 days of incubation (Figure 6. 8). The trend of size alteration in CM-10 was shown to be different from size alteration in NM-10 and SM-

10. A dynamic aggregation-disaggregation of NPs in CM-10 was suggested by the appearance of two size peaks by DLS with dynamic peak area changes during 21 days of incubation (Figure 6.8.a). The peak area belong to larger size particle increased within the first 24 hours but then continuously decreased until end of 21 days of incubation, consumed by the increased of peak area of smaller size paticles. On the other hand, continuous growth of NPs in NM-10 and SM-10 was exhibited by continuous shift of DLS peak into larger size (Figure 6.8 b-c). This discrepancy was indicated by different colour changes of AgNPs in diluted media, where only CM-10 preserved yellow colour of AgNPs after 21 days of incubation.

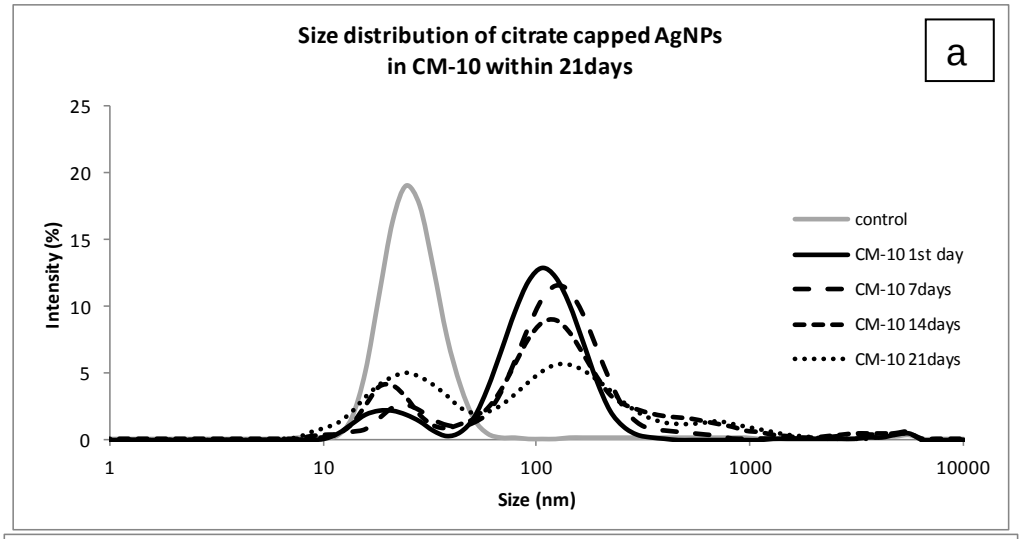

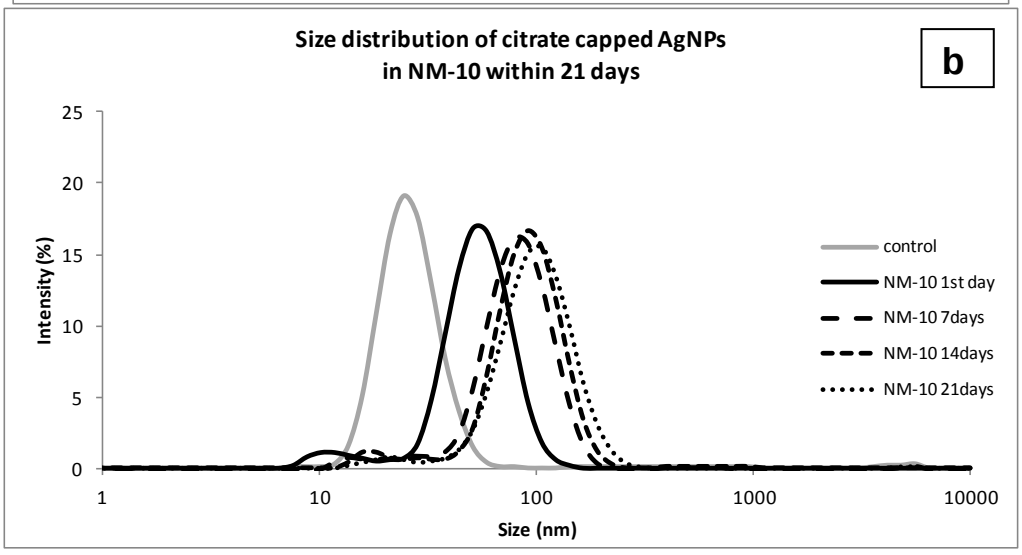

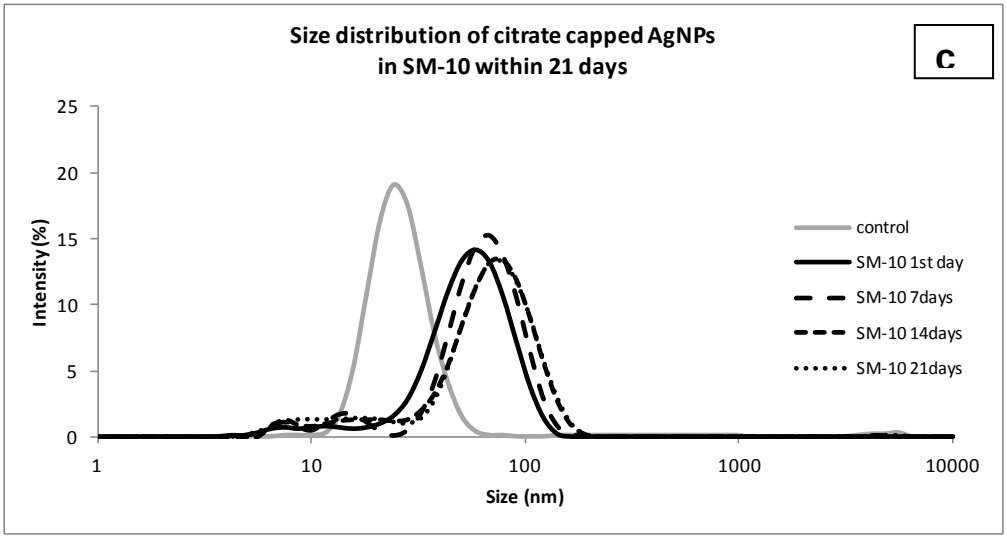

Figure 6. 8 Size distribution by intensity of citrate-capped AgNPs in (a) CM-10; (b) NM-10; and (c) SM-10 within 21 days incubation

The zeta potential (ζ) of citrate capped AgNPs in various media was measured at day 0, 7, and 21 of incubation (Figure 6. 9). The results show that the media altered the NP's zeta potential significantly, especially in concentrated media with no substantial pH changes (pH range = 6.8-7.5).

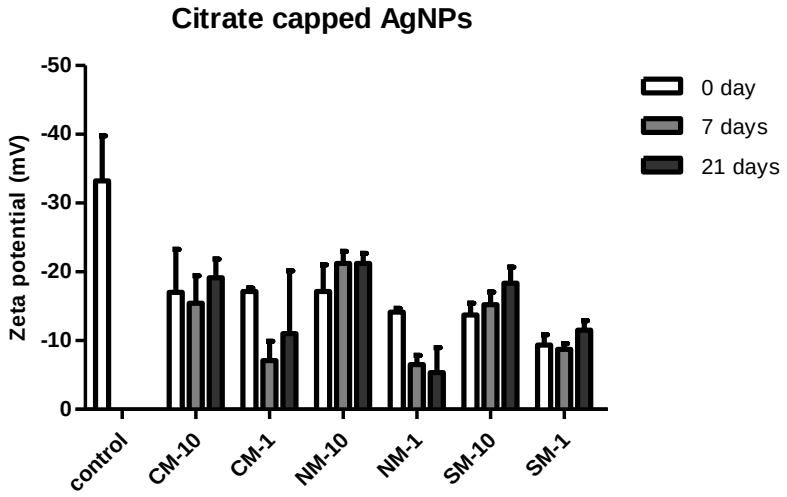

Figure 6. 9 The ζ of citrate capped AgNPs incubated in various media measured at 0; 7 and 21 days

Table 6. 3 The ζ of citrate capped AgNPs in various media measured at 0,7 and 21 days.

Media	zeta potential (mV)		
	0 day	7 days	21 days
CM-10	-17 ± 6.21	-15.4 ± 3.99	-19.1 ± 2.7
CM-1	-17.1 ± 0.52	-7.07 ± 2.78	-11 ± 9.1
NM-10	-17.1 ± 3.87	-21.2 ± 1.75	-21.2 ± 1.45
NM-1	-14.1 ± 0.53	-6.48 ± 1.35	-5.32 ± 3.6
SM-10	-13.7 ± 1.69	-15.2 ± 1.83	-18.3 ± 2.36
SM-1	-9.31 ± 1.52	-8.68 ± 0.83	-11.5 ± 1.36
control	-33.2 ± 6.51		

Table 6. 4 pH of citrate capped AgNPs suspension in different media

Incubation time	CM-10	CM-1	NM-10	NM-1	SM-10	SM-1
0 day	6.8	6.7	7.2	6.9	6.9	7
6 days	7	7.3	7.4	7.4	7.4	7.5
14 days	7.3	6.9	7.3	6.9	7.2	6.9
21 days	7.2	6.8	7.1	6.7	7	6.7

The decrease of zeta potential (ζ), a measure of electrostatic potential at the stern plane, indicates the decrease of repulsive forces of citrate capped AgNPs in concentrated media. In high purity water, the ζ was around -33mV but then altered into less than -12mV in concentrated media and -21mV in dilute media with no significant pH changes (Table 6.4). Since the zeta potential moved away from cut off -30mV toward point 0 in all media, the NPs was predicted to be less stable in the media than in high purity water (control).

TEM was used for visualization of remaining NPs in all media after 21 days incubation. NPs could only be detected in dilute media (Figure 6. 10) but nothing remained in the concentrated media.

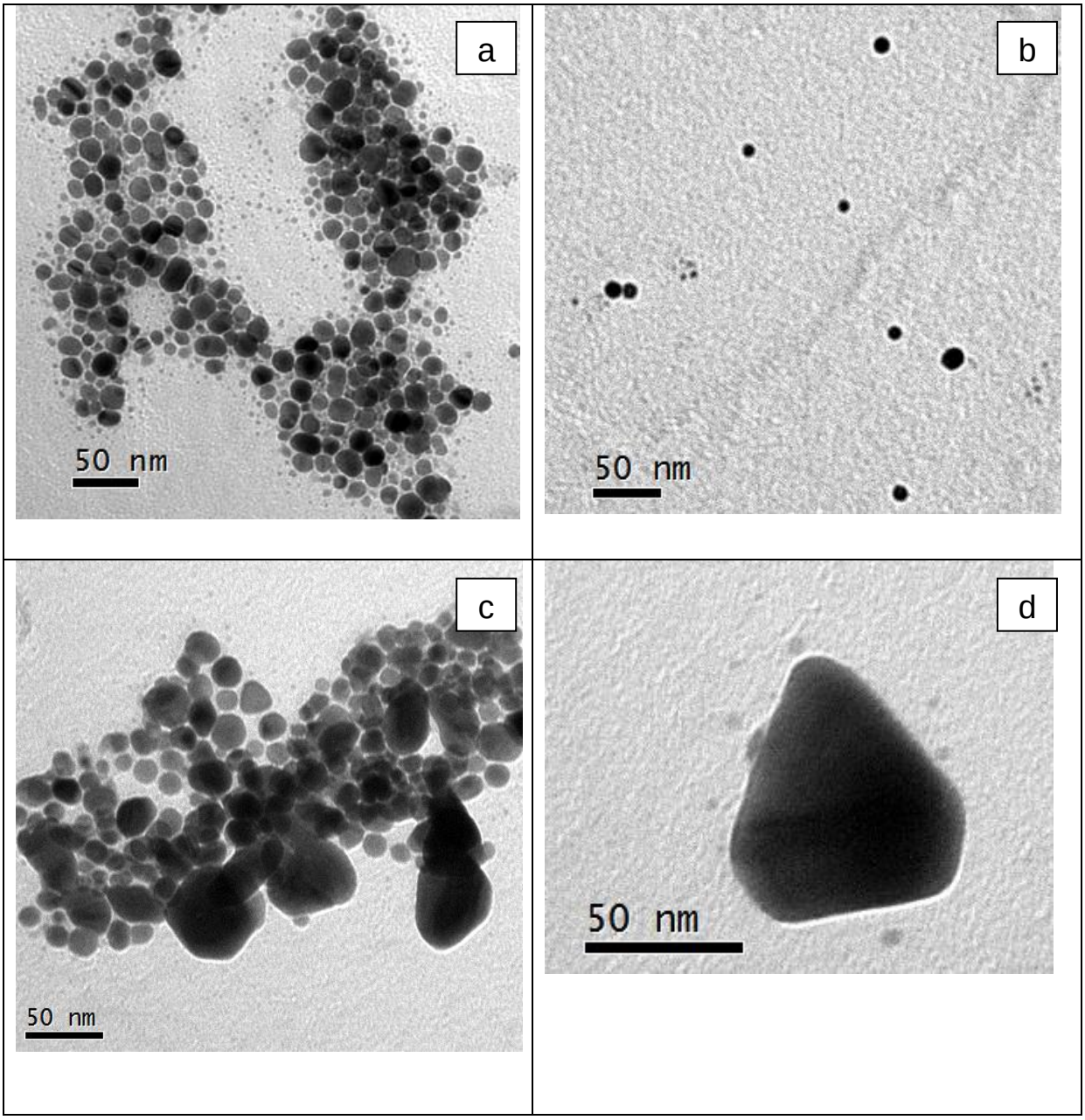
a
50 nm
b
50 nm
c
50 nm
d
50 nm

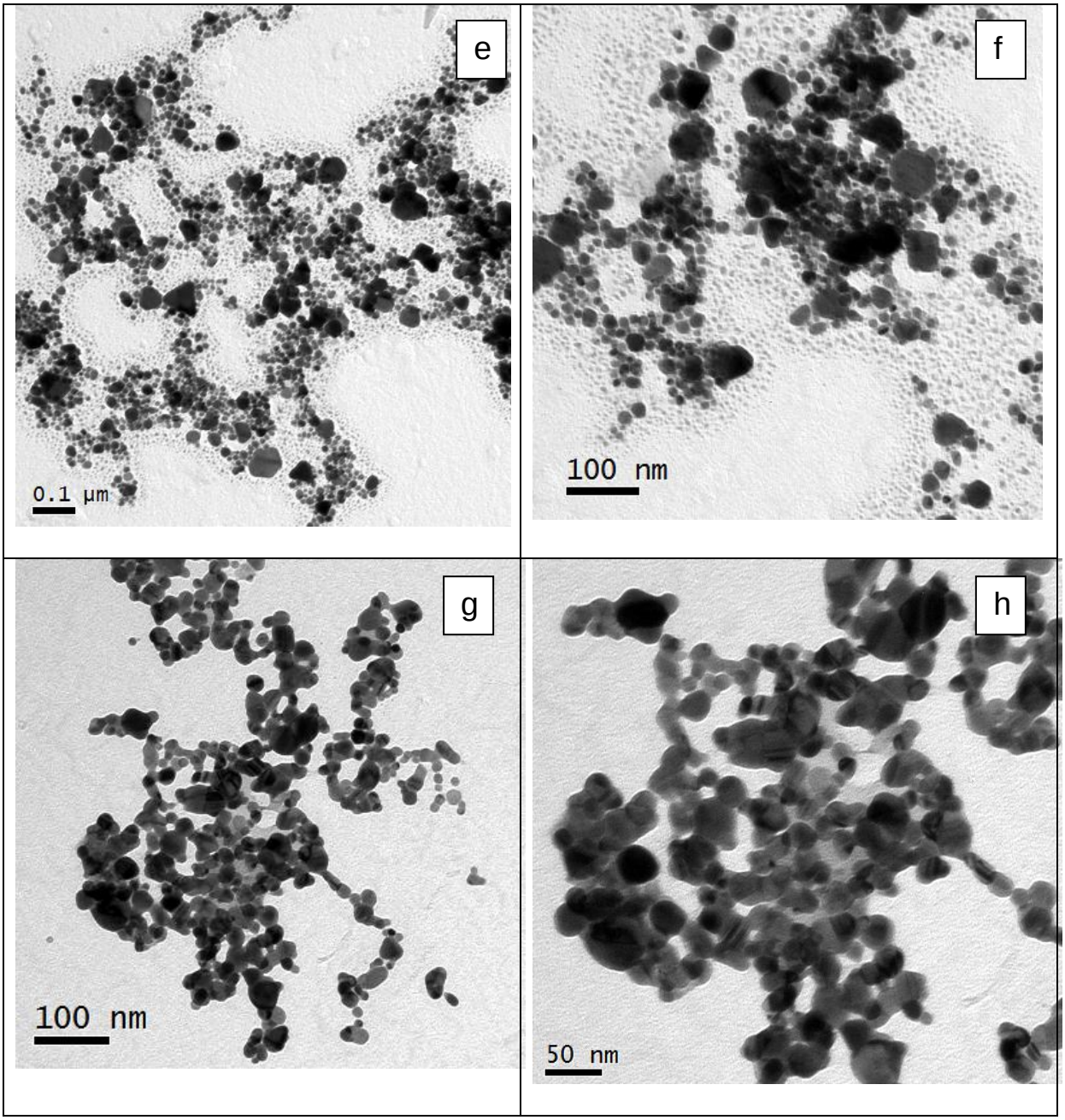
e
0.1 µm
f
100 nm
g
100 nm
h
50 nm

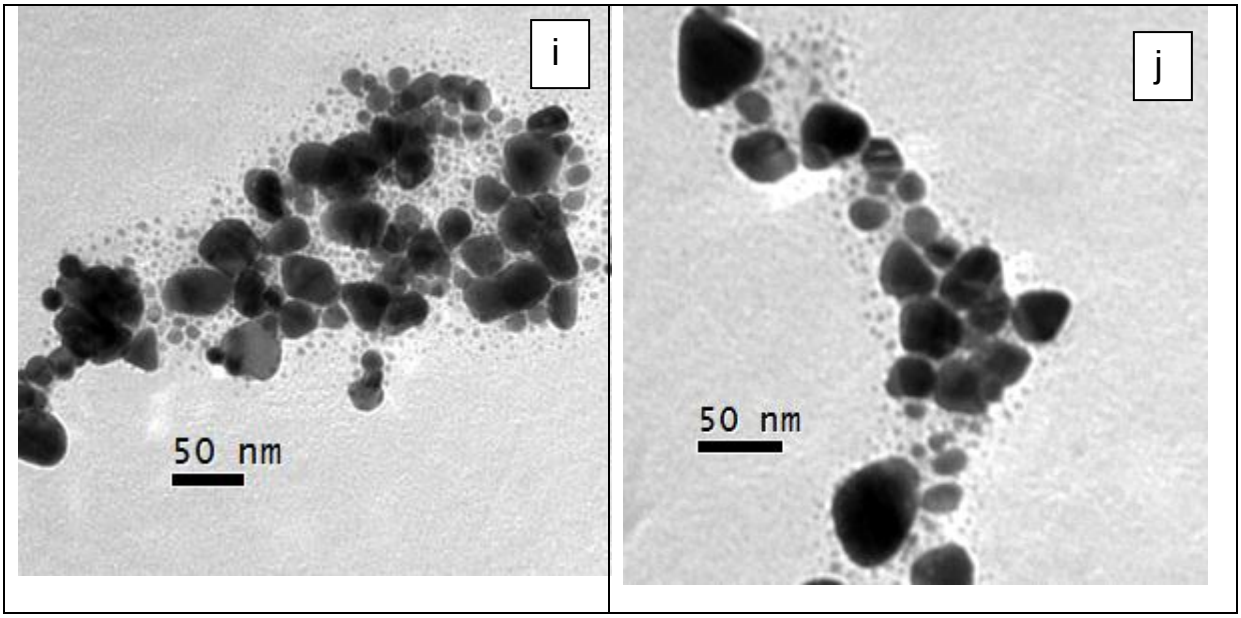

Figure 6. 10 TEM images of citrate-capped AgNPs in diluted media: (a) and (b) in CM-10 after 21 days; (c) and (d) in NM-10 after 2 weeks; (e) and (f) in NM-10 after 21 days; (g) and (h) in SM-10 after 2 weeks; and (i) and (j) in SM-10 after 21 days

No AgNPs were observed by TEM imaging in concentrated media by the end of 21 days incubation as the AgNPs formed large aggregates and settled down (Figure 6. 2). Only in CM-10 the dispersion of AgNPs with minor aggregation was observed, in fact shape transformation of AgNPs in NM-10 and SM-10 were observed.

.

6.4.2. Behaviour of PEG-capped AgNPs in CM-1; NM-1 and SM-1

Unlike citrate-capped AgNPs, throughout 21 days incubation the PEG-capped AgNPs retained its yellow colour in all media including in concentrated media. During the first five minutes of incubation in concentrated media, no significant fluctuation of A_t/A_o at λ_{max} 398nm of PEG-capped AgNPs (Figure 6. 11) while there was a large decrease of A_t/A_o at λ_{max} of citrate-capped AgNPs in concentrated media (Figure 6. 4). It indicates a better AgNPs stability imparted by PEG-SH capping agent. The SPR of PEG-capped AgNPs after 2 hours incubation in different media was analysed and is presented in Figure 6. 12. The alteration of plasmon peak position and width were analysed and is presented in Table 6. 5.

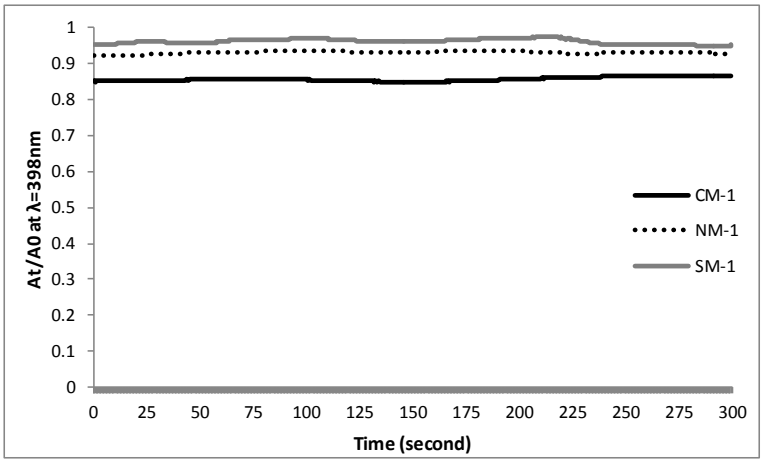

Figure 6. 11 Kinetics (A_t/A_0) of PEG capped AgNPs in concentrated media within the first 5 minutes of incubation.

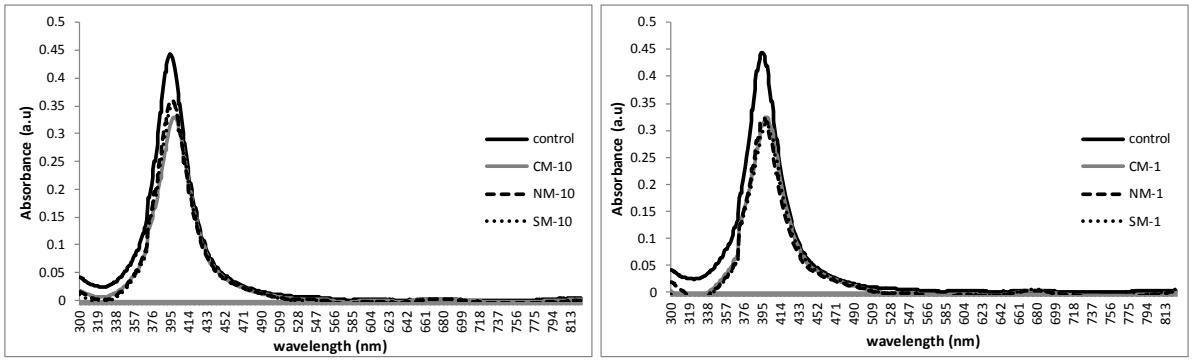

Figure 6. 12 The SPR of PEG-capped AgNPs in (a) various dilute media; and (b) various concentrated media measured after 2 hours incubation.

Table 6. 5 The λ_{max} and FWHM of PEG-capped AgNPs suspended in different media and measured after 2 hours incubation.

	control	CM-10	NM-10	SM-10	CM-1	NM-1	SM-1
λmax	395	400	397	398	398	397	398
FWHM	38	41	39.5	41	42	38	42

Within 2 hours of incubation, it was shown that the SPR area decreased by 21-33%, and the decrease was greater in concentrated media. Then the SPR behaviour of PEG-capped AgNPs was continuously monitored throughout 21 days of incubation and the results are presented in Figure 6. 13. Table 6. 6 shows the decrease of SPR area of AgNPs during 21 days incubation in different media, calculated according to Equation 6.1.

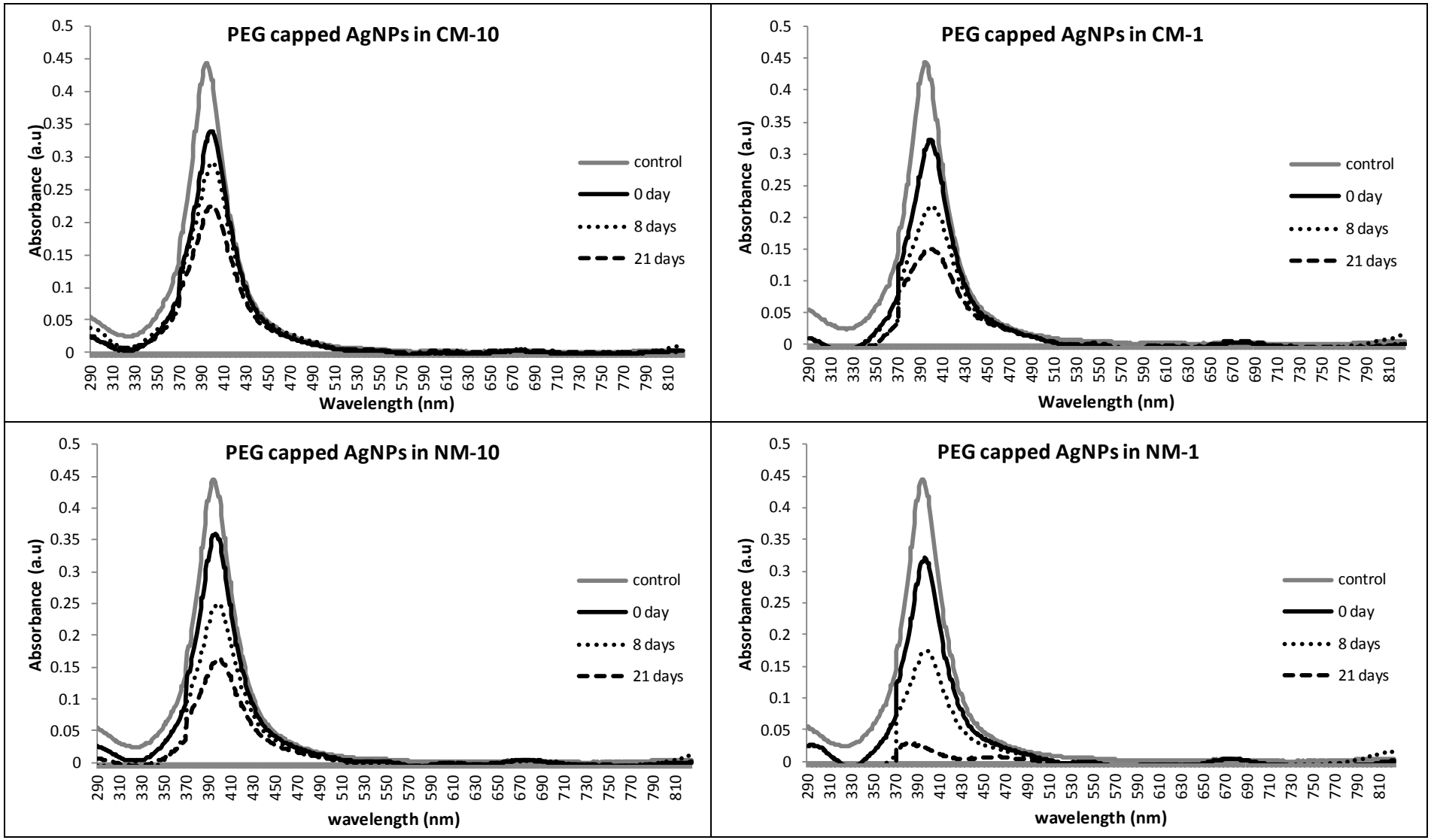
PEG capped AgNPs in CM-10
Absorbance (a.u)
Wavelength (nm)
control
0 day
8 days
21 days
PEG capped AgNPs in CM-1
Absorbance (a.u)
Wavelength (nm)
control
0 day
8 days
21 days
PEG capped AgNPs in NM-10
Absorbance (a.u)
wavelength (nm)
control
0 day
8 days
21 days
PEG capped AgNPs in NM-1
Absorbance (a.u)
wavelength (nm)
control
0 day
8 days
21 days

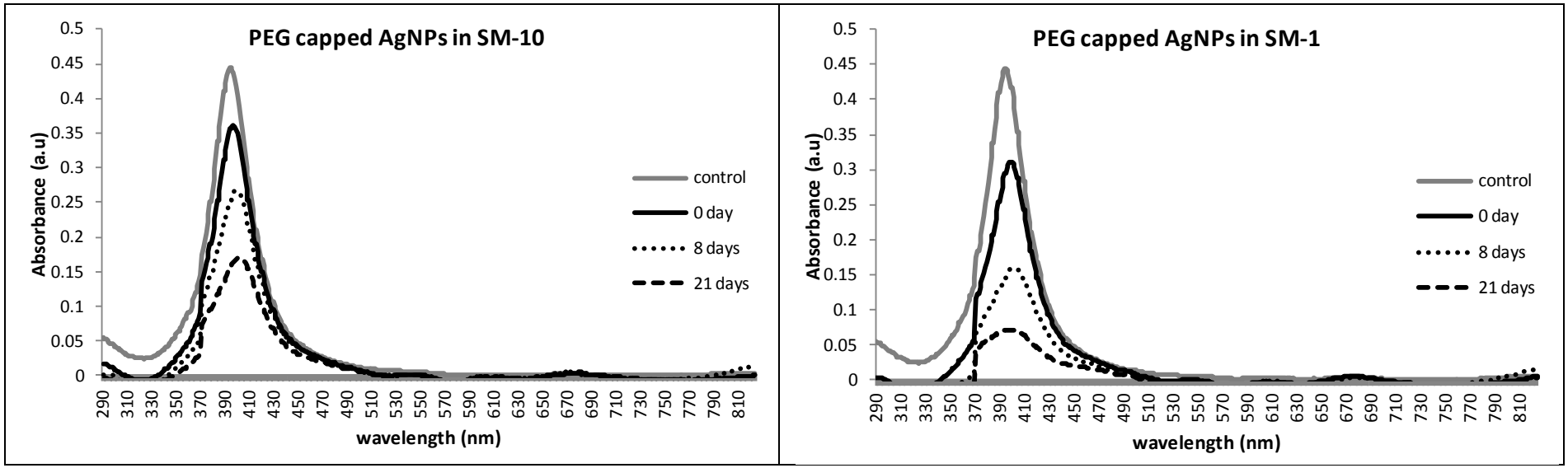

Figure 6. 13 The SPR of PEG-capped AgNPs in various media during 21 days incubation

Table 6. 6 The alteration of SPR's peak area of PEG-capped AgNPs after 21 days incubation

	CM-10	NM-10	SM-10	CM-1	NM-1	SM-1
t= 2hrs	**-24.24 ± 4.53**	**-21.15 ± 1.45**	**-21.69 ± 0.94**	**-28.02 ± 0.28**	**-33.28 ± 1.19**	**-31.52 ± 1.00**
t= 8 days	**-35.04 ± 7.08**	**-43.35 ± 3.61**	**36.40 ± 2.75**	**-49.97 ± 6.16**	**-68.62 ± 3.77**	**-61.79 ± 3.98**
t= 21 days	**-45.09 ± 5.29**	**59.33 ± 4.48**	**55.18 ± 3.04**	**61.79 ± 7.47**	-96.52 ± 2.76	-88.06 ±3. 5

It was observed that within 21 days of incubation in various media the absorbance of PEG-capped AgNPs at λ_{max} 395nm continuously dropped off although the yellow colour was preserved. The smallest decrease was again found in the dilute media and in the chloride containing (ca 45% in CM-10 and 62% in the CM-1). However, in some cases essentially the entire peak disappeared (e.g. NM-1) indicating a complete loss of material.

The d_H of PEG-capped AgNPs after suspended in different media was measured by DLS. The z average, PdI and Peak 1 size by intensity after 24 hrs of incubation is presented in Table 6. 7. Size distributions of PEG-capped AgNPs in different media after 24hrs incubation are illustrated in Figure 6. 14.

Table 6. 7 The size and PdI of PEG-capped AgNPs in different media after 24hrs incubation measured by DLS

Property / Media	Z average	PdI	Peak 1 by intensity
High purity water	40.88 ± 1.53	0.15 ± 0.02	42.65 ± 2.09
CM-1	44.34 ± 1.72	0.24 ± 0.03	46.98 ± 2.84
NM-1	49.34 ± 3.73	0.29 ± 0.04	44.93 ± 7.16
SM-1	51.19 ± 4.41	0.29 ± 0.09	45.63 ± 2.00
CM-10	43.79 ± 2.51	0.28 ± 0.10	44.36 ± 2.34
NM-10	46.52 ± 3.23	0.25 ± 0.06	44.39 ± 5.43
SM-10	52.08 ± 5.83	0.31 ± 0.09	49.02 ± 8.08

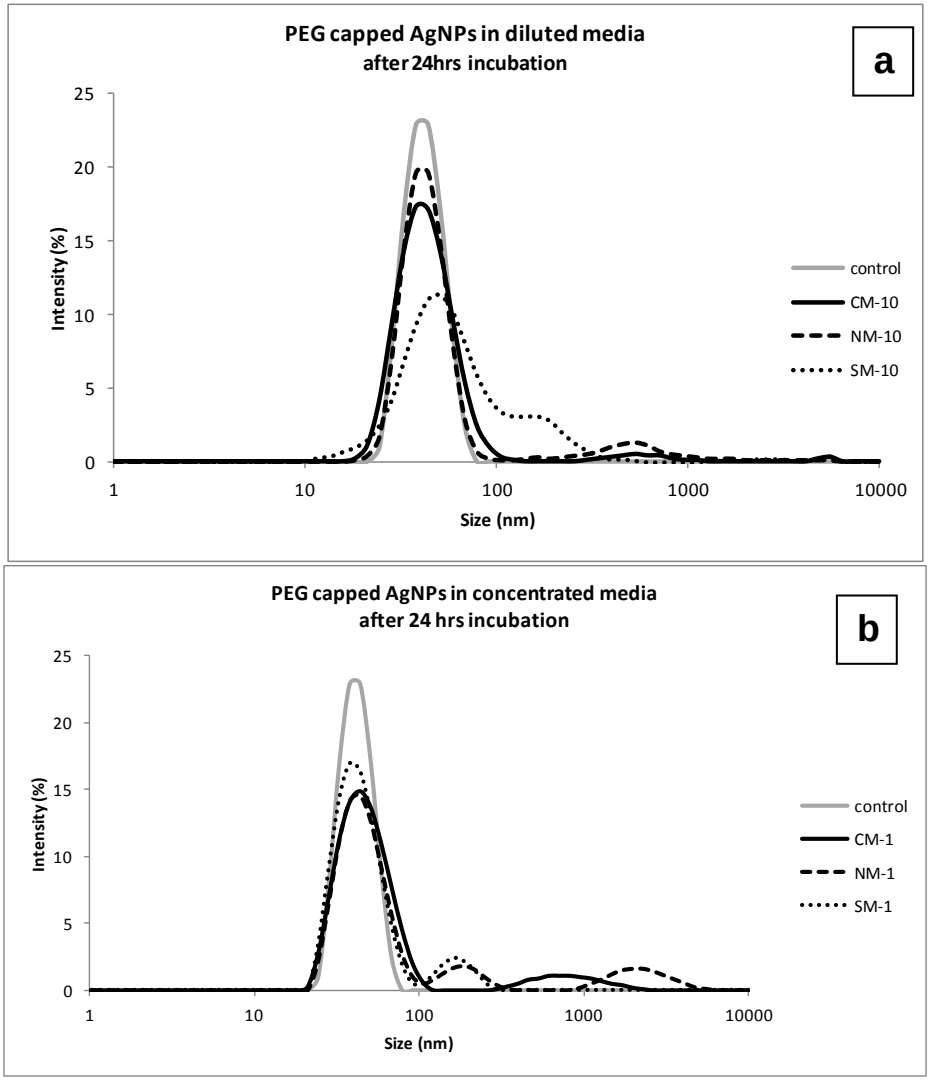

Figure 6. 14 Size distribution of PEG-capped AgNPs after 24 hrs incubation in (a) concentrated media and (b) dilute media

The d_H (z-average) of PEG-capped AgNPs during 21 days incubation in different media was measure by DLS. Figure 6. 15 and **Error! Reference source not found.** show the trend of z-average size and size distribution of PEG-capped AgNPs during 21 days incubation in different media respectively.

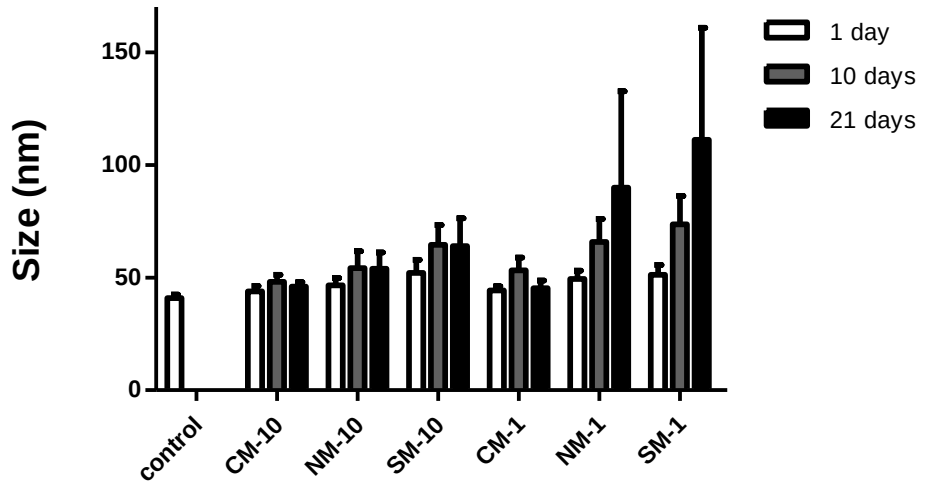

Figure 6. 15 z-average of PEG-capped AgNPs in different media within 21 days

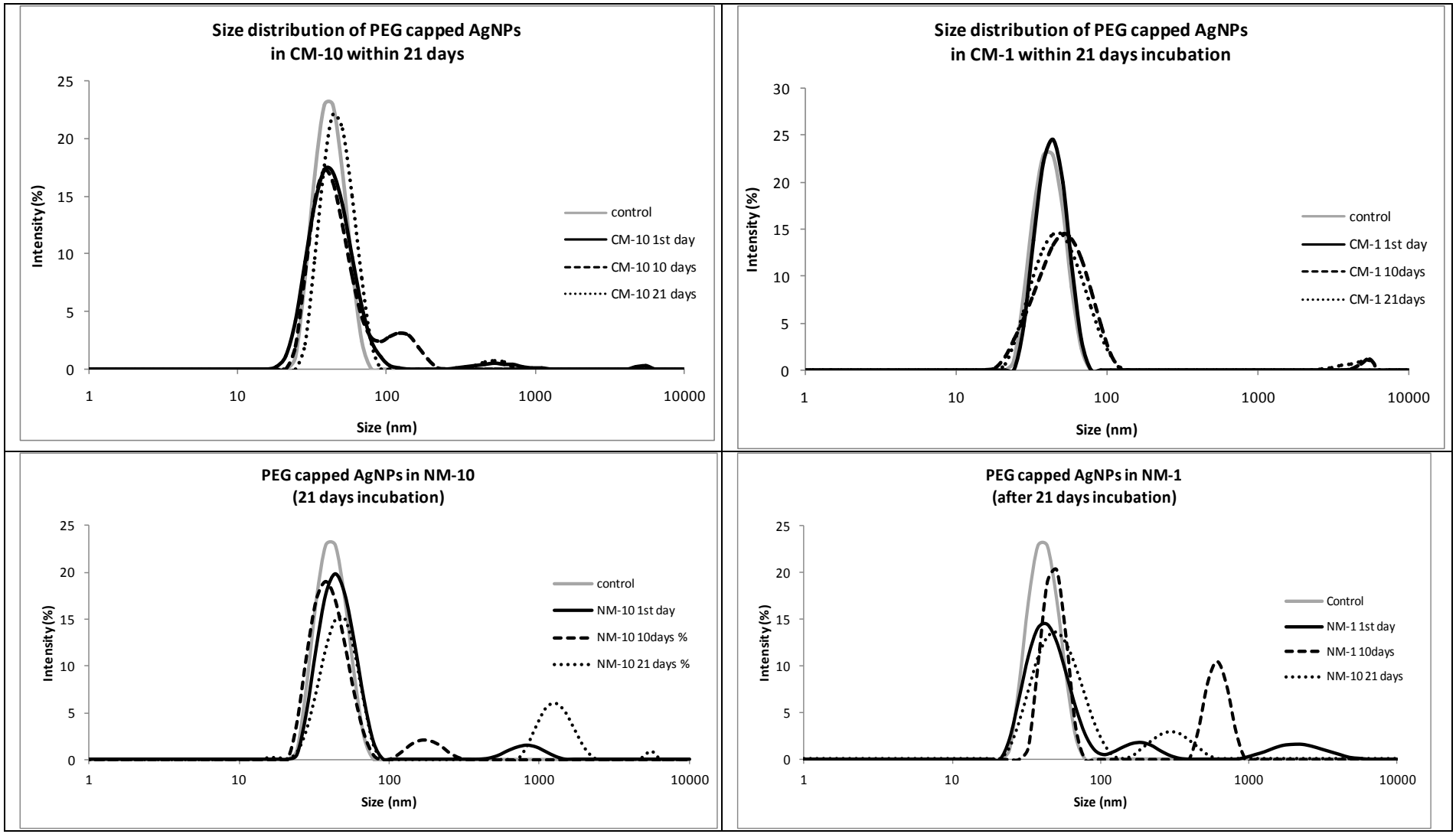
Size distribution of PEG capped AgNPs in CM-10 within 21 days
Intensity (%)
Size (nm)
control
CM-10 1st day
CM-10 10 days
CM-10 21 days
Size distribution of PEG capped AgNPs in CM-1 within 21 days incubation
Intensity (%)
Size (nm)
control
CM-1 1st day
CM-1 10days
CM-1 21days
PEG capped AgNPs in NM-10 (21 days incubation)
Intensity (%)
Size (nm)
control
NM-10 1st day
NM-10 10days %
NM-10 21 days %
PEG capped AgNPs in NM-1 (after 21 days incubation)
Intensity (%)
Size (nm)
Control
NM-1 1st day
NM-1 10days
NM-10 21 days

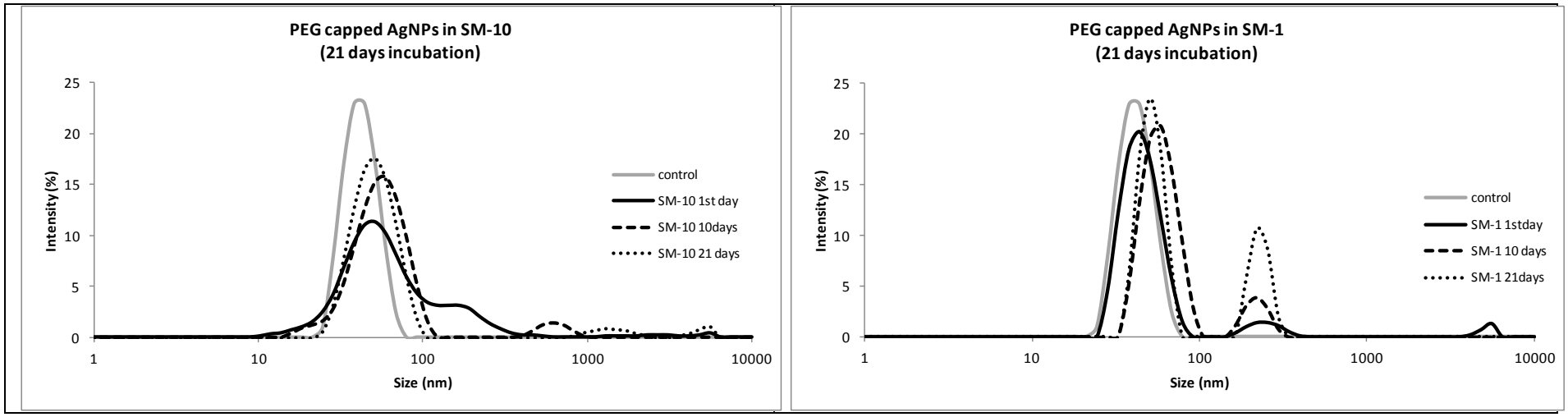

Figure 6. 16 Size distribution by intensity of PEG-capped AgNPs in different media within 21 days

Similar with the SPR data, the size distribution of PEG-capped AgNPs in different media both in concentrated and diluted media was also more stable than citrate-capped AgNPs. Minor aggregation of PEG-capped AgNPs in CM-10, NM-10 and NM-1 after 24hrs of incubation was corroborated by the increase of z-average and the PdI value while preserving the Peak 1 size by intensity. During 21 days of incubation, the z-average of PEG capped AgNPs in dilute media was relatively unchanged Figure 6. 16. In some concentrated media (NM-1 and SM-1), however the NPs grew tremendously at the end of incubation period, in agreement with the SPR extinction finding, suggesting aggregation of NPs.

The ζ and pH of PEG-capped AgNPs during 21 days incubation in different media were measured Figure 6. 17 and Table 6. 8. It was found that ζ of PEG-capped AgNPs in all media became less negative than the control, especially in concentrated media while there was no significant pH variance. However as PEG polymer stabilised the NPs sterically, the ζ value in fact, is not relevant for NPs stability estimation.

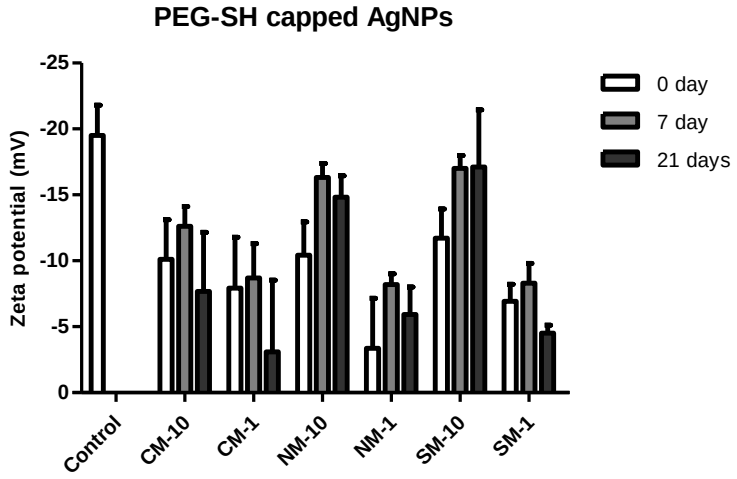

Figure 6. 17 The ζ of PEG-capped AgNPs in different media measured at incubation day = 0; 7; and 21 days

Table 6. 8 The ζ of PEG-capped AgNPs indifferent media

Media	zeta potential (mV)		
	0 day	7 days	21 days
CM-10	-10.1 ± 3	-12.6 ± 1.5	-7.66 ± 4.5
CM-1	-7.91 ± 3.9	-8.67 ± 2.6	-3.07 ± 5.5
NM-10	-10.4 ± 2.5	-16.3 ± 1.1	-14.8 ± 1.6
NM-1	-3.35 ± 3.8	-8.18 ± 0.8	-5.91 ± 2.1
SM-10	-11.7 ± 2.2	-17 ± 1.0	-17.1 ± 4.3
SM-1	-6.9 ± 1.3	-8.28 ± 1.5	-4.48 ± 0.6
control	-19.5 ± 2.3		

Table 6. 9 pH of PEG-capped AgNPs in different media

Incubation time	CM-10	CM-1	NM-10	NM-1	SM-10	SM-1
0 day	6.9	6.6	6.7	6.8	6.8	7
7 days	6.9	7.2	7.4	7.2	7.4	7.4
21 days	7.5	7.1	7.2	7.1	7.2	6.8

The remaining PEG-capped AgNPs in different media after 21 days incubation were analysed by TEM (Figure 6. 18). It was revealed that the PEG-capped AgNP maintained its dispersion form in all diluted media with some aggregates in SM-10. However, there were no noticeable single NPs in NM-1 after 21 days incubation except large aggregates as indicated by the disappearance of SPR in NM-1. Interestingly, in CM-1 well dispersed AgNPs were found. Better stability of PEG-capped AgNPs than citrate was due to steric repulsion formation by PEG-SH polymer on NPs surface that hindered the NPs from aggregation as has been shown in the work of gold NPs (AuNPs) (Wang et al., 2008).

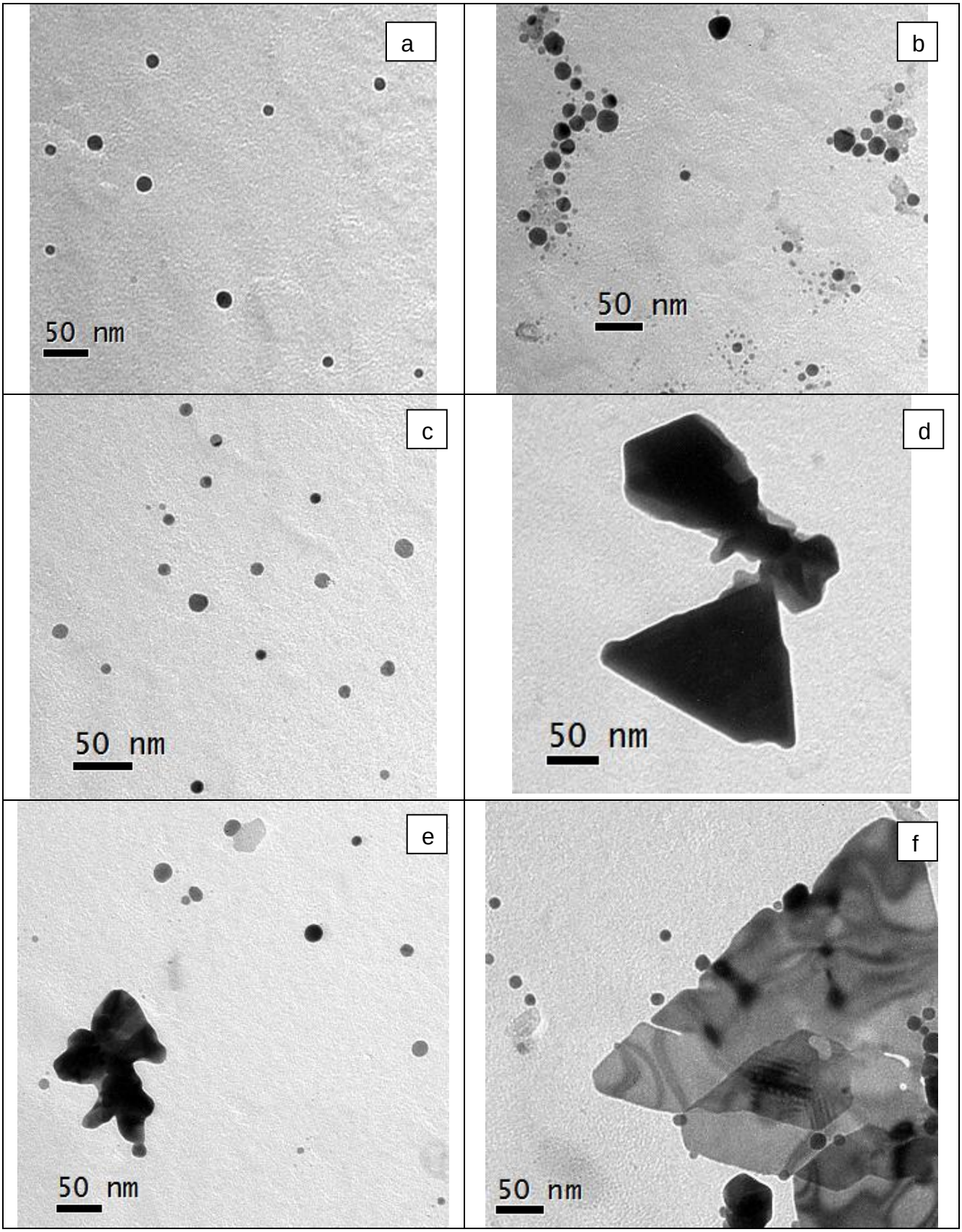

Figure 6. 18 TEM images of PEG-capped AgNPs after 21 days in (a) CM-10; (b) CM-1; (c) NM-10; (d) NM-1; (e) SM-10 and (f) SM-1.

6.4.3. Behaviour of PVP-capped AgNPs in CM, NM and SM

Similar to the PEG-stabilised AgNPs, the distinctive yellow colour of PVP-capped AgNPs was preserved in all media until end of the study (Figure 6. 19). This was confirmed by the preservation of AgNPs's SPR for both after 24 hrs and during 21 days incubation (Figure 6. 20 and Figure 6. 21). The alteration of plasmon peak position and width after 24hrs incubation in different media are presented in Table 6. 10. The decrease of SPR area after 21 days incubation in different media was calculated by Equation 6.1 and is presented in Table 6. 11.

Figure 6. 19 PVP-capped AgNPs in different media preserved the yellow characteristic colour within 21 days study period.

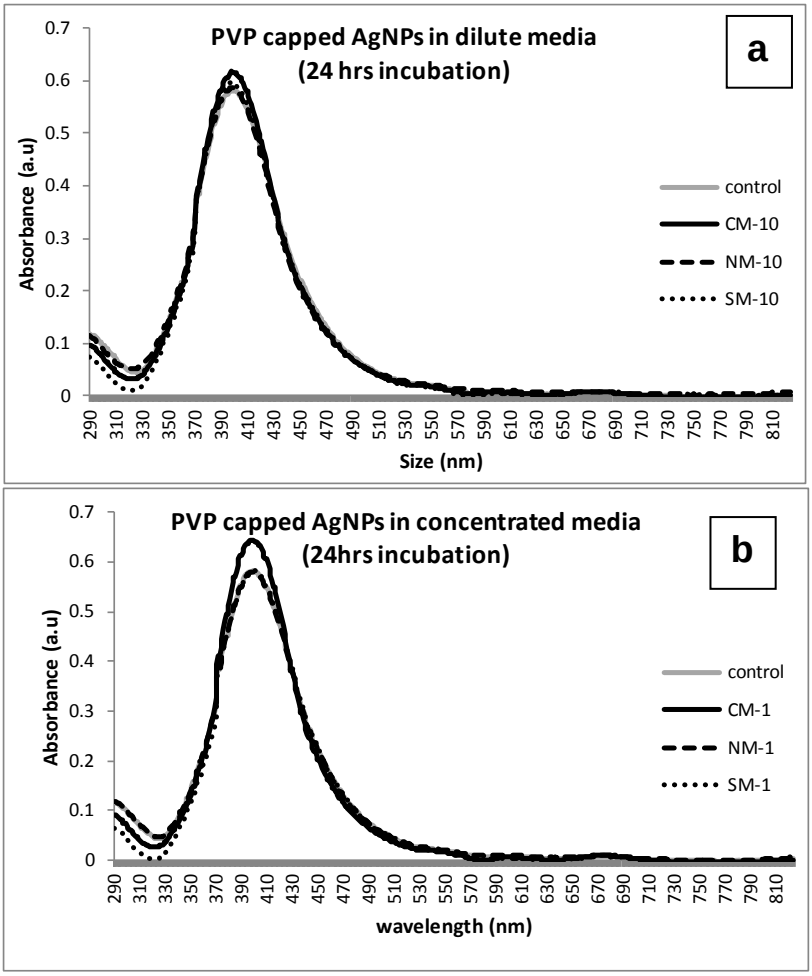

Figure 6. 20 The SPR behaviour of PVP-capped AgNPs in: (a) dilute and (b) concentrated media after 24hrs of incubation.

Table 6. 10 The λ_{max} and FWHM of the PVP-capped AgNPs SPR in various media after 24hrs incubation

	control	CM-10	NM-10	SM-10	CM-1	NM-1	SM-1
λmax	399	398	398	399	400	401	401
FWHM	72	67	69	68	58	72	70

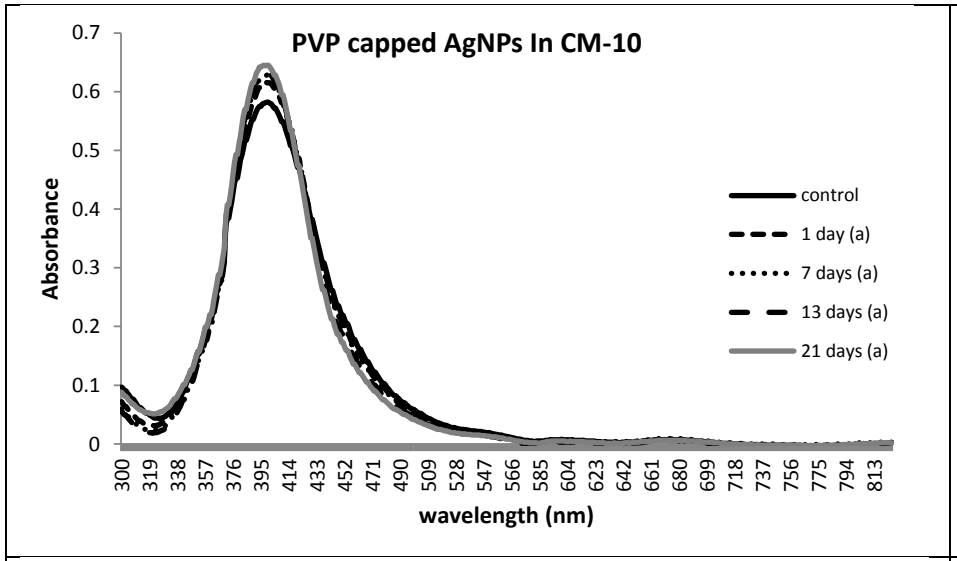
PVP capped AgNPs In CM-10
Absorbance
wavelength (nm)
control
1 day (a)
7 days (a)
13 days (a)
21 days (a)

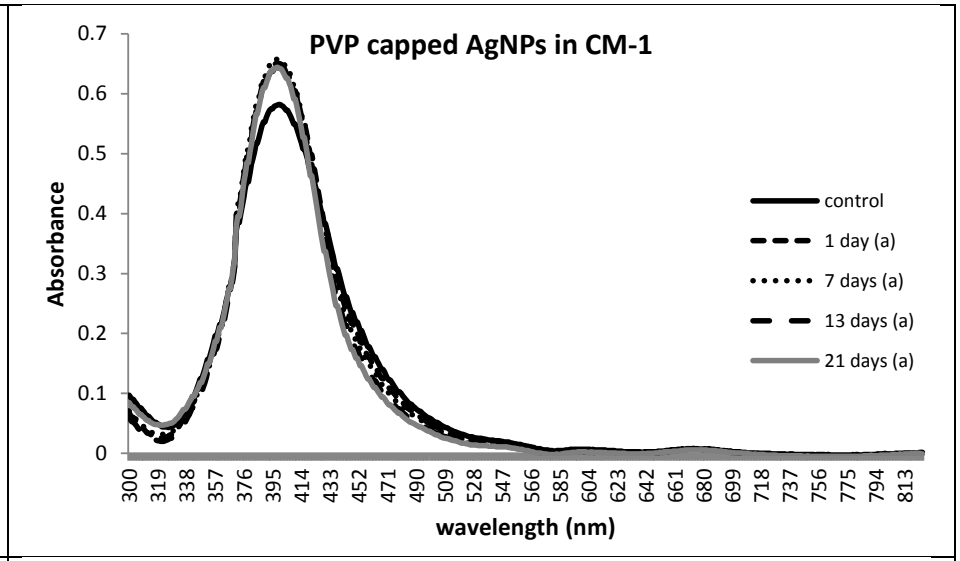
PVP capped AgNPs in CM-1
Absorbance
wavelength (nm)
control
1 day (a)
7 days (a)
13 days (a)
21 days (a)

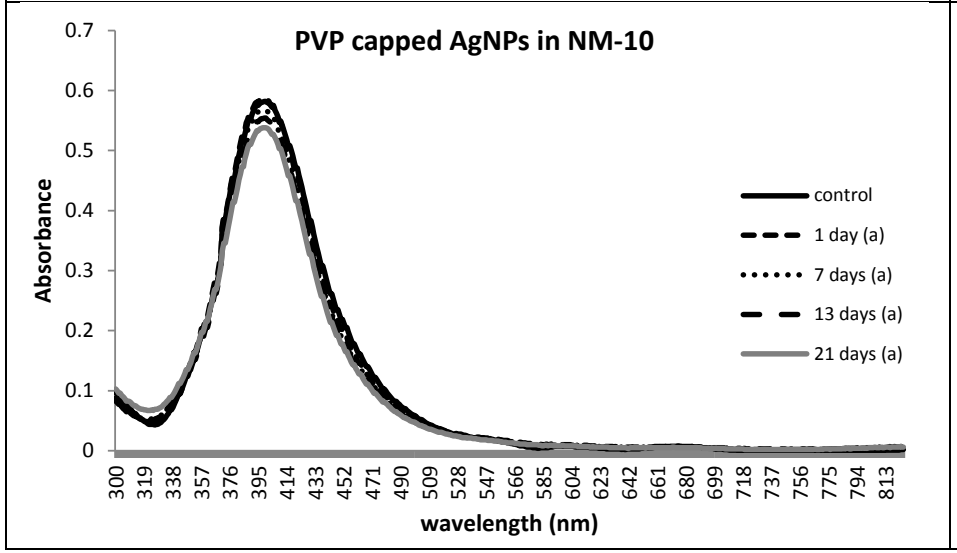
PVP capped AgNPs in NM-10
Absorbance
wavelength (nm)
control
1 day (a)
7 days (a)
13 days (a)
21 days (a)

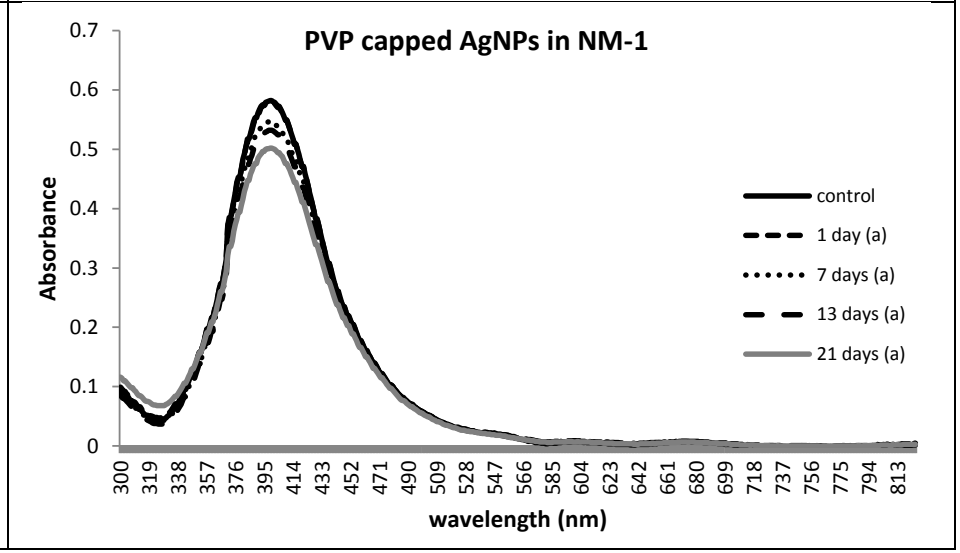
PVP capped AgNPs in NM-1
Absorbance
wavelength (nm)
control
1 day (a)
7 days (a)
13 days (a)
21 days (a)

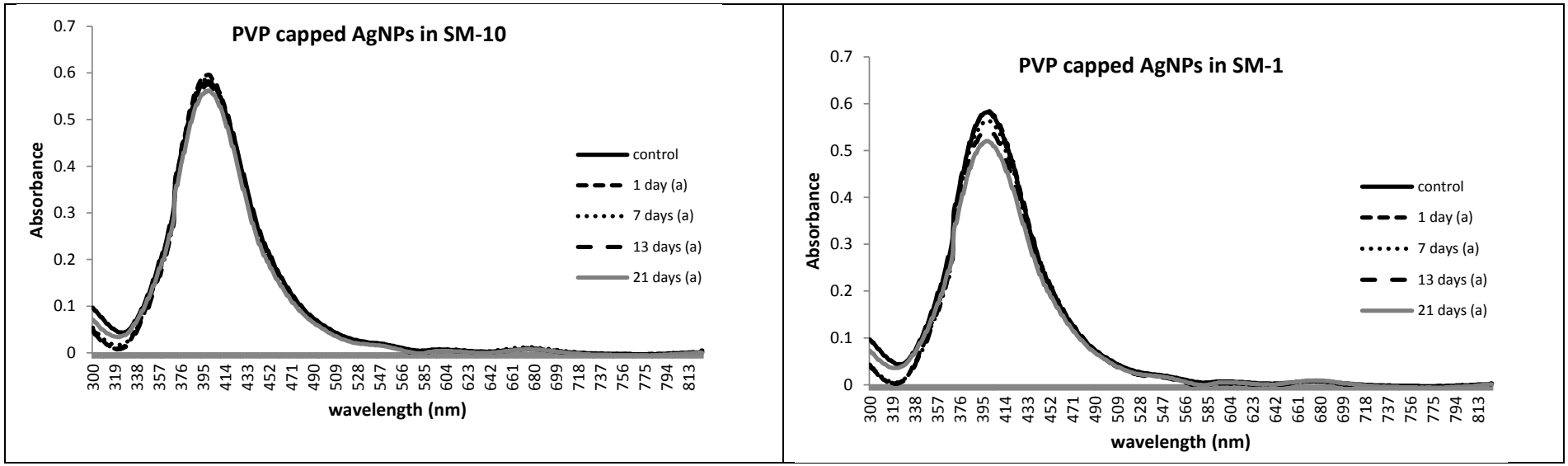

Figure 6. 21 The SPR behaviour of PVP capped AgNPs in variety of media during 21 days of incubation

Table 6. 11 The peak area decrease of the PVP-capped AgNPs over time monitored during 21 days incubation in variety media

	CM-10	NM-10	SM-10	CM-1	NM-1	SM-1
t = 2hrs	Stable	-1.59 ± 0.90	-2.31 ± 0.15	-0.20 ± 2.04	-0.42 ± 0.75	-2.47 ± 0.59
t = 7 days	-0.73 ± 1.15	-6.08 ± 1.26	-4.51 ± 1.64	-1.22 ± 2.15	-4.08 ± 0.60	-5.58 ± 0.20
t = 13 days	-2.95 ± 0.34	-8.84 ± 0.97	-6.38 ± 0.28	-5.11 ± 1.69	-6.96 ± 0.50	-9.11 ± 0.40
t = 21 days	-0.57 ± 0.61	-9.41 ± 1.91	-7.57 ± 0.56	-5.77 ± 1.27	-10.04 ± 0.75	-10.55 ± 0.32

PVP-capped AgNPs showed the most stable plasmon peak during 21 days incubation in any media compared to the citrate- and PEG-capped AgNPs, as indicated by the yellow colour preservation. Only minor absorbance decrease of PVP-capped AgNPs in chloride containing media (less than 1% in CM-10 and less than 6% in CM-1) observed at the end of 21 days of incubation and slightly larger SPR area reduction in media without chloride (8-11%) (Table 6. 11). The d_H size average (z-average and peak 1 size by intensity) and size distribution of PVP capped AgNPs in ultrapure water (control) and in media after 24 hrs incubation was analysed by DLS and the results are presented in Table 6. 12 and Figure 6. 22. There were a slight increase of z-average size of PVP-capped AgNPs after 24hrs incubation in the media, however only a minor changes of peak 1 size by intensity.

Size distribution of PVP-capped AgNPs in different media during 21 days incubation is presented in Figure 6. 23 and Figure 6. 24. It is seen that the NPs become more polydisperse with formation of larger particles, yet the original and main size of NPs was still remained.

Table 6. 12 The size of PVP capped AgNPs in media after 24hrs incubation.

Property / Media	Z average	PdI	Peak 1 by intensity
High purity water	22.89 ± 0.46	0.31 ± 0.02	26.74 ± 2.10
CM-1	42.76 ± 3.85	0.65 ± 0.09	26.13 ± 6.09
NM-1	29.82 ± 2.30	0.43 ± 0.06	26.67 ± 0.80
SM-1	37.40 ± 4.71	0.41 ± 0.05	25.78 ± 1.98
CM-10	34.64 ± 2.73	0.46 ± 0.03	23.7 ± 1.54
NM-10	42.26 ± 1.94	0.43 ± 0.03	27.47 ± 2.38
SM-10	30.02 ± 1.83	0.46 ± 0.06	24.73 ± 1.24

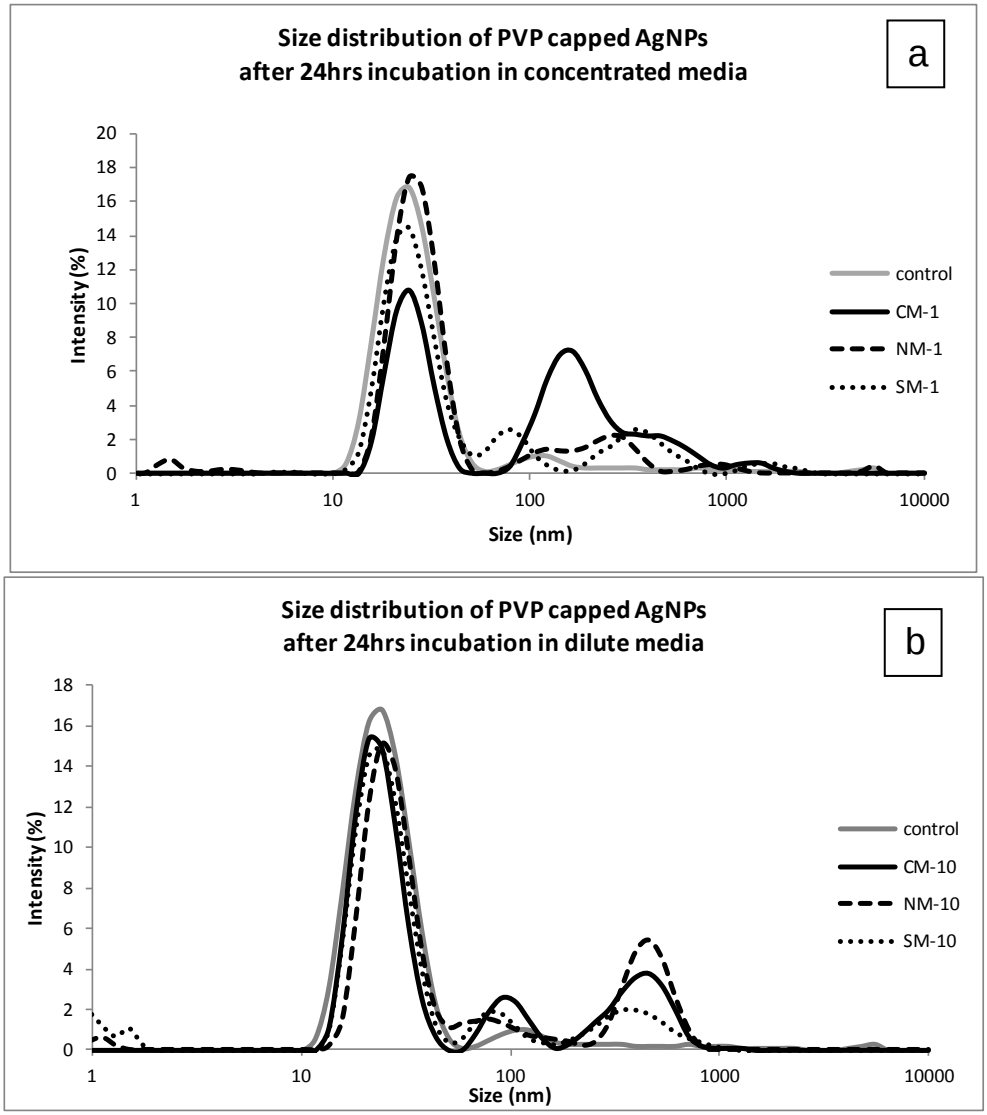

Figure 6. 22 The size distribution by intensity of PVP-capped AgNPs in (a) concentrated media; and (b) dilute media, after 24hrs incubation measured by DLS

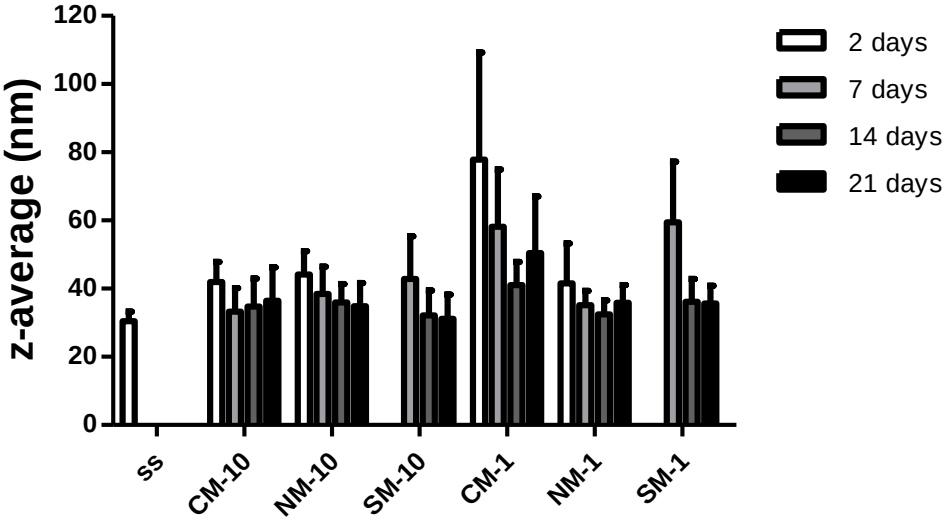

Figure 6. 23 The z average of PVP-capped AgNPs in variety of media within 21 days study period.

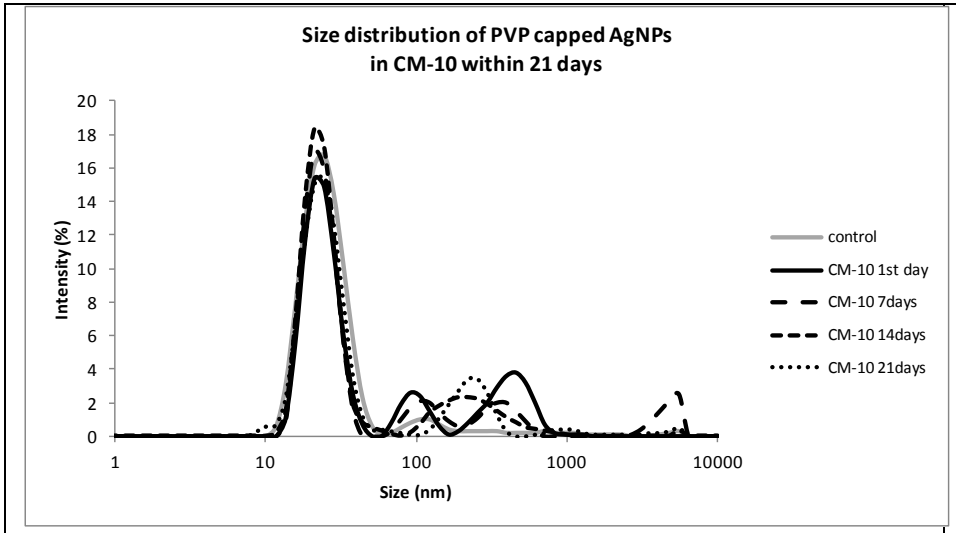
Size distribution of PVP capped AgNPs
in CM-10 within 21 days
Intensity (%)
Size (nm)
control
CM-10 1st day
CM-10 7days
CM-10 14days
CM-10 21days

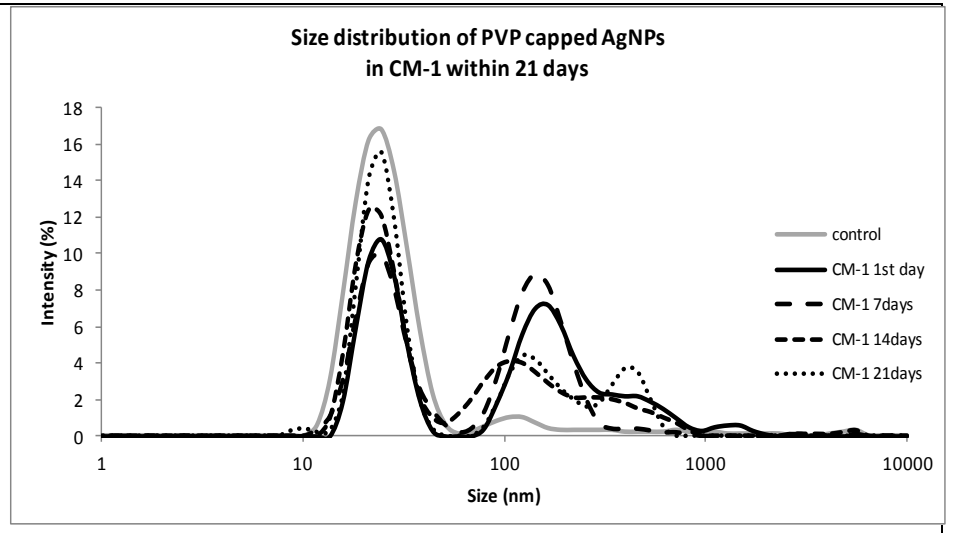
Size distribution of PVP capped AgNPs
in CM-1 within 21 days
Intensity (%)
Size (nm)
control
CM-1 1st day
CM-1 7days
CM-1 14days
CM-1 21days

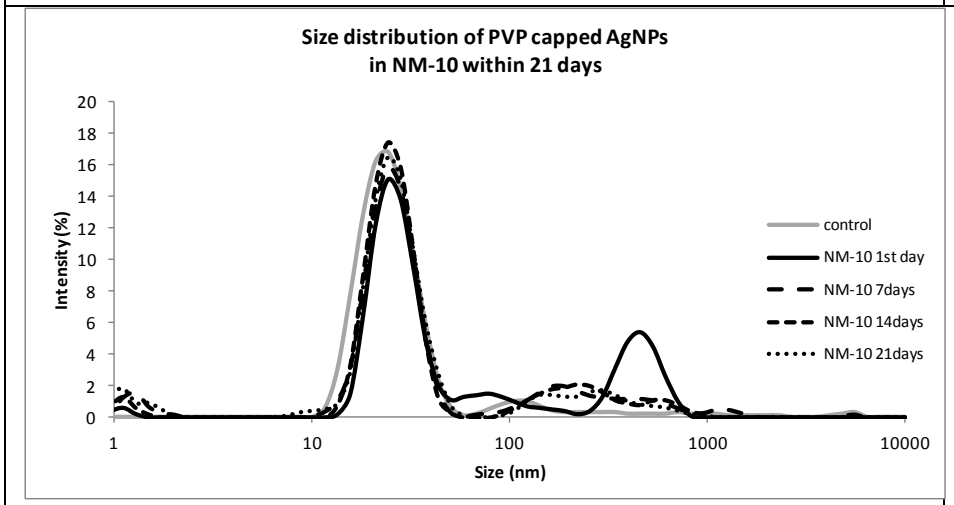
Size distribution of PVP capped AgNPs
in NM-10 within 21 days
Intensity (%)
Size (nm)
control
NM-10 1st day
NM-10 7days
NM-10 14days
NM-10 21days

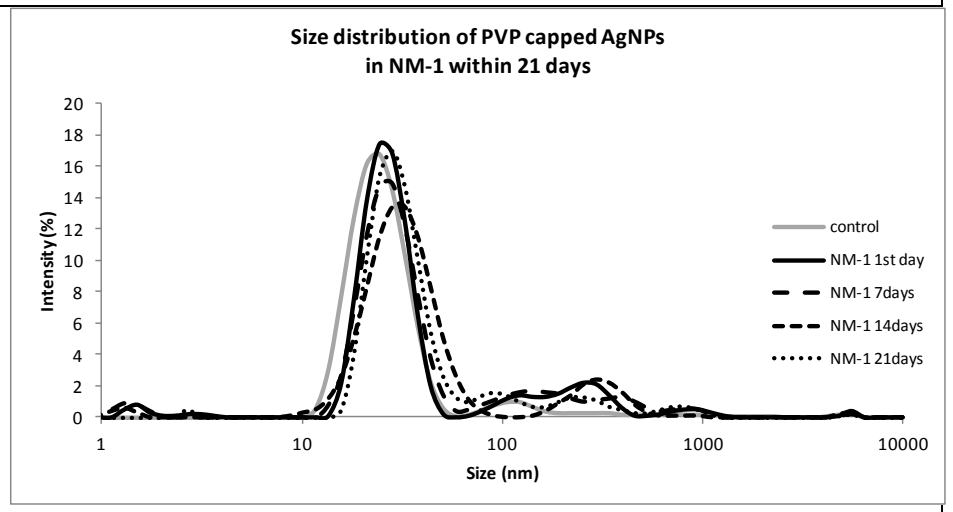
Size distribution of PVP capped AgNPs
in NM-1 within 21 days
Intensity (%)
Size (nm)
control
NM-1 1st day
NM-1 7days
NM-1 14days
NM-1 21days

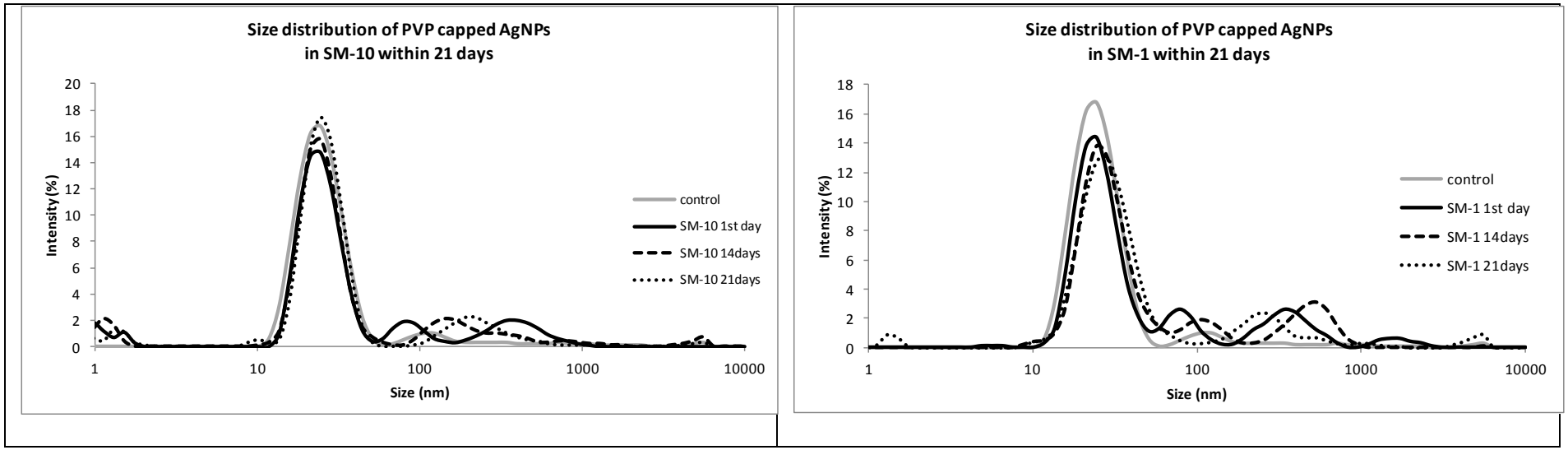

Figure 6. 24 Size distribution by intensity of PVP-capped AgNPs in different media within 21 days

The ζ and pH of the PVP-capped suspension in media were measured during 21 days of incubation (Table 6. 13, Figure 6. 25 and Table 6. 14). It was shown that in general the ζ of the NPs suspension became less negative and moved away from -17.8mV (control), particularly in concentrated media without chloride with no significant pH changes. Similar with PEG, PVP polymer stabilised the NPs via steric stabilization thus the ζ data do not directly reflect the stability of NPs.

Table 6. 13 The ζ of PVP-capped AgNPs in various media within 21 days study period

Media	zeta potential (mV)		
	0 day	7 days	21 days
CM-10	-11.5 ± 2.39	-11.6 ± 3.47	-11.4 ± 4.67
CM-1	-10.5 ± 1.53	-15.8 ± 2.75	-17.4 ± 2.37
NM-10	-8.51 ± 3.55	-7.48 ± 2.25	-10.3 ± 1.76
NM-1	-4.94 ± 0.55	-6.8 ± 0.64	-7.11 ± 1.29
SM-10	-10.8 ± 1.71	-11.4 ± 2.47	-11 ± 2.72
SM-1	-6.99 ± 0.89	-8.49 ± 1.38	-9.43 ± 1.62
control	-17.8 ± 1.79		

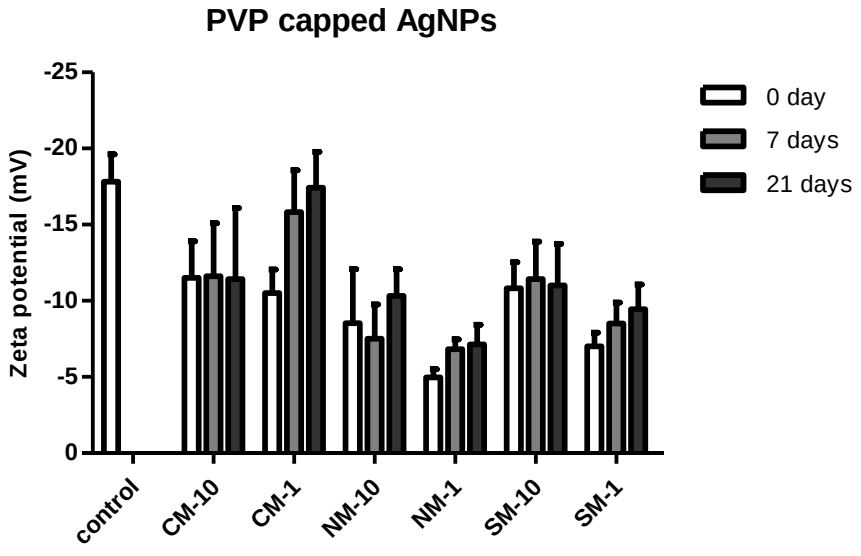

Figure 6. 25 The ζ of PVP-capped AgNPs in variety of media within 21 days

Table 6. 14 pH of PVP-capped AgNPs suspension in different media

Incubation time	CM-10	CM-1	NM-10	NM-1	SM-10	SM-1
0 day	6.9	7	6.9	7	6.8	7
7 days	7.2	7.2	7.4	7.4	7.7	7.5
21 days	7.5	7	7.3	6.9	7.5	7

The TEM was used for visualization of remaining PVP-capped AgNPs in media at the end of 21 days incubation. As predicted from the SPR data, the NPs in most of the media remained as disperse NPs except in SM-1 as some large aggregates were found together with some single particles.

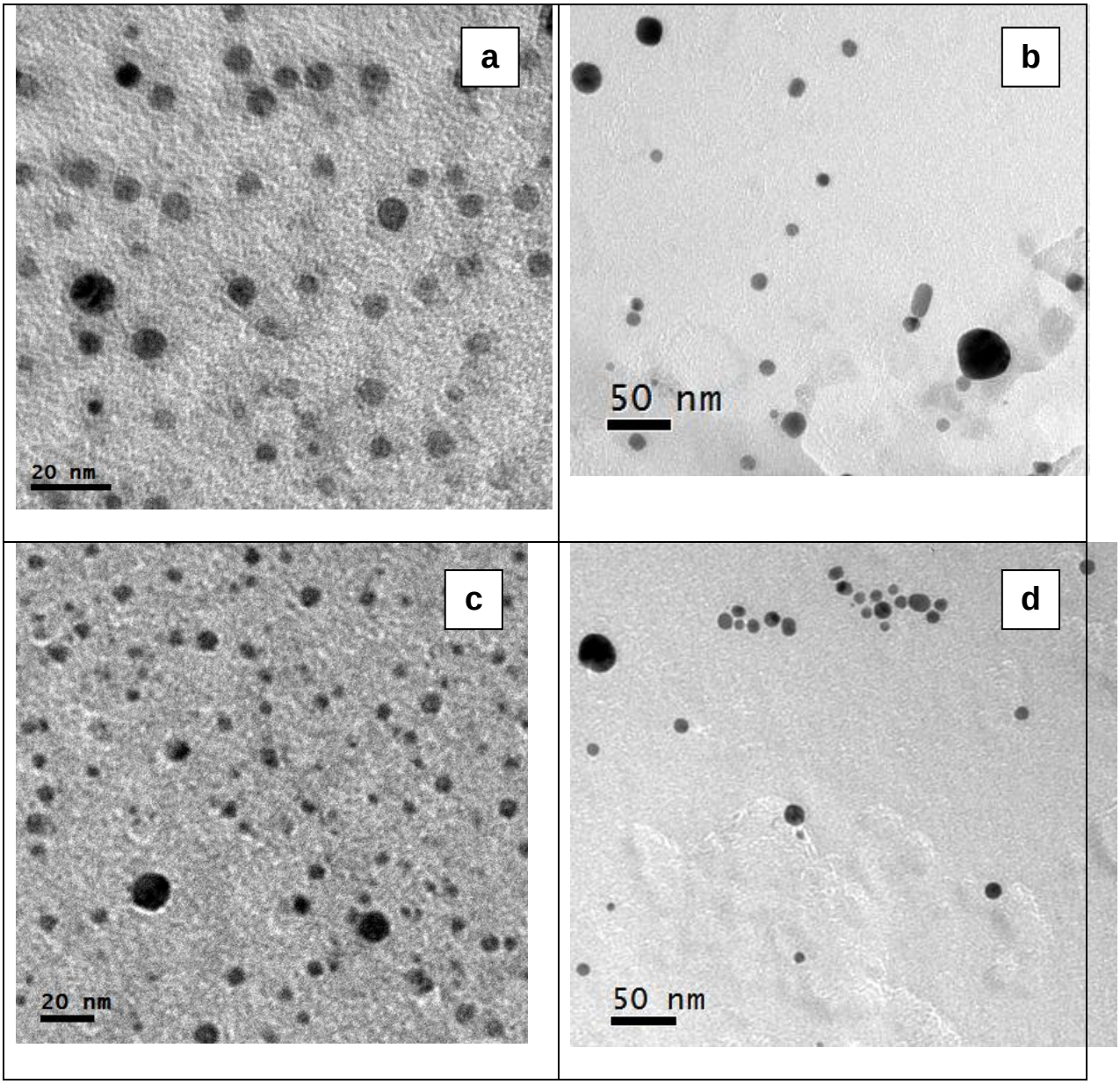

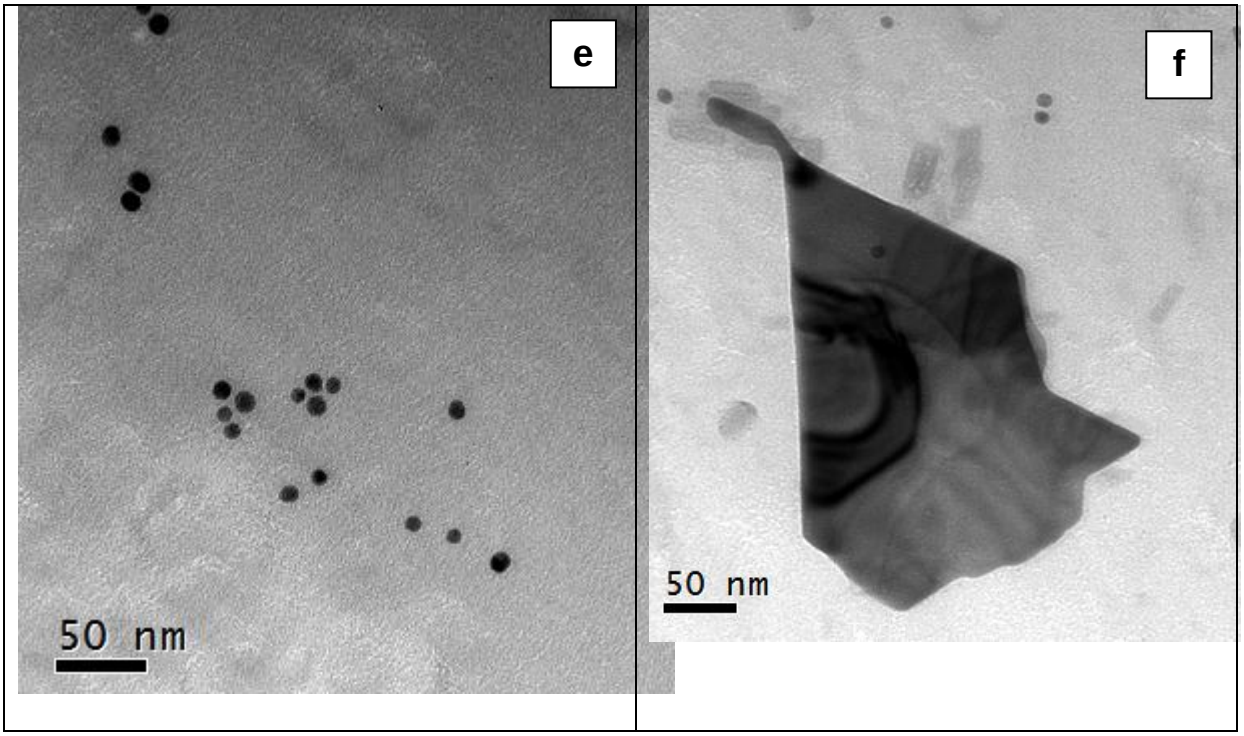

Figure 6. 26 TEM images of PVP-capped AgNPs in (a) CM-10; (b) CM-1; (c) NM-10; (d) NM-1; (e) SM-10 and (f) SM-1

6.4.4. Behaviour of citrate-, PEG-, and PVP-capped AgNPs in algae media

The SPR behavior of AgNPs with three different capping agents in algae media (AM) within 72 hours of incubation time was examined and presented in Figure 6. 27. The SPR area are presented in Table 6. 15.

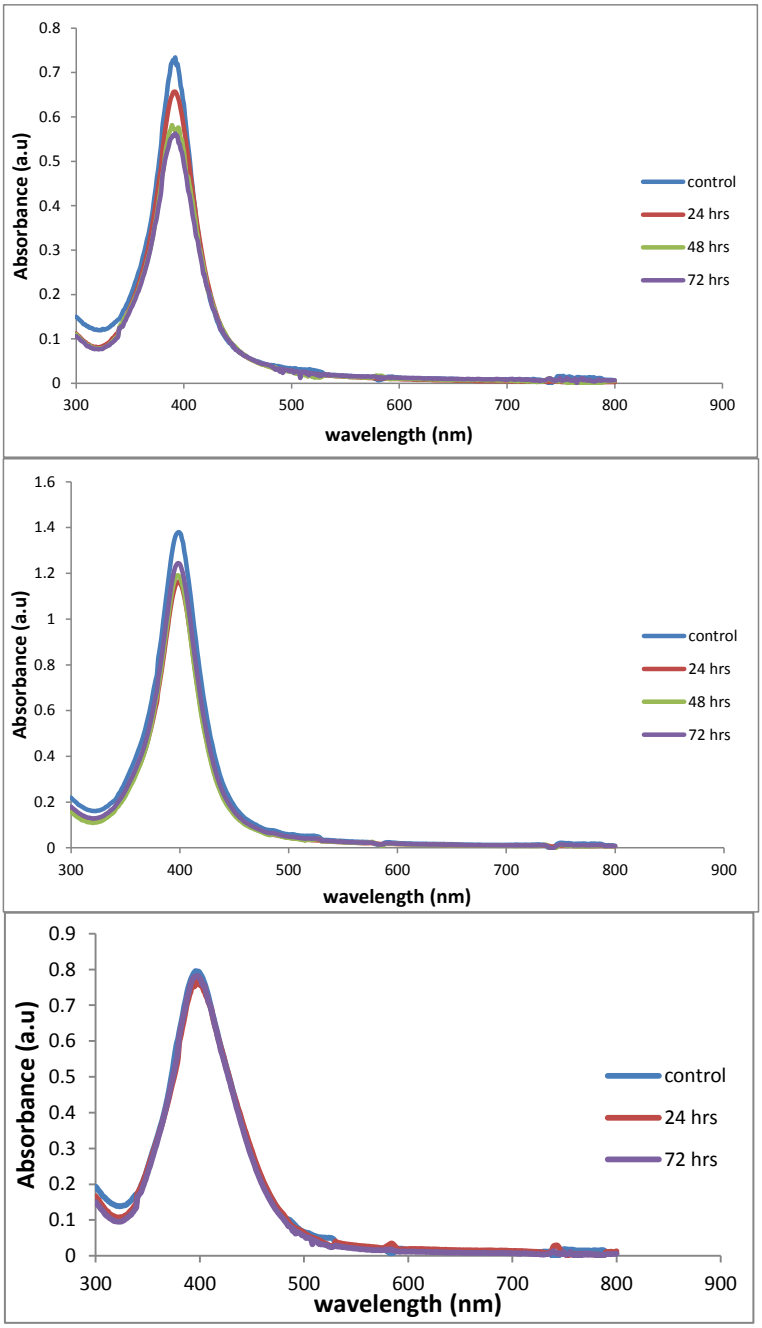

Figure 6. 27 The SPR of (a) citrate-; (b) PEG-; and (c) PVP-capped AgNPs in algae media monitored within 72 hours incubation.

Table 6. 15 The changes of SPR area of AgNPs during incubation in algae media

Time	Citrate	PEG	PVP10
24hrs	-7.74 ± 0.30	-15.37 ± 8.56	-2.79 ± 0.23
48hrs	-14.07 ± 0.33	-17.60 ± 0.47	Not available
72hrs	-15.88 ± 0.11	-21.75 ± 0.19	-5.24 ± 0.36

As presented in Figure 6. 27, there was an approximately 8% absorbance decrease at λ_{max} of citrate-capped AgNPs within 24 hrs of incubation in AM, and further decreased up to 16% after 72 hrs incubation time. On the other hand, there was only minor SPR alteration of PVP- capped AgNPs in algae media until end of 72hrs incubation (at about 5% plasmon peak area decrease) as corroborated by their yellow colour preservation. Interestingly, the PEG-capped AgNPs which showed better stability in OECD Daphnia media, demonstrated higher SPR area decrease than citrate-capped AgNPs. This finding indicates lesser stability of PEG-capped AgNPs than citrate-capped AgNPs in AM.

The d_H size distribution of AgNPs in algae media (presented as z-average and Peak 1 size by intensity) and the PdI value were monitored within 72hrs of incubation and the result is presented in Table 6. 16 and Figure 6. 28.

Table 6. 16 Hydrodynamic size of AgNPs during 72hrs incubation in algae media

Capping agent	Incubation duration	Z average	PdI	Peak 1 by intensity
Citrate	Control	23.8 ± 0.65	0.23 ± 0.02	26.47 ± 1.96
	24 hrs	76.9 ± 3.06	0.43 ±0.03	118.9 ± 10.15
	72 hrs	66.50 ± 1.86	0.45 ± 0.01	113.5 ± 14.67
PEG	Control	40.85 ± 0.74	0.29 ± 0.03	39.61 ± 2.68
	24 hrs	158.9 ± 27.4	0.46 ± 0.07	37.85 ± 3.66
	72 hrs	67.78 ± 8.93	0.58 ± 0.13	41.49 ± 3.36
PVP	Control	23.4 ± 1.01	0.31 ± 0.05	25.25 ± 2.91
	24 hrs	111.5 ± 32.5	0.45 ± 0.05	21.75 ± 1.61
	72 hrs	35.3 ± 5.32	0.55 ± 0.06	19.38 ± 1.33

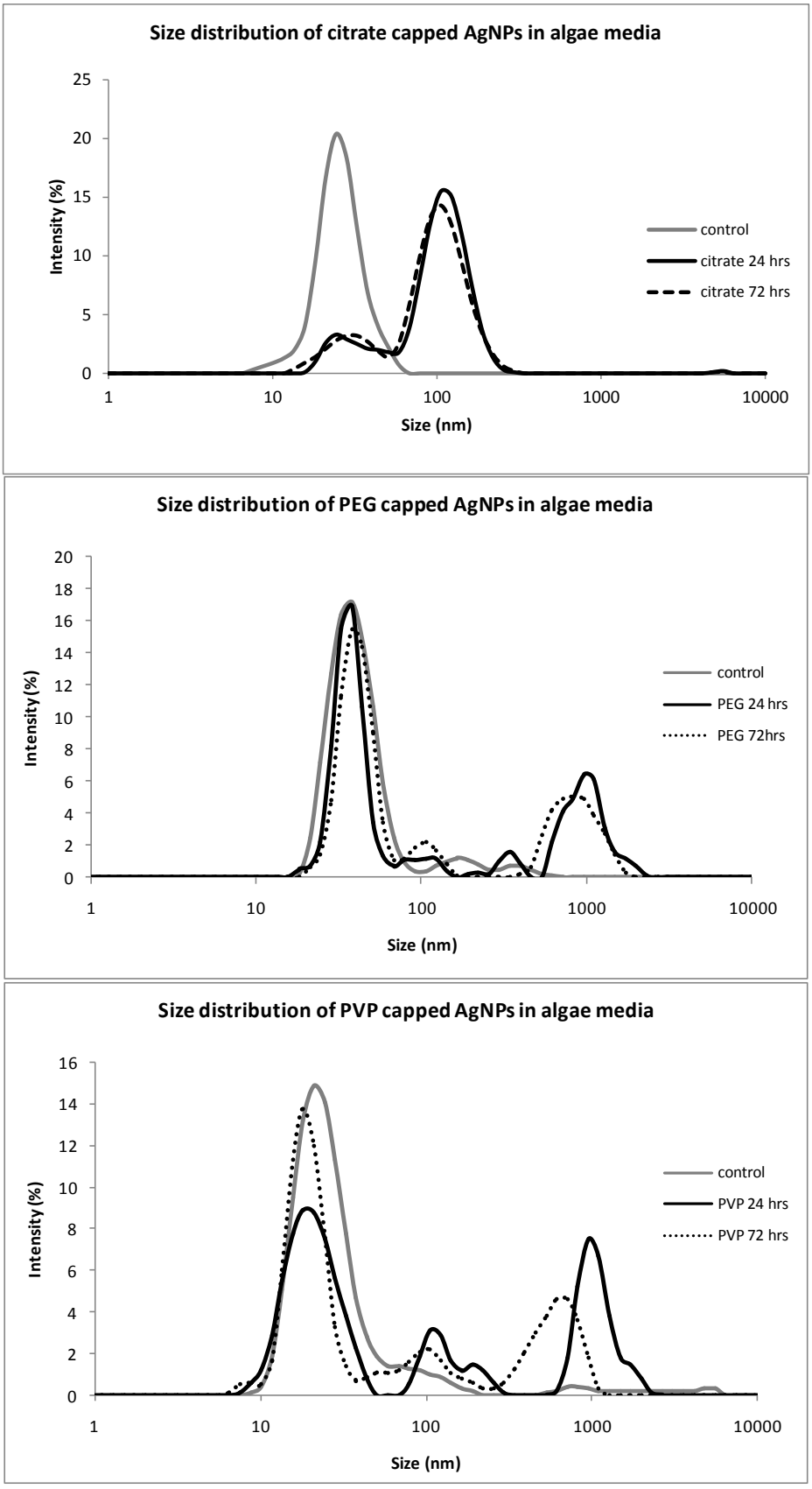

Figure 6. 28 Size distribution of citrate, PEG and PVP capped AgNPs incubated in algae media up to 72 hours

In general, the d_H size and size distribution of AgNPs after incubation in AM became larger and more polydisperse than their corresponding controls as shown by the DLS analyses result. Further d_H analyses were done by using Fl-FFF after 72 hours incubation in AM. The FFF fractograms are illustrated in Figure 6. 29. The calculated average sizes are presented in Table 6. 17. Consistent with the DLS result, observed size distribution and size average of citrate- and PEG-capped AgNPs became broader and larger than their corresponding control, suggesting formation of large aggregate. The PVP-capped AgNPs fractogram, however, showed a stable d_H in AM with minor peak broadening.

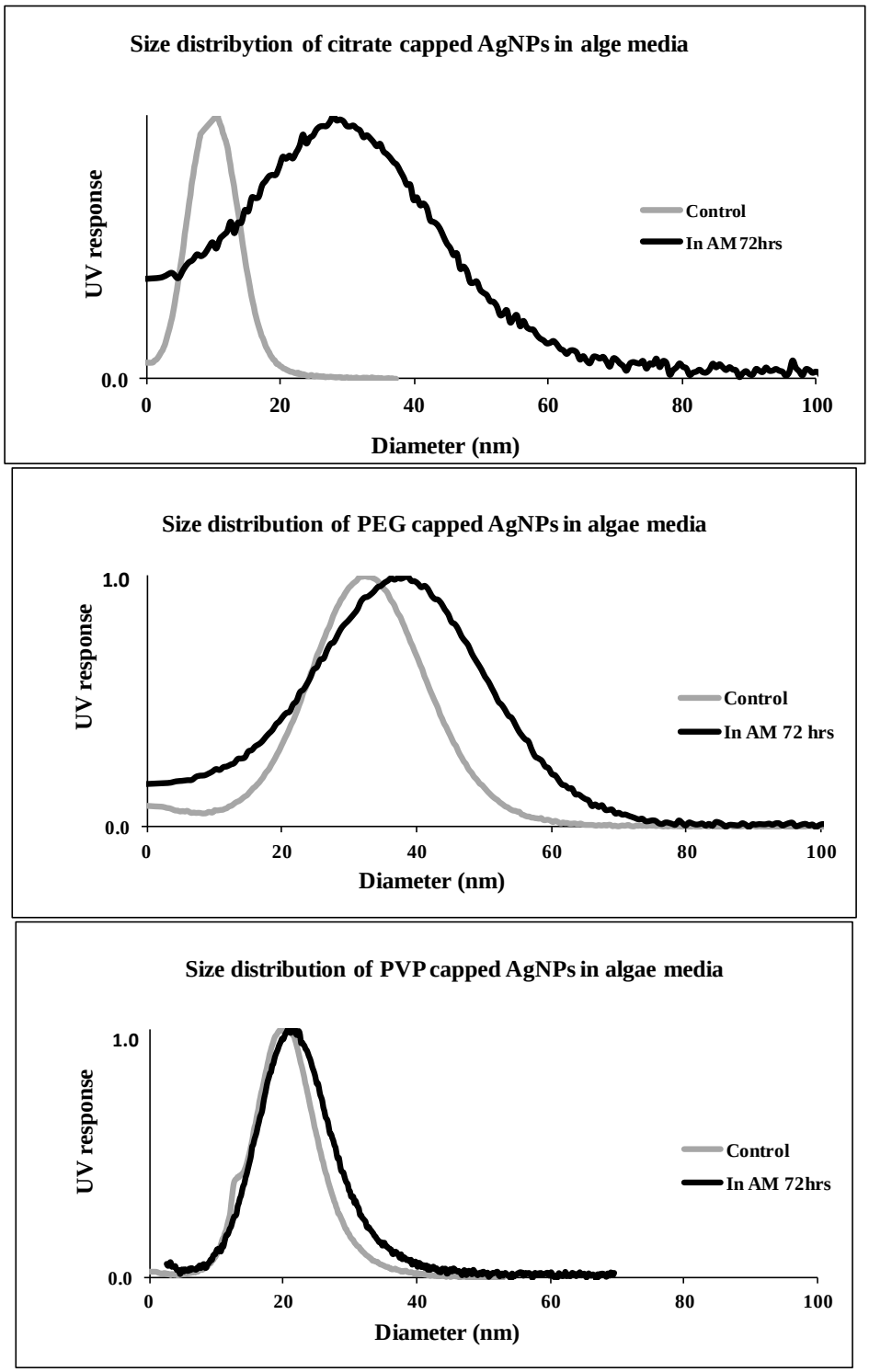

Figure 6. 29 The fractogram of citrate-; PEG- and PVP-capped AgNPs after 72hrs incubation in algae media

Table 6. 17 The size (diameter weight/dw) of citrate-, PEG- and PVP-capped AgNPs before and after 72 hours incubation

Capping agent	Size (dw) of AgNPs pristine suspension	Size (dw) of AgNPs after 72 hrs incubation
citrate	13.12 ± 0.63	43.16 ± 2.88
PEG	36.07 ± 0.28	43.27 ± 0.73
PVP	22.92 ± 1.12	25.06 ± 0.63

The likelihoodl of citrate-capped AgNPs aggregation was also emphasized by zeta potential alteration of citrate-capped AgNPs in AM. Significant changes of zeta potential value from -38.5 into -23.8 mV (Table 6. 18) potentially lead to aggregation of citrate-capped AgNPs in AM. There was no pH difference between the clean media (without NPs) and media-NPs suspension, both in the beginning and at the end of the study, at pH value about 6.4. Since PEG- and PVP-polymer stabilised the NPs sterically, the stability of polymer capped AgNPs cannot be inferred from ζ data.

Table 6. 18 The ζ of citrate-, PEG- and PVP-capped AgNPs before and after incubation in algae media

Capping agent	zeta potential (mV)		
	Pristine suspension	in algae media	
		0 hr	72 hrs
citrate	(-) 38.5 ± 1.7	(-) 24.7 ± 0.6	(-) 23.8 ± 1.6
PEG	(-) 6.80 ± 3.7	(-) 22.9 ± 1.8	(-) 19.1 ± 1.7
PVP	(-) 24.6 ± 1.9	(-) 24.4 ± 1.4	(-) 21.0 ± 2.1

The image of remaining AgNPs in AM-NPs suspension was taken by TEM at the end of 72hours of incubation (Figure 6. 30). The size are then compared with their corresponding control (Figure 6. 31). It was found that the average core size of citrate and PEG capped AgNPs increased after 72hrs incubation in AM yet the PVP capped AgNPs remained stable (Table 6. 19).

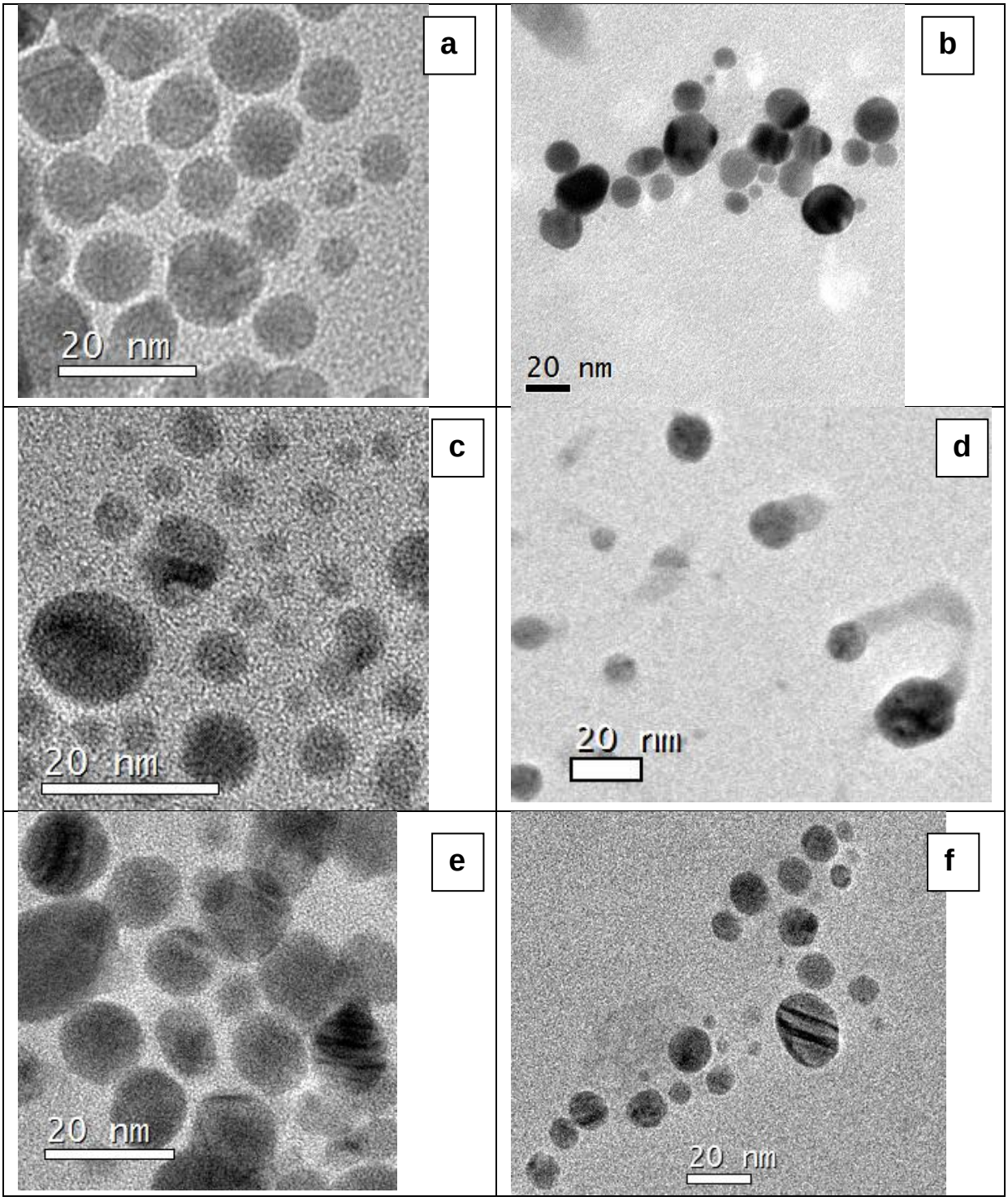

Figure 6. 30 TEM images of citrate-, PEG- and PVP-capped AgNPs controls (a,c,e) and after 72hrs incubation in algae media (b,d,f)

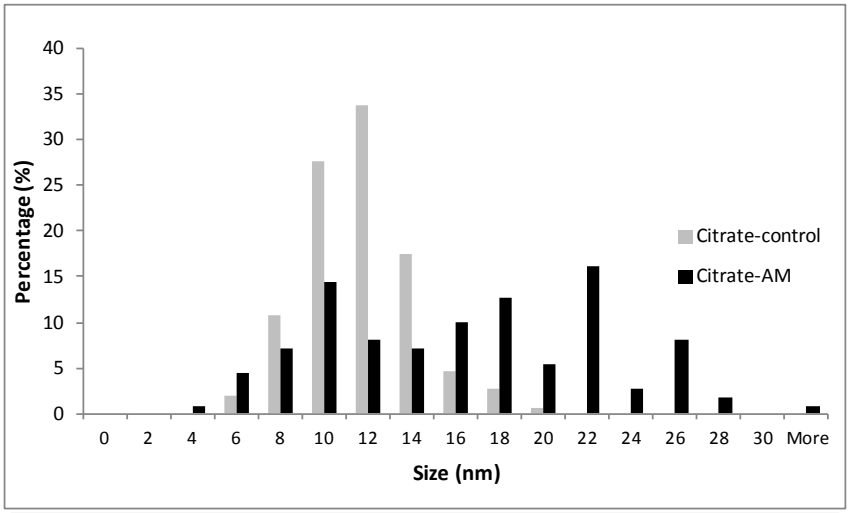

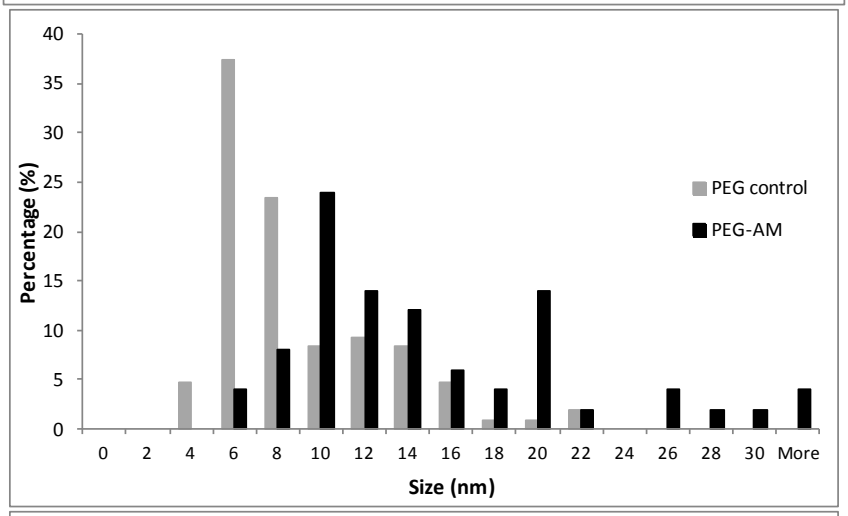

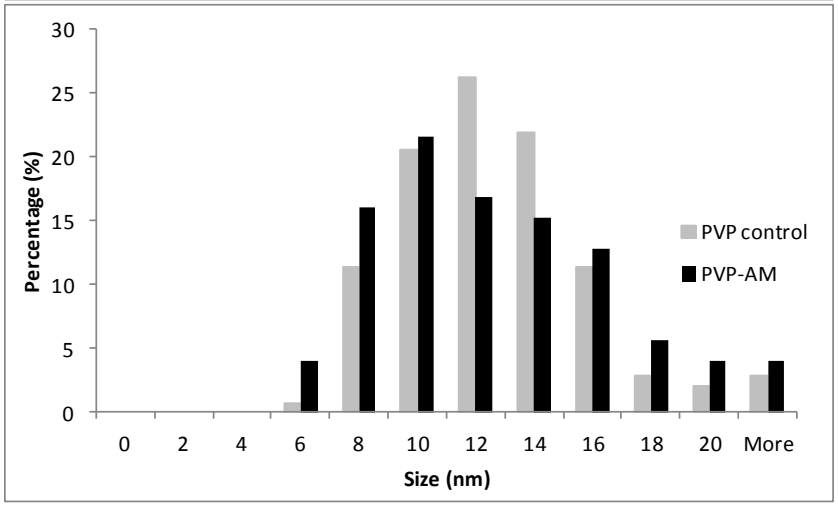

Figure 6. 31 The comparison of size distribution comparison of control and 72hrs algae media-AgNPs suspension: (a)citrate-, (b) PEG- and (c) PVP-capped AgNPs

Table 6. 19 Core size average of citrate-, PEG- and PVP-capped AgNPs in algae media by TEM

Capping agent and media	core size (nm)
Citrate - high purity water (control)	10.65 ± 2.52
Citrate - AM	15.57 ± 6.22
PEG – high purity water (control)	7.81 ± 3.85
PEG - AM	14.78 ± 10.19
PVP – high purity water (control)	11.74 ± 3.63
PVP - AM	11.73 ± 4.16

6.5. Discussion

This study observed number of factors influencing the stability of AgNPs in ecotoxicology media and will be discussed in the following paragraph.

6.5.1. The influence of capping agent into the stability and behaviour of AgNPs

Previous study found the effect of organic capping agent into stability of NPs (Sharma et al., 2014) and SPR analysis is one of powerful technique for NPs suspension stability evaluation (MacCuspie, Rogers et al., 2011). Three different capping agents used in this study were citrate as an electrostatic capping agent, and thiolated-PEG (PEG-SH) and polyvivylpyrrolidone (PVP) as steric capping agents. According to the SPR analysis data, it was shown that steric capping agents stabilized the NPs in a greater extend than electrostatic capping agent. However, PEG-SH exerted less stabilizing effect than PVP polymer as shown by greater SPR area decrease in all media. In Algae media (AM), interestingly, PEG-capped AgNPs showed a lesser stabilizing effect than citrate.

Possible mechanisms that can be related to the extinction of SPR peak are dissolution, aggregation and loss of materials due to adsorption onto container walls (MacCuspie, Rogers et al., 2011; Handy, Cornelis et al., 2012). The observation of greater dissolution of PEG-capped AgNPs in pristine suspension has been

presented in Chapter 5, section 5.3.2, and most likely increased in ecotoxicology media as also revealed in other studies (Zook, Long et al., 2011; Li and Lenhart, 2012). As a result, the reduction of PEG-capped AgNPs SPR peak was greater than PVP-capped AgNPs in all media, and greater than citrate-capped AgNPs in Algae media.

Aggregation was also another potential reason of SPR extinction in this study, citrate-capped AgNPs in particular. The enlargement of d_H size, the appearance of sediments and the disappearance of NPs from the suspension corroborated citrate-capped AgNPs aggregation. Although DLS and Fl-FFF d_H size of PEG-capped AgNPs in all media became larger, the occurrence of aggregation seemed to be minor since well-dispersed PEG-capped AgNPs was found by TEM, apart from the suspension in NM-1 and SM-1. Instead, dissolution-redeposition might be the case, as the dissolution of PEG-capped AgNPs was followed by the increase of core size of PEG-capped AgNPs, both in CM-10 and AM.

The potential of AgNPs adsorption into container walls was not evaluated in this study. The implementation of acid wash and $Ca(NO_3)_2$ treatment to the plastic ware as has been presented in section 3.2.4, however, could prervent NPs loss due to adsorption. Thus, the reduction of SPR absorbance due to container adsorption in this study was trivial.

In all media, PVP was shown to be imparted extensive stabilization effect. By the action of loan pair donation from the amine functional head group, PVP polymer coats the AgNPs surface and increases AgNPs stability in electrolyte media (Henglein, 1993). Enhancing NPs stability by coating the NPs with PVP polymer has been presented in number of studies (Reed, 1993; Zhang et al., 2007; Panacek, Kolar et al., 2009).

6.5.2. Ionic strength dependence of stability and behaviour of AgNPs

The effect of ionic strength (IS) of media into NPs stability, both electrostatic (Yoo, 1998; Komarneni et al., 2002; Sardar et al., 2009; Liu, Zhou et al., 2011) and steric capped NPs studies (Guo et al., 2000; Li and El-Sayed, 2001; Liu et al., 2003; Gerbec et al., 2005; EU, 2013), has been shown by many studies. In this study, two concentrations of media, full strength and 10 fold dilution of CM, NM and SM were used to evaluate the IS effect to AgNPs. Algae media (AM), having IS about 10% less than CM-1 was also used.

It was clearly shown that electrostatically, citrate-capped AgNPs were more sensitive to high IS media (CM-1; NM-1; SM-1) as presented by its rapid disappearance of SPR, the vast increase of d_H size, the appearance of sediment in the container and NPs removal from the media as shown by TEM analysis. According to DLVO (Derjaguin and Landau, Verweey and Overbeek) theory, the stability of NPs was influenced by the extent of attractive and repulsive forces act on the NPs (Mittal et al., 2013). The formation of electrostatic double layer (EDL) surrounding the NPs can increase the repulsive force between NPs and stabilize the dispersion electrostatically against aggregation. Any interruption to the thickness of EDL will disrupt the stability of NPs and induce aggregation.

According to Debye-Hückel approximation, the thickness of EDL (by the size of $1/\kappa$) depends on the temperature and the bulk electrolyte concentration as presented in (Equation 6. 2) (Mittal, Chisti et al., 2013):

$$K = \sqrt{\frac{2000\,\mathrm{F}^2}{\varepsilon_0 \varepsilon_r RT}} \times \sqrt{I}\ \ (\text{meter})^{-1} \qquad \text{(Equation 6. 2)}$$

where K is Debye-Hückel parameter, ***F*** is Faraday's constant (96,485 C.mol^{-1}), ***I*** is ionic strength, $\boldsymbol{\varepsilon_0}$ is permittivity of a vacuum (8.85 x 10^{-12} farad.m^{-1}), $\boldsymbol{\varepsilon_r}$ is dielectric constant of solution, ***R*** is gas constant (8.31 J.K^{-1}.mol^{-1}) and ***T*** is temperature (K).

At 25^{0}C in water (ε_r at 25^{0}C = 78.57), than the K = 3.288 $\sqrt{I}$ (nm^{-1}), shows that the EDL ($\sim 1/\kappa$) is only influenced by media's ionic strength where

$$\boldsymbol{I} = \frac{1}{2} \sum c_i z_i^2 \qquad \text{(Equation 6. 3)}$$

where c_i is ionic concentration and z_i is the ionic charge.

Given that the CM-1; NM-1 and SM-1 had a higher ionic strength than the high purity water (the media of pristine suspension) as calculated in appendix 1, the increase of ***I*** amplified the ***K*** value, point to the contraction of NPs's EDL layer and lead to NPs aggregation. In dilution media (lower ionic strength), however, the aggregation process was slower than in concentrated media as the ionic strength (IS) was smaller than concentrated media.

In Algae media, where the IS difference was only 10% lower than CM-1, the stability of citrate-capped AgNPs enhanced significantly. Loss of SPR area was only about 16%, smaller than the SPR decrease of PEG-SH capped AgNPs (ca 22%). Thus, other factors, such as cation and anion composition of media might contribute to the stability of electrostatic capped AgNPs in electrolyte media.

6.5.3. Media composition dependence of stability and behaviour of AgNPs

One of interesting findings from this study was the observation of a better stability of citrate-capped AgNPs in Algae media (AM) than in OECD Daphnia media (CM-1). Even though the IS difference between CM-1 (8.88 mM) and AM (8.02 mM) was less than 10%, but lower concentration of divalent cation in AM (ca 8%) than in CM-1 (ca 74%) increase the stability of citrate-capped AgNPs. Dramatic effect of divalent cation content in the media into NPs stability has also been revealed in other studies (Haiss et al., 2007; French, Jacobson et al., 2009; Badawy, Luxton et al., 2010) in fact Schulze-Hardy rule emphasized the dependences of colloid stability on

the valency of counter-ions only (Gerbec, Magana et al., 2005). Moreover higher concentration of Ca^{2+} in media increases the likely of aggregation due to complexation of Ca^{2+} with the carbonyl group of citrate coating (Komarneni, Li et al., 2002; Yin et al., 2004). Since Ca^{2+} concentration in AM and CM-1 were 0.17 and 2 mM respectively, less aggregation of citrate-capped AgNPs in AM.

Another effect of media composition to the NPs stability was shown by the appearance of SPR shoulder peak and shape transformation of citrate-capped AgNPs in dilution media without chloride (NM-10 and SM-10). Since the presence of shoulder peak can be explained by: (1) strong coupling between NPs due to Ostwald ripening driven aggregation (Handy, von der Kammer et al., 2008; Baalousha, Stolpe et al., 2011); (2) in-plane dipole resonance of nanoplate with edge length greater than 100nm (Warheit, 2008) and or (3) dissolution-recrystallization of NPs (Anderson, 1987; Yang, Zhang et al., 2007), these mechanisms might occur in dilution media without chloride. NPs shapes other than spherical were also found from PEG-SH capped AgNPs after 21 days incubation in NM-1 and SM-1. Large non-spherical aggregates were also found from PVP-capped AgNPs after suspended in SM-1 for 21 days. Yet no shape transformation was found in chloride containing media.

The shape stability of AgNPs in chloride containing media potentially due to the formation of Ag-Cl complexes on the AgNPs surface, and protect the particles from further transformation. Both in dilution and concentrated chloride containing media, all particles showed less SPR area decreases, indicating less transformation of AgNPs. Similar findings was found from other studies (Badawy, Luxton et al., 2010; Li, Lenhart et al., 2010) and also suggested earlier by Henglein (1993) that the Cl^- content prevents the aggregation of citrate-caped AgNPs.

6.6. Conclusion

This study showed that behaviour of AgNPs in ecotoxicology media were manifested as colour preservation; SPR peak area alteration; d_H and core size changes; lesser zeta potential value (closer to zero); and shape transformation. The stability was influenced by types of capping agent; ionic strength and chemical composition of the media.

In general, steric capping agent (PEG-SH and PVP polymer) imparted better stability than electrostatic capping agent (citrate) and PVP gave the best stabililization effect in all media under study. In Algae media, however, PEG-capped AgNPs showed less SPR stability than citrate-capped AgNPs due to dissolution-redeposition of NPs. Lower divalent cation and Ca^{2+} content of Algae media than OECD Daphnia media less interrupted the stability of citrate-capped AgNPs.

The effect of media ionic strength to the stability of electrostatic-capped AgNPs was due to contraction of electrostatic double layer (EDL) of NPs. Chloride containing media, however increased the stability of citrate-capped AgNPs at some extent potentially due to formation of Ag-Cl complexes on the NPs surface. In contrast, media without chloride transformed the shape of AgNPs potentially due to Ostwald ripening driven aggregation, nanoplate formation and or dissolution-recrystalization of NPs.

CHAPTER VII

DISCUSSION, CONCLUSION AND FURTHER WORK

7.1. Discussion and Conclusion

PVP-capped AgNPs with intended core size ±10nm and spherical shape have successfully been synthesized via direct (hot and cold method) and indirect method (ligand-exchange of citrate capped AgNPs). Mulfinger et al. (2007) synthesis method was modified by adding PVP capping agent and found to generate more monodisperse PVP-capped AgNPs compared to hot process as corroborated by lower PdI value, narrower SPR width and single DLS size peak. From this study, it was found that lower PdI value was achieved by adding the PVP polymer before the reduction of Ag^{+} by $NaBH_4$ took place and the volume ratio of reactants (2mM $NaBH_4$; 1mM $AgNO_3$ (aq); and 0.3% m/v PVP_{10}) was 15 : 5 : 1.

Indirect method was also successful in synthesizing PVP-capped AgNPs. By mixing PVP polymer with citrate-capped AgNPs, PVP polymer replaced citrate from the surface of AgNPs as polymer provide stronger affinity. The occurrence of ligand-replacement was seen by the increase of AgNPs stability over electrolyte media, nitrate media (NM) that was used as an indicator. No characteristics alteration of core AgNP due to ligand replacement by PVP. Advantages and drawback of direct and indirect method inferred from this study is presented in Table 7.1.

Table 7. 1 Comparison of PVP-capped synthesis method within this study

Synthesis method		Advantages	Drawbacks
Direct Route	Hot Process	• Strongly attached and thick layer of PVP polymer on the surface of NPs • No contamination from reducing agent	• Troublesome, need longer and constant heating at 70^0C for 7 hours • Thorough washing by acetone • Polydisperse NPs (PdI ± 0.4) • Zeta potential close to zero (less than 5mV)

	Cold Process	• Simple, fast, and generates more homogeneous size of NPs (PdI ± 0.2). • Stable in high ionic strength media • Low solubility (± 0.19%) • More negative zeta potential (ca 12 mV) compared to HP-AgNPs	• Changing the ratio of reactant concentration, stirring time, could not control the size of generated NPs. • Need an ice bath to perform the reaction • Need washing to remove the excess reactants
Indirect Route	Ligand-Exchange	• Simple, fast and easy • Generated PVP-AgNPs stable in high ionic strength media	• Need to characterize the original electrostatic NPs, make sure the homogeneity of NPs • Added polymer may influence the NPs core characteristics • Need washing to remove the excess reactants

Following the success of recapping citrate-capped AgNPs by PVP polymer via indirect method, ligand exchange of citrate-capped AgNPs by other polymers such as thiolated-PEG (PEG-SH); Suwannee River Fulvic acid (FA) and Tween-80 were also investigated. Thiolated PEG and Tween polymer were found to change the core size of AgNPs, but not with fulvic acid. Ligand exchange of citrate capped AgNPs by all polymers, however improved the stability of AgNPs in OECD *Daphnia magna sp*. media.

Characterization of as synthesized AgNPs by multi method techniques was performed in this study. It was shown that presenting SPR, d_H size, core size (both vertical and lateral dimension), polydispersity index (PdI), single elemental analysis and zeta potential of AgNPs was sufficient for the characterization purpose of this study. Additional dissolution data was very useful although performing dissolution study was difficult and expensive. Understanding the effect of ligand-exchange into NP core properties was also satisfactorily seen by performing SPR, d_H, core size, PdI and zeta potential analysis.

The stability of NPs in ecotoxicology media can also be evaluated by analyzing the SPR, d_H size, core size and zeta potential alteration of NPs during and

after incubated in media. The changes of λ_{max} and FWHM of AgNP's SPR indicates size, aggregation state and shape transformation. Further confirmation of size changes can be done by DLS, Fl-FFF, TEM, and AFM method, and shape transformation by TEM. EDX was also useful to analyse chemical composition of NPs both before and after incubation. This study found that PVP-polymer stabilized AgNPs at greater extent compared to citrate, and thiolated PEG. Chloride content in media apparently stabilized AgNPs, potentially due to formation Ag-Cl complexes on AgNPs surface. On the other hand, media without chloride induced shape transformation of AgNPs. Shape transformation was potentially caused by dissolution-redeposition mechanism, but it needs further confirmation. Lower ionic strength and lower divalent cation content in media gave lesser effect to both electrostatically and sterically capped AgNPs.

Dissolution properties of PVP-capped AgNPs generated by cold process was partly characterized by dialysis method and ICP-MS. It was shown that the silver ion concentration in the bulk media was controlled by the chloride content of the media. In ten fold dilution of OECD *Daphnia magna sp.* media, three phases of AgNPs transformation were observed which were: (1) dissolving of Ag^0 into Ag^+, (2) reduction of Ag^+ concentration in the bulk suspension due to Ag-Cl complexes formation, and (3) equilibrium state.

7.2. Further works

For the purpose of ecotoxicology study, tight constrained, fully characterized and stable NPs are required. As this study is part of larger ecotoxicology study, all those requirements was tried to be fulfilled. In this short study, due to time and resources limitation, however, several attemps regarding synthesis, characterization

and stability test of AgNPs could not be performed, but suggested to be done in future work.

In the synthesis process, to have a better monodispersity of NPs, separation technique such as ultracentrifugation and Fl-FFF can be utilized for NPs size segregation. It was expected to have a lower PdI value after separation process. More polymers such as gum Arabic, SDS, chitosan, etc can be used in indirect synthesis to have a stable AgNPs. Characterising dissolution properties of AgNPs has not been comprehensively done in this study and suggested to be done in further work not only by dialysis and ultrafiltration, but also using centrifugation, DGT, and other techniques. NPs surface analysis after ligand-exchange by Raman spectrometry, FTIR, H-NMR, STEM, etc, are also suggested to fully understand the occurrence of ligand-exchange, and media effect onto AgNPs.

From this study, it was observed that PVP-capped AgNPs, both generated from direct cold process and indirect method showed a satisfactory monodispersity and stability in OECD Daphnia magne sp. and Algae media. Therefore this particular NPs can be utilized for further ecotoxicology study.

Special acknowledgment

I would like to acknowledge Isabella Römer and Angelina Camina for synthesizing some of citrate and PEG-SH capped AgNPs for this study. Also Isabella work with FFF for size characterization of AgNPs after incubated in algae media is highly appreciated.

LIST OF REFERENCES

(2005). Zetasizer Nano Series: User Manual, Malvern Instrument.

(2011). "Solution-phase, dual LSPR-SERS plasmonic sensors of high sensitivity and stability based on chitosan-coated anisotropic silver nanoparticles." Journal of Materials Chemistry **21**(11): 3625.

Ahamed, M., M. S. AlSalhi, et al. (2010). "Silver nanoparticle applications and human health." Clinica Chimica Acta **411**(23-24): 1841-1848.

Alasonati, E., V. I. Slaveykova, et al. (2010). "Characterization of the colloidal organic matter from the Amazonian basin by asymmetrical flow field-flow fractionation and size exclusion chromatography." Water Research **44**(1): 223-231.

Allen, B. L., P. D. Kichambare, et al. (2008). "Biodegradation of Single-Walled Carbon Nanotubes through Enzymatic Catalysis." Nano Letters **8**(11): 3899-3903.

Allen, B. L., G. P. Kotchey, et al. (2009). "Mechanistic Investigations of Horseradish Peroxidase-Catalyzed Degradation of Single-Walled Carbon Nanotubes." Journal of the American Chemical Society **131**(47): 17194-17205.

Alvarez, P. J. J., V. Colvin, et al. (2009). "Research Priorities to Advance Eco-Responsible Nanotechnology." ACS Nano **3**(7): 1616-1619.

An, J., B. Tang, et al. (2008). "Sculpturing Effect of Chloride Ions in Shape Transformation from Triangular to Discal Silver Nanoplates." The Journal of Physical Chemistry C **112**(39): 15176-15182.

Anderson, R. L. (1987). "Practical statistics for analytical chemists."

Andrievski, R. (2009). "Size-dependent effects in properties of nanostructured materials." Rev. Adv. Mater. Sci **21**(2): 107-133.

Araki, J. (2013). "Electrostatic or steric? - preparations and characterizations of well-dispersed systems containing rod-like nanowhiskers of crystalline polysaccharides." Soft Matter **9**(16): 4125-4141.

Auffan, M., J. Rose, et al. (2009). "Towards a definition of inorganic nanoparticles from an environmental, health and safety perspective." Nat Nano **4**(10): 634-641.

Auffan, M., J. Rose, et al. (2009). "Chemical stability of metallic nanoparticles: A parameter controlling their potential cellular toxicity in vitro." Env. Pollut. **157**(4): 1127-1133.

Aymonier, C., U. Schlotterbeck, et al. (2002). "Hybrids of silver nanoparticles with amphiphilic hyperbranched macromolecules exhibiting antimicrobial properties." Chemical Communications **0**(24): 3018-3019.

Baalousha, M. and J. R. Lead (2007). "Characterization of Natural Aquatic Colloids (<5 nm) by Flow-Field Flow Fractionation and Atomic Force Microscopy." Environmental Science & Technology **41**(4): 1111-1117.

Baalousha, M. and J. R. Lead (2009). Overview of nanoscience in the environment. Environmental and human health impacts of nanotechnology. J. R. Lead and E. Smith. West Sussex, John Wiley & Sons, Ltd.

Baalousha, M. and J. R. Lead (2012). "Rationalizing Nanomaterial Sizes Measured by Atomic Force Microscopy, Flow Field-Flow Fractionation, and Dynamic Light Scattering: Sample Preparation, Polydispersity, and Particle Structure." Environmental Science & Technology **46**(11): 6134-6142.

Baalousha, M., Y. Nur, et al. (2013). "Effect of monovalent and divalent cations, anions and fulvic acid on aggregation of citrate-coated silver nanoparticles." Science of The Total Environment **454–455**(0): 119-131.

Baalousha, M., B. Stolpe, et al. (2011). "Flow field-flow fractionation for the analysis and characterization of natural colloids and manufactured nanoparticles in environmental systems: a critical review." Journal of Chromatography A **1218**(27): 4078-4103.

Baalousha, M., B. Stolpe, et al. (2011). "Flow field-flow fractionation for the analysis and characterization of natural colloids and manufactured nanoparticles in environmental systems: A critical review." Journal of Chromatography A **1218**(27): 4078-4103.

Badawy, A. M. E., T. P. Luxton, et al. (2010). "Impact of environmental conditions (pH, ionic strength, and electrolyte type) on the surface charge and aggregation of silver nanoparticles suspensions." Environmental Science & Technology **44**(4): 1260-1266.

Balazs, A. C., T. Emrick, et al. (2006). "Nanoparticle Polymer Composites: Where Two Small Worlds Meet." Science **314**(5802): 1107-1110.

Balnois, E., G. Papastavrou, et al. (2007). Force microscopy and force measurement of environmental colloids. Environmental colloids and particles: behaviour, separation and characterisation. K. J. Wilkinson and J. R. Lead. Chichester, John Wiley & Sons.

Barillet, S., A. Simon-Deckers, et al. (2010). "Toxicological consequences of TiO2, SiC nanoparticles and multi-walled carbon nanotubes exposure in several mammalian cell types: an in vitro study." Journal of Nanoparticle Research **12**(1): 61-73.

Batley, G. E., J. K. Kirby, et al. (2012). "Fate and Risks of Nanomaterials in Aquatic and Terrestrial Environments." Accounts of Chemical Research **46**(3): 854-862.

Baun, A., N. Hartmann, et al. (2008). "Ecotoxicity of engineered nanoparticles to aquatic invertebrates: a brief review and recommendations for future toxicity testing." Ecotoxicology **17**(5): 387-395.

Baur, C., A. Bugacov, et al. (1998). "Nanoparticle manipulation by mechanical pushing: underlying phenomena and real-time monitoring." Nanotechnology **9**: 360.

Beckett, R., Z. Jue, et al. (1987). "Determination of molecular weight distributions of fulvic and humic acids using flow field-flow fractionation." Environmental Science & Technology **21**(3): 289-295.

Benn, T. M. and P. Westerhoff (2008). "Nanoparticle silver released into water from commercially available sock fabrics." Env. Sci. & Tech. **42**(13): 7.

Binnig, G., C. Gerber, et al. (1987). "Atomic resolution with atomic force microscope." Surface Science **189–190**(0): 1-6.

Binnig, G., C. F. Quate, et al. (1986). "Atomic Force Microscope." Physical Review Letters **56**(9): 930-933.

Bleeker, E. A. J., W. H. de Jong, et al. (2013). "Considerations on the EU definition of a nanomaterial: Science to support policy making." Regulatory Toxicology and Pharmacology **65**(1): 119-125.

Bone, A. J., B. P. Colman, et al. (2012). "Biotic and abiotic interactions in aquatic microcosms determine fate and toxicity of Ag nanoparticles: Part 2–Toxicity and Ag speciation." Environmental science & technology **46**(13): 6925-6933.

Bonet, F., V. Delmas, et al. (1999). "Synthesis of monodisperse Au, Pt, Pd, Ru and Ir nanoparticles in ethylene glycol." Nanostructured Materials **11**(8): 1277-1284.

Borm, P., F. C. Klaessig, et al. (2006). "Research strategies for safety evaluation of nanomaterials, part V: role of dissolution in biological fate and effects of nanoscale particles." Toxicological Sciences **90**(1): 23-32.

Brown, L. O. and J. E. Hutchison (2001). "Formation and Electron Diffraction Studies of Ordered 2-D and 3-D Superlattices of Amine-Stabilized Gold Nanocrystals†." The Journal of Physical Chemistry B **105**(37): 8911-8916.

Brunner, T. J., P. Wick, et al. (2006). "In vitro cytotoxicity of oxide nanoparticles: comparison to asbestos, silica and the effect of particle solubility." Env. Sci. & Tech. **40**(14): 8.

Brust, M. and C. J. Kiely (2002). "Some recent advances in nanostructure preparation from gold and silver particles: a short topical review." Colloids and Surface A: Physicochemical and Engineering Aspects **202**: 12.

BSI (2005). Vocabulary-Nanoparticles. PAS 71:2005. UK, British Standard Institution.

Burda, C., T. Green, et al. (2000). Optical spectroscopy of nanophase material. Characterization of nanophase materials. Z. L. Wang. Weineim, Wiley-VCH.

Caragheorgheopol, A. and V. Chechik (2008). "Mechanistic aspects of ligand exchange in Au nanoparticles." Physical Chemistry Chemical Physics **10**(33): 5029-5041.

Casals, E., T. Pfaller, et al. (2011). "Hardening of the nanoparticle–protein corona in metal (Au, Ag) and oxide (Fe3O4, CoO, and CeO2) nanoparticles." Small **7**(24): 3479-3486.

Cedervall, T., I. Lynch, et al. (2007). "Understanding the nanoparticle–protein corona using methods to quantify exchange rates and affinities of proteins for nanoparticles." Proceedings of the National Academy of Sciences **104**(7): 2050-2055.

Chambers, B. A., A. Afrooz, et al. (2014). "Effects of Chloride and Ionic Strength on Physical Morphology, Dissolution, and Bacterial Toxicity of Silver Nanoparticles." Environmental Science & Technology **48**(1): 761-769.

Chen, C.-Y. and C. T. Jafvert (2011). "The role of surface functionalization in the solar light-induced production of reactive oxygen species by single-walled carbon nanotubes in water." Carbon **49**(15): 5099-5106.

Chen, K. L., B. A. Smith, et al. (2010). "Assesing the colloidal properties of engineered nanoparticles in water: case studies from fullerene C60 nanoparticles and carbon nanotubes." Env. Chem. **7**(1): 18.

Cheng, Y., L. Yin, et al. (2011). "Toxicity reduction of polymer-stabilized silver nanoparticles by sunlight." The Journal of Physical Chemistry C **115**(11): 4425-4432.

Cheng, Y., L. Yin, et al. (2011). "Toxicity Reduction of Polymer-Stabilized Silver Nanoparticles by Sunlight." The J. of Phy. Chem. C **115**(11): 4425-4432.

Chernousova, S. and M. Epple (2013). "Silver as Antibacterial Agent: Ion, Nanoparticle, and Metal." Angewandte Chemie-International Edition **52**(6): 1636-1653.

Chi, L. and C. Rothig (2000). Scanning Probe Microscopy of Nanoclusters. Characterization of nanophase materials. Z. L. Wang. Weinheil, Wiley-VCH.

Choi, O., T. E. Clevenger, et al. (2009). "Role of sulfide and ligand strength in controlling nanosilver toxicity." Water Research **43**(7): 1879-1886.

Chou, K.-S. and Y.-S. Lai (2004). "Effect of polyvinyl pyrrolidone molecular weights on the formation of nanosized silver colloids." Materials Chemistry and Physics **83**: 7.

Christian, P. (2009). Nanomaterials: Properties, preparation and application. Environmental and Human Health Impacts of Nanotechnology. J. R. Lead and E. Smith. West Sussex, John Wiley & Sons, Ltd.

Christian, P., F. Kammer, et al. (2008). "Nanoparticles: structure, properties, preparation and behaviour in environmental media." Ecotoxicology **17**(5): 326-343.

Coleman, J. N., U. Khan, et al. (2006). "Small but strong: a review of the mechanical properties of carbon nanotube–polymer composites." Carbon **44**(9): 1624-1652.

Crane, M., R. D. Handy, et al. (2008). "Ecotoxicity test methods and environmental hazard assessment for engineered nanoparticles." Ecotoxicology **17**(5): 421-437.

Crespo, P., R. Litrán, et al. (2004). "Permanent Magnetism, Magnetic Anisotropy, and Hysteresis of Thiol-Capped Gold Nanoparticles." Physical Review Letters **93**(8): 087204.

Cumberland, S. A. and J. R. Lead (2009). "Particle size distributions of silver nanoparticles at environmentally relevant conditions." Journal of Chromatography A **1216**(52): 9099-9105.

Curtis, J., M. Greenberg, et al. (2006). "Nanotechnology and nanotoxicology." Toxicological reviews **25**(4): 245-260.

Dalai, S., S. Pakrashi, et al. (2013). "Cytotoxicity of TiO2 nanoparticles and their detoxification in a freshwater system." Aquatic Toxicology **138–139**(0): 1-11.

Daniel, M.-C. and D. Astruc (2004). "Gold Nanoparticles: Assembly, Supramolecular Chemistry, Quantum-size-related properties, and Applications toward biology, catalysis and nanotechnology." Chemical Reviews **104**(1): 54.

de Lima, R., A. B. Seabra, et al. (2012). "Silver nanoparticles: a brief review of cytotoxicity and genotoxicity of chemically and biogenically synthesized nanoparticles." Journal of Applied Toxicology **32**(11): 867-879.

Derfus, A. M., W. C. W. Chan, et al. (2003). "Probing the Cytotoxicity of Semiconductor Quantum Dots." Nano Letters **4**(1): 11-18.

Derjaguin, B. V. (1989). Theory of stability of colloids and thin films. New York, Consultant Bureau.

Dolgaev, S. I., A. V. Simakin, et al. (2002). "Nanoparticles produced by laser ablation of solids in liquid environment." Applied Surface Science **186**(1-4): 6.

Domingos, R. F., M. A. Baalousha, et al. (2009). "Characterizing manufactured nanoparticles in the environment: Multimethod determination of particle sizes." Env. Sci. & Tech. **43**(19): 8.

Driver, S. M. and D. P. Woodruff (2000). "Adsorption Structures of 1-Octanethiol on Cu(111) Studied by Scanning Tunneling Microscopy." Langmuir **16**(16): 6693-6700.

Ducamp-Sanguesa, C., R. Herrera-Urbina, et al. (1992). "Synthesis and characterization of fine and monodisperse silver particles of uniform shape." Journal of Solid State Chemistry **100**(2): 272-280.

Duffin, R., L. Tran, et al. (2007). "Proinflammogenic effects of low-toxicity and metal nanoparticles in vivo and in vitro: highlighting the role of particle surface area and surface reactivity." Inhalation toxicology **19**(10): 849-856.

Eaton, P. and P. West (2010). Atomic Force Microsocpy. Oxford, Oxford university press.

EFSA, S. C. (2011). "Guidance on the risk assessment of the application of nanoscience and nanotechnologies in the food and feed chain." EFSA J **9**(5): 2140.

El-Sayed, M. A. (2004). "Small Is Different: Shape-, Size-, and Composition-Dependent Properties of Some Colloidal Semiconductor Nanocrystals." Accounts of Chemical Research **37**(5): 326-333.

El Badawy, A. M., A. Aly Hassan, et al. (2013). "Key Factors Controlling the Transport of Silver Nanoparticles in Porous Media." Environmental Science & Technology **47**(9): 4039-4045.

El Badawy, A. M., R. G. Silva, et al. (2010). "Surface Charge-Dependent Toxicity of Silver Nanoparticles." Environmental Science & Technology **45**(1): 283-287.

Elechiguerra, J. L., J. L. Burt, et al. (2005). "Interaction of silver nanoparticles with HIV-I." Journal of Nanobiotechnology **3**(6): 10.

Elechiguerra, J. L., L. Larios-Lopez, et al. (2005). "Corrosion at the nanoscale: the case of silver nanowires and nanoparticles." Chemistry of materials **17**(24): 6042-6052.

Elimelech, M. and C. R. O'Melia (1990). "Effect of particle size on collision efficiency in the deposition of Brownian particles with electrostatic energy barriers." Langmuir **6**(6): 1153-1163.

Endo, T., S. Yamamura, et al. (2005). "Localized surface plasmon resonance based optical biosensor using surface modified nanoparticle layer for label-free monitoring of antigen–antibody reaction." Science and Technology of Advanced Materials **6**(5): 491-500.

EPA (2013). "Priority Polutants." from http://water.epa.gov/scitech/methods/cwa/pollutants.cfm.

EU (2013). "Nanotechnology." Retrieved 28th March, 2014, from http://ec.europa.eu/nanotechnology/index_en.html.

Fabrega, J., S. R. Fawcett, et al. (2009). "Silver nanoparticle impact on bacterial growth: effect of pH, concentration, and organic matter." Environmental Science and Technology **43**(19): 6.

Fabrega, J., S. N. Luoma, et al. (2011). "Silver nanoparticles: Behaviour and effects in the aquatic environment." Env. Intl. **37**(2): 517-531.

Fabrega, J., R. Zhang, et al. (2011). "Impact of silver nanoparticles on natural marine biofilm bacteria." Chemosphere **85**(6): 961-966.

Faraday, M. (1857). "The Bakerian Lecture: Experimental Relations of Gold (and Other Metals) to Light." Philosophical Transactions of the Royal Society of London **147**: 145-181.

Farkas, J., H. Peter, et al. (2011). "Characterization of the effluent from a nanosilver producing washing machine." Environment International **37**(6): 1057-1062.

Fauss, E. (2008). The silver nanotechnology commercial inventory, Woodrow WilsonInternational Centre for Scholar.

Fonseca, F. C., G. F. Goya, et al. (2002). Superparamagnetism and magnetic properties of Ni nanoparticles embedded in SiO2. Physical Review B, American Physical Society. **66:** 104406.

Foss Hansen, S., B. H. Larsen, et al. (2007). "Categorization framework to aid hazard identification of nanomaterials." Nanotoxicology **1**(3): 243-250.

Franklin, N. M., N. J. Rogers, et al. (2007). "Comparative Toxicity of Nanoparticulate ZnO, Bulk ZnO, and ZnCl2 to a Freshwater Microalga (Pseudokirchneriella subcapitata): The Importance of Particle Solubility." Environmental Science & Technology **41**(24): 8484-8490.

Franklin, N. M., N. J. Rogers, et al. (2007). "Comparative toxicity of nanoparticulate ZnO, bulk ZnO, and $ZnCl_2$ to a freshwater microalga (*Pseudokirchneriella subcapitata*): the importance of particle solubility." Env. Sci. and Tech. **41**(24): 7.

Freitas, C. and R. H. Müller (1998). "Effect of light and temperature on zeta potential and physical stability in solid lipid nanoparticle (SLN™) dispersions." International Journal of Pharmaceutics **168**(2): 221-229.

French, R. A., A. R. Jacobson, et al. (2009). "Influence of Ionic Strength, pH, and Cation Valence on Aggregation Kinetics of Titanium Dioxide Nanoparticles." Environmental Science & Technology **43**(5): 1354-1359.

Gangula, A., J. Chelli, et al. (2012). "Thione-gold nanoparticles interactions: Vroman-like effect, self-assembly and sensing." Journal of Materials Chemistry **22**(43): 22866-22872.

Gao, J., S. Youn, et al. (2009). "Dispersion and Toxicity of Selected Manufactured Nanomaterials in Natural River Water Samples: Effects of Water Chemical Composition." Env. Sci. & Tech. **43**(9): 3322-3328.

Geranio, L., M. Heuberger, et al. (2009). "The behavior of silver nanotextiles during washing." Environmental Science and Technology **43**(21): 6.

Gerbec, J. A., D. Magana, et al. (2005). "Microwave-Enhanced Reaction Rates for Nanoparticle Synthesis." Journal of the American Chemical Society **127**(45): 15791-15800.

Ghosh, S. K., S. Nath, et al. (2004). "Solvent and Ligand Effects on the Localized Surface Plasmon Resonance (LSPR) of Gold Colloids." The Journal of Physical Chemistry B **108**(37): 13963-13971.

Giddings, J. (1993). "Field-flow fractionation: analysis of macromolecular, colloidal, and particulate materials." Science **260**(5113): 1456-1465.

Gigault, J., B. Grassl, et al. (2012). "A new analytical approach based on asymmetrical flow field-flow fractionation coupled to ultraviolet spectrometry and light scattering detection for SWCNT aqueous dispersion studies." Analyst **137**(4): 917-923.

Glover, R. D., J. M. Miller, et al. (2011). "Generation of Metal Nanoparticles from Silver and Copper Objects: Nanoparticle Dynamics on Surfaces and Potential Sources of Nanoparticles in the Environment." ACS Nano **5**(11): 8950-8957.

Gubbins, E. J., L. C. Batty, et al. (2011). "Phytotoxicity of silver nanoparticles to Lemna minor L." Env. Pollut. **159**(6): 1551-1559.

Guo, L., S. Yang, et al. (2000). "Highly monodisperse polymer-capped ZnO nanoparticles: Preparation and optical properties." Applied Physics Letters **76**(20): 2901-2903.

Haes, A. J. and R. P. Van Duyne (2002). "A Nanoscale Optical Biosensor: Sensitivity and Selectivity of an Approach Based on the Localized Surface Plasmon Resonance Spectroscopy of Triangular Silver Nanoparticles." Journal of the American Chemical Society **124**(35): 10596-10604.

Haiss, W., N. T. K. Thanh, et al. (2007). "Determination of size and concentration of gold nanoparticles from UV-Vis spectra." Analytical Chemistry **79**(11): 4215-4221.

Handy, R., R. Owen, et al. (2008). "The ecotoxicology of nanoparticles and nanomaterials: current status, knowledge gaps, challenges, and future needs." Ecotoxicology **17**(5): 315-325.

Handy, R. D., G. Cornelis, et al. (2012). "Ecotoxicity test methods for engineered nanomaterials: practical experiences and recommendations from the bench." Environmental Toxicology and Chemistry **31**(1): 15-31.

Handy, R. D., F. v. d. Kammer, et al. (2008). "The ecotoxicology and chemistry of manufactured nanoparticles." Ecotoxicology **17**(4): 28.

Handy, R. D., F. von der Kammer, et al. (2008). "The ecotoxicology and chemistry of manufactured nanoparticles." Ecotoxicology **17**(4): 287-314.

Hansen, S. F., B. H. Larsen, et al. (2007). "Categorization framework to aid hazard identification of nanomaterials." Nanotoxicology **1**(3): 243-U369.

Hartmann, N. B., F. Von der Kammer, et al. (2010). "Algal testing of titanium dioxide nanoparticles—Testing considerations, inhibitory effects and modification of cadmium bioavailability." Toxicology **269**(2–3): 190-197.

Haruta, M. (1997). "Size-and support-dependency in the catalysis of gold." Catalysis Today **36**(1): 153-166.

Haruta, M. (2004). "Gold as a novel catalyst in the 21st century: preparation, working mechanism and applications." Gold bulletin **37**(1-2): 27-36.

Haruta, M., N. Yamada, et al. (1989). "Gold catalysts prepared by coprecipitation for low-temperature oxidation of hydrogen and of carbon monoxide." Journal of Catalysis **115**(2): 301-309.

Hassellov, M., F. V. D. Kammer, et al. (2007). Characterization of aquatic colloids and macromolecules by Field-flow fractionation. Environmental colloids and particles: behaviour, separation and characterization. K. J. Wilkinson and J. R. Lead. Chichester, John Wiley & Sons. **10**.

Hassellöv, M., J. Readman, et al. (2008). "Nanoparticle analysis and characterization methodologies in environmental risk assessment of engineered nanoparticles." Ecotoxicology **17**(5): 344-361.

Hassellov, M., J. W. Readman, et al. (2008). "Nanoparticle analysis and characterization methodologies in environmental risk assessment of engineered nanoparticles." Ecotoxicology **17**: 18.

Hassellov, M., F. von der Kammer, et al. (2007). "Characterisation of aquatic colloids and macromolecules by field-flow fractionation." IUPAC Series on Analytical and Physical Chemistry of Environmental Systems **10**: 223.

He, Y. T., J. Wan, et al. (2008). "Kinetic stability of hematite nanoparticles: the effect of particle sizes." Journal of Nanoparticle Research **10**(2): 321-332.

Heard, S. M., F. Grieser, et al. (1983). "The characterization of ag sols by electron microscopy, optical absorption, and electrophoresis." Journal of Colloid and Interface Science **93**(2): 545-555.

Henglein, A. (1993). "Physicochemical properties of small metal particles in solution: "microelectrode" reactions, chemisorption, composite metal particles, and the atom-to-metal transition." The J. of Phy. Chem. **97**(21): 5457-5471.

Henglein, A. and M. Giersig (1999). "Formation of Colloidal Silver Nanoparticles, capping action of citrate." Journal of Physical Chemistry **103**: 7.

Ho, C.-M., S. K.-W. Yau, et al. (2010). "Oxidative Dissolution of Silver Nanoparticles by Biologically Relevant Oxidants: A Kinetic and Mechanistic Study." Chemistry – An Asian Journal **5**(2): 285-293.

Hoppe, C. E., M. Lazzari, et al. (2006). "One-step synthesis of gold and silver hydrosols using Poly (N-vinyl-2-pyrrolidone) as a reducing agent " Langmuir **22**: 8.

Hori, H., Y. Yamamoto, et al. (2004). "Diameter dependence of ferromagnetic spin moment in Au nanocrystals." Physical Review B **69**(17): 174411.

Hostetler, M. J., J. E. Wingate, et al. (1998). "Alkanethiolate Gold Cluster Molecules with Core Diameters from 1.5 to 5.2 nm: Core and Monolayer Properties as a Function of Core Size." Langmuir **14**(1): 17-30.

Hu, W., C. Peng, et al. (2011). "Protein Corona-Mediated Mitigation of Cytotoxicity of Graphene Oxide." ACS Nano **5**(5): 3693-3700.

Huang, C.-Y., D.-Y. Wang, et al. (2011). "Efficient light harvesting and carrier transport in PbS quantum dots/silicon nanotips heterojunctions." Journal of Physics D: Applied Physics **44**(8): 085103.

Huang, H. H., X. P. Ni, et al. (1996). "Photochemical Formation of Silver Nanoparticles in Poly(N-vinylpyrrolidone)." Langmuir **12**(4): 909-912.

Hunter, R. J. (1986). Foundations of colloid science. Oxford, Oxford University Press.

Hunter, R. J. (1986). Foundations of colloids science. New York, Oxford University Press.

Hussain, S., S. Boland, et al. (2009). "Oxidative stress and proinflammatory effects of carbon black and titanium dioxide nanoparticles: role of particle surface area and internalized amount." Toxicology **260**(1): 142-149.

Hwang, M. G., H. Katayama, et al. (2007). "Inactivation of< i> Legionella pneumophila</i> and< i> Pseudomonas aeruginosa</i>: Evaluation of the bactericidal ability of silver cations." Water Research **41**(18): 4097-4104.

Impellitteri, C. A., S. Harmon, et al. (2013). "Transformation of silver nanoparticles in fresh, aged, and incinerated biosolids." Water research **47**(12): 3878-3886.

Impellitteri, C. A., T. M. Tolaymat, et al. (2009). "The speciation of silver nanoparticles in antimicrobial fabric before and after exposure to a hypochlorite/detergent solution." Journal of environmental quality **38**(4): 1528-1530.

Jalili, N. and K. Laxminarayana (2004). "A review of atomic force microscopy imaging systems: application to molecular metrology and biological sciences." Mechatronics **14**(8): 907-945.

Jana, N. R., L. Gearheart, et al. (2001). "Wet chemical synthesis of silver nanorods and nanowires of controllable aspect ratio." Chemical Communications **0**(7): 617-618.

Jin, X., M. Li, et al. (2010). "High-Throughput Screening of Silver Nanoparticle Stability and Bacterial Inactivation in Aquatic Media: Influence of Specific Ions." Env. Sci. & Tech. **44**(19): 7321-7328.

Jo, Y.-K., B. H. Kim, et al. (2009). "Antifungal Activity of silver ions and nanoparticles on phytopathogenic fungi." Plant Disease **93**(10): 7.

Jonte, J. H. and D. S. Martin Jr (1952). "The Solubility of Silver Chloride and the Formation of Complexes in Chloride Solution1." Journal of the American Chemical Society **74**(8): 2052-2054.

Ju-Nam, Y. and J. R. Lead (2008). "Manufactured nanoparticles: An overview of their chemistry, interactions and potential environmental implications." Science of the Total Environment **400**: 19.

Kaegi, R., B. Sinnet, et al. (2010). "Release of silver nanoparticles from outdoor facades." Env. Pollut. **158**(9): 2900-2905.

Kaegi, R., A. Voegelin, et al. (2013). "Fate and transformation of silver nanoparticles in urban wastewater systems." Water research **47**(12): 3866-3877.

Kamat, P. V., M. Gevaert, et al. (1997). "Photochemistry on Semiconductor Surfaces. Visible Light Induced Oxidation of C60 on TiO2 Nanoparticles." The Journal of Physical Chemistry B **101**(22): 4422-4427.

Kanninen, P., C. Johans, et al. (2008). "Influence of ligand structure on the stability and oxidation of copper nanoparticles." Journal of Colloid and Interface Science **318**(1): 88-95.

Kapoor, S. (1998). "Preparation, characterization, and surface modification of silver particles." Langmuir **14**(5): 1021-1025.

Keller, A. A., H. Wang, et al. (2010). "Stability and Aggregation of Metal Oxide Nanoparticles in Natural Aqueous Matrices." Environmental Science & Technology **44**(6): 1962-1967.

Kelly, K. L., E. Coronado, et al. (2002). "The Optical Properties of Metal Nanoparticles: The Influence of Size, Shape, and Dielectric Environment." The Journal of Physical Chemistry B **107**(3): 668-677.

Kelly, K. L., E. Coronado, et al. (2003). "The optical properties of metal nanoparticles: The influence of size, shape and dielectric environment." Journal of Physical Chemistry **107**(3): 10.

Kendall, M. and S. Holgate (2012). "Health impact and toxicological effects of nanomaterials in the lung." Respirology **17**(5): 743-758.

Kent, R. D. and P. J. Vikesland (2011). "Controlled Evaluation of Silver Nanoparticle Dissolution Using Atomic Force Microscopy." Environmental Science & Technology.

Khanna, S. N. and A. W. Castleman (2003). Quantum phenomena in clusters and nanostructures, Springer.

Kim, B., C.-S. Park, et al. (2010). "Discovery and Characterization of Silver Sulfide Nanoparticles in Final Sewage Sludge Products." Environmental Science & Technology **44**(19): 7509-7514.

Kim, D., S. Jeong, et al. (2006). "Synthesis of silver nanoparticles using the polyol process and the influence of precursor injection." Nanotechnology **17**: 6.

Kirby, B. J. and E. F. H. Jr (2004). "Zeta potential of microfluidic substrate: 1. Theory, experimental techniques, and effect on separation." Electrophoresis **25**(2): 187-202.

Kittler, S., C. Greulich, et al. (2010). "Toxicity of silver nanoparticles increases during storage because of slow dissolution under release of silver ions." Chemistry of Materials **22**(16): 7.

Klaine, S. J., P. J. J. Alvarez, et al. (2008). "Nanomaterials in the environment: behavior, fate, bioavailability and effects." Environmental Toxicology and Chemistry **27**(9): 27.

Klein, J. (2007). "Probing the interactions of proteins and nanoparticles." Proceedings of the National Academy of Sciences **104**(7): 2029-2030.

Komarneni, S., D. Li, et al. (2002). "Microwave-polyol process for Pt and Ag nanoparticles." Langmuir **18**(15): 5959-5962.

Krüger, D., H. Fuchs, et al. (2001). "Interaction of short-chain alkane thiols and thiolates with small gold clusters: Adsorption structures and energetics." Journal of Chemical Physics **115**(10): 4776-4786.

Kvitek, L., A. Panaček, et al. (2008). "Effect of Surfactants and Polymers on Stability and Antibacterial Activity of Silver Nanoparticles (NPs)." The J. Phy. Chem. C **112**(15): 5825-5834.

Kvitek, L., M. Vanickova, et al. (2009). "Initial Study on the Toxicity of Silver Nanoparticles (NPs) against Paramecium caudatum." The Journal of Physical Chemistry C **113**(11): 4296-4300.

Laaksonen, T., P. Ahonen, et al. (2006). "Stability and Electrostatics of Mercaptoundecanoic Acid-Capped Gold Nanoparticles with Varying Counterion Size." ChemPhysChem **7**(10): 2143-2149.

Lajunen, L. H. and P. Perämäki (2004). Spectrochemical analysis by atomic absorption and emission, Royal Society of Chemistry.

Lead, J. R. and E. Smith, Eds. (2009). Environmental and human health impacts of nanotechnology, Wiley.

Ledwith, D. M., D. Aherne, et al. (2009). Approaches to the synthesis and characterization of spherical and anisotropic silver nanomaterials. Metallic Nanomaterials. C. Kumar. Weinheim, Wiley-VCH Verlag GmbH&Co.

Ledwith, D. M., D. Aherne, et al. (2009). Approaches to the synthesis and characterization of spherical and anisotropic silver nanomaterials. Weinheim, Wiley-VCH Verlag GmbH & Co.KGaA.

Lee, J. H., B. E. Park, et al. (2009). "Synthesis of fullerene[C60]-silver nanoparticles using various non-ionic surfactants under microwave irradiation." Current Applied Physics **9**(2, Supplement): e152-e156.

Lee, Y. S. (2008). Nanoparticles: Metals, Semiconductors, and Oxides. Self-Assembly and Nanotechnology. New Jersey, John Wiley and Sons.

Levard, C., E. M. Hotze, et al. (2012). "Environmental Transformations of Silver Nanoparticles: Impact on Stability and Toxicity." Environmental Science & Technology **46**(13): 6900-6914.

Levard, C., S. Mitra, et al. (2013). "Effect of Chloride on the Dissolution Rate of Silver Nanoparticles and Toxicity to E. coli." Environmental Science & Technology **47**(11): 5738-5745.

Levard, C., B. C. Reinsch, et al. (2011). "Sulfidation processes of PVP-coated silver nanoparticles in aqueous solution: impact on dissolution rate." Environmental science & technology **45**(12): 5260-5266.

Li, X. and J. J. Lenhart (2012). "Aggregation and Dissolution of Silver Nanoparticles in Natural Surface Water." Environmental Science & Technology **46**(10): 5378-5386.

Li, X., J. J. Lenhart, et al. (2010). "Dissolution-Accompanied Aggregation Kinetics of Silver Nanoparticles." Langmuir **26**(22): 16690-16698.
null

Li, X., J. J. Lenhart, et al. (2011). "Aggregation kinetics and dissolution of coated silver nanoparticles." Langmuir **28**(2): 1095-1104.

Li, Y. and M. A. El-Sayed (2001). "The effect of stabilizers on the catalytic activity and stability of Pd colloidal nanoparticles in the Suzuki reactions in aqueous solution." The Journal of Physical Chemistry B **105**(37): 8938-8943.

Lidén, G. (2011). "The European Commission Tries to Define Nanomaterials." Annals of Occupational Hygiene **55**(1): 1-5.
I

Lin, W., Y.-w. Huang, et al. (2006). "In vitro toxicity of silica nanoparticles in human lung cancer cells." Toxicology and Applied Pharmacology **217**(3): 252-259.

Lin, X.-M. and A. C. Samia (2006). "Synthesis, assembly and physical properties of magnetic nanoparticles." Journal of Magnetism and Magnetic Materials **305**(1): 10.

Linnert, T., P. Mulvaney, et al. (1993). "Surface chemistry of colloidal silver: surface plasmon damping by chemisorbed iodide, hydrosulfide (SH-), and phenylthiolate." The Journal of Physical Chemistry **97**(3): 679-682.

Liu, J. and R. H. Hurt (2010). "Ion Release Kinetics and Particle Persistence in Aqueous Nano-Silver Colloids." Environmental Science & Technology **44**(6): 2169-2175.

null

Liu, J., D. A. Sonshine, et al. (2010). "Controlled Release of Biologically Active Silver from Nanosilver Surfaces." ACS Nano **4**(11): 6903-6913.

Liu, S., X. Qian, et al. (2003). "Preparation and characterization of polymer-capped CdS nanocrystals." Journal of physics and chemistry of solids **64**(3): 455-458.

Liu, W., Q. Zhou, et al. (2011). "Environmental and biological influences on the stability of silver nanoparticles." Chinese Science Bulletin **56**(19): 2009-2015.

Liu, Z., Z. Li, et al. (2006). "Manipulation, dissection, and lithography using modified tapping mode atomic force microscope." Microscopy Research and Technique **69**(12): 998-1004.

Liz-Marzán, L. M., M. Giersig, et al. (1996). "Synthesis of Nanosized Gold−Silica Core−Shell Particles." Langmuir **12**(18): 4329-4335.

Lohrke, J., A. Briel, et al. (2008). "Characterization of superparamagnetic iron oxide nanoparticles by asymmetrical flow-field-flow-fractionation." Nanomedicine **3**(4): 437-452.

Lopez, N. and J. K. Nørskov (2002). "Catalytic CO Oxidation by a Gold Nanoparticle: A Density Functional Study." Journal of the American Chemical Society **124**(38): 11262-11263.

Lorenz, C., L. Windler, et al. (2012). "Characterization of silver release from commercially available functional (nano)textiles." Chemosphere **89**(7): 817-824.

Lowry, G. V., B. P. Espinasse, et al. (2012). "Long-Term Transformation and Fate of Manufactured Ag Nanoparticles in a Simulated Large Scale Freshwater Emergent Wetland." Environmental Science & Technology **46**(13): 7027-7036.

Lowry, G. V., K. B. Gregory, et al. (2012). "Transformations of Nanomaterials in the Environment." Environmental Science & Technology **46**(13): 6893-6899.

Lu, L., R. W.-Y. Sun, et al. (2008). "Silver nanoparticles inhibit hepatitis B virus replication." Antiviral Therapy **13**: 10.

Luoma, S. N. (2008). Silver nanotechnologies and the environment: old problems or new challenges, Woodrow Wilson International Center for Scholar, Project on Emerging Nanotechnologies.

Luoma, S. N. (2008). Silver nanotechnologies and the environment: old problems or new challenges?, Woodrow Wilson International Centre for Scholars. **PEN 15**.

MacCuspie, R. (2011). "Colloidal stability of silver nanoparticles in biologically relevant conditions." Journal of Nanoparticle Research **13**(7): 2893-2908.

MacCuspie, R. I., K. Rogers, et al. (2011). "Challenges for physical characterization of silver nanoparticles under pristine and environmentally relevant conditions." Journal of Environmental Monitoring **13**(5): 1212-1226.

Mafune, F., J.-y. Kohno, et al. (2000). "Structure and stability of silver nanoparticles in aqueous solution produced by laser ablation." The Journal of Physical Chemistry **104**(35): 5.

Mak, K. F., C. H. Lui, et al. (2009). "Observation of an electric-field-induced band gap in bilayer graphene by infrared spectroscopy." Physical review letters **102**(25): 256405.

Malinsky, M. D., K. L. Kelly, et al. (2001). "Chain Length Dependence and Sensing Capabilities of the Localized Surface Plasmon Resonance of Silver Nanoparticles Chemically Modified with Alkanethiol Self-Assembled Monolayers." Journal of the American Chemical Society **123**(7): 1471-1482.

Malvern Zeta potential an introduction in 30 minutes.

Marambio-Jones, C. and E. V. Hoek (2010). "A review of the antibacterial effects of silver nanomaterials and potential implications for human health and the environment." Journal of Nanoparticle Research **12**(5): 1531-1551.

Marques-Hueso, J., R. Abargues, et al. (2012). Plasmon dumping in Ag-nanoparticles/polymer composite for optical detection of amines and thiols vapors.

McFarland, A. D. and R. P. Van Duyne (2003). "Single Silver Nanoparticles as Real-Time Optical Sensors with Zeptomole Sensitivity." Nano Letters **3**(8): 1057-1062.

Mehra, M. and A. Gubeli (1971). "COMPLEXING CHARACTERISTICS OF INSOLUBLE SELENIDES. PT. 3.--MERCURIC SELENIDE." J LESS-COMMON METALS **25**(2): 221-224.

Meyers, M. A., A. Mishra, et al. (2006). "Mechanical properties of nanocrystalline materials." Progress in Materials Science **51**(4): 427-556.

Miao, A.-J., X.-Y. Zhang, et al. (2010). "Zinc oxide–engineered nanoparticles: Dissolution and toxicity to marine phytoplankton." Environmental Toxicology and Chemistry **29**(12): 2814-2822.

Misra, S. K., A. Dybowska, et al. (2012). "The complexity of nanoparticle dissolution and its importance in nanotoxicological studies." Science of the Total Environment **438**: 225-232.

Mittal, A. K., Y. Chisti, et al. (2013). "Synthesis of metallic nanoparticles using plant extracts." Biotechnology Advances **31**(2): 346-356.

Mock, J., M. Barbic, et al. (2002). "Shape effects in plasmon resonance of individual colloidal silver nanoparticles." The Journal of Chemical Physics **116**: 6755.

Monteiller, C., L. Tran, et al. (2007). "The pro-inflammatory effects of low-toxicity low-solubility particles, nanoparticles and fine particles, on epithelial cells in vitro: the role of surface area." Occupational and environmental medicine **64**(9): 609-615.

Mulfinger, L., S. D. Solomon, et al. (2007). "Synthesis and Study of Silver Nanoparticles." J. of Chem. Edu. **84**(2): 322.

Mulvaney, P., T. Linnert, et al. (1991). "Surface chemistry of colloidal silver in aqueous solution: observations on chemisorption and reactivity." The Journal of Physical Chemistry **95**(20): 7843-7846.

Napper, D. H. (1977). "Steric stabilization." Journal of Colloid and Interface Science **58**(2): 390-407.

Navarro, E., F. Piccapietra, et al. (2008). "Toxicity of Silver Nanoparticles to Chlamydomonas reinhardtii." Environmental Science & Technology **42**(23): 8959-8964.

Navarro, E., F. Piccapietra, et al. (2008). "Toxicity of silver nanoparticles to *Chlamydomonas reinhardtii*." Environmental Science and Technology **42**: 6.

Nobs, L., F. Buchegger, et al. (2004). "Current methods for attaching targeting ligands to liposomes and nanoparticles." Journal of Pharmaceutical Sciences **93**(8): 1980-1992.

Novotny, L. and B. Hecht (2012). Principles of nano-optics, Cambridge university press.

Nowack, B. and T. D. Bucheli (2007). "Occurence, behaviour and effects of nanoparticles in the environment." Env. Pollut. **150**: 18.

Nowack, B. and T. D. Bucheli (2007). "Occurrence, behavior and effects of nanoparticles in the environment." Env. Pollution **150**(1): 5-22.

Oberdörster, G., J. Ferin, et al. (1994). "Correlation between particle size, in vivo particle persistence, and lung injury." Environmental health perspectives **102**(Suppl 5): 173.

Oberdörster, G., E. Oberdörster, et al. (2005). "Nanotoxicology: an emerging discipline evolving from studies of ultrafine particles." Environmental health perspectives **113**(7): 823.

OECD (2002). "OECD Guidelines for the testing of chemicals number 201: Freshwater algae and Cyanobacteris, Growth Inhibition Test." Retrieved 31st March, 2014, from http://www.oecd.org/chemicalsafety/testing/1946914.pdf.

OECD (2004). Test No. 202: Daphnia sp. Acute Immobilisation Test, OECD Publishing.

OECD/OCDE (2004). OECD Guideline for Testing of Chemicals: Daphnia sp., Acute Immobilisation Test, number 202. France, OECD/OCDE.

Owens, F. J. and C. P. Poole Jr (2008). The physics and chemistry of nanosolids, John Wiley & Sons.

Pal, T., T. K. Sau, et al. (1997). "Reversible Formation and Dissolution of Silver Nanoparticles in Aqueous Surfactant Media†." Langmuir **13**(6): 1481-1485.

Panacek, A., M. Kolar, et al. (2009). "Antifungal activity of silver nanoparticles against *Candida* spp." Biomaterials0 **30**(31): 8.

Panáček, A., L. Kvítek, et al. (2006). "Silver Colloid Nanoparticles: Synthesis, Characterization, and Their Antibacterial Activity." The Journal of Physical Chemistry B **110**(33): 16248-16253.
null

Park, H.-J., J. Y. Kim, et al. (2009). "Silver-ion-mediated reactive oxygen species generation affecting bactericidal activity." Water Research **43**(4): 1027-1032.

Park, K., G. Tuttle, et al. (2013). "Stability of citrate-capped silver nanoparticles in exposure media and their effects on the development of embryonic zebrafish (Danio rerio)." Archives of pharmacal research **36**(1): 125-133.

Park, S. and K. Hamad-Schifferli (2008). "Evaluation of Hydrodynamic Size and Zeta-Potential of Surface-Modified Au Nanoparticle-DNA Conjugates via Ferguson Analysis." The Journal of Physical Chemistry C **112**(20): 7611-7616.

Park, T.-J., G. C. Papaefthymiou, et al. (2007). "Size-Dependent Magnetic Properties of Single-Crystalline Multiferroic BiFeO3 Nanoparticles." Nano Letters **7**(3): 766-772.

Park, Y. and R. C. Advincula (2011). "Hybrid Semiconductor Nanoparticles: pi-Conjugated Ligands and Nanostructured Films." Chemistry of Materials **23**(19): 4273-4294.

Parr, R. G., L. v. Szentpály, et al. (1999). "Electrophilicity Index." Journal of the American Chemical Society **121**(9): 1922-1924.

Patakfalvi, R., S. Papp, et al. (2007). "The kinetic of homogeneous nucleation of silver nanoparticles stabilized by polymers." Journal of nanoparticle Research **9**(3): 12.

Pattanaik, M. and S. K. Bhaumik (2000). "Adsorption behaviour of polyvinyl pyrrolidone on oxide surfaces." Materials Letters **44**(6): 352-360.

PEN (2013). "The Project on Emerging Nanotechnologies ". Retrieved 28th March, 2014, from http://www.nanotechproject.org/cpi/about/analysis/.

Pettitt, M. E. and J. R. Lead (2013). "Minimum physicochemical characterisation requirements for nanomaterial regulation." Environment International **52**: 41-50.

Poda, A. R., A. J. Bednar, et al. (2011). "Characterization of silver nanoparticles using flow-field flow fractionation interfaced to inductively coupled plasma mass spectrometry." Journal of Chromatography A **1218**(27): 4219-4225.

Popa, M., T. Paradell, et al. (2007). "Stable silver colloidal dispersions using short chain polyethylene glycol." Colloids and Surface A: Physicochemical and Engineering Aspects **303**: 7.

Porel, S., S. Singh, et al. (2004). "Nanoparticle-Embedded Polymer: In Situ Synthesis, Free-Standing Films with Highly Monodisperse Silver Nanoparticles and Optical Limiting." Chemistry of Materials **17**(1): 9-12.

Powers, K. W., S. C. Brown, et al. (2006). "Research strategies for safety evaluation of nanomaterials. Part VI. Characterization of nanoscale particles for toxicological evaluation." Toxicological Sciences **90**(2): 296-303.

Prathna, T. C., N. Chandrasekaran, et al. (2011). "Studies on aggregation behaviour of silver nanoparticles in aqueous matrices: Effect of surface functionalization and matrix composition." Colloids and Surfaces A: Physicochemical and Engineering Aspects **390**(1–3): 216-224.

Premkumar, T., D. Kim, et al. (2007). "Polysorbate 80 as a Tool: Synthesis of Gold Nanoparticles." Macromolecular Rapid Communications **28**(7): 888-893.

Rahman, I. A. and V. Padavettan (2012). "Synthesis of silica nanoparticles by sol-gel: size-dependent properties, surface modification, and applications in silica-polymer nanocomposites—a review." Journal of Nanomaterials **2012**: 8.

Rao, C. N. R., G. U. Kulkarni, et al. (2002). "Size-Dependent Chemistry: Properties of Nanocrystals." Chemistry – A European Journal **8**(1): 28-35.

Ratte, H. T. (1999). "Bioaccumulation and toxicity of silver compounds: A review." Environmental Toxicology and Chemistry **18**(1): 89-108.

Rauscher, H., G. Roebben, et al. (2014). Towards a review of the EC Recommendation for a definition of the term "nanomaterial"

Part 1: Compilation of information concerning the experience with the definition. JRC Scientific and policy report. H. Rauscher and G. Roebben. Luxembourg, Joint Research Centre European Commission. **50:** 289.

Reed, S. J. B. (1993). Electron Microprobe Analysis. Cambridge, University Cambridge, Press.

Rehn, B., F. Seiler, et al. (2003). "Investigations on the inflammatory and genotoxic lung effects of two types of titanium dioxide: untreated and surface treated." Toxicology and Applied Pharmacology **189**(2): 84-95.

Reidy, B., A. Haase, et al. (2013). "Mechanisms of Silver Nanoparticle Release, Transformation and Toxicity: A Critical Review of Current Knowledge and Recommendations for Future Studies and Applications." Materials **6**(6): 2295-2350.

Reimer, L. (1997). Transmission electron microscopy: Physics of image formation and microanalysis. Berlin, Springer.

Rejeski, D. (2009). Testimony of Project on Emerging Nanotechnology (PEN): Consumer Product Safety Commison (CPSC) FY 2010 Agenda and Priorities. Washington, Woodrow Wilson International Center for Scholars.

Resch, R., D. Lewis, et al. (2000). "Manipulation of gold nanoparticles in liquid environments using scanning force microscopy." Ultramicroscopy **82**(1–4): 135-139.

Riddick, T. M. (1968). "Control of colloid stability through zeta potential." Blood **10**: 1.

Rochow, T. G. and P. A. Tucker (1994). Introduction to microscopy by means of light, electrons, X rays, or acoustics. New York, Plenum Press.

Rogers, N. J., N. M. Franklin, et al. (2010). "Physico-chemical behaviour and algal toxicity of nanoparticulate CeO2 in freshwater." Environmental Chemistry **7**(1): 50-60.

Römer, I., T. A. White, et al. (2011). "Aggregation and dispersion of silver nanoparticles in exposure media for aquatic toxicity tests." J. of Chrom. A **1218**(27): 4226-4233.

RS (2004). Nanoscience and nanotechnologies: opportunities and uncertainties. London, The Royal Society.

Rugar, D. and P. Hansma (1990). "Atomic force microscopy." Physics today **43**(10): 23-30.

Sardar, R., A. M. Funston, et al. (2009). "Gold Nanoparticles: Past, Present, and Future." Langmuir **25**(24): 13840-13851.

Sartor, M. Dynamic Light Scattering to determine the radius of small beads in Brownian motion in a solution, University of California San Diego. **2012**.

Sau, T. K., A. Pal, et al. (2001). "Size Regime Dependent Catalysis by Gold Nanoparticles for the Reduction of Eosin." The Journal of Physical Chemistry B **105**(38): 9266-9272.

Schenk, J., L. Trobs, et al. (2012). "Simultaneous UV/Vis spectroscopy and surface enhanced Raman scattering of nanoparticle formation and aggregation in levitated droplets." Analytical Methods **4**(5): 1252-1258.

Schinca, D. C. and L. B. Scaffardi (2008). "Core and shell sizing of small silver-coated nanospheres by optical extinction spectroscopy." Nanotechnology **19**(49): 495712.

Schmitt, J., G. Decher, et al. (1997). "Metal nanoparticle/polymer superlattice films: Fabrication and control of layer structure." Advanced Materials **9**(1): 61-65.

Scown, T. M., E. M. Santos, et al. (2010). "Effects of Aqueous Exposure to Silver Nanoparticles of Different Sizes in Rainbow Trout." Toxicol. Sci. **115**(2): 521-534.

Seo, J., S. J. Kim, et al. (2009). "Enhancement of the photovoltaic performance in PbS nanocrystal:P3HT hybrid composite devices by post-treatment-driven ligand exchange." Nanotechnology **20**(9): 095202.

Seo, W. S., H. H. Jo, et al. (2004). "Size-Dependent Magnetic Properties of Colloidal Mn3O4 and MnO Nanoparticles." Angewandte Chemie International Edition **43**(9): 1115-1117.

Shakhashiri, B. Z., G. E. Dirreen, et al. (1980). "Solubility and complex ion equilibria of silver(I) species in aqueous solution." Journal of Chemical Education **57**(11): 813.

Sharma, V. K., K. M. Siskova, et al. (2014). "Organic-coated silver nanoparticles in biological and environmental conditions: Fate, stability and toxicity." Advances in Colloid and Interface Science **204**(0): 15-34.

Shi, H. B., R. Magaye, et al. (2013). "Titanium dioxide nanoparticles: a review of current toxicological data." Particle and Fibre Toxicology **10**: 15-15.

Shin, H. S., H. J. Yang, et al. (2004). "Mechanism of growth of colloidal silver nanoparticles stabilized by polyvinyl pyrrolidone in< i> γ</i>-irradiated silver nitrate solution." Journal of colloid and interface science **274**(1): 89-94.

Shinde, M., A. Pawar, et al. (2009). "Uncapped silver nanoparticles synthesis by DC arc thermal plasma technique for conductor paste formulation." Journal of Nanoparticle Research **11**: 5.

Shrivastava, S., T. Bera, et al. (2007). "Characterization of enhanced antibacterial effects of novel silver nanoparticles." Nanotech. **18**(225103): 9.

Shvedova, A. A., A. Pietroiusti, et al. (2012). "Mechanisms of carbon nanotube-induced toxicity: Focus on oxidative stress." Toxicology and Applied Pharmacology **261**(2): 121-133.

Silva, A. R. and G. Unali (2011). "Controlled silver delivery by silver–cellulose nanocomposites prepared by a one-pot green synthesis assisted by microwaves." Nanotechnology **22**(31): 315605.

Silva, B. F. d., S. Pérez, et al. (2011). "Analytical chemistry of metallic nanoparticles in natural environments." TrAC Trends in Analytical Chemistry **30**(3): 528-540.

Silvert, P.-Y., R. Herrera-Urbina, et al. (1997). "Preparation of colloidal silver dispersions by the polyol process, Part 2: Mechanism of particle formation." Journal of Materials Chemistry **7**(2): 7.

Skandan, G. and A. Singhal (2006). Perspectives on the science and technology of nanoparticle synthesis. Nanomaterials Handbook. Y. Gogotsi. Boca Raton, CRC Press.

Slistan-Grijalva, A., R. Herrera-Urbina, et al. (2005). "Assessment of growth of silver nanoparticles synthesized from an ethylene glycol-silver nitrate-polyvinylpyrrolidone solution." Physica E **25**: 10.

Smitha, S. L., K. M. Nissamudeen, et al. (2008). "Studies on surface plasmon resonance and photoluminescence of silver nanoparticles." Spectrochimica Acta Part A: Molecular and Biomolecular Spectroscopy **71**(1): 186-190.

Sondag-Huethorst, J. A. M., C. Schonenberger, et al. (1994). "Formation of Holes in Alkanethiol Monolayers on Gold." The Journal of Physical Chemistry **98**(27): 6826-6834.

Stobiecka, M., K. Coopersmith, et al. (2010). "Resonance elastic light scattering (RELS) spectroscopy of fast non-Langmuirian ligand-exchange in glutathione-induced gold nanoparticle assembly." Journal of Colloid and Interface Science **350**(1): 168-177.

Stolpe, B., L. Guo, et al. (2010). "Size and composition of colloidal organic matter and trace elements in the Mississippi River, Pearl River and the northern Gulf of Mexico, as characterized by flow field-flow fractionation." Marine Chemistry **118**(3–4): 119-128.

Stone, V., B. Nowack, et al. (2010). "Nanomaterials for environmental studies: Classification, reference material issues, and strategies for physico-chemical characterisation." Sci. of the Tot. Env. **408**(7): 1745-1754.

Struempler, A. W. (1973). "Adsorption characteristics of silver, lead, cadmium, zinc, and nickel on borosilicate glass, polyethylene, and polypropylene container surfaces." Analytical Chemistry **45**(13): 2251-2254.

Sugimoto, T. (1987). "Preparation of monodisperse colloidal particles." Advances in Colloid and Interface Science **28**: 44.

Sun, Y., S. K. Gray, et al. (2011). "Surface chemistry: a non-negligible parameter in determining optical properties of small colloidal metal nanoparticles." Physical Chemistry Chemical Physics **13**(25): 11814-11826.

Tantra, R., S. Jing, et al. (2011). "Dispersion stability of nanoparticles in ecotoxicological investigations: the need for adequate measurement tools." Journal of Nanoparticle Research **13**(9): 3765-3780.

Tantra, R., S. Jing, et al. (2011). "Dispersion stability of nanoparticles in ecotoxicological investigations: the need for adequate measurement tools." Journal of Nanoparticle Research **13**(9): 3765-3780.

Taylor, H. E., J. R. Garbarino, et al. (2002). "Inductively coupled plasma-mass spectrometry as an element-specific detector for field-flow fractionation particle separation." Analytical chemistry **64**(18): 2036-2041.

Templeton, A. C., W. P. Wuelfing, et al. (1999). "Monolayer-Protected Cluster Molecules." Accounts of Chemical Research **33**(1): 27-36.

Templeton, R. C., P. L. Ferguson, et al. (2006). "Life-Cycle Effects of Single-Walled Carbon Nanotubes (SWNTs) on an Estuarine Meiobenthic Copepod†." Environmental Science & Technology **40**(23): 7387-7393.

Thomas, D. N., S. J. Judd, et al. (1999). "Flocculation modelling: a review." Water Research **33**(7): 1579-1592.

Thomas, J. C. (1987). "The determination of log normal particle size distributions by dynamic light scattering." Journal of Colloid and Interface Science **117**(1): 187-192.

Tolaymat, T. M., A. M. El Badawy, et al. (2010). "An evidence-based environmental perspective of manufactured silver nanoparticle in syntheses and applications: A systematic review and critical appraisal of peer-reviewed scientific papers." Science of the Total Environment **408**(5): 999-1006.

Torrey, D., K. Michael, et al. (2006). "Optimizing silicone emulsion stability using zeta potential." American Laboratory News, June/July.

Tourinho, P. S., C. A. Van Gestel, et al. (2012). "Metal-based nanoparticles in soil: Fate, behavior, and effects on soil invertebrates." Environmental Toxicology and Chemistry **31**(8): 1679-1692.

Treuel, L. and G. U. Nienhaus (2012). "Toward a molecular understanding of nanoparticle–protein interactions." Biophysical Reviews **4**(2): 137-147.

Tsunoyama, H., H. Sakurai, et al. (2005). "Size-Specific Catalytic Activity of Polymer-Stabilized Gold Nanoclusters for Aerobic Alcohol Oxidation in Water." Journal of the American Chemical Society **127**(26): 9374-9375.

Tsuzuki, T. and P. G. McCormick (2004). "Mechanochemical synthesis of nanoparticles." Journal of Materials Science **39**(16-17): 4.

Unrine, J. M., B. P. Colman, et al. (2012). "Biotic and abiotic interactions in aquatic microcosms determine fate and toxicity of Ag nanoparticles. Part 1. Aggregation and dissolution." Environmental science & technology **46**(13): 6915-6924.

Verwey, E. J. W., J. T. G. Overbeek, et al. (1999). Theory of the stability of lyophobic colloids, Courier Dover Publications.

Vollath, D. (2008). Nanomaterials: An Introduction to Synthesis, Properties and Applications. Germany, WILEY-CH.

Vollath, D. (2008). Nanomaterials: an introduction to synthesis, properties and applications. Weinheim, Wiley-VCH.

Wang, C.-H., C.-J. Liu, et al. (2008). "Optimizing the size and surface properties of polyethylene glycol (PEG)–gold nanoparticles by intense x-ray irradiation." Journal of Physics D: Applied Physics **41**(19): 195301.

Wang, C., D. van der Vliet, et al. (2009). "Monodisperse Pt3Co nanoparticles as a catalyst for the oxygen reduction reaction: Size-dependent activity." The Journal of Physical Chemistry C **113**(45): 19365-19368.

Wang, X., X. Xu, et al. (1999). "Thermal conductivity of nanoparticle-fluid mixture." Journal of thermophysics and heat transfer **13**(4): 474-480.

Wang, Y. and Y. Xia (2004). "Bottom-Up and Top-Down Approaches to the Synthesis of Monodispersed Spherical Colloids of Low Melting-Point Metals." Nano Letters **4**(10): 2047-2050.

Warheit, D. B. (2008). "Absence of adequate material characterization?" Toxicological Sciences **101**(2): 3.

Washio, I., Y. Xiong, et al. (2006). "Reduction by the end groups of poly(vinyl pyrrolidone): A new and versatile route to the kinetically controlled synthesis of Ag Triangular Nanoplates." Advance Materials **18**(13): 5.

West, F. K., P. W. West, et al. (1966). "Adsorption of Traces of Silver on Container Surfaces." Analytical Chemistry **38**(11): 1566-1570.

Wilcoxon, J. P. and P. Provencio (2003). "Etching and Aging Effects in Nanosize Au Clusters Investigated Using High-Resolution Size-Exclusion Chromatography." The Journal of Physical Chemistry B **107**(47): 12949-12957.

Wiley, B. J., S. H. Im, et al. (2006). "Maneuvering the Surface Plasmon Resonance of Silver Nanostructures through Shape-Controlled Synthesis." The Journal of Physical Chemistry B **110**(32): 15666-15675.

Wilkinson, K. J. and J. R. Lead, Eds. (2007). Environmental colloids and particles: behaviour, separation and characterization. IUPAC series on analytical and physical chemistry of environmental system. Chicester, England, John Wiley & Sons.

Williams, P. S., M. H. Moon, et al. (1996). "Effect of viscosity on retention time and hydrodynamic lift forces in sedimentation/steric field-flow fractionation." Chemical engineering science **51**(19): 4477-4488.

Woehrle, G. H., L. O. Brown, et al. (2005). "Thiol-Functionalized, 1.5-nm Gold Nanoparticles through Ligand Exchange Reactions: Scope and Mechanism of Ligand Exchange." Journal of the American Chemical Society **127**(7): 2172-2183.

Xiong, Y., I. Washio, et al. (2006). "Poly(vinyl pyrrolidone): A Dual Functional Reductant and Stabilizer for the Facile Synthesis of Noble Metal Nanoplates in Aqueous Solutions." Langmuir **22**(20): 8563-8570.
null

Xiu, Z.-M., J. Ma, et al. (2011). "Differential Effect of Common Ligands and Molecular Oxygen on Antimicrobial Activity of Silver Nanoparticles versus Silver Ions." Environmental Science & Technology **45**(20): 9003-9008.

Yan, S., Y. Wang, et al. (2006). "A study on the optical absorption properties of dielectric-mediated gold nanoshells." Physica E: Low-dimensional Systems and Nanostructures **33**(1): 139-143.

Yang, J., Q. Zhang, et al. (2007). "Dissolution-recrystallization mechanism for the conversion of silver nanospheres to triangular nanoplates." J. of Coll. and Inter. Sci. **308**(1): 157-161.

Yang, X., A. P. Gondikas, et al. (2011). "Mechanism of silver nanoparticle toxicity is dependent on dissolved silver and surface coating in Caenorhabditis elegans." Environmental science & technology **46**(2): 1119-1127.

Yin, B., H. Ma, et al. (2003). "Electrochemical synthesis of silver nanoparticles under protection of poly (N-vinylpyrrolidone)." The Journal of Physical Chemistry B **107**(34): 8898-8904.

Yin, H., T. Yamamoto, et al. (2004). "Large-scale and size-controlled synthesis of silver nanoparticles under microwave irradiation." Materials Chemistry and Physics **83**(1): 66-70.

Yoo, J. S. (1998). "Selective gas-phase oxidation at oxide nanoparticles on microporous materials." Catalysis today **41**(4): 409-432.

Zhang, L., Y. Jiang, et al. (2007). "Investigation into the antibacterial behaviour of suspensions of ZnO nanoparticles (ZnO nanofluids)." Journal of Nanoparticle Research **9**(3): 479-489.

Zhang, M. and B.-C. Ye (2011). "Colorimetric Chiral Recognition of Enantiomers Using the Nucleotide-Capped Silver Nanoparticles." Analytical Chemistry **83**(5): 1504-1509.

Zhang, P. and T. K. Sham (2003). "X-Ray Studies of the Structure and Electronic Behavior of Alkanethiolate-Capped Gold Nanoparticles: The Interplay of Size and Surface Effects." Physical Review Letters **90**(24): 245502.

Zhang, Y.-W., R. Si, et al. (2003). "Facile alcohothermal synthesis, size-dependent ultraviolet absorption, and enhanced CO conversion activity of ceria nanocrystals." The Journal of Physical Chemistry B **107**(37): 10159-10167.

Zhang, Z., B. Zhao, et al. (1996). "PVP Protective Mechanism of Ultrafine Silver Powder Synthesized by Chemical Reduction Processes." Journal of Solid State Chemistry **121**(1): 105-110.

Zhou, W. P., A. Lewera, et al. (2006). "Size Effects in Electronic and Catalytic Properties of Unsupported Palladium Nanoparticles in Electrooxidation of Formic Acid." The Journal of Physical Chemistry B **110**(27): 13393-13398.

Zook, J. M., S. E. Long, et al. (2011). "Measuring silver nanoparticle dissolution in complex biological and environmental matrices using UV–visible absorbance." Analytical and bioanalytical chemistry **401**(6): 1993-2002.

APPENDIX A

IONIC STRENGTH CALCULATION

$$I = \frac{1}{2}\sum_{i=1}^{n} c_i z_i^2$$

Table A. 1 Chemical composition of OECD Daphnia sp. Media and its variation

Media	Chemicals name	Formula	Released ions	Concentration (mM)
OECD Daphnia Media (CM)	Calcium dichloride dihydrate	$CaCl_2.2H_2O$	$Ca^{2+} + 2Cl^-$	2
	Magnesium sulfate heptahydrate	$MgSO_4.2H_2O$	$Mg^{2+} + SO_4^{2-}$	0.5
	Sodim bicharbonate	$NaHCO_3$	$Na^+ + HCO_3^-$	0.77
	Potassium chloride	KCl	$K^+ + Cl^-$	0.08
	Sodium selenite	Na_2SeO_3	$2Na^+ + SeO_3^{2-}$	0.01
Nitrate media (NM)	Calcium dinitrate tetrahydrate	$Ca(NO_3)_2.2H_20$	$Ca^{2+} + 2NO_3^-$	2
	Magnesium sulfate heptahydrate	$MgSO_4.2H_2O$	$Mg^{2+} + SO_4^{2-}$	0.5
	Sodim bicharbonate	$NaHCO_3$	$Na^+ + HCO_3^-$	0.77
	Potassium nitrate	KCl	$K^+ + NO_3^-$	0.07
	Sodium selenite	Na_2SeO_3	$2Na^+ + SeO_3^{2-}$	0.01
Sulfate Media (SM)	Calcium sulfate	$CaSO_4$	$Ca^{2+} + SO_4^{2-}$	2
	Magnesium sulfate heptahydrate	$MgSO_4.2H_2O$	$Mg^{2+} + SO_4^{2-}$	0.5
	Sodium bicharbonate	$NaHCO_3$	$Na^+ + HCO_3^-$	0.77
	dipotassium sulphate	K_2SO_4	$2K^+ + SO_4^{2-}$	0.04
	Sodium selenite	Na_2SeO_3	$2Na^+ + SeO_3^{2-}$	0.01

Table A. 2 Ionic Strength calculation of OECD Daphnia sp. Media and its variation

Ions	Ion's charge	CM		NM		SM	
		Ion's conc (c)	z^2 x c	c	z^2 x c	c	z^2 x c
	(z)	(mM)	mM		mM		mM
Ca^{2+}	2	2	8	2	8	2	8
Cl^-	1	4.08	4.08	0	0	0	0
Mg^{2+}	2	0.5	2	0.5	2	0.5	2
SO_4^{2-}	2	0.5	2	0.5	2	2.5	10
Na^+	1	0.79	0.79	0.799	0.799	0.79	0.79
HCO_3^-	1	0.77	0.77	0.77	0.77	0.77	0.77
K^+	1	0.08	0.08	0.08	0.08	0.08	0.08
SeO_3^{2-}	2	0.01	0.04	0.01	0.04	0.01	0.04
NO_3^-	1	0	0	4.08	4.08	0	0
			17.76		17.769		21.68
Ionic Strength			8.88		8.8845		10.84

Table A. 3 Chemicals content of algae media (Bold basal medium)

No	Name	Formula	Released ions:	Concentration (mM)
1	di-potassium hydrogen orthophosphate	K_2HPO_4 *	$2K^+ + HPO_4^{2-}$	4.306E-01
2	Potassium di-hydrogen orthophosphate	KH_2PO_4 *	$K^+ + H_2PO_4^-$	1.286E+00
3	Magnesium sulphate	$MgSO_4.7H_2O$	$Mg^{2+} + SO_4^{2-}$	3.043E-01
4	Sodium Nitrate	$NaNO_3$	$Na^+ + NO_3^-$	2.941E+00
5	Calcium chloride	$CaCl_2.2H_2O$	$Ca^{2+} + 2Cl^-$	1.701E-01
6	Sodium Chloride	NaCl	$Na^+ + Cl^-$	4.278E-01
7	Ferrous sulphate	$FeSO_47H_2O$	$Fe^{2+} + SO_4^{2-}$	1.791E-02
8	Sulphuric acid conc. (wt per mL = 1.84g)	H_2SO_4	$2H^+ + SO_4^{2-}$	1.876E-02
9	Boric acid	H_3BO_3 **	$H^+ + B(OH)_4^-$	1.847E-01
10	Zinc sulphate	$ZnSO_4.7H_2O$	$Zn^{2+} + SO_4^{2-}$	4.911E-03
11	Manganese chloride	$MnCl_2.4H_2O$	$Mn^{2+} + 2Cl^-$	1.172E-03
12	Cupric sulphate	$CuSO_4.5H_2O$	$Cu^{2+} + SO_4^{2-}$	1.009E-03
13	Cobaltous nitrate	$Co(NO_3)_2.6H_2O$	$Co^{2+} + 2NO_3^-$	2.749E-04
14	Sodium molybdate	$Na_2MoO_4.2H_2O$	$2Na^+ + MoO_4^{2-}$	7.936E-04

Note:

Second and third dissociation of $H_2PO_4^-$ and HPO_4^{2-} were ignored as the K_{a2} and K_{a3} of phosphoric acid were very low: 6.2×10^{-8} and 4.8×10^{-13} respectively

The dissociation of H_3BO_3 is $H_3BO_3 + H_2O \rightarrow H_3O^+ + B(OH)_4^-$

Table A. 4 Ionic Strength calculation of algae media

Ions	Ion's charge	Ion's concentration (mM)	charge^2 x conc
K^+	1	2.147E+00	2.147092
HPO_4^{2-}	2	4.306E-01	1.722356
$H_2PO_4^-$	1	1.286E+00	1.285914
Mg^{2+}	2	3.043E-01	1.217137
SO_4^{2-}	2	3.469E-01	1.387511
Na^+	1	3.371E+00	3.370553
NO_3^-	1	2.942E+00	2.941726
Ca^{2+}	2	1.701E-01	0.680272
Cl^-	1	7.703E-01	0.77027
Fe^{2+}	2	1.791E-02	0.071652
H^+	1	2.222E-01	0.22222
$B(OH)_4^-$	1	1.847E-01	0.1847
Zn^{2+}	2	4.911E-03	0.019643
Mn^{2+}	2	1.172E-03	0.004689
Cu^{2+}	2	1.009E-03	0.004037
Co^{2+}	2	2.749E-04	0.0011
MoO_4^{2-}	2	7.936E-04	0.003174
		Sum	16.03
		Ionic Strength (mM)	8.02

Table A. 5 The ion content comparison of daphnia media (CM-1) and algae media (AM)

Cations				**Anion**			
CM-1		**AM**		**CM-1**		**AM**	
Ions	**conc (mM)**	**Ions**	**conc (mM)**	**Ions**	**conc (mM)**	**Ions**	**conc (mM)**
Ca^{2+}	2.0000	K^{+}	2.1471	Cl^{-}	4.0771	HPO_4^{2-}	0.4306
Mg^{2+}	0.5000	Mg^{2+}	0.3043	SO_4^{2-}	0.5000	$H_2PO_4^{-}$	1.2859
Na^{+}	0.7940	Na^{+}	3.3706	HCO_3^{-}	0.7708	SO_4^{2-}	0.3469
K^{+}	0.0771	Ca^{2+}	0.1701	SeO_3^{2-}	0.0116	NO_3^{-}	2.9417
		Fe^{2+}	0.0179			Cl^{-}	0.7703
		H^{+}	0.2222			$B(OH)_4^{-}$	0.1847
		Zn^{2+}	0.0049			MoO_4^{2-}	0.0008
		Mn^{2+}	0.0012				
		Cu^{2+}	0.0010				
		Co^{2+}	0.0003				
Total conc (mM)	3.37		6.24		5.36		5.96
monovalent (%)	**25.84**		**91.99**		**90.45**		**86.94**
bivalent (%)	**74.16**		**8.01**		**9.55**		**13.06**

APPENDIX B

TEM IMAGES OF SILVER NANOPARTICLES IN ECOTOXICOLOGY MEDIA

	TEM Images	Parameter	Value
Triangular 1	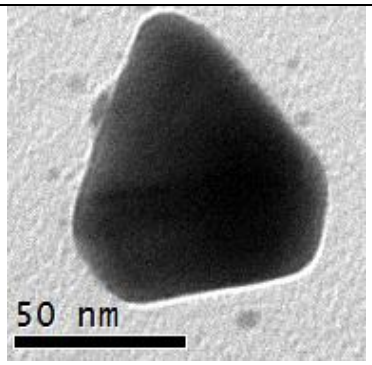	Area (nm^2)	4194.927
		Perimeter (nm)	281.591
		Average edge length (nm)	93.86
		Shape factor	0.665
Triangular 2	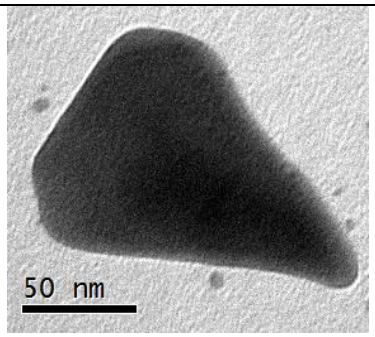	Area (nm^2)	9579.454
		Perimeter (nm)	460.166
		Average edge length (nm)	153.39
		Shape factor	0.568
Triangular 3	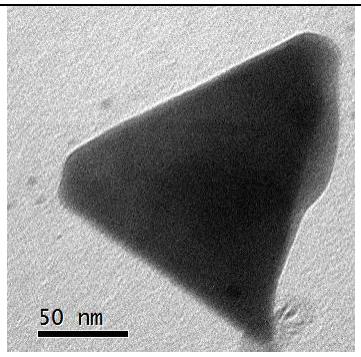	Area (nm^2)	14517.338
		Perimeter (nm)	639.942
		Average edge length (nm)	213.31
		Shape factor	0.445

Figure B. 1 Shape transformation of citrate capped AgNPs in NM-10 after 21 days of incubation

$\text{Average edge length (nm)} = \frac{\text{Perimeter (nm)}}{3}$; and $\text{Shape factor} = 4\Pi \times \frac{\text{area}}{\text{perimeter}^2}$

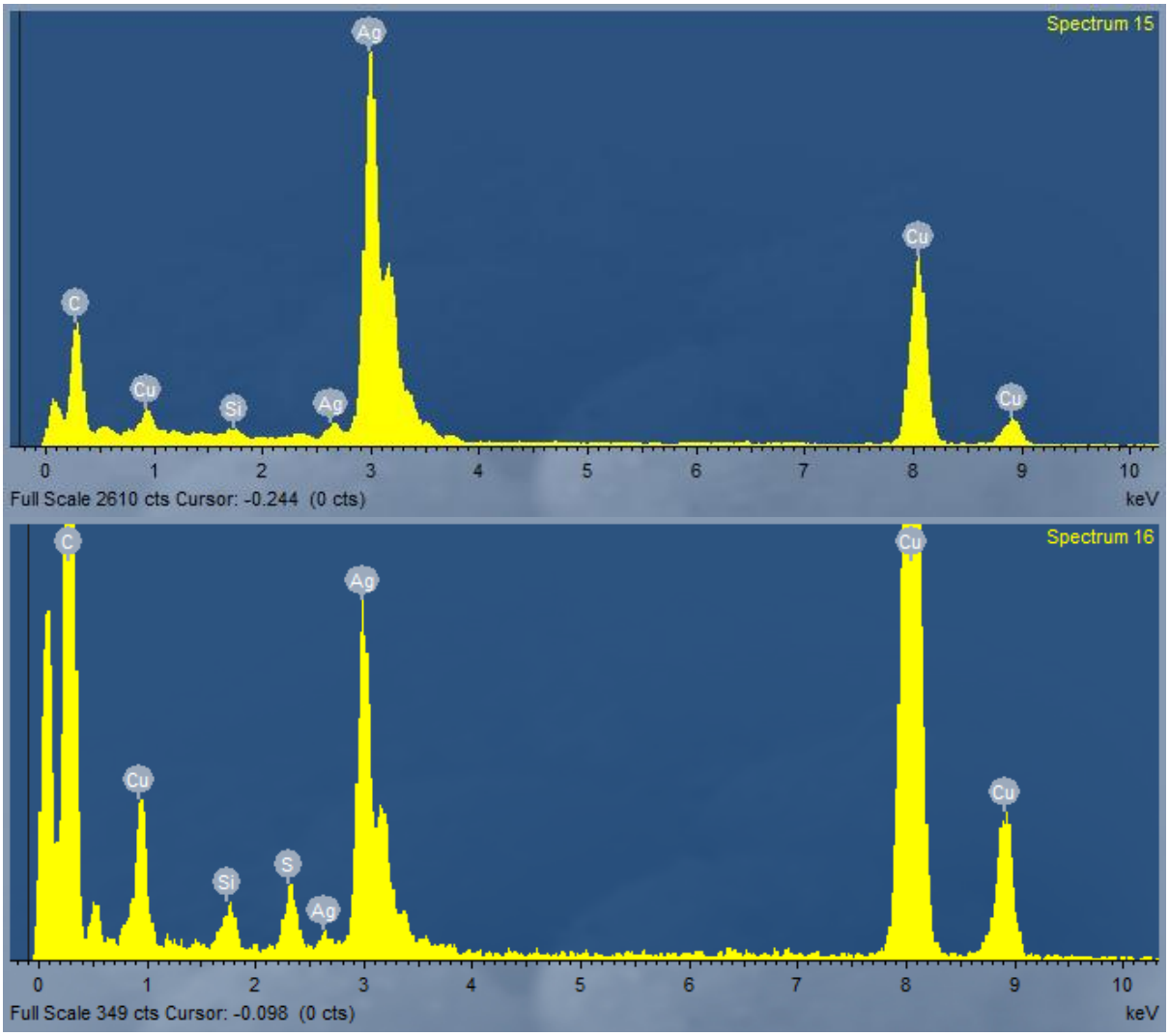

Figure B. 2 EDX Spectrum of Triangular AgNPs shape, found in AgNPs-NM-10 suspension after 21 days of incubation.